MODELING AND SIMULATION OF BIOETHANOL PRODUCTION FROM SILA SORGHUM STALKS AND MAIZE COBS

BY

WISEMAN TUMBO NGIGI

A THESIS SUBMITTED TO THE SCHOOL OF ENGINEERING IN PARTIAL FULFILLMENT OF THE REQUIREMENTS FOR THE AWARD OF THE DEGREE OF DOCTOR OF PHILOSOPHY IN ENERGY STUDIES

MOI UNIVERSITY

2024

DECLARATION

Declaration by Student:

This thesis is my original work and has not been presented for the award of a degree in any other University. No part of this thesis may be reproduced without the prior written permission of the author and/or Moi University.

Signature :_____ Date :_____

Tumbo, Wiseman Ngigi
ENG/DPHIL/MP/01/18

Declaration by Supervisors

We declare that this thesis has been submitted for examination with our approval as university supervisors.

SUPERVISORS:

Signature :_____ Date :_____

Prof. Zachary Siagi
Dept. of Mechanical, Production & Energy Eng.,
Moi University.

Signature :_____ Date :_____

For. Prof. Er Anil Kumar
Dept. of Chemical & Process Eng.,
Moi University.

Signature :_____ Date :_____

Dr. Moses NyoTonglo Arowo
Dept. of Chemical & Process Eng.,
Moi University.

DEDICATION

To

My father, the Late Leonard Ngigi Kimani,

My mother

My wife

&

My sons,

Whose support, love and guidance have been the fountain of my inspiration to a series of successes

ACKNOWLEDGEMENTS

A large number of individuals have contributed to the success of this thesis: Thanks to all of them for their assistance materially and morally. Special thanks to my supervisors Prof. Siagi, Prof. Kumar and Dr. Arowo for their guidance during the preparation of this thesis. I wish to thank my classmates for the mutual encouragement they offered. I would like to give credit to all my Lecturers at Moi University, School of Engineering for generously enriching me with Knowledge. Special thanks to Africa Development Bank (AFDB) for supporting my studies by way of scholarship. I also wish to thank World Bank, Moi University, Indian Institute of Technology Bombay, Africa Centre of Excellence (ACEII PTRE) and Government of India for organizing and financially supporting my exchange programme at IITB. To Prof. Srinivas of IITB, thank you for teaching me modeling and simulation using Aspen Plus software. Special thanks to the technicians in the Department of Chemical and Process Engineering, Civil and Structural Engineering and Manufacturing, Industrial and Textile Engineering and Mr. Swapnil, computer laboratory technician at IITB for guiding me during experimental work, analysis of samples, modeling and simulation studies. God bless them all. Finally, I would like to give credit to all the sources from where I have drawn information for this thesis.

ABSTRACT

Commercialization of bioethanol production from lignocellulosic biomass is hindered by low yield of fermentable sugars as well as insufficient techno-economic data on large-scale production. Simulation of the production process is a feasible way to obtain the necessary techno-economic data while the yield of fermentable sugars can be improved through optimization of the hydrolysis process. The main objective of this research was to model and simulate a large-scale bioethanol production process from Sila sorghum stalks and maize cobs (substrates) found in Kenya. The specific objectives were to select the most suitable pretreatment, hydrolysis and fermentation technologies in terms of bioethanol production rate, energy demand and energy intensity; determine the effect of varying cost and process parameters on the minimum bioethanol selling price (MBSP); hydrolyse the substrates using concentrated acid and establish conditions for optimal yield of fermentable sugars; establish kinetic parameters for glucose production and degradation during hydrolysis of substrates. Dilute acid, steam explosion and alkaline pretreatment, separate hydrolysis and co-fermentation (SHCF) and simultaneous saccharification and co-fermentation (SSCF) bioethanol production technologies were separately modeled and simulated using Aspen Plus software. The MBSP was calculated from the discounted cash flow rate of return (DCFROR) model. Hydrolysis of substrates was done by varying temperature (40^{o}C– 80^{o}C), time (30- 90 min) and concentration of acid (30 - 70%, w/w). Optimization of hydrolysis parameters was done using Central Composite Rotatable Design (CCRD). Kinetic study was done by varying reaction temperature (30^{o}C – 80^{o}C) and time (0 - 60 min). From the simulation results, the bioethanol production rate from dilute sulphuric acid, steam explosion, alkaline pretreatment and SSCF technologies was 21664.5, 18698.6, 12032.7 and 31074.4, 24749.4 and 13266.6 kg/h from sorghum stalks and maize cobs respectively. The energy demand for pretreatment and SSCF was 169787.23, 200053.08 and 93411 MJ/h for sorghum stalks and 225707.51, 242852.04 and 104211 MJ/h for maize cobs when using dilute sulphuric acid, steam explosion and alkaline pretreatment. The energy intensity for pretreatment, SSCF and product purification was 12.39, 16.50 and 19.79 MJ/L of bioethanol from sorghum stalks and 11.96, 13.53 and 15.34 MJ/L of bioethanol from maize cobs when using dilute sulphuric acid, steam explosion and alkaline pretreatment technologies. The MBSP increased from $0.81/L and $0.68 /L to $1.11/L and $0.89/L using sorghum stalks and maize cobs respectively when the cost of substrate increased from $20/ton to $100/ton. From experimental results, glucose yield reached a maximum of 87.54 and 90.02% (w/w) using sorghum stalks and maize cobs respectively. Optimum hydrolysis conditions were established as 60°C, 60 min and 50 % (w/w) acid concentration. The activation energy for glucose formation and degradation was 25.41 kJ/mol, 75.69 kJ/mol and 26.80 kJ/mol, 52.02 kJ/mol for sorghum stalks and maize cobs respectively. In conclusion, dilute acid pretreatment and SSCF is the most suitable technology. The main factors that impact the MBSP are cost of substrate, conversion of cellulose to glucose in the SSCF reactor and the flow rate of substrate. Concentrated acid hydrolysis results in high yield of fermentable sugars due to high activation energy of glucose degradation during hydrolysis of substrates. The findings herein provide insight on techno-economic feasibility of large-scale bioethanol production from sorghum stalks and maize cobs. In order to develop a single model that can handle alternative substrates, further research is recommended to update the models used in this study so as to handle other types of substrates.

TABLE OF CONTENTS

DECLARATION ii
DEDICATION iii
ACKNOWLEDGEMENTS iv
ABSTRACT v
TABLE OF CONTENTS vi
LIST OF TABLES xv
LIST OF FIGURES xx
LIST OF PLATES xxii
ACRONYMS AND SYMBOLS xxiii
CHAPTER ONE: INTRODUCTION 1
1.1 Background Information 1
1.1.1 Global energy mix 2
1.1.2 Global energy demand projections 3
1.2 Biofuels 5
1.3 Biomass 7
1.4 Lignocellulosic Biomass 12
1.5 The Problem Statement 13
1.6 The Objectives of the Research 14
1.6.1 General Objective 14
1.6.2 Specific Objectives 14
1.7 Scope of the Study 15
1.8 Justification of the Study 15
1.9 Sorghum 16
1.10 Maize Plant 18
1.11 Significance of the Study 19
1.12 Outline of the Research 19
CHAPTER TWO: LITERATURE REVIEW 21
2.1 Review of Previous Research 21
2.1.1 Simple sugars 21
2.1.2 Previous research on hydrolysis and kinetic studies of LGB 22
2.1.3 Previous research on techno-economic studies 33
2.1.4 Summary of existing research gaps 37

2.2 Sources of Biomass 37
2.2.1 Classification of biomass 38
2.2.1.1 Forestry woody substrates 38
2.2.1.2 Agricultural residues 38
2.2.1.3 Energy Crops 38
2.2.1.4 Aquatic plants 39
2.2.2 Herbaceous crops 39
2.2.3 Municipal Solid Waste 39
2.2.4 Animal Waste 39
2.3 Characteristics of Lignocellulosic Biomass 40
2.3.1 Cellulose 40
2.3.2 Hemicellulose 41
2.3.3 Lignin 41
2.3.4 Ash 42
2.4 Pretreatment of LGB 42
2.4.1 Physical pretreatment 43
2.4.1.1 Extrusion 43
2.4.1.2 Mechanical Pretreatment 43
2.4.1.3 Microwave 43
2.4.2 Chemical pretreatment 44
2.4.2.1 Acid pretreatment 44
2.4.2.2 Alkaline pretreatment 44
2.4.2.3 Organosolvent pretreatment 45
2.4.2.4 Ionic liquid pretreatment 45
2.4.2.5 Deep Eutectic Solvents 45
2.4.2.6 Oxidizing agents 46
2.4.2.7 Ozonolysis 46
2.4.3 Physio-chemical pretreatment 46
2.4.3.1 Steam explosion pretreatment 46
2.4.3.2 Liquid hot water pretreatment 47
2.4.3.3 Ammonia fibre explosion pretreatment 47
2.4.3.4 Carbon dioxide explosion 47
2.4.3.5 Wet Oxidation 48
2.4.4 Biological pretreatment 48

2.5 Pretreatment Inhibitors....48
2.6 Acid Hydrolysis....49
2.6.1 Dilute acid hydrolysis....50
2.6.2 Concentrated acid hydrolysis....51
2.7 Enzymatic Hydrolysis....52
2.8 Fermentation....53
2.9 Integrated Fermentation Technologies....53
2.9.1 Separate hydrolysis and fermentation....54
2.9.2 Simultaneous saccharification and fermentation....54
2.9.3 Separate hydrolysis and co-fermentation....54
2.9.4 Simultaneous saccharification and co-fermentation....54
2.9.5 Consolidated bioprocessing....55
2.9.6 Thermochemical Approach....55
2.10 Bioethanol Purification....55
2.10.1 Bioethanol distillation....55
2.10.2 Bioethanol dehydration....56
2.11 Safety Aspects of Large-Scale Bioethanol Production....56
2.12 Process Modeling and Simulation....57
2.12.1 Aspen Plus....59
2.12.2 Unit operation models....60
2.12.3 Physical property methods....60
2.12.4 Chemical components....61
2.12.5 Thermodynamic model selection....61
2.13 Economics of the Bioethanol Production Process....63
2.13.1 Costing and Project Evaluation....63
2.13.2 Economic analysis....63
2.13.2.1 Fixed capital investment....64
2.13.2.2 Working capital investment....64
2.13.2.3 Direct costs....64
2.13.2.4 Indirect costs....64
2.13.2.5 Operating cost....65
2.13.3 Estimating capital costs....65
2.13.4 Discounted cash-flow rate of return....66
2.14 Reaction Kinetics....66

2.14.1 Chemical kinetics 66
2.14.2 Factors affecting reaction rate 67
2.14.3 Activation energy 67
2.14.4 The Arrhenius equation 67
2.15 Kinetics of Glucose Production From LGB 68
2.15.1 Models used in kinetic studies during acid hydrolysis of LGB 69
2.15.1.1 The Saeman kinetic model 69
2.15.1.1 The biphasic kinetic model 71
2.16 Optimization 73
2.16.1 Central Composite Design 73
2.16.2 Full factorial design 74
2.16.3 The empirical model 75
2.16.4 Testing the significance of a regression 76
2.16.5 F- Test for regression model and lack of fit 76
2.16.6 Coefficient of determination 77
2.17 Software Application 77
2.18 Current Outlook for Large-Scale Bioethanol Production 77
CHAPTER THREE: EXPERIMENTAL MATERIALS, EQUIPMENT AND PROCEDURE 80
3.1 Experimental Materials 80
3.1.1 Reagents and standards 80
3.2 Experimental Equipment 80
3.3 Experimental Procedure 80
3.3.1 Methodology 82
3.3.1.1 Collection of Samples 82
3.3.1.2 Drying and Milling of Substrate 82
3.3.2 Modeling and simulation 83
3.3.2.1 Chemical components 84
3.3.2.2 Thermodynamic model selection 84
3.3.2.3 Reactor Models 84
3.3.2.4 Stream Input and equipment specification 86
3.3.2.5 Simulation output 86
3.3.2.6 Sensitivity analysis studies 86
3.3.3 Summary of the process 87

3.3.4 Pretreatment processes 87
3.3.4.1 Dilute sulphuric acid pretreatment 87
3.3.4.2 Steam explosion pretreatment 88
3.3.4.3 Alkaline pretreatment 89
3.3.5 Enzymatic hydrolysis 90
3.3.5.1 Hydrolysis reactions 91
3.3.6 Fermentation 91
3.3.6.1 Fermentation reactions 92
3.3.7 Product recovery and purification 93
3.3.8 Drying of ethanol 94
3.3.9 Economic analysis 94
3.3.9.1 Purchased equipment costs 95
3.3.9.2 Raw material costs 96
3.3.9.3 Estimation of working capital investment, direct costs, indirect costs, service facilities and fixed charges 96
3.3.9.4 Estimation of labour costs 98
3.3.9.5 Estimation of total capital investment 98
3.3.9.6 Discounted cash flow 99
3.3.10 Procedure for hydrolysis of substrate 99
3.3.11 Analysis of glucose: Summary 100
3.3.11.1 Procedure for analysis of glucose 101
3.3.12 Kinetic studies 103
CHAPTER FOUR: EXPERIMENTAL RESULTS AND DISCUSSION 104
4.1 Introduction 104
4.2 Characterization of Substrates 104
4.3 Process Modeling and Simulation: Sorghum Stalks and Maize Cobs 105
4.3.1 Modeling and simulation of dilute sulphuric acid pretreatment and SSCF process 106
4.3.2 Modeling and simulation of dilute sulphuric acid pretreatment and SHCF process 106
4.3.3 Modeling and simulation of steam explosion pretreatment and SSCF process 107
4.3.4 Modeling and simulation of the steam explosion pretreatment and SHCF process 107

4.3.5 Modeling and simulation of the alkaline pretreatment and SSCF process ... 107
4.3.6 Modeling and simulation of the alkaline pretreatment and SHCF process .. 108
4.3.7 Modeling and simulation of the beer column, rectification column, molecular sieve dehydration and energy recovery process ... 108
4.4 Sorghum Stalks: Simulation Results Obtained From Various Models ... 109
4.4.1 Simulation results for dilute sulphuric acid pretreatment and SSCF process for sorghum stalks ... 109
4.4.2 Simulation results for dilute sulphuric acid pretreatment and SHCF process for sorghum stalks ... 110
4.4.3 Simulation results for steam explosion pretreatment and SSCF process for sorghum stalks ... 111
4.4.4 Simulation results for steam explosion pretreatment and SHCF process for sorghum stalks ... 111
4.4.5 Simulation results for alkaline pretreatment and SSCF process for sorghum stalks ... 112
4.4.6 Simulation results for alkaline pretreatment and SHCF process for sorghum stalks ... 112
4.5 Sorghum Stalks: Energy Analysis and Ethanol Production Rate for Pretreatment, Hydrolysis and Fermentation Processes ... 113
4.5.1 Energy analysis for dilute sulphuric acid, steam explosion, alkaline pretreatment and SHCF process ... 113
4.5.2 Energy analysis for dilute sulphuric acid, steam explosion, alkaline pretreatment and SSCF process ... 113
4.6 Sorghum Stalks: Summary of Energy Analysis and Ethanol Production Rate for Pretreatment, Hydrolysis and Fermentation Processes ... 114
4.6.2 Summary of heating, cooling demand and ethanol production rate for SHCF process for sorghum stalks ... 114
4.6.3 Summary of heating, cooling demand and ethanol production rate for SSCF processes for sorghum stalks ... 115
4.7 Sorghum Stalks: Energy Analysis and Ethanol Production Rate for Pretreatment, Hydrolysis, Fermentation, Beer Purification and Energy Recovery Process ... 116
4.7.1 Heating and cooling demand for purification of beer from dilute sulphuric acid, steam explosion, alkaline pretreatment methods and SSCF process . 116

4.8 Sorghum Stalks: Summary of Energy Analysis and Ethanol Production Rate for Pretreatment, SSCF and Beer Purification Processes 117
4.9 Sila Sorghum Stalks: Development and Simulation of Full-Scale Model for 2GBE Production 119
4.10 Economic Analysis: Production of Bioethanol from Sorghum Stalks 120
4.10.1 Purchased equipment costs 121
4.10.2 Direct costs, indirect costs, TCI, fixed charges and service facilities 121
4.10.3 Total labour costs 122
4.10.4 Analysis of cash flow 123
4.11 Maize Cobs: Simulation Results Obtained From Various Models 124
4.11.1 Simulation results for dilute sulphuric acid pretreatment and SSCF process for maize cobs 124
4.11.2 Simulation results for steam explosion pretreatment and SSCF process for maize cobs 125
4.11.3 Simulation results for alkaline pretreatment and SSCF process for maize cobs 126
4.12 Maize Cobs: Energy Analysis and Ethanol Production Rate for Pretreatment, Hydrolysis and Fermentation Processes 126
4.12.1 Energy analysis for dilute sulphuric acid, steam explosion, alkaline pretreatment and SSCF process 126
4.13 Maize Cobs: Summary of Energy Analysis and Ethanol Production Rate for Pretreatment, Hydrolysis and Fermentation Processes 127
4.14 Maize Cobs: Energy Analysis and Ethanol Production Rate for Pretreatment, Hydrolysis, Fermentation, Beer Purification and Energy Recovery Process 128
4.14.1 Energy analysis and ethanol production rate for dilute sulphuric acid pretreatment, SSCF and beer purification process 128
4.15 Maize Cobs: Summary of Energy Analysis and Ethanol Production Rate for Pretreatment, SSCF and Beer Purification Processes 129
4.16 Economic Analysis: Production of Ethanol from Maize Cobs 130
4.16.1 Analysis of cash flow 132
4.17 Production of Bioethanol from Sorghum Stalks and Maize Cobs: Overall Results and Discussion 133
4.18 Effect of Varying Cost and Process Parameters on Bioethanol Production Rate, Bioethanol Production Cost and MBSP 139

4.18.1 Effect of varying LGB flow rate on bioethanol production rate 139
4.18.2 Effect of varying the conversion of cellulose to glucose in the SSCF reactor on ethanol production rate 141
4.18.3 Effect of varying LGB cost on bioethanol production cost and MBSP 144
4.18.4 Effect of varying cost of enzyme on MBSP 146
4.18.5 Effect of varying discount rate on MBSP 147
4.18.6 Effect of varying FCI on MBSP 148
4.18.7 Effect of varying plant life on MBSP 148
4.18.8 Effect of varying income tax rate on MBSP 149
4.19 Optimal Hydrolysis Conditions 150
4.19.1 Glucose yield from sorghum stalks 151
4.19.2 Optimization of concentrated acid hydrolysis of sorghum stalks 153
4.19.3 Glucose yield from maize cobs 157
4.19.4 Optimization of concentrated acid hydrolysis of maize cobs 162
4.20 Model Validation 165
4.21 Glucose Yield from Sorghum Stalks and Maize Cobs: Literature Based Comparison 165
4.22 Kinetics Studies 168
4.22.1 Optimization of glucose production during kinetics studies 173
4.23 Modeling and Simulation of Concentrated Sulphuric Acid Hydrolysis of Sorghum Stalks and Maize Cobs 174
4.23.1 Comparison of kinetic parameters for glucose formation and degradation 177
CHAPTER FIVE: CONCLUSIONS AND RECOMMENDATIONS 179
5.1 Conclusions 179
5.2 Recommendations 183
REFERENCES 186
APPENDIXES 198
Appendix A: Modeling and Simulation results 198
Appendix B: Economic analysis and variation of techno-economic parameters 201
Appendix C: Calculations involving glucose yield 203
Appendix C. 1: Determination of glucose yield 203
Appendix C. 2: Maximum/theoretical yield of glucose 204
Appendix D: Saeman and biphasic model 206
Appendix D. 1: Integration of the proposed Saeman model 206

Appendix E: Scientific Output 209
Appendix F: Plagiarism Awareness Certificate 210

LIST OF TABLES

Table 3. 1: Equipment used during the study 81
Table 3. 2: Conditions for dilute sulphuric acid pretreatment 88
Table 3. 3: Main reactions that occur during dilute sulphuric acid pretreatment 88
Table 3. 4: Main reaction during ammonia conditioning 88
Table 3. 5: Conditions for steam explosion pretreatment 89
Table 3. 6: Reactions that occur during steam explosion pretreatment 89
Table 3. 7: Conditions for alkaline pretreatment 89
Table 3. 8: Output from separation unit during alkaline pretreatment 90
Table 3. 9: Conditions for separate hydrolysis 90
Table 3. 10: Main reaction that occur during separate hydrolysis 90
Table 3. 11: Conditions for co- fermentation 91
Table 3. 12: Main reactions that occur during co-fermentation 92
Table 3. 13: Conditions for SSCF 92
Table 3. 14: Main reactions that occur during SSCF 92
Table 3. 15: Parameters used in economic analysis 94
Table 3. 16: Working capital investment 97
Table 3. 17:Direct costs 97
Table 3. 18: Indirect costs 97
Table 3. 19: Service facilities 97
Table 3. 20: Fixed charges 98
Table 3. 21: CCRD matrix for actual and coded level of hydrolysis factors 100
Table 3. 22: Experimental design matrix for the hydrolysis process: actual and coded 101
Table 4. 1: Chemical composition of substrates 104
Table 4. 2: Comparison of substrate composition with literature data 105
Table 4. 3: Results of dilute sulphuric acid pretreatment and SSCF process for sorghum stalks 110
Table 4. 4: Results of dilute sulphuric acid pretreatment and SHCF process for sorghum stalks 110
Table 4. 5: Results of steam explosion pretreatment and SSCF process for sorghum stalks 111

Table 4. 6: Results of steam explosion pretreatment and SHCF process for sorghum stalks 111
Table 4. 7: Results of alkaline pretreatment and SSCF process for sorghum stalks . 112
Table 4. 8: Results of sodium hydroxide pretreatment and SHCF process for sorghum stalks 112
Table 4. 9: Heating and cooling demand for dilute sulphuric acid, steam explosion and alkaline pretreatment methods and SHCF process for sorghum stalks.... 113
Table 4. 10: Heating and cooling demand for dilute sulphuric acid, steam explosion and alkaline pretreatment methods and SSCF process for sorghum stalks 114
Table 4. 11: Summary of heating, cooling demand and ethanol production rate for SHCF processes for sorghum stalks 114
Table 4. 12: Summary of heating, cooling demand and ethanol production rate for SSCF processes for sorghum stalks 115
Table 4. 13: Heating and cooling demand for purification of beer from dilute sulphuric acid, steam explosion, alkaline pretreatment methods and SSCF process..... 117
Table 4. 14: Combined summary of results for dilute sulphuric acid, steam explosion, alkali pretreatment, SSCF and purification process for sorghum stalks .. 117
Table 4. 15: Results of dilute sulphuric acid pretreatment and SSCF process with flash separator for sorghum stalks 119
Table 4. 16: Composition of product stream from the purification and dehydration section 120
Table 4. 17: Assumptions for techno-economic analysis 120
Table 4. 18: Purchased equipment costs 121
Table 4. 19: Direct costs 121
Table 4. 20: Indirect costs 122
Table 4. 21: Total capital investment..... 122
Table 4. 22: Fixed charges 122
Table 4. 23: Service facilities..... 122
Table 4. 24: Total labour costs..... 123
Table 4. 25: Summary of direct production costs 123
Table 4. 26: Total product costs..... 123
Table 4. 27: Analysis of cash flow..... 123

Table 4. 28: Summary of cash flow analysis 124
Table 4. 29: Results of dilute sulphuric acid pretreatment and SSCF process for maize cobs 125
Table 4. 30: Results of steam explosion pretreatment and SSCF process for maize cobs 125
Table 4. 31: Results of alkaline pretreatment and SSCF process for maize cobs 126
Table 4. 32: Heating and cooling demand for dilute sulphuric acid, steam explosion, alkaline pretreatment methods and SSCF process 127
Table 4. 33: Summary of heating demand, cooling demand and ethanol production rate for SSCF processes for maize cobs 127
Table 4. 34: Heating and cooling demand for purification of beer from dilute sulphuric acid, steam explosion, alkaline pretreatment methods and SSCF process 128
Table 4. 35: Combined summary of results for dilute sulphuric acid, steam explosion, alkali pretreatment, SSCF and purification processes for maize cobs 129
Table 4. 36: Purchased equipment costs 130
Table 4. 37: Direct costs 131
Table 4. 38: Indirect costs 131
Table 4. 39: Total capital investment 131
Table 4. 40: Service facilities 131
Table 4. 41: Fixed charges 132
Table 4. 42: Direct production costs 132
Table 4. 43: Total product cost 132
Table 4. 44: Summary of cash flow analysis 132
Table 4. 45: Combined summary of heating, cooling demand and ethanol production rate for acid pretreatment, SSCF and purification process for sorghum stalks and maize cobs 133
Table 4. 46: Ethanol production rate: comparison between results from the current study with results from literature 134
Table 4. 47: Ethanol production rate, concentration of ethanol in the fermentation broth, heating demand and cooling demand: comparison between results from the current study with results from literature 135
Table 4. 48: Pretreatment energy consumption: comparison between results from the current study with results from literature 136

Table 4. 49: Energy intensity: comparison between results from the current study with results from literature 137
Table 4. 50: Comparison of bioethanol production cost from sorghum stalks and maize cobs 137
Table 4. 51: Effect of varying enzyme cost on MBSP 146
Table 4. 52: Cost contribution for sorghum stalks and maize cobs 146
Table 4. 53: Effect of varying FCI on MBSP 148
Table 4. 54: Glucose yield from sorghum stalks 151
Table 4. 55: ANOVA for testing significance of the model equation 152
Table 4. 56: Glucose yield from maize cobs 158
Table 4. 57: ANOVA for testing significance of the model equation 159
Table 4. 58: ANOVA for testing significance of the reduced model 161
Table 4. 59: Comparison of hydrolysis yield results from this study with results from literature 167
Table 4. 60: Rate constants for glucose formation and degradation during kinetic studies of sorghum stalks 168
Table 4. 61: Rate constants for glucose formation and degradation during kinetic studies of maize cobs 168
Table 4. 62: Kinetic parameters for glucose formation and degradation during hydrolysis of sorghum stalks and maize cobs 172
Table 4. 63: Hydrolysis of sorghum stalks and maize cobs: Results of optimization 173
Table 4. 64: Results of modeling and simulation of concentrated acid hydrolysis of sorghum stalks 174
Table 4. 65: Results of modeling and simulation of concentrated acid hydrolysis of maize 175
Table 4. 66: Comparison of glucose yield for experimental, model and simulation results at 60^{o}C for sorghum stalks and maize cobs 175
Table 4. 67: Heating demand, glucose production rate and glucose yield: Comparison between concentrated acid hydrolysis and dilute acid pretreatment and enzymatic hydrolysis of sorghum stalks and maize cobs 176
Table 4. 68: Comparison of kinetic parameters in this study with those from literature for acid catalysed hydrolysis of cellulose 177
Table A. 1: Overall mass balance around the dilute sulphuric acid pretreatment reactor for SSS 198

Table A. 2: Overall mass balance around the dilute sulphuric acid pretreatment reactor for maize cobs 198
Table A. 3: Overall mass balance around the steam explosion pretreatment reactor for SSS 199
Table A. 4: Overall mass balance around the steam explosion pretreatment reactor for maize cobs 199
Table A. 5: Overall mass balance around the alkaline pretreatment reactor for SSS 200
Table A. 6: Overall mass balance around the alkaline pretreatment reactor for maize cobs 200

LIST OF FIGURES

Figure 1. 1: World energy consumption 1
Figure 1. 2: Global energy mix 3
Figure 2. 1: Structure of cellulose 40
Figure 2. 2: Structure of hemicellulose 41
Figure 2. 3: Structure of lignin 42
Figure 2. 4: Conversion of cellulose and hemicellulose into sugar monomers and inhibitors 49
Figure 4. 1: PFD for dilute sulphuric acid pretreatment and SSCF process 106
Figure 4. 2: PFD for dilute sulphuric acid pretreatment and SHCF process 106
Figure 4. 3: PFD for steam explosion pretreatment and SSCF process 107
Figure 4. 4: PFD for steam explosion pretreatment and SHCF process 107
Figure 4. 5: PFD for alkaline pretreatment and SSCF process 108
Figure 4. 6: PFD for alkaline pretreatment and SHCF process 108
Figure 4. 7: PFD for ethanol purification, dehydration and energy recovery 109
Figure 4. 8: PFD of dilute acid pretreatment and SSCF process for sorghum stalks 119
Figure 4. 9: Effect of varying LGB flow rate on ethanol production rate for sorghum stalks 140
Figure 4. 10: Effect of varying LGB flow rate on ethanol production rate for maize cobs 140
Figure 4. 11: Effect of varying SSCF conversion on ethanol production rate for sorghum stalks 142
Figure 4. 12: Effect of varying SSCF conversion on ethanol production rate for maize cobs 142
Figure 4. 13: Effect of varying LGB cost on bioethanol cost 144
Figure 4. 14: Effect of varying cost of LGB on MBSP 145
Figure 4. 15: Effect of varying discount rate on MBSP 147
Figure 4. 16: Effect of varying plant life on MBSP 149
Figure 4. 17: Effect of varying income tax rate on MBSP 150
Figure 4. 18: RSM plot: effect of temperature (X1) and time (X2) on glucose yield (R1) 154
Figure 4. 19: RSM plot: effect of temperature (X1) and acid concentration (X3) on glucose yield (R1) 155

Figure 4. 20: RSM plot: effect of time and acid concentration on glucose yield 156
Figure 4. 21: RSM plot: effect of temperature (X1) and time (X2) on glucose yield (R1)..... 162
Figure 4. 22: RSM plot: effect of temperature (X1) and acid concentration (X3) on glucose yield (R1) 163
Figure 4. 23: RSM plot: effect of time (X2) and acid concentration (X3) on glucose yield (R1)..... 164
Figure 4. 24: Arrhenius plot of lnk1 against 1/T for sorghum stalks..... 170
Figure 4. 25: Arrhenius plot of lnk2 against 1/T for sorghum stalks..... 170
Figure 4. 26: Arrhenius plot of lnk1 against 1/T for maize cobs..... 171
Figure 4. 27: Arrhenius plot of lnk2 against 1/T for maize cobs..... 171
Figure 4. 28: PFD for concentrated acid hydrolysis of sorghum stalks and maize cobs..... 174
Figure B. 1: IRR against % change in selling price, income tax rate, LGB cost and plant Life for SSS 202
Figure B. 2: IRR against % change in selling price, income tax rate, LGB cost and plant Life for maize cobs..... 202

LIST OF PLATES

Plate 3. 1: Sorghum stalks samples 83
Plate 3. 2: Maize cobs samples 83

ACRONYMS AND SYMBOLS

$	Dollar
A_o	Pre-exponential Factor or Frequency Factor
C_1	Capital Cost of Project with Capacity S_1
C_2	Capital Cost of Project with Capacity S_2
C_A	Concentration of Cellulose/Glucan
C_B	Concentration of Glucose
C_{Bmax}	Maximum Concentration of Glucose
C_C	Concentration of Decomposition Product
$\eta_{Overall}$	Overall Efficiency
S_1	Project with Capacity S_1
S_2	Project with Capacity S_2
t_{max}	Hydrolysis time at which maximum concentration of glucose occurs
V_a	Value of Assets in n Years
V_s	Salvage Value of Assets
1GB	First Generation Biofuels
1GBE	First Generation Bioethanol
2GB	Second Generation Biofuels
2GBE	Second Generation Bioethanol
3GB	Third Generation Biofuels
AFEX	Ammonia fibre explosion
ANOVA	Analysis of Variance
AP	Aspen Plus
ASTM	American Society for Testing and Materials

ATP	Adenosine Triphosphate
bcm	Billion Cubic Metres
BMIMAc	1-N-Butyl-3-Methylimidazolium Acetate
BMIMCl	1- N-Butyl-3 Methylimidazolium Chloride
BPS	Banana Pseudostem
C_2H_5OH	Ethanol
C5	Five Carbon Sugars
$C_5H_{10}O_5$	Xylose
$C_5H_8O_4$	Hemicellulose
C6	Six Carbon Sugars
$C_6H_{10}O_5$	Cellulose
$C_6H_{12}O_6$	Glucose
$Ca(OH)_2$	Calcium Hydroxide
C_{AO}	Initial Cellulose/Glucan Concentration
C_B	Instantaneous Glucose Concentration
CBP	Consolidated Bioprocessing
CHO	Carbon Hydrogen Oxygen
CO	Carbon Monoxide
CO_2	Carbon Dioxide
CSTR	Continuous Stirred Tank Reactor
DCFROR	Discounted Cash Flow Rate of Return
DESs	Deep Eutectic Solvents
E_a	Activation Energy
EABL	East Africa Breweries Limited
EJ	Exajoules
EMIMCl	1-Ethyl-3-Methylimidazolium Chloride

EOS	Equation of State
et al	And Others
EV	Electric Vehicles
f	Depreciation factor
FAME	Fatty Acid Methyl Esters
FCI	Fixed Capital Investment
G6P	Glucose-6-Phosphate
G6PD	Glucose-6-Phosphate Dehydrogenase
GAPDH	Glyceraldehydes-3-Phosphate Dehydrogenase
GDP	Gross Domestic Product
GHG	Greenhouse Gas
gm/cc	Gram Per Cubic Centimeter
H_2O	Water
H_2O_2	Hydrogen Peroxide
H_2SO_4	Sulphuric Acid
HCl	Hydrochloric Acid
HK	Hexokinase
HMF	Hydroxymethylfurfural
HNO_3	Nitric Acid
HPLC	High Performance Liquid Chromatography
IEA	International Energy Agency
ILs	Ionic Liquids
IRR	Internal Rate of Return
J/mol	Joules per mole
K	Kelvin

k_1	Kinetic Constant for Glucose Formation
k_2	Kinetic Constant of Glucose Degradation
k_A	Reaction Rate Constant
KALRO	Kenya Agricultural and Livestock Research Organization
KJ/mol	Kilojoules per mole
kmol/h	Kilomole per hour
KNBS	Kenya National Bureau of Statistics
kWh	Kilowatt hour
LAP	Laboratory Analytical Procedures
LGB	Lignocellulosic Biomass
LHW	Liquid Hot Water
mbd	Million Barrels Per Day
MBSP	Minimum Bioethanol Selling Price
MCC	Microcrystalline Cellulose
MJ	Megajoules
MJ/h	Megajoules per Hour
MJ/L	Megajoules per Litre
MOA	Ministry of Agriculture
mol/L	Moles per Litre
MSW	Municipal Solid Waste
NAD	Nicotinamide Adenine Dinucleotide
NADH	Nicotinamide Adenine Dinucleotide +H
NaOH	Sodium Hydroxide
NFW	Net Future Worth
NOx	Oxides of Nitrogen

NPV	Net Present Value
NPW	Net Present Worth
NREL	National Renewable Energy Laboratory
NRTL	Non-Random Two Liquids
O_2	Oxygen
PFD	Process Flow Diagram
PFDs	Process Flow Diagrams
PPP	Public-Private-Partnership
R	Universal Gas Constant
RID	Refractive Index Detector
ROR	Rate of Return
RSM	Response Surface Methodology
RSP	Response Surface Plots
SCB	Sugarcane Bagasse
SHCF	Separate Hydrolysis and Co-fermentation
SHF	Separate Hydrolysis and Fermentation
SLR	Solid to Liquid Ratio
SOx	Oxides of Sulphur
SRK	Soave-Redlich-Kwong
SSB	Sweet Sorghum Bagasse
SSCF	Simultaneous Saccharification and Co-Fermentation
SSF	Simultaneous Saccharification and Fermentation
SSS	Sila Sorghum Stalks
T	Absolute Temperature
TCI	Total Capital Investment

TJ	Terajoules
TPC	Total Product Cost
TWh	Terawatt-hours
UNEP	United Nations Environment Program
USA	United States of America
V	Initial Value of Assets
v/v	Volume by Volume
VOCs	Volatile Organic Carbons
w/v	Weight by Volume
w/w	Weight by Weight
WCI	Working Capital Investment

CHAPTER ONE: INTRODUCTION

1.1 Background Information

One of the major challenges facing the world in the 21st century is the need to meet the energy demand for heating, transportation, lighting and industrial processes. The world's population is increasing faster, which makes the provision of energy a big challenge. The global energy demand is on the rise due to rapid population growth and rising standards of living (Yolcan, 2023; McKinsey & Company, 2022). According to Joy et al. (2021), rapid economic development has led to an increase in demand for transportation fuel. "Energy has become a priority in every country due to its great influence in the creation of jobs, the modernization of infrastructure, military, politics etc" (Triana, 2016, p.19). According to Cheah et al. (2020), the consumption of energy worldwide is estimated to increase by 49% from 2007 to 2035 with China and India contributing a bigger proportion of this increase. Figure 1.1 shows the world energy consumption over the last twenty years.

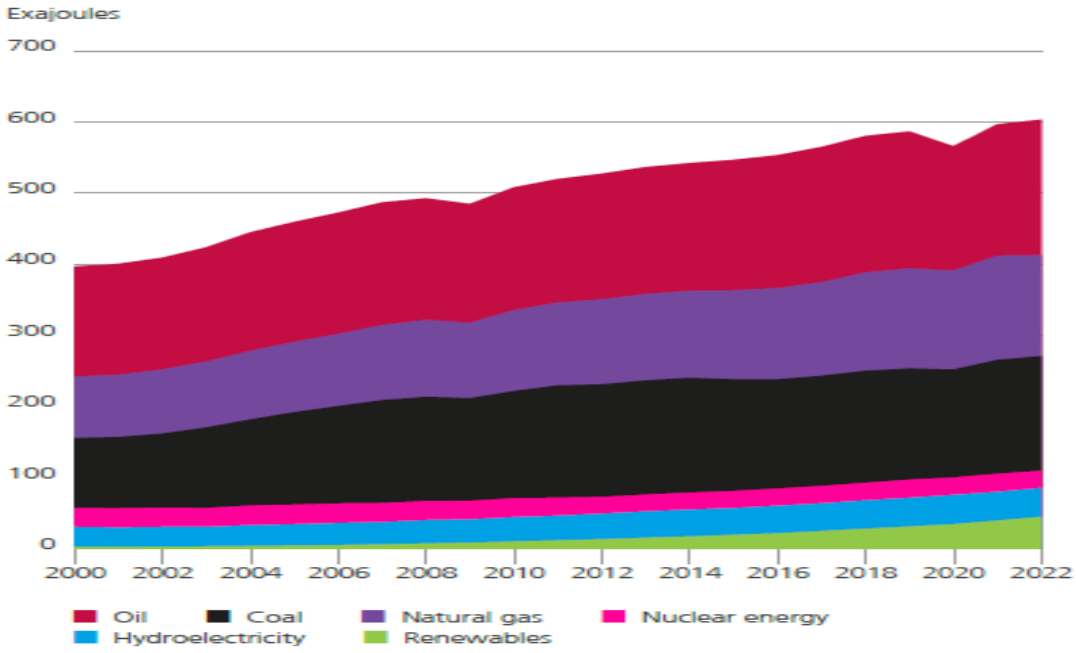

Figure 1. 1: World energy consumption (Energy Institute, 2023)

1.1.1 Global energy mix

"The global energy mix is projected to shift rapidly towards power and hydrogen" (McKinsey & Company, 2022, p.10). Due to electrification and the growth in living standards, the consumption of power is expected to triple by 2050 (McKinsey & Company, 2022). The fastest transition to electricity will be witnessed in the transport sector due to the use of electric vehicles (EV) (McKinsey & Company, 2022). For the long term, "green hydrogen production is projected to be the biggest driver of additional power demand (42% of the growth between 2035–2050)" (McKinsey & Company, 2022, p.11). "Peak oil demand is projected to occur between 2024 and 2027 driven largely by EV uptake" (McKinsey & Company, 2022, p.6). The demand for coal peaked in 2013 and after a temporary rebound in 2021, it is projected to continue its downward trajectory (McKinsey & Company, 2022). According to McKinsey & Company (2022), thermal power generation is expected to mainly act as a back-up provider to support grid stability. On the other hand, nuclear power generation will require support by way of economic policies and further public awareness in order to promote public acceptance (McKinsey & Company, 2022). The share of natural gas in the energy mix has increased gradually. The demand for natural gas in power generation is set to grow until between 2035 and 2040 after which it is projected that it will act as a back-up to renewables (McKinsey & Company, 2022). The contribution to the global energy mix by renewable energy is projected to reach 80–90% by 2050 mainly due to the growth in solar and wind energy sources (McKinsey & Company, 2022). Figure 1.2 shows the global energy mix where the energy consumption by fuel is shown in terajoules (TJ).

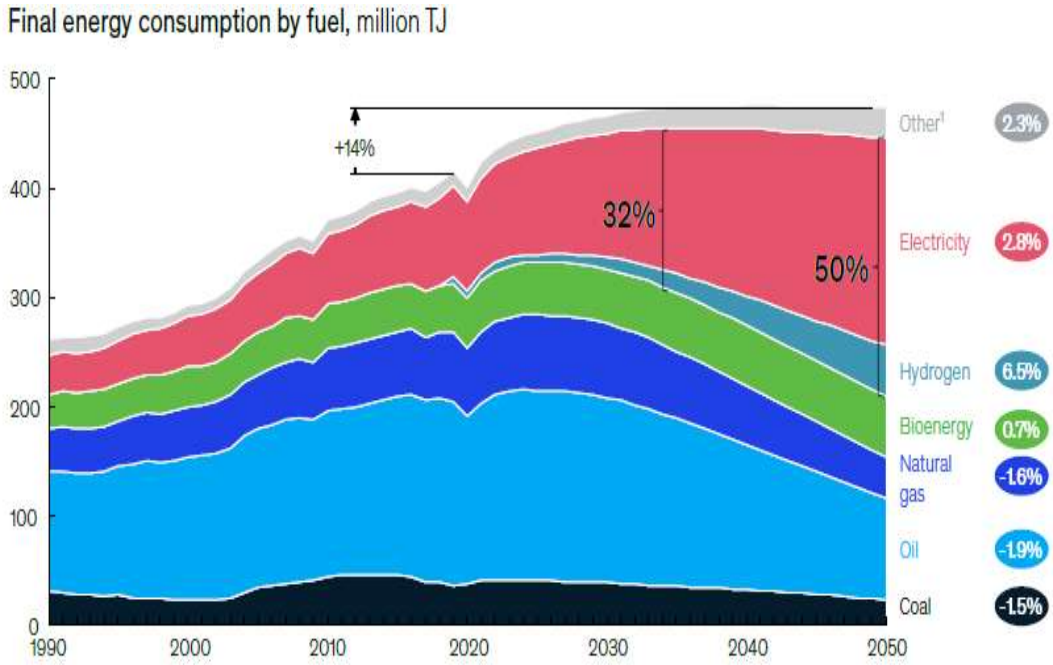

Figure 1. 2: Global energy mix (McKinsey & Company, 2022)

1.1.2 Global energy demand projections

It is projected that by 2050, the demand for hydrogen will increase by 500% mainly due to increased use by road transport, aviation and maritime sectors (McKinsey & Company, 2022). In addition, by 2050, hydrogen is projected to add approximately 18,000 terawatt-hours (TWh) of electricity consumption (McKinsey & Company, 2022). The demand for sustainable source of energy such as bioethanol is projected to triple over the next 20 years (McKinsey & Company, 2022). However, the production of sustainable fuels such as bioethanol faces challenges that include lack of sustainable supply of feedstocks. In order to meet the demand for sustainable fuels, feedstocks such as lignocellulosic biomass (LGB) will be required (McKinsey & Company, 2022). The use of renewable energy globally has been increasing over the years (Yolcan, 2023). According to the International Energy Agency [IEA] (2023), the demand for oil globally has increased by 18 million barrels per day (mb/d). This increase has largely been driven by a rise in demand in the transportation sector, with road transport

accounting for 45% of global oil demand (IEA, 2023; Yolcan, 2023). According to IEA (2023), the global demand for coal is set to decline in the next five years. This is mainly attributed to changes in iron and steel production (IEA, 2023). “In China – the world’s largest coal consumer – the impressive growth of renewables and nuclear alongside macroeconomic shifts point to a decrease in coal use by the mid-2020s” (IEA, 2023, p.28). The global natural gas use has increased by an annual average of 2% since 2011 (IEA, 2023). However, it is projected that this growth will slow to less than 0.4% per year until 2030 (IEA, 2023). The main consumers of natural gas are in power generation and building sectors which account for 39% and 21% respectively of the total natural gas demand (IEA, 2023).

According to Xiao et al. (2021), 80% of energy sources globally are obtained from fossil fuels. “Non-renewable energy source like petroleum, natural gas, coal and nuclear energy will continue to dominate the global energy supply” (Gebreyohannes, 2010, p.1). The demand for fossil fuels is still on the rise and the use of this source of energy will continue causing environmental pollution (Yolcan, 2023; IEA, 2023; McKinsey & Company, 2022; Xiao et al., 2021). Several attempts have been made to come up with other sources of energy that are environmentally friendly, but the current situation indicates that fossil fuels lead in global energy supply (IEA, 2023; McKinsey & Company, 2022). Due to the decline in crude oil reserves and the environmental impact associated with the use of petroleum, alternative sources of energy must be found. There has been an increased focus on alternative sources of energy due to the impact of fossil fuel consumption on global warming which results from greenhouse gas (GHG) emissions, the increased energy demand worldwide and the depletion of fossil fuel reserves (Yolcan, 2023; Xiao et al., 2021; Dias et al., 2011).

According to Xiao et al. (2021), one way of reducing the overdependence on fossil fuels is by producing energy from renewable sources such as LGB. Several alternative sources of energy exist which include biofuels such as ethanol which is derived from fermentation of simple sugars (Beluhan et al., 2023). Fuel ethanol is known as bioethanol because it is produced from starch and sugar-based substrates (corn, wheat or sugar) or from LGB through chemical or biological processes (Cheah et al., 2020). According to Beluhan et al. (2023), bioethanol is a suitable alternative to fossil-based fuels because it is considered a renewable, sustainable, environmentally friendly and clean fuel. In addition, it blends easily with gasoline and has a higher-octane number than gasoline which make it suitable for spark ignition engines (Joy et al., 2021). The use of bioethanol contributes to climate change mitigation by curtailing the emission of greenhouse gases (Beluhan et al., 2023). Svetlana et al. (2016) reported that bioethanol is a clean and renewable source of energy with tremendous environmental benefits and is a promising biofuel especially when blended with gasoline. The authors noted that bioethanol can be produced from different kinds of renewable substrates (Svetlana et al., 2016).

1.2 Biofuels

The environmental impact associated with the use of fossil fuels can be addressed by using biofuels (Beluhan et al., 2023). Biofuels are sources of energy that are derived from energy containing substances which originate from plants and animal biomass (Shukla et al., 2023). Biofuels include biodiesel (from oils), bioethanol (from fermentation of sugars), hydrogen and biogas (from anaerobic fermentation of organic substrates). The annual production of biofuels globally increased from 139.4 billion liters in 2016 to 174.9 billion liters in 2022 (Beluhan et al., 2023). The type and source of the biofuel is used to classify them into two categories i.e., primary and secondary biofuels. Biofuels that are

used in raw (unprocessed) form fall under the primary type. They are mainly used for cooking and heating. Examples of primary biofuels include wood chips and pellets, which are mainly by-products of activities such as agriculture (commonly referred to as agri-residues), food processing and deforestation (Khandelwal et al., 2023; Triana, 2016). On the other hand, secondary biofuels are obtained from organic materials through processes such as hydrolysis and fermentation or transesterification. In other words, secondary biofuels are as a result of some form of processing of organic materials. Further, secondary biofuels can either be first generation biofuels (1GB), second generation biofuels (2GB) or third generation biofuels (3GB) (Khandelwal et al., 2023). This classification is based on the source of biomass and the type of technology that is used in production (Khandelwal et al., 2023). 1GB are obtained from food-based biomass feedstocks. Examples include ethanol, also refered to as first generation bioethanol (1GBE), which is obtained from starch and sucrose sources through hydrolysis, fermentation and distillation processes, and biodiesel which is obatined through transesterification of vegetable oil (Beluhan et al., 2023; Khandelwal et al., 2023). 2GB are mainly obtained from inedible plant portions and non-food substrates such as LGB and waste cooking oil (Beluhan et al., 2023; Khandelwal et al., 2023). They include bioethanol which is produced from LGB through hydrolysis, fermentation and distillation processes. Bioethanol produced from LGB is referred to as second generation bioethanol (2GBE). Other examples of 2GB include biohydrogen which can be obtained from fermentation of biomass-derived sugars, biomethane which is produced through anaerobic digestion of biomass and biodiesel which is produced through transesterification of waste cooking oil (Khandelwal et al., 2023; El Bari et al., 2022). 3GB are obtained from microalgae biomass (Khandelwal et al., 2023). According to Khandelwal et al. (2023), algae biomass can be converted to biodiesel, biomethane and

bioethanol. Biodiesel is derived from the intracellular lipids of microalgae (Khandelwal et al., 2023). The lipids are converted to biodiesel through a transesterification reaction between methanol and triacylglycerols. This reaction results in fatty acid methyl esters (FAME) and glycerol. The FAME are purified to biodiesel (Khandelwal et al., 2023). Algae biomass produces biogas when subjected to anaerobic digestion. In addition, Algae biomass can ferment to bioethanol under anaerobic conditions. (Khandelwal et al., 2023).

The production costs for 1GB are significantly lower compared to 2GB and 3GB (Beluhan et al., 2023). For example, the selling price of 1GBE (from sugarcane) was $0.56/L in 2018 compared to 2GBE (from sugarcane bagasse) at $1.33/L (Beluhan et al., 2023). This is attributed to the fact that IGBE production technology has lower capital and production costs due to fewer processing units (Beluhan et al., 2023). In addition, the production of 2GBE require 10–60% more energy than 1GBE (Jarunglumlert and Prommuak, 2021). This is mainly due to the complex nature of the LGB structure, which require energy intensive pretreatment and hydrolysis processes (Jarunglumlert and Prommuak, 2021).

1.3 Biomass

Biomass refers to substances derived from living organisms (plant and animals). According to the United Nations Environment Program [UNEP] (2013), biomass can be used as a source of food, raw materials for building, construction and energy. Biomass is mainly composed of carbon, hydrogen and oxygen (CHO). The use of biomass as a source of energy is preferred over fossil fuels because biomass is renewable in nature while fossil fuels are non-renewable (Beluhan et al., 2023). According to UNEP (2013), biomass derives energy from the sun. Solar energy is used to grow plants through a process called photosynthesis. During the process of

photosynthesis, water (H_2O) and carbon dioxide (CO_2) molecules are broken down in the presence of light forming a carbohydrate molecule known as glucose ($C_6H_{12}O_6$) and oxygen (O_2) (UNEP 2013). This reaction can be represented by Equation 1.1.

$$6CO_2 + 6H_2O + \text{Light} \xrightarrow{\text{Chorophyll}} C_6H_{12}O_6 + 6O_2 \qquad 1.1$$

Biomass is available in many forms including forestry woody substrates, agricultural residues, energy crops, aquatic plants, herbaceous crops, municipal solid waste and animal waste (Shukla et al., 2023; Cheah et al., (2020).

The use of biomass in energy production can contribute to energy security through diversification of energy supply, generate employment opportunities especially in the rural areas which in turn provide additional income further leading to improvements in living standards of the rural communities. In addition, establishment of the biofuel industry contributes to the overall gross domestic product (GDP) of a country. The government is also able to raise more revenue by way of taxes, save on foreign exchange that could have been used to import fossil fuels and participate in environmental protection endeavors by advocating for the use of biofuels.

The current research study deals with bioethanol that is produced from simple sugars derived from LGB. There is a growing need worldwide to find abundant and sustainable substrates that can be used to produce simple sugars which can be fermented to bioethanol. Substrates for simple sugars production can be divided into three major groups: substrates containing sucrose such as table sugar, starchy substrates such as wheat, potatoes, corn and LGB such as wood, straws and grasses (Beluhan et al., 2023; Kumar et al., 2016). Currently the production of simple sugars which can be fermented to bioethanol is almost entirely dependent on starch and sugars from existing food crop substrates such as sucrose, cereals and starch. The main disadvantage of producing

simple sugars from sucrose, cereals or starch is that the substrate tends to be expensive and is also used in other applications such as food supply making such sources unsustainable (Beluhan et al., 2023; Kumar et al., 2016). This leads to supply constraints which result into price increases rendering the final products expensive and contributes to food insecurity (Cheah et al., 2020). Due to the above reasons, alternative substrates such as LGB can be utilized to produce simple sugars (Beluhan et al., 2023). In order to avoid competition with food supply that is being experienced in the production of 1GBE, LGB is considered as an alternative substrate for bioethanol production (Joy et al., 2021). Research on non-food substrates such as LGB as a source of simple sugars for the production of bioethanol and organic chemicals such as citric and lactic acids is attracting great attention worldwide because they are cheap, abundant, sustainable, environmentally friendly and profitable. According to Beluhan et al. (2023), LGB is one of the most important alternative substrates for the production of energy. LGB can be converted into liquid sources of energy such as bioethanol. According to da Silva et al. (2019), LGB has a capacity to generate 161 Exajoules (EJ) of energy annually which can substitute 73% of the annual global oil consumption. Bioethanol is produced through fermentation of simple sugars derived from LGB (Beluhan et al., 2023). The initial stages of this process involve pretreatment and hydrolysis of cellulose and hemicellulose polymers found in LGB using chemicals such as acids or enzymes (Shukla et al., 2023). Hydrolysis of cellulose and hemicellulose gives rise to glucose and xylose sugars respectively. Using microorganisms such as *Saccharomyces cerevisiae*, *Escherichia coli* and *Trichoderma reesei*, fermentation of these sugars can be carried out to obtain bioethanol (Salimi et al., 2017).

In order to produce 2GBE for commercial purposes, large-scale processing plants are required. Commercialization of 2GBE production requires the design of large-scale

processes involving pretreatment, hydrolysis, fermentation, product recovery, purification and dehydration (Humbird et al., 2011). In addition, techno-economic analysis of the entire process is required in order to establish the techno-economic viability of the process (da Silva et al., 2019).

Process design plays an important role in developing a cost-effective method of large-scale production of 2GBE by analyzing different process technologies/configurations and parameters (Humbird et al., 2011). According to Jarunglumlert and Prommuak (2021), laboratory research can be scaled to commercial production through techno-economic analysis. In order to evaluate the techno-economic feasibility of large-scale 2GBE production process, it is important to assess the efficiency of all the process steps involved in the entire production system (pretreatment, hydrolysis/saccharification, fermentation, distillation and dehydration). Assessing the efficiency of the above processes by conducting experiments in a laboratory set-up requires huge resources in terms of costs and time. It is therefore necessary to devise a better tool of evaluating the techno-economic performance of the 2GBE production process without conducting laboratory experiments.

There is a lot of data on experiments involving pretreatment, hydrolysis and fermentation process steps involved in the production of 2GBE (Beluhan et al., 2023; Gebreyohannes, 2010). However, this data does not reveal much about the techno-economic viability of the process steps involved in the production of 2GBE on a large-scale. In addition, experimental data cannot be relied upon to make accurate decisions when selecting 2GBE production technologies/routes that are optimal from techno-economic point of view (Gebreyohannes, 2010). However, the experimental data can be used to design large-scale processes for producing 2GBE (Gebreyohannes, 2010).

This can be achieved by studying all steps involved in the production of 2GBE simultaneously (in a manner similar to real commercial plant). What is required is combining of experimental data, different 2GBE production technologies that are currently available and accurate cost estimates data in order to model, simulate and optimize 2GBE production processes while selecting the optimal route which gives the Minimum Bioethanol Selling Price (MBSP) (Humbird et al., 2011). In addition, there are many possible technological routes of producing 2GBE that it is difficult to evaluate them techno-economically in terms of varying capacity, varying feedstock composition and varying process parameters (Gebreyohannes, 2010). The successful development of a large-scale 2GBE production facility depends on proper selection of a technology that will ensure the highest yield of bioethanol and most cost-effective performance (Humbird et al., 2011).

Process modeling and simulation is a convenient way of evaluating the techno-economic performance of a 2GBE production process. In this approach, a model of the process of producing 2GBE on a large-scale is designed and simulated using computer software. Different models are designed to represent the different types of technologies/configurations of producing 2GBE that need to be evaluated. The models are simulated under varying parameters and the results of the simulation are analyzed, compared and the optimum design is selected for further evaluation and possible commercialization (Aspen Plus, 2000).

The Advanced System for Process Engineering (ASPEN Plus) is a computer modeling and simulation software (Aspen Plus, 2000). Aspen Plus is a tool that can be used to analyze a large-scale 2GBE production plant. Finally, there is a lot of information in literature concerning the production of ethanol (Humbird et al., 2011). Data on

stoichiometry and conversion of LGB to simple sugars (glucose and xylose) and subsequent fermentation of these sugars to bioethanol is well established and available in literature (Humbird et al., 2011). This data can be used in the simulation of process models for producing 2GBE on a large-scale (Humbird et al., 2011).

1.4 Lignocellulosic Biomass

Lignocellulosic biomass (LGB) refers to plant biomass consisting of cellulose, hemicellulose and lignin (Shukla et al., 2023). LGB is a renewable, sustainable and environmentally friendly energy source with the potential to improve the economy and energy security in many countries (Cheah et al., (2020). Despite the major interest in the production of bioethanol from LGB, several challenges exist. The main challenges include multistage production process, high costs associated with pretreatment, hydrolysis, fermentation and distillation processes (Shukla et al., 2023; Cheah et al., 2020), formation of inhibitors (especially furfural, hydroxymethylfurfural (HMF) and weak acids) during pretreatment, insufficient yield of simple sugars and bioethanol during hydrolysis and fermentation respectively and large amount of solid and liquid wastes which poses a threat to the environment and presents additional cost in an attempt to manage these wastes (Triana, 2016; Kumar et al., 2016; Janga et al., 2012; Humbird et al., 2011). Obtaining simple sugars from LGB is hindered to a greater extent by the recalcitrant nature of LGB (Janga et al., 2012). This limits the yield of simple sugars and makes the overall process of producing bioethanol from LGB costly (Janga et al., 2012). According to Muktham et al. (2016), efficient conversion of LGB to bioethanol is currently an active research area. Whereas 1GBE is commercially established, it is not sustainable as food crops are used as substrate (Beluhan et al., 2023). On the other hand, 2GBE production is not fully commercialized but can be produced from sustainable (non-food crop) substrates (Jarunglumlert and Prommuak,

2021). According to Ioelovich (2015), the cost of producing bioethanol from LGB can be reduced by co- producing valuable by-products from solid and liquid wastes associated with the production of bioethanol. Svetlana et al. (2016) reported that there is a lot of documented information about 1GBE while 2GBE requires further research in order to bring down the cost of production so as to make the entire process economically viable.

In order to obtain simple sugars from LGB, some form of pretreatment and hydrolysis is required prior to fermentation (Cheah et al., 2020). According to Shukla et al., (2023), pretreatment of LGB is required in order to decrystallize the recalcitrant LGB. Cheah et al. (2020) reported that pretreatment is normally done to disrupt and disintegrate the lignin and break down the hemicellulose portion of LGB. In addition, pretreatment removes inorganic salts and amorphous cellulose found in LGB. The yield of glucose from cellulose together with minimum decomposition of glucose to HMF are highly dependent upon the type of LGB, the composition of LGB and the process conditions (Janga et al., 2012). Therefore, each LGB should be studied independently in order to optimize and select suitable process conditions for maximum yield of simple sugars during pretreatment and hydrolysis. Mezule et al. (2015) asserted that optimization of processes involved in the production of bioethanol from LGB can increase the quantity of fermentable sugars and reduce the production costs which in turn will support full commercialization of 2GBE production.

1.5 The Problem Statement

Biofuels such as bioethanol are increasingly being used as sources of energy as the world economy tends to substitute fossil fuels due to global warming and declining supplies. However, large-scale production of 2GBE faces technological and economic

feasibility challenges due to insufficient data. Such data can be obtained from experiments and/or pilot and demonstration plants. However, performing experiments or setting up pilot and demonstration plants in order to obtain techno-economic data on large-scale 2GBE production is cumbersome, time consuming and expensive in terms of the required resources. Computer software such as Aspen Plus can be used to model and simulate a large-scale 2GBE production process. Using data from Aspen Plus, economic analysis of the entire process can be carried out using suitable economic models such as the discounted cash flow rate of return (DCFROR) or the net present value (NPV). This research seeks to model and simulate a large-scale process of producing 2GBE from Sila sorghum stalks (SSS) and maize cobs found in Kenya using Aspen Plus. In addition, the research seeks to establish optimum hydrolysis conditions and kinetic parameters of concentrated sulphuric acid hydrolysis of Sila sorghum stalks and maize cobs found in Kenya.

1.6 The Objectives of the Research

1.6.1 General Objective

The main objective of this research is to model and simulate a large-scale bioethanol production process from Sila sorghum stalks and maize cobs.

1.6.2 Specific Objectives

The specific objectives are to;

1) Select the most suitable pretreatment, hydrolysis and fermentation technology in terms of bioethanol production rate, energy demand and energy intensity.
2) Simulate a full-scale model of producing bioethanol.
3) Determine the effects of varying the flowrate of LGB, conversion of cellulose to glucose in the simultaneous saccharification and co-fermentation (SSCF) reactor,

cost of LGB and enzymes, plant life, fixed capital investment (FCI), discount rate and income tax rate on the economic viability of large-scale bioethanol production in Kenya.

4) Hydrolyse SSS and maize cobs using concentrated sulphuric acid and identify conditions for optimal yield of fermentable sugars.
5) Develop kinetic models for glucose production and establish kinetic constants and kinetic parameters for glucose formation and degradation during concentrated sulphuric acid hydrolysis of SSS and maize cobs.

1.7 Scope of the Study

The current research study focused on characterization, modeling and simulation of large-scale bioethanol production from SSS and maize cobs, hydrolysis and kinetic study of concentrated sulphuric acid hydrolysis of SSS and maize cobs. SSS were obtained from Bungoma County while maize cobs were obtained from Nakuru County. The study included literature review, laboratory experimentation, Aspen Plus and Design-Expert 13 software application.

1.8 Justification of the Study

According to the Ministry of Energy [MOE] (2018), some of the main challenges facing biofuels production in Kenya include limited research data/information for the use and sustainable production of biofuels, inadequate research and development on alternative biofuel feed-stocks and technologies and the lack of efficient technologies for production, conversion and consumption of biomass energy (MOE, 2018). The production of alternative sources of energy such as 2GBE need to be fully commercialized so as to substitute fossil fuels whose supply is declining and are known to contribute to global warming (Lugani et al., 2020). The development of cost-effective

methods of producing 2GBE relies on process design which enables the analysis and selection of available process parameters and production technologies (Humbird et al., 2011). The use of experiments is unrealistic, time and resource consuming in selecting and analyzing the suitability of a large-scale 2GBE production process (Gebreyohannes, 2010). The use of computer software can address this challenge since it is possible to model and simulate different large-scale 2GBE production technologies/routes and select the most economically viable in an efficient and less costly manner (Gebreyohannes, 2010). The use of SSS and maize cobs (agri-wastes) in the production of bioethanol contributes significantly in reducing the use of fossil fuels, environmental pollution and over reliance on food-based substrates to produce bioethanol (Xiao et al., 2021; Lugani et al., 2020). Since the proposed substrates are wastes, their use will help reduce land and air pollution in cases where these wastes are dumped in landfills or burnt during land preparation (Shukla et al., 2023). Despite the wide interests in the production of bioethanol from agricultural residues, no study has been done in Kenya regarding the techno-economic viability of producing 2GBE from SSS and maize cobs. In order to deconstruct the LGB, chemicals especially acids are used. The main challenge is the low yield of simple sugars realized during acid hydrolysis of LGB, which is mainly caused by disintegration of the resulting simple sugars into inhibitors such as furfural (from xylose) and HMF (from glucose). This problem can be addressed by optimizing the hydrolysis process.

1.9 Sorghum

Sorghum (Sorghum bicolor *(L.*) *Moench*) belongs to the grass family Poaceae, tribe *Andropogoneae*, and subtribe *Sorghinae* (Xiao et al., 2021). Sorghum is categorized into four main varieties that include grain sorghum, sweet sorghum, forage sorghum and fiber sorghum (Hu et al., 2022). Sila sorghum, also known as Gadam sorghum, is

a new variety of sorghum (Agfax On-line, 2011). Sila sorghum was introduced in Kenya within Bungoma, Siaya, Kitui, Makueni, Tharaka Nithi and Machakos Counties (Mailu & Mulinge, 2016). The major features that distinguish it from the usual varieties of sorghum include drought resistance, fast growing and high yielding variety (Agfax On-line, 2011). The production of Sila sorghum is being promoted by various operators through a Public-Private-Partnership (PPP) formed by the Ministry of Agriculture (MOA), Kenya Agricultural and Livestock Research Organization (KALRO), the provincial administration, Smart Logistics Ltd, Equity Bank and East African Breweries Limited (EABL) (Mailu & Mulinge, 2016). Sila sorghum grain is a promising raw material for beer manufacture due to its high carbohydrate content. Samples analysed by EABL revealed that Sila sorghum contained 75% carbohydrates, compared to 67% and 66% in barley and maize respectively, making Sila sorghum a good source of fermentable sugars (Mailu & Mulinge, 2016).

EABL introduced Senator Keg into the local market in 2003 (East African Breweries Limited [EABL], 2014). Senator keg is a sorghum based alcoholic drink that is cheaper than barley-based beer (EABL, 2014). Senator keg targets the low-income consumers because it is cheaper and a safe alternative to illicit liquors while at the same time giving farmers a reliable source of income through the supply of Sila sorghum grain to EABL (EABL, 2014). Due to this development, EABL intends to substitute barley with Sila sorghum grain in beer production (Agfax On-line, 2011). EABL stated in a press briefing that it will require 12 million kilograms of Sila sorghum grain for beer production in 2011 (New Agriculturist On-line, 2011). According to Standard Newspaper On-line (2014), EABL has increased the use of Sila sorghum in beer production. To this end, it has brought on board farmers from Tharaka Nithi County, a region estimated to produce 7,000 tonnes of Sila sorghum grain per season. EABL has

a capacity of 60,000 metric tonnes of sorghum grain (Njagi et al., 2019). According to Hu and Chen (2022), the sorghum plant has a potential yield of 60,000 kg/hectare of sorghum stalks and 2250 to 6000 kg/hectare of sorghum grain. According to Roziafanto et al. (2023), mature sorghum plant consists of 15% grain, 10% leaves and 75% stalks by weight. It is projected that Sila sorghum grain will eventually substitute barley in beer making, thus ensuring sustainable supply of sorghum stalks.

1.10 Maize Plant

Maize (corn) also referred to as *Zea mays L*. is a plant (grass) that grows to a height of 2 to 5 m depending on the variety (Australian Government, 2008). The genus *Zea* is a Greek word, *Zea* meaning cereal or grain which belongs to the tribe *Andropogoneae* in the subfamily *Panicoideae* in the family *Poaceae* (Australian Government, 2008). There are five main species of maize namely: *Zea mays L., Zea diploperennis, Zea perennis, Zea luxurians* and *Zea nicaraguensis*. *Zea mays L*. is the only cultivated species while the rest species are wild grasses commonly referred to as teosintes (Australian Government, 2008). The main parts of the plant include the tassel, stalk, leaves, grain and cobs (Miya, 2015). Maize was first introduced in Kenya in the sixteenth century by the Portuguese (Tarus, 2019). Initially, the cultivation of maize was concentrated within the coastal regions of Kenya (Tarus, 2019). It was the European settlers who later started growing maize in other parts of the country (Tarus, 2019). Data from the MOA indicated that maize accounted for more than 51% of all the staple food grown in Kenya in the year 2011 (Tarus, 2019). Kenya's per capita maize consumption is estimated at 103 kg/person/year (Tarus, 2019). The current maize yield is estimated at 1622 kg/ha, with average production of nearly 3.5 million tonnes annually (Tarus, 2019). Maize is cultivated for domestic consumption and commercial purposes, with small-scale farmers selling an estimated 20% of their produce (Tarus,

2019). During harvesting, husks are removed leaving the grain on the cob, which is then shelled to give about 80% grain and 20% cob by weight (Tandzi and Mutengwa 2019). Maize cobs are agricultural residues found in plenty in many parts of Kenya. In most cases, maize cobs are used as sources of energy without any processing. This leads to environmental pollution and a reduction in its economic value.

1.11 Significance of the Study

This research will have the following benefits to the current and future generations: it will lead to the generation of techno-economic data on large-scale production of 2GBE from SSS and maize cobs found in Kenya. Optimization of hydrolysis conditions will improve the yield of simple sugars which in turn will lead to cost reductions during 2GBE production. In addition, the study will generate data on the suitability of sorghum stalks and maize cobs found in Kenya as alternative, low cost, renewable and sustainable sources of energy. The use of alternative non-food substrates such as sorghum stalks and maize cobs to produce biofuels will address the high cost of food-based substrates such as corn and sucrose which are currently used to produce bioethanol. With the current global focus being on the reduction in greenhouse gases that cause global warming, this research provides a solution to these problems by offering alternative raw material for large-scale production of alternative sources of energy such as bioethanol which will go a long way in mitigating global warming. Finally, the study will provide a database of information for future researchers.

1.12 Outline of the Research

This research comprises of five chapters. It covers the introduction, literature review, experimental materials, equipment and procedures, results and discussion, conclusion and recommendations. Chapter one presents the background information about the

study, world energy consumption, biofuels and policies related to biofuels in Kenya. It further points out the problem statement, research objectives, scope, justification and significance of the study. Chapter two reviews the existing literature on hydrolysis and kinetic studies of LGB, techno-economic studies on largescale bioethanol production plants, sources of biomass, classification of biomass, pretreatment of biomass, fermentation and bioethanol purification technologies, process modelling and simulation, economics of bioethanol production process, reaction kinetics, kinetics of glucose production from LGB, process optimization and statistical analysis. Chapter three reports on various research equipment, chemicals/reagents, modeling and simulation, experimental and statistical procedures employed in this research. Chapter four presents results, analyses, and discussions of various research findings. Finally, chapter five gives the overall conclusion and recommendations arising from this study.

CHAPTER TWO: LITERATURE REVIEW

2.1 Review of Previous Research

2.1.1 Simple sugars

Simple sugars are the smallest sugar monomers that form the basic unit of LGB. Simple sugars include glucose and xylose that can be fermented to bioethanol using suitable microorganisms such as *Saccharomyces cerevisiae*, *Escherichia coli* and *Trichoderma reesei*. LGB include agricultural, food processing and municipal wastes, perennial grasses and woody biomass (Cheah et al., 2020). LGB consists of cellulose, hemicellulose and lignin (Cheah et al., 2020). To convert LGB to simple sugars, several steps including pretreatment and saccharification/hydrolysis are necessary. The aim of pretreatment is to free cellulose from lignin and hemicellulose in order to facilitate disintegration of LGB to simple sugars during a process known as hydrolysis (Lugani et al., 2020). Pretreatment methods normally use chemical, physical, mechanical or biological techniques to disintegrate LGB (Cheah et al., 2020). Normally, an effective pretreatment should disintegrate the LGB effectively so as to allow for maximum hydrolysis of both the cellulose and hemicellulose to glucose and xylose respectively (Hu et al., 2008).

Cellulose is a polymer consisting of six carbon sugars (C6). The structure of cellulose consists of a crystalline and amorphous lattice that is made up of glucose monomers. This crystallinity hinders the disintegration of cellulose to glucose. However, when pretreated and hydrolyzed, cellulose disintegrates into glucose that can be fermented into bioethanol using yeast. Hemicellulose is a polymer consisting of five carbon sugars (C5) and can be broken down to individual sugars such as xylose and arabinose (Beluhan et al., 2023). On the other hand, Lignin consists of phenols which are not fermentable, but can be recovered after hydrolysis and fermentation for use as a source

of energy through combustion in steam boilers (Humbird et al., 2011).

Hydrolysis of LGB is a key process step in the production of 2GBE. During this process, cellulose and hemicellulose are broken down into simple sugars. This process can be carried out using chemicals (mainly acids) or enzymes (biological hydrolysis) (Legodi et al., 2021).

2.1.2 Previous research on hydrolysis and kinetic studies of LGB

Several studies concerning bioethanol production from LGB have been reported in literature. Wyman (1994) did a review on bioethanol production. This review looked at the various steps involved in the production of bioethanol. The author asserted that current research in bioethanol is being driven by the need to reduce the cost of production. The author indicated that improvement in feedstock selection, use of low-cost substrates with high content of carbohydrate fraction, improving the overall yield of cellulose hydrolysis and shortening of fermentation time could be the basis of bringing down bioethanol production costs (Wyman, 1994). In addition, integration of the process into an existing plant, or recovery of higher value lignin co-products could lower the projected price of bioethanol due to additional revenues realized from the sale of such co-products (Wyman, 1994).

Camacho et al. (1996) studied the effects of temperature and concentration of sulphuric acid on the solubilization rate of microcrystalline cellulose (MCC) (pure form of cellulose) and on the rate of glucose production. Temperature levels investigated were 25, 30, 35 and 40°C, sulphuric acid concentrations were varied from 31% to 70% (weight by volume, w/v) and the solid to liquid ratio (SLR) was set at 1.0, 1.5, 2.0, 3.0, 4-0 and 5.0 cm^3 of acid per gram of substrate. The authors concluded that cellulose hydrolysis using concentrated sulphuric acid at room temperature gave total

solubilization of cellulose and appreciable glucose yields (Camacho et al., 1996). The major shortcoming in this study was the use of pure cellulose as substrate instead of real LGB.

Research on hydrolysis of LGB to simple sugars and fermentation of these sugars to bioethanol started in Finland in 1970 (Shawn et al., 2003). The energy crisis experienced in 1973 contributed to further research on hydrolysis of LGB using enzymes.

Roberto et al. (2003) studied the dilute acid hydrolysis of rice straw and reported that for maximum hydrolysis efficiency, the best conditions were 1.0 % (w/v) sulphuric acid (H_2SO_4) concentration, 27 minutes of reaction time at a temperature of 121^oC.

Sanchez et al. (2004) carried out a two-stage acid hydrolysis of Bolivian straw. In the first stage, the straw was pretreated with steam followed by dilute sulphuric acid hydrolysis using 0.5 - 1.0 % (weight by weight, w/w) acid concentration while the hydrolysis temperature was 170 - 230^oC for a time period of 3 - 10 minutes. Results of the first stage revealed that the highest sugar yield was realized at 190^oC and 5–10 minutes (Sanchez et al., 2004). In order to hydrolyze the remaining cellulose fraction during the second stage hydrolysis reaction, 230^oC was found to be suitable (Sanchez et al., 2004).

Rahman et al. (2006) studied the production of xylose from oil palm waste using H_2SO_4. They reported that the optimum conditions were 6.0 % (w/v) H_2SO_4 concentration, 120^oC and 15 minutes of reaction time which resulted in 29.4 g/L xylose concentration.

Ming et al. (2007) investigated the enzymatic saccharification of corncob and fermentation of simple sugars obtained to bioethanol. The authors pretreated the

substrate using H_2SO_4 and hydrolyzed the resulting residue using cellulases realizing simple sugars yield of 67.5% by weight. During the study, they reported that poor activity of cellobiase lead to product inhibition due to cellobiose accumulation. They supplemented cellobiase and the yield improved to 83.9% by weight (Ming et al., 2007).

Sarrouh et al. (2007) did a study on hydrolysis of bagasse using 70%, (w/w) sulphuric acid solution. During the study, the reaction temperature was set at between 30^oC and 70^oC. At various time intervals between 10 and 90 minutes, a sample was taken from the reaction medium and analysed for fermentable sugars. The authors reported that the yield of fermentable sugars increased as temperature increased up to 50^oC. The maximum reported yield of fermentable sugars was 87.6% (w/w) which was obtained at 60 minutes and a temperature of 50^oC (Sarrouh et al., 2007). This was followed by a decrease in the yield of fermentable sugars (to 86.4%, w/w) when the reaction was carried on after one hour (Sarrouh et al., 2007).

Akpinar et al. (2009) studied acid hydrolysis of sunflower and tobacco stalks. They reported that the optimized parameters for the hydrolysis of sunflower and tobacco stalks were a temperature of 120^oC, 30 minutes of reaction time and 4 % (w/v) acid concentration and a temperature of 133^oC, 27 minutes of reaction time and 4.9 % (w/v) acid concentration respectively.

During their study, Rodrigues et al. (2010) obtained 74 % (w/w) yield of xylose when they hydrolyzed sugarcane bagasse (SCB) at a temperature of 130^oC for 10 minutes using 100 mg of H_2SO_4 per gram of SCB.

Chu et al. (2011) did a study on cotton cellulose hydrolysis using concentrated sulphuric acid. The range of acid and solid concentration was 45 - 60% (volume by volume, v/v) and 30 - 70 g/L respectively. In addition, the reaction temperature was set at 27 – 50^oC.

The authors reported that at an acid concentration of 55%, (v/v), reaction temperature of 40^{o}C, initial cotton cellulose concentration of 70 g/L and 90 minutes of hydrolysis, the yield of reducing sugars was 73.9 % (w/w). Further experiments were done to establish the activation energy and pre-exponential factor for cellulose hydrolysis using concentrated sulphuric acid. The authors reported that the activation energy and the pre-exponential factor were 98.98 kJ/mol and 2.36 x 10^{15}/min respectively.

Jeevan et al. (2011) studied optimization of acid hydrolysis of corn cob hemicellulosic hydrolysate for microbial production of xylitol. The authors used dilute sulfuric acid as a catalyst. In the study, the effect of four parameters (SLR, acid concentration, reaction temperature and time) on the production of simple sugars (xylose, glucose and arabinose) and fermentation inhibitors (furfural, HMF and acetic acid) were studied during hydrolysis of the hemicellulose fraction of corn cob (Jeevan et al.,2011). From the results, the optimal conditions for the recovery of xylose were: sulfuric acid concentration of 1.5% (w/v), reaction temperature of 130^{o}C, reaction time of 20 min and a SLR of 1:10 (Jeevan et al.,2011). However, the study did not establish optimum conditions for glucose production.

According to Chandel et al. (2012), most researchers have reported that mild temperature leads to substantial recovery of fermentable sugars during acid hydrolysis of LGB, while higher temperatures cause more sugar degradation, contributing to the formation of fermentation inhibitors which leads to lower bioethanol yields (Chandel et al., 2012).

Janga et al. (2012) did a study of the influence of acid concentration, temperature and time on decrystallization of cellulose in a two - stage concentrated sulphuric acid hydrolysis of pine wood and aspen wood. The optimum predicted yield of total sugars

obtained during the study were 74% (w/w) and 91% (w/w) for aspen wood and pine wood respectively (Janga et al., 2012). The authors reported that the most influential variables on total sugar yield were acid concentration and temperature. The authors further reported that the formation of sugar degradation products such as HMF was mostly influenced by the reaction temperature.

Esther et al. (2012) studied the production of xylose from wheat straw. The concentration of H_2SO_4 used was varied between 1.0 -5.0 % w/w while the temperature was 130^oC. The results revealed that 99% of hemicellulose and 11% glucan were hydrolysed to xylose and glucose respectively (Esther et al., 2012). Optimal conditions for xylose production were established as 2% (w/w) H_2SO_4 concentration at a temperature of 130^oC for 29 min. During this study, the authors did not establish optimum conditions for glucose production.

Ioelovich (2012) reported that treating cellulose with 50% - 60% (w/v) sulphuric acid solution at room temperature gave rise to a reduction in crystallinity of cellulose by 25% - 30%. The solubility of the resulting cellulose increased while the polymerization degree decreased (Ioelovich, 2012). This study indicated that sulphuric acid has the potential of hydrolyzing LGB to simple sugars.

During their study on saccharification of LGB for biofuel production, Moe et al. (2012) reported that a two-stage concentrated sulphuric acid hydrolysis of soft wood gave rise to good sugar yields and a low concentration of fermentation inhibitors.

Liu et al. (2012) studied kinetic model analysis of dilute H_2SO_4 catalyzed hemicellulose hydrolysis of sweet sorghum bagasse (SSB) for xylose production. The concentration of H_2SO_4 used was 3% (w/w) and the SLR was 1:10 by mass (Liu et al., 2012). The temperature was varied from 110 to 150^oC (Liu et al., 2012). The results indicated that

elevated reaction temperatures promoted the hydrolysis of hemicellulose into xylose and the degradation of xylose into furfural (Liu et al., 2012). The xylose yield increased in proportion to reaction time in the initial stages and then declined due to the degradation of xylose to furfural (Liu et al., 2012). The pre-exponential factors for the 'easy-to-hydrolyze' fraction, the 'hard-to-hydrolyze' fraction of hemicellulose and xylose degradation were 3.53×10^6, 1.80×10^5 and 0.62/min, respectively, while the activation energies were 60.7, 58.1 and 14.5 kJ/mol, respectively. The ideal hydrolysis condition for xylose production was 140^{o}C for 50 min, under which the xylose yield reached 60% of hemicellulose weight. In addition, the authors reported that the hydrolysis of cellulose to glucose was not significant under the reaction conditions since the yield of glucose did not exceed 6.0% by weight of hemicellulose. The source of this glucose was hemicellulose heteropolymers (Liu et al., 2012).

Ali et al. (2014) studied the saccharification of corn cobs using H_2SO_4 for the production of monomeric sugars. Two types of corn cobs (red and white corn cobs) were investigated. The corn cobs were delignified using 1% (w/w) sodium hydroxide (NaOH) followed by hydrolysis using H_2SO_4 in different proportion (5, 10 and 15%). The results from this study revealed that the maximum yield of sugars from red and white cobs was 49.51% (w/w) and 43.08% (w/w) respectively, which was obtained after 90 minutes and at 10% (w/w) acid strength.

Wijaya et al. (2014) did a study on the effect of acid concentration (65-80%, w/w), hydrolysis temperature (80^{o}C-100^{o}C) and time (2 hours) on sugar recovery for different biomass species (oak wood, pine wood and empty fruit bunch (EFB) of palm oil). Under optimized conditions, the range of theoretically extractable sugars was 78-96% (w/w) for the three biomass species (Wijaya et al., 2014). The authors further reported that the

hydrolysis reaction time affected the concentration of sugar at higher temperature (100^{o}C) because extending the hydrolysis reaction time decreased the overall sugar yield at this temperature due to the degradation of sugars into fermentation inhibitors.

Zhu et al. (2014) carried out acid hydrolysis of maize cobs to produce xylose using formic acid under varying concentration (2.0% - 6.0%, w/w), time (30-150 min), reaction temperature (120-160 ^{o}C), and SLR (3-11 mL/g). The results of the study indicated that the optimal yield of xylose was 81.6% (w/w) which was achieved at 5.0% (w/w) acid concentration, 150 min, 135^{o}C and SLR of 1:7 (Zhu et al., 2014). However, during this study, the authors did not consider optimization of glucose production.

According to a study by Kumar et al. (2015), acid hydrolysis of bagasse can be described by a first-order, two-step consecutive reaction model, where the polysaccharides first undergo hydrolysis into monomers and thereafter, degrade into various products in the second step.

Kanchanalai et al. (2016) carried out kinetic studies of concentrated acid hydrolysis of microcrystalline cellulose (MCC), which is a pure form of cellulose (Avicel) and xylan, the major component in hemicellulose. The concentration of sulphuric acid used was varied (10% to 50%, w/w) while temperature was varied (80 to 100^{o}C) (Kanchanalai et al., 2016). The authors reported that the amount of glucose increased as the concentration of acid and hydrolysis time increased. However, there was a decline in glucose concentration as the hydrolysis time increased past 120 minutes, mainly due to the decomposition of glucose. On the other hand, there was a notable decrease in glucose concentration at constant acid concentration (40%, w/v) as temperature and time increased (Kanchanalai et al., 2016). The major shortcoming in this study was the use of pure cellulose and xylan as substrates instead of real LGB.

Puttaswamy et.al (2016) studied the production of bioethanol from different biomass resources (bagasse, wheat straw, rice straw, ragi straw and water hyacinth). The results of this study indicated that the highest amount of bioethanol was obtained from bagasse at 11.90 g/L on the 6^{th} day which also coincided with the highest release of TRS during saccharification of bagasse followed by wheat straw at 9.56 g/L, rice straw at 8.84 g/L, and ragi straw at 7.01 g/L. The least amount of bioethanol was produced from water hyacinth at 6.19 g/L (Puttaswamy et.al, 2016). The authors concluded that renewable LGB such as bagasse, wheat straw, water hyacinth, rice straw, and ragi straw can be used as a potential source of simple sugars for the production of bioethanol.

Rasmey et al. (2017) studied chemical pretreatment and saccharification of SCB into simple sugars for bioethanol production through fermentation using *Saccharomyces cerevisiae*. Saccharification of pretreated biomass was achieved using crude cellulase extracted from *Trichoderma harzianum*. The highest bioethanol concentration (1.34%, w/v) was obtained after a fermentation period of 48 hours with a fermentation efficiency of 51.81% (w/w) and a volumetric productivity 0.275 $gl^{-1}h^{-1}$ (Rasmey et al., 2017). The main challenge was the high cost of enzymes used in the hydrolysis step.

Chang et al. (2018) did a study on two step acid hydrolysis of pronghorn spring triticale straws with the aim of establishing the best conditions for maximum glucose yield. During the first stage, the straws were treated with H_2SO_4 (62 – 82%, w/w) at 30^oC for 2 hours followed by partial neutralization using 20- 40% (w/w) NaOH and 29% (w/w) aqueous ammonia. The second stage involved treatment at 97 - 121^oC for 3 hours. The authors established that the optimal conditions were 72% (w/w) H_2SO_4 concentration at 30^oC for 2 hours for the first stage, neutralization using 20% (w/w) NaOH and 121^oC

for 10 minutes in the second stage. The maximum glucose yield obtained under the optimal conditions was 88% (w/w).

Kim (2018) realized 90.9% (w/w) glucose yield efficiency from soybean straw pretreated using NaOH and hydrolysed using enzyme cellulase at 42^{o}C and 48 hours hydrolysis period. The main drawback in this study was the use of costly enzymes in the hydrolysis reaction.

Tizazu and Moholkar (2018) investigated kinetic and thermodynamic features of dilute acid hydrolysis of SCB. Hydrolysis of SCB was carried out using 2% (v/v) H_2SO_4 at temperatures of between 100°C - 130°C and reaction time of between 5 - 120 min at a SLR of 1:30. The authors reported that activation energies for hydrolysis of hemicellulose to xylose and degradation of xylose were 60.3 and 83.4 kJ/mol respectively. They further reported that the optimum hydrolysis conditions were temperature (120^{o}C) and time (30 min) while the yield of xylose was 0.76 g/g hemicellulose. However, the study did not consider hydrolysis of cellulose to glucose.

Rusanen et al. (2019) obtained 62% (w/w) hemicellulose sugars from pine sawdust hydrolysed using a mixture of 0.5% (w/w) H_2SO_4 and 5.5-10% (w/w) formic acid at 120^{o}C for 2 hours. The authors studied the influence of acid type and concentration, time and reaction temperature on sugar yield. The authors concluded that by using a mixture of acids, the concentration of a single acid could be reduced significantly.

Kolo et al. (2020) obtained 66.57% (w/w) saccharification efficiency from microwave - assisted sodium hydroxide pretreatment and H_2SO_4 hydrolysis of elephant grass (biomass). Hydrolysis was performed at 2% (w/w) H_2SO_4 concentration, 95^{o}C and 30 minutes reaction time.

Suryadi et al. (2020) did a study on oxalic acid hydrolysis of hemicellulose found in oil palm empty fruit bunch for xylose production. The aim was to establish the best hydrolysis conditions by varying temperature (95^{o}C - 135^{o}C), hydrolysis time (10 - 110 minutes) and concentration of oxalic acid (1% - 7% (w/v). The authors reported that the optimal hydrolysis conditions were 121^{o}C, 85 minutes and 4% (w/v) oxalic acid concentration. Under optimized conditions, 93.8% (w/w) xylose recovery was realized.

Swiatek et al. (2020) carried out hydrolysis reactions involving beech wood, spruce wood and *Miscanthus x giganteus* in a semi-continuous plant using 0.05 moles per litre (mol/L) dilute H_2SO_4 solution for 40 minutes. The aim was to establish the time dependent formation of fermentable sugars (glucose, xylose and mannose) and fermentation inhibitors (HMF, furfural, acetic acid and formic acid). The authors used three different temperatures (180, 200 and 220^{o}C) to investigate the influence of hydrolysis temperature on the formation of sugar monomers and inhibitors. The authors observed that there was a sharp increase in the concentration of sugars monomers during the initial stages of the reaction. In addition, increasing the temperature and reaction time led to the formation of inhibitors. The authors concluded that optimization of hydrolysis conditions to maximize the desired products is essential for efficient use of LGB.

Zhang et al. (2020) studied dilute H_2SO_4 hydrolysis of hemicelluloses found in rice husk for xylose production by varying reaction temperature, time and acid concentration. Optimum hydrolysis conditions obtained were 4.0% (w/w) acid concentration, 25 minutes hydrolysis reaction time and 150^{o}C. The optimal yield of xylose was 32.96% (w/w). However, the study did not consider hydrolysis of cellulose found in rice husk.

Beckendorff et al. (2021) did a study on optimization of corn cob and beech wood xylan hydrolysis for xylose production using H_2SO_4. The aim was to find optimal hydrolysis conditions for maximum yield of xylose. The maximum yield of xylose was 77.3% (w/w) and 65.1% (w/w) from corn cob and beech wood xylan respectively. Optimal hydrolysis conditions were 100^oC, 2.0% (w/w) H_2SO_4 concentration and 120 minutes hydrolysis period for both substrates. However, the study did not consider hydrolysis of cellulose.

Legodi et al. (2021) obtained 86.7% (w/w) hydrolysis efficiency from enzymatic hydrolysis of liquid hot water (LHW) pretreated banana pseudostem (BPS). The authors performed the hydrolysis reaction at 50^oC for 76 hours. In this study, the major shortcoming was the long hydrolysis reaction period. The authors recommended that optimization of the whole process was necessary.

Lu et al. (2021) reported that 74.75% (w/w) xylose was obtained from hydrolysis of *Miscanthus sacchariflorus* using 0.3% (w/w) H_2SO_4 at 180^oC for 10 minutes. In addition, the authors reported that the yield of xylose and inhibitors (furfural, HMF and acetic acid) depends on the temperature, reaction time and acid concentration. The total sugar (xylose, glucose and arabinose) recovered was 85.5% (w/w), which was obtained using 1.76% (w/w) H_2SO_4 at 152.6^oC for 21 minutes.

Nasohaa et al. (2023) optimized conditions for pineapple peel biomass hydrolysis for xylose production using nitric acid (HNO_3). The authors varied temperature (80-130^oC), time (5-50 minutes) and acid concentration (0.5-7%, w/w). Optimum xylose yield (85%, w/w) was obtained under 105^oC, 20 minutes reaction time and 5% (w/w) acid concentration. However, the study did not consider hydrolysis of cellulose found in pineapple peel biomass.

2.1.3 Previous research on techno-economic studies

Quintero et al. (2013) did a comparative study on the techno –economics of 2GBE production from several agricultural wastes. Aspen Plus software was used for modeling and simulation of the large-scale process using dilute acid pretreatment of LGB. From their study, the yield of bioethanol from empty fruit branches, coffee cut stems, SCB and rice husks were 313.83, 305.11, 298.21 and 250.56 liters per tonne of LGB respectively. The authors reported that the cost of producing bioethanol was $0.5779/L, $0.6393/L, $0.6807/L and $0.7662/L from empty fruit branches, rice husks, coffee cut stems and SCB respectively.

According to Porzio et al. (2012), facilities that produce bioethanol differ in terms of type of substrate, operating conditions, bioethanol yield, type of process technology used, bioethanol production rate and the level of process integration and implementation.

Porzio et al. (2012) did a study on modeling and simulation of a process to produce bioethanol from poplar (substrate). The process entailed steam explosion catalyzed pretreatment of substrate followed by SSCF. In addition, the authors performed a literature based comparative analysis of bioethanol production technologies in terms of efficiency, process yield, type of feedstock and the level of process integration. The authors reported that the bioethanol production yield ranged from 303 to 316 liters per tonne of dry LGB. The net process energy efficiency ranged from 35% to 37% (Porzio et al., 2012).

da Silva et al. (2016) compared different pretreatment technologies during their study on large-scale 2GBE production using Aspen Plus. The authors compared dilute acid, LHW and ammonia fiber explosion (AFEX) pretreatment methods. They evaluated the

effect of several pretreatment parameters on energy consumption and the concentration of bioethanol in the fermentation broth. The authors reported that the energy demand and concentration of ethanol in the fermentation broth were 103971 kWh and 5.85%, w/w, 179363 kWh and 5.20%, w/w, 100285 kWh and 5.40%, w/w for dilute acid, LHW and AFEX pretreatment methods respectively.

Frankó, et al. (2016) performed a techno-economic analysis on the feasibility of producing bioethanol from forest residues (fuel logs, sawdust and shavings, hog fuel and pulpwood, tops and branches, early thinning) which differed in composition of the bark. The main aim was to evaluate the feasibility of utilizing these residues as substrates for bioethanol production. The impact of bark content on the production rate of bioethanol and cost of production was investigated. The feedstocks were pretreated using steam catalyzed by sulphur dioxide followed by simultaneous saccharification and fermentation (SSF). The authors reported that the MBSP from the forest residues ranged from $0.77/L to $1.52/L.

Barreraa et al. (2016) did a study on techno-economic evaluation of bioethanol production from SCB and blue agave bagasse. They modelled and simulated the pretreatment, hydrolysis and fermentation process using “Superpro Designer” (Barreraa et al., 2016). In their study, they used ozonolysis pretreatment method and separate hydrolysis and co-fermentation (SHCF) process. The authors reported that the yield of bioethanol was 431.38 and 389.08 liters per tonne of dry blue agave bagasse and SCB respectively. In addition, they reported that the cost of producing bioethanol from blue agave bagasse and SCB was $0.352/L and $0.384/L respectively.

da Silva et al. (2017) did a techno-economic analysis of a complete process of producing bioethanol from spruce biomass using H_2SO_4 catalyzed ethanol organo-

solvent pretreatment technology. The authors reported that the total energy consumption and the MBSP were 41.82 megajoules per litre (MJ/L) and $1.0/L of bioethanol respectively.

Tgarguifa et al. (2017) did a literature-based study on modeling and optimization of the distillation process for bioethanol production. Their study focused on the distillation column only. They performed a sensitivity study on the effect of distillation column feed stage position and the reflux ratio on the production rate of bioethanol. The aim of the study was to improve bioethanol production rate by optimizing the distillation column operating parameters. The authors reported that bioethanol production rate and the reboiler duty increased while the condenser duty decreased as the reflux ratio increased. On the other hand, the production rate of bioethanol increased as the feed stage position was varied from feed stage number 8 to feed stage number 17, followed by a drastic fall in bioethanol production rate upon further increase in feed stage position (Tgarguifa et al., 2017).

According to Boakye-Boaten et al. (2017), the economic viability of producing 2GBE is hindered by the complex nature of the main process steps (pretreatment, hydrolysis, fermentation, purification and dehydration) involved in the production of bioethanol from LGB. Performing a techno-economic analysis of the complete process involved in the production of 2GBE can be useful in identifying and addressing potential areas that may require improvements in process conditions and process configuration.

Boakye-Boaten et al. (2017) did a study on the economic viability of using *Miscanthus x giganteus* as a substrate for bioethanol production. The study was based on a report by the National Renewable Energy Laboratory (NREL), which entailed process modeling and simulation of bioethanol production from corn stover using dilute acid

pretreatment and SHCF. The authors reported that MBSP ranged from $0.65/L to $0.71/L of bioethanol when the cost of substrate was varied between $0.08/kg to $0.1/kg.

da Silva et al. (2018) did a techno-economic analysis of large-scale 2GBE production from corn stover using modified AFEX pretreatment technology. The authors modified the reactor conditions in order to increase the productivity which contributed to a 28% reduction in the MBSP. In addition, in order to recover ammonia used in the pretreatment process, water quenching was used. This resulted in a decrease in the make-up ammonia. The authors reported that the total energy consumption and the MBSP were 18.75 MJ/L and $0.55/L of ethanol respectively.

da Silva et al. (2019) assessed the economic and environmental impact of large-scale 2GBE production from corn stover using dilute sulphuric acid, steam explosion, organo-solvent, LHW and AFEX pretreatment technologies with separate hydrolysis and fermentation (SHF) process. The authors reported that dilute sulphuric acid pretreatment had the highest substrate conversion which resulted in high ethanol productivity. LHW and steam explosion pretreatment methods had the lowest pretreatment costs due to simpler operation process. AFEX and organo-solvent pretreatment methods had the highest utility costs due to the need for recovery of chemicals. Steam explosion pretreatment had the highest CO_2 contribution due to emissions from the cogeneration area.

According to Lopes et al. (2019), the feasibility of large-scale processes for the production of 2GBE can be evaluated using modeling and simulation. Process modeling and simulation can be used as a tool to select the best technology for use in large-scale 2GBE production because it is possible to have a wider insight of the entire process and

be able to identify and understand technical issues that hinder full scale commercialization of the 2GBE production process (Barreraa et al., (2016).

2.1.4 Summary of existing research gaps

The following is a summary of the shortcomings that were identified in literature. These shortcomings formed the basis of investigation in this research study.

1. Lack of sufficient information on optimum conditions governing hydrolysis of cellulose found in LGB.
2. Low yield of fermentable sugars obtained during hydrolysis of LGB.
3. Multistage LGB hydrolysis process which has the potential of increasing capital and operating costs during large-scale 2GBE production process.
4. Lack of sufficient data on the impact of varying process and economic factors on the techno-economic viability of large-scale 2GBE production process. This hinders decision making as to whether or not investments should be done on large-scale 2GBE production.
5. Literature does not report significant studies that compare different pretreatment methods on large-scale 2GBE production.
6. Lack of sufficient kinetic data for pretreatment, hydrolysis and fermentation reactors involved in 2GBE production.
7. Large amount of solid and liquid wastes generated during 2GBE production which poses a threat to the environment and presents additional cost in an attempt to manage these wastes.

2.2 Sources of Biomass

The main sources of biomass that can be used as substrate for the production of biofuels include forestry woody substrates, agricultural residues, energy crops, aquatic plants,

herbaceous crops, municipal solid waste and animal waste (Shukla et al., 2023; Cheah et al., 2020).

2.2.1 Classification of biomass

A general classification of biomass according to the origin is presented below.

2.2.1.1 Forestry woody substrates

Trees such as pine, cedar and cypress are referred to as forestry woody substrates (Cheah et al., 2020). They have less ash compared to crop-based substrates and are easy to transport from one point to another due to their high density (Cheah et al., 2020; Obieogu et al., 2016; UNEP, 2013).

2.2.1.2 Agricultural residues

Agricultural residues describe organic materials which are produced as by-products from agricultural activities. They include rice straws, corn stover, corn cobs, wheat straws etc (Cheah et al., (2020). These substrates are lignocellulosic in nature (consist of cellulose, hemicellulose and lignin) and represent ideal substrate for the production of 2GBE because they are renewable, available in abundance and they are cheap (Beluhan et al., 2023). In addition, these substrates are sustainable in nature because they do not require additional land for their production (UNEP, 2013).

2.2.1.3 Energy Crops

These are crops such as vegetable oil, canola, groundnuts etc which are grown for use as raw materials for energy production. For example, vegetable oil can be converted to biodiesel through transesterification process (Khandelwal et al., 2023).

2.2.1.4 Aquatic plants

Aquatic plants such as algae and reeds are being used as substrates for the production of biodiesel, biogas and bioethanol (Cheah et al., (2020). They are advantageous because they are fast growing substrates (UNEP, 2013).

2.2.2 Herbaceous crops

Grasses such as napier and switch grass are categorized as herbaceous crops (Beluhan et al., 2023). They have high biomass yield and are considered as suitable substrates for the production of biofuels (Beluhan et al., 2023).

2.2.3 Municipal Solid Waste

Municipal solid waste (MSW) consists of waste generated by residential, schools, hotels, industries etc, that is normally collected for disposal in dumpsites (Beluhan et al., 2023). It consists of food remains, fats, oils, polymers, glass, garden waste etc (Obieogu et al., 2016). Upon sorting the various constituents of MSW, substantial amount of biomass can be obtained which can be used to produce biofuels through technologies such as anaerobic fermentation (which yield biogas) or transesterification (which yield biodiesel). This presents an opportunity of managing MSW in an environmentally friendly and sustainable manner.

2.2.4 Animal Waste

Animal waste is obtained from animals such as cows, goats, pigs, poultry etc that are normally reared for eggs, meat and milk. Animal waste can be used as substrate for the production of biofuels through technologies such as anaerobic fermentation, which generate biogas. This presents an opportunity of managing animal waste in an environmentally friendly and sustainable manner.

2.3 Characteristics of Lignocellulosic Biomass

The term Lignocellulose describes a three-dimensional polymer that consists of cellulose, hemicellulose and lignin (Cheah et al., 2020; Habibi et al., 2010). In addition, LGB contains compounds such as salts, acids, proteins and minerals (Kumar et al., 2009).

2.3.1 Cellulose

Cellulose is quite strong, resists hydrolysis and is insoluble in water (Shukla et al., 2023; Habibi et al., 2010). According to Habibi et al. (2010), the basic building block of cellulose is cellobiose which is formed by two glucose molecules. Cellulose molecules are linear and tend to form intra and intermolecular hydrogen bonds (Habibi et al., 2010). Bundles of cellulose molecules are aggregated together in the form of microfibrils, in which highly ordered crystalline domains alternate with less ordered amorphous regions (Shukla et al., 2023). Cellulose has high tensile strength due to intermolecular hydrogen bonds. During hydrolysis of cellulose, cellobiose appears as an intermediary product while glucose is the final product (Hector et al., 2008). The structure of cellulose is shown in Figure 2.1.

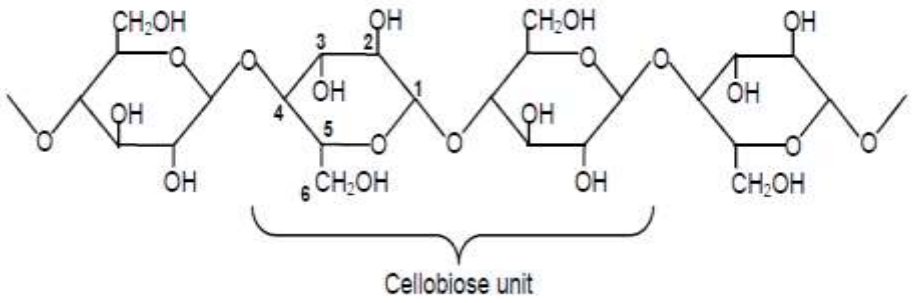

Figure 2. 1: Structure of cellulose (Hector et al., 2008)

2.3.2 Hemicellulose

Hemicellulose is a polymer consisting of five (C5) and six (C6) carbon sugars (Yuan et al., 2021). Hemicellulose bonds with cellulose fibrils forming a framework that provides the structural backbone to the plant cell wall (Hector et al., 2008). Hemicellulose provides strength to the secondary cell wall and facilitates transport of water to the plant (Shukla et al., 2023). The hemicellulose content in LGB varies widely depending on plant genus, cell type, growth conditions, extraction method and storage conditions (Shukla et al., 2023). The structure of hemicellulose is shown in Figure 2.2.

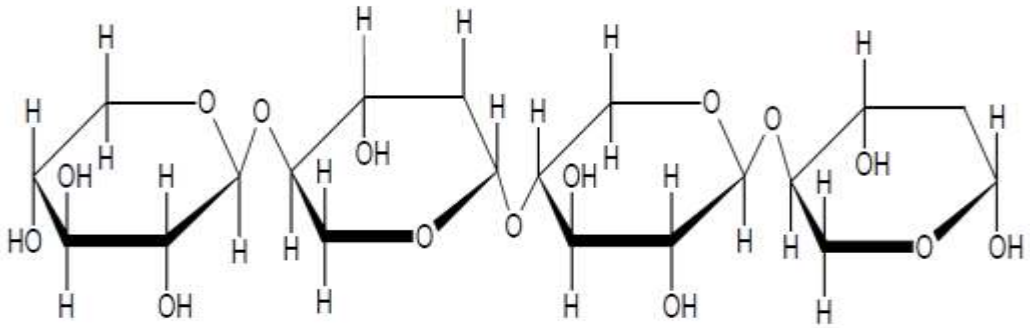

Figure 2. 2: Structure of hemicellulose (Hector et al., 2008)

2.3.3 Lignin

Lignin is the largest non-carbohydrate fraction of LGB (Shukla et al., 2023). It is highly crystalline and quite recalcitrant. Lignin provides additional strength and resistance against pests and diseases (Hector et al., 2008). Cellulose and hemicellulose are normally tightly bound to lignin. LGB with high lignin content tends to resist chemical and enzymatic depolymerization. Lignin is insoluble in water and in many occasions, it resists acidic attack. However, lignin is easily altered under alkali conditions (Shukla et al., 2023). The structure of lignin is shown in Figure 2.3.

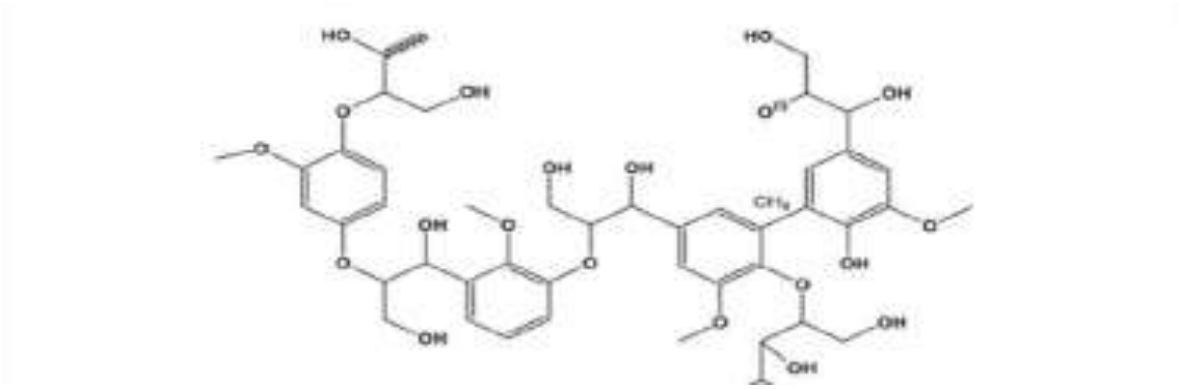

Figure 2. 3: Structure of lignin (Shukla et al., 2023)

2.3.4 Ash

LGB contains varying amounts of proteins, ash and extractives (Kumar et al., 2009). When LGB is ignited at 575^{o}C, the residue that remains is referred to as ash. This residue is 3–10% of the total dry weight of LGB and normally contains minerals such as aluminium and potassium. Extractives include resins and fats, (Kumar et al., 2009).

2.4 Pretreatment of LGB

The production of bioethanol from LGB involves several steps including pretreatment, hydrolysis, fermentation, product recovery, purification and dehydration (Beluhan et al., 2023; Humbird et al., 2011). Cellulose and hemicellulose are the main carbohydrate fractions found in LGB, while lignin is the main non-carbohydrate fraction. In order to unwind and redistribute the complex structure of LGB, pretreatment is required (Lugani et al., 2020). Pretreatments work by separating the LGB into its structural components (cellulose, hemicellulose and lignin) (Shukla et al., 2023; Lugani et al., 2020; Cheah et al., 2020). Pretreatment reduces the crystallinity and degree of polymerization found in cellulose thereby increasing the porosity of the LGB. A suitable pretreatment method is key in breaking down the recalcitrant lignin structure leading to the accessibility of cellulose and hemicellulose by hydrolytic enzymes for their conversion into glucose and xylose respectively (Lugani et al., 2020). An efficient pretreatment method should

facilitate the hydrolysis process leading to improved yields of monomeric sugars, reduced degradation of carbohydrates and reduced formation of inhibitors (Lugani et al., 2020). According to Shukla et al. (2023), pretreatment methods can be categorized into physical, chemical, physio-chemical and biological.

2.4.1 Physical pretreatment

According to Beluhan et al. (2023), physical pretreatment methods of LGB include extrusion, mechanical size reduction, microwave and ultrasound (sonification).

2.4.1.1 Extrusion

According to Beluhan et al. (2023), extrusion is the most conventional mechanical pretreatment method, where the LGB is subjected to temperatures above 300^{o}C under shear mixing. Extrusion combines thermal, chemical and mechanical techniques to alter the structure of LGB (Shukla et al., 2023). The crystalline and amorphous fractions of LGB are altered due to the twin effect of elevated temperature in the reactor and the shearing force caused by rotating screw blades (Beluhan et al., 2023).

2.4.1.2 Mechanical Pretreatment

Mechanical pretreatment methods include chipping, milling and grinding which are mainly used to reduce the size of the LGB (Beluhan et al., 2023; Legodi et al., 2021). Ball mills and hammer mills are the main types of equipments used in mechanical pretreatment of LGB (Legodi et al., 2021). During size reduction of LGB, the crystallinity and degree of polymerization of the cellulose fraction are reduced thereby contributing to improved hydrolysis of cellulose (Cheah et al., 2020).

2.4.1.3 Microwave

LGB can be subjected to microwave – assisted pretreatment, which results in high lignin removal (Beluhan et al., 2023). Microwave irradiation breaks down the structure

of cellulose and degrades hemicellulose and lignin found in LGB. The breakdown of LGB is achieved through molecular collisions due to bending and stretching caused by dielectric polarization on covalent bonds between hemicellulose and cellulose (Shukla et al., 2023). The pretreated biomass has a high yield of fermentable sugars. Microwave – assisted pretreatment can be combined with chemical pretreatment for improved hydrolysis efficiency (Beluhan et al., 2023).

2.4.2 Chemical pretreatment

Chemical pretreatment includes acid, alkaline, organosolvent, ionic liquid, deep eutectic solvents (DESs), oxidizing agents and ozonolysis (Beluhan et al., 2023; Cheah et al., 2020; Alicia, 2013).

2.4.2.1 Acid pretreatment

Dilute acid pretreatment is the most common pretreatment method applied in most types of LGB (Cheah et al., 2020; da Silva et al., 2019). This type of pretreatment involves soaking the LGB in a dilute acid solution with a given acid concentration for a specific period of time. The acid concentration is normally below 4.0%, (w/w) at temperatures within the range of 140- 200°C for a time period of one hour (Alicia, 2013). The acid catalyzes the hydrolysis of hemicellulose found in LGB into xylose and removes lignin. This action renders the cellulose fraction accessible to hydrolysis enzymes (Cheah et al., 2020). The major drawback of dilute acid pretreatment is the generation of fermentation inhibitors such as furfural and HMF (Cheah et al., 2020).

2.4.2.2 Alkaline pretreatment

Alkaline pretreatment can also be used to pretreat LGB. According to Cheah et al., (2020), alkaline pretreatment breaks the bonds between lignin and carbohydrates. The removal of lignin is achieved by destroying links between lignin and other

carbohydrates (Alicia, 2013). The main types of bases used in alkaline pretreatment include sodium hydroxide, calcium hydroxide, magnesium hydroxide, potassium hydroxide and ammonia hydroxide (Cheah et al., 2020; Alicia, 2013; Conde-Mejíaa et al., 2012). Sodium hydroxide pretreatment of LGB is preferred due to higher lignin removal than other types of bases (Cheah et al., 2020; Alicia, 2013).

2.4.2.3 Organosolvent pretreatment

The organosolvent pretreatment process involves the use of an organic or aqueous organic solvent mixture with inorganic acid catalysts such as hydrochloric acid (HCl) or H_2SO_4 to break the internal lignin and hemicellulose bonds (Shukla et al., 2023). Methanol, ethanol, acetone, glycerol and ethylene glycol are examples of organic solvents which can be used in this process (Shukla et al., 2023).

2.4.2.4 Ionic liquid pretreatment

Novel pretreatment technologies have focused on the use of ionic liquids (ILs) as cellulose dissolving agents. Due to the presence of a variety of component ions and their low melting point, it is practical to vary their physiochemical properties so as to suit a given need (Lugani et al., 2020). ILs which include salts of alkylimidazolium containing anion derivatives like 1-ethyl-3-methylimidazolium chloride (EMIMCl), 1-N-butyl-3 methylimidazolium chloride (BMIMCl) and 1-N-butyl-3-methylimidazolium acetate (BMIMAc) are often referred to as green solvents that are able to dissolve cellulose (Cheah et al., 2020; Fukaya et al., 2008).

2.4.2.5 Deep Eutectic Solvents

DESs are an emerging class of solvents used in the delignification of LGB (Beluhan et al., 2023). DESs are efficient in dissolving LGB components, which results in high cellulose and hemicellulose recovery yield (Beluhan et al., 2023). In terms of

environmental safety, DESs are considered green solvents. In addition, they are cheaper and easier to prepare than ILs (Beluhan et al., 2023).

2.4.2.6 Oxidizing agents

Hydrogen peroxide (H_2O_2) is the most common oxidizing agent used to pretreat LGB through the delignification process (Beluhan et al., 2023). H_2O_2 is effective in dissolving about 50% lignin and the recovery of hemicellulose in LGB (Beluhan et al., 2023).

2.4.2.7 Ozonolysis

This method involves the use of ozone to pretreat LGB. The ozone attacks the structure of lignin and does not affect the cellulose and hemicellulose content of LGB (Beluhan et al., 2023). Ozonolysis occurs at room temperature and pressure and it does not lead to the formation of fermentation inhibitors (Beluhan et al., 2023).

2.4.3 Physio-chemical pretreatment

Physio-chemical pretreatment methods include steam explosion, LHW, AFEX, CO_2 explosion and wet oxidation (Beluhan et al., 2023; Cheah et al., 2020; Galbe and Wallberg, 2019; Alicia, 2013).

2.4.3.1 Steam explosion pretreatment

During steam explosion pretreatment, the LGB is treated with high pressure steam for a short period of time (Cheah et al., 2020; Alicia, 2013). The pressure is then reduced instantly resulting in explosive decompression of LGB (Cheah et al., 2020; Alicia, 2013). Steam explosion pretreatment is normally carried out at temperatures of 160^{o}C to 260^{o}C which corresponds to pressures of 0.69 to 4.83 MPa for residence time which ranges from seconds to a few minutes (Cheah et al., 2020; Alicia, 2013). During steam explosion pretreatment, the structure of hemicellulose and lignin is altered with the

production of xylose from hemicellulose while cellulose remains in solid form (Beluhan et al., 2023).

2.4.3.2 Liquid hot water pretreatment

LHW pretreatment involves soaking the LGB in water at elevated temperatures (up to 240^{o}C) and pressures (up to 2.8 MPa) in order to keep the water in liquid state at these conditions (Cheah et al., 2020). This method is also known as autohydrolysis or pressure cooking in water (Galbe and Wallberg, 2019). Due to the existing conditions, the water is acidic in nature, which results in hydrolysis of hemicellulose to xylose. In addition, under these conditions, a large portion of lignin is removed (Cheah et al., 2020).

2.4.3.3 Ammonia fibre explosion pretreatment

AFEX is a pretreatment process that is similar in operation principle to the steam explosion method except that it uses hot liquid ammonia under high pressure for a specified holding time (Cheah et al., 2020). AFEX involves subjecting the LGB to a pressurized solution of ammonia at high temperature and pressure (Alicia, 2013). The pressure is held for a short time and released suddenly resulting into an explosive degradation of LGB which breaks the bonds between lignin and hemicellulose (Alicia, 2013).

2.4.3.4 Carbon dioxide explosion

This pretreatment method involves the use of CO_2 (Beluhan et al., 2023). In this process, CO_2 is fed in a high-pressure reactor containing LGB which is subjected to constant agitation at temperatures of about 200^{o}C. During this process, carbonic acid that is formed by CO_2 diffuses into the LGB and causes hydrolysis of hemicellulose

(Shukla et al., 2023). Once the LGB is pretreated, the explosive release of CO_2 breaks down the cellulose and hemicellulose fractions (Beluhan et al., 2023).

2.4.3.5 Wet Oxidation

Wet oxidation pretreatment involves treating of LGB with air (oxygen) and water for about 30 minutes at temperatures above 120^{o}C (Beluhan et al., 2023). The cellulose, hemicellulose and lignin content of LGB is affected during wet oxidation pretreatment which results in cellulose that is easily accessible by enzymes during hydrolysis (Beluhan et al., 2023).

2.4.4 Biological pretreatment

The biological method uses micro-organisms (such as fungi and bacteria) or enzymes in the pretreatment of LGB (Beluhan et al., 2023; Cheah et al., 2020). LGB can be modified biologically using brown, white or soft rot fungi because of their ability to undergo oxidation (Cheah et al., 2020).

2.5 Pretreatment Inhibitors

The formation of inhibitors varies from one pretreatment method to another and depends on the pressure, pH, temperature, reaction time and concentration of added chemicals (Sjulander and Kikas, 2020). Pretreatment inhibitors are mainly formed during chemical pretreatment methods (Sjulander and Kikas, 2020). The main causes of inhibitor formation during chemical pretreatment includes the use of high temperature, use of harsh/very reactive chemicals and long pretreatment period. In addition, the type and concentration of inhibitor depends on the type of LGB (Sjulander and Kikas, 2020). According to Beckendorff et al. (2021), high temperatures (above 140°C) and long pretreatment time (over 3 hours) during cellulose and hemicellulose hydrolysis leads to the degradation of sugar monomers into inhibitors. Examples of

inhibitors resulting from chemical pretreatment of LGB include organic acids (formic acid, levulinic acid and acetic acid), sugar degradation products (HMF and furfural), and lignin degradation products (vanillin and aldehydes) (Parameswaran et al., 2011). According to Sjulander and Kikas (2020), furfural is formed as a result of degradation of hemicellulose when the pretreatment method is performed at a temperature below 150^{o}C, in acidic conditions, for a long period of time and high concentration of water. On the other hand, the concentration of formic acid which is formed as a result of degradation of HMF and furfural increases with an increase in pretreatment temperature and time. The use of low to moderate temperature, less severe chemicals and shorter pretreatment reaction time reduces inhibitor formation during pretreatment of LGB (Sjulander and Kikas, 2020). Therefore, during chemical pretreatment of LGB, reaction conditions should be carefully selected so as ensure that the conditions existing in the pretreatment reactor do not support inhibitor formation (Lugani et al., 2020). Figure 2.4 shows the conversion of cellulose and hemicellulose to sugar monomers and inhibitors (Beckendorff et al., 2021).

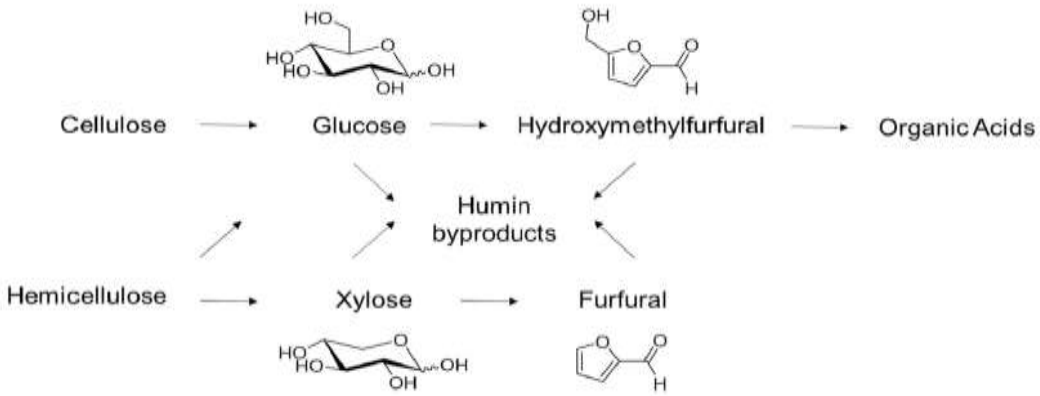

Figure 2. 4: Conversion of cellulose and hemicellulose into sugar monomers and inhibitors (Beckendorff et al., 2021)

2.6 Acid Hydrolysis

Hydrolysis is defined as a reaction which leads to the breaking of chemical bonds through the addition of a water molecule. This reaction is important in the production

of simple sugars because it disintegrates cellulose and hemicellulose into simple sugars that can be converted to bioethanol through the process of fermentation. Acid hydrolysis of LGB can be carried out using dilute or concentrated acid (Kunar et al., 2015). The concentration of acid during dilute acid hydrolysis of LGB is normally below 10% (w/w) while during concentrated acid hydrolysis, it is above 10% (w/w) (Kumar et al., 2015). The acid reacts with the cellulose and hemicellulose found in LGB to produce mainly glucose and xylose respectively. The main advantage of the acid hydrolysis process is that acids can penetrate lignin without any preliminary pretreatment of biomass, thus breaking down the cellulose and hemicellulose polymers to form individual sugar molecules (Kumar et al., 2015; Chandel et al., 2012). Acid hydrolysis of LGB is influenced by factors such as hydrolysis temperature, reaction time, particle size of LGB, concentration of acid and SLR (Muktham et al., 2016; Chandel et al., 2012).

2.6.1 Dilute acid hydrolysis

This is the oldest technology for converting LGB into simple sugars. Common acids used as catalysts in dilute acid hydrolysis of LGB include HCl, H_2SO_4, phosphoric acid, HNO_3 and acetic acid (Xiao et al. (2021). The acid catalyzes the reaction leading to breaking of bonds between the constituents of LGB. The breaking of these bonds releases several compounds including simple sugars (such as xylose, glucose and arabinose), and fermentation inhibitors (such as furfural, HMF and acetic acid). Dilute acid hydrolysis of LGB occurs in two stages in order to maximize the yield of simple sugar from cellulose and hemicellulose fraction of the LGB. Size reduction of LGB is necessary in order to allow adequate penetration of acid within the entire LGB (Mustafa & Cahide 2008). After each stage, liquid hydrolysates are recovered, neutralized and fermented to bioethanol or concentrated into sugar syrup (Lenihan et al., 2010). Dilute

acid hydrolysis of LGB is influenced by several factors including reaction temperature and time, acid concentration, particle size of LGB and SLR (Muktham et al., 2016; Chandel et al., 2012). The concentration of acid and the reaction temperature are the most important factors affecting the formation of simple sugars during dilute acid hydrolysis of LGB (Chandel et al., 2012).

2.6.2 Concentrated acid hydrolysis

Concentrated acid hydrolysis process provides a rapid and complete conversion of cellulose and hemicelluloses present in LGB into glucose and xylose respectively, with little degradation into furfural and HMF. This leads to high yield of simple sugars which in turn promotes higher fermentation yields (Kanchanalai et al., 2016). The main types of acids used in concentrated acid hydrolysis include H_2SO_4, HCL, and HNO_3. The critical factors needed to make this process economically viable include optimization of the hydrolysis process through selection of optimum levels of reaction parameters (temperature, acid concentration and time) and cost-effective recovery of the acid for recycling (Chandel et al., 2012; Mustafa & Cahide 2008).

The concentrated acid hydrolysis process uses relatively mild temperatures and pressure which reduces chances of glucose and xylose sugar degradation into HMF and furfural respectively (Mustafa & Cahide 2008). The concentrated acid hydrolysis process offers more potential for cost reductions than the dilute acid hydrolysis process because during concentrated acid hydrolysis, the crystalline fraction of cellulose is disintegrated into glucose which leads to higher yield of glucose (Xiao et al., 2021; Mustafa & Cahide 2008).

After concentrated acid hydrolysis of LGB, separation of acid from the simple sugars, acid recovery and acid re-concentration for recycling is done (Mustafa & Cahide 2008).

The main advantage of the concentrated acid hydrolysis process is the potential for high sugar recovery efficiency, because upto 90% of hemicellulose and cellulose fractions of the LGB are depolymerized into xylose and glucose respectively (Chandel et al., 2007). LGB is mixed with concentrated acid to decrystallize cellulose in a reaction where the concentrated acid disrupts inter and intra molecular hydrogen bonding responsible for cellulose crystallinity and renders the cellulose amorphous and easy to hydrolyse under mild conditions with the formation of minimum fermentation inhibitors (Janga et al., 2012).

The overall yield of bioethanol during acid hydrolysis and fermentation is affected by the degradation of simple sugars into fermentation inhibitors. This leads to a reduction in overall efficiency of biomass to ethanol conversion process making the entire process not commercially competitive (Janga et al., 2012). Improvements in sugar – acid recovery technologies such as the simulated moving bed chromatographic separation has increased interest in concentrated acid hydrolysis of LGB (Kanchanalai et al., 2016).

2.7 Enzymatic Hydrolysis

The enzymatic hydrolysis process uses enzymes known as cellulases and hemicellulases to hydrolyse cellulose and hemicellulose into glucose and xylose respectively (Lugani et al., 2020). The mechanism involved in the enzymatic degradation of LGB depends on the chemical nature and physical structure of the substrate (Lugani et al., 2020; Taherzadeh & Karimi, 2008). The structural features of the substrate that affect enzymatic hydrolysis include crystallinity, specific surface area, accessibility to enzyme adsorption, degree of polymerization and unit cell dimensions of the lignocellulosic material (Taherzadeh & Karimi, 2008). The main drawbacks of

enzymatic hydrolysis include high quantity of enzymes required, deactivation of enzymes due to long incubation period and the tendency of lignin to adsorb enzymes during hydrolysis (Lugani et al., 2020; Parameswaran et al., 2011).

2.8 Fermentation

Fermentation is a metabolic process that involves the conversion of carbohydrates into alcohols such as ethanol and organic acids such as lactic acid and citric acid (Mustafa & Cahide, 2008). It is a natural process initiated by microorganisms such as *saccharomyces cerevisiae* which act on sugars such as glucose and sucrose to produce ethanol and CO_2 under anaerobic conditions (Beluhan et al., 2023; UNEP, 2013). These microorganisms (yeasts, fungi and bacteria) break down organic substrates under anaerobic conditions (fermentation) to produce ethanol and organic acids (Beluhan et al., 2023). The raw materials (substrates) used in fermentation are classified into three categories i.e., sugars, starches and cellulose (Beluhan et al., 2023). Sugars (from sugarcane, beet sugar and fruits) can be converted into ethanol directly. Starches (corn, cassava and potatoes) and cellulose (mainly from agricultural residues, forest residues, aquatic plants and MSW) require pretreatment and hydrolysis prior to fermentation (Mustafa & Cahide, 2008). Ethanol is then recovered through a distillation process (Ray, 2023). The fermentation process can be configured and carried out as batch, fed - batch and continuous fermentation (Lugani et al., 2020).

2.9 Integrated Fermentation Technologies

The main steps for converting LGB into 2GBE can be implemented separately or they can be combined in various ways to form integrated processes aimed at minimizing the cost of producing 2GBE. There are several ways of integrating these processes including separate hydrolysis and fermentation (SHF), simultaneous saccharification

and fermentation (SSF), separate hydrolysis and co-fermentation (SHCF), simultaneous saccharification and co-fermentation (SSCF), consolidated bioprocessing (CBP) and thermochemical approach (Lugani et al., 2020).

2.9.1 Separate hydrolysis and fermentation

In this method, hydrolysis of LGB and fermentation of sugars are handled separately. After the completion of the hydrolysis process, fermentation of the resulting liquid hydrolysate is achieved separately using *Saccharomyces cerevisiae* (Lugani et al., 2020; Monir et al., 2020).

2.9.2 Simultaneous saccharification and fermentation

In simultaneous saccharification and fermentation (SSF) process, cellulose hydrolysis and fermentation of glucose are carried out in the presence of fermentation microorganism in a single step (Lugani et al., 2020). The cellulase enzymes hydrolyze cellulose to glucose, which in turn is fermented to bioethanol by *Saccharomyces cerevisiae* (Lugani et al., 2020).

2.9.3 Separate hydrolysis and co-fermentation

In separate hydrolysis and co-fermentation (SHCF), hydrolysis of LGB is carried out in a separate reactor while fermentation of the resulting C5 and C6 sugars is carried out in a single reactor (Lugani et al., 2020).

2.9.4 Simultaneous saccharification and co-fermentation

In simultaneous saccharification and co-fermentation (SSCF), hydrolysis of LGB and fermentation of the resulting C5 and C6 sugars is carried out in a single reactor (Lugani et al., 2020).

2.9.5 Consolidated bioprocessing

During consolidated bioprocessing (CBP), cellulase enzyme production, substrate hydrolysis and fermentation of C5 and C6 sugars are carried out in one reactor (Beluhan et al., 2023; Lugani et al., 2020).

2.9.6 Thermochemical Approach

During thermochemical approach, the carbon in the LGB feedstock is converted to synthesis gas through incomplete combustion (gasification) (Monir et al., 2020). The hydrogen and carbon oxides (synthesis gas) produced are then fed into special fermenters where microorganisms such as *Saccharomyces cerevisiae, Escherichia coli* and *Trichoderma reesei* are used to convert the gas into bioethanol through fermentation (Monir et al., 2020).

2.10 Bioethanol Purification

The fermentation process leads to the formation of several undesired compounds including organic acids, alcohols (such as methanol) and aldehydes (Parameswaran et al., 2011). These compounds can be removed through distillation in order to enhance the quality of bioethanol (Beluhan et al., 2023).

2.10.1 Bioethanol distillation

The separation of liquid substances into the different constituents can be achieved through distillation. According to Ray (2023), distillation is mainly used in separating liquid mixtures into various components in the chemical process industry. Distillation is preferred in the purification of bioethanol because it is fast, simple, efficient and effective compared to other separation techniques such as chromatography (Ray, 2023). Up to 96% (w/w) bioethanol can be obtained during distillation. Distillation can be carried out as batch, equilibrium or rectification process configurations (Ray, 2023).

2.10.2 Bioethanol dehydration

The purity of bioethanol from the distillation process can be improved through the dehydration process. This process can be done using molecular sieves which uses an adsorbent that has high affinity for water and less affinity for ethanol (Ray, 2023). After leaving the rectification column, the ethanol vapor stream is passed through a column packed with an adsorbent such as zeolite (Ray, 2023). Since zeolite has high affinity for water, it removes the water from the stream as it flows through using the principle of adsorption (Gebreyohannes, 2010; Ray, 2023). The recovery of these beds is achieved by passing a stream of pure ethanol which entrains water molecules thereby renewing the zeolite capacity to adsorb water again (Ray, 2023). The stream from regeneration of zeolite is returned back to the rectifying column (Ray, 2023). The product from the molecular sieve adsorption is pure ethanol that is stored in product tanks.

2.11 Safety Aspects of Large-Scale Bioethanol Production

During bioethanol production, hazards may be encountered from raw materials, catalysts, intermediates and finished products. They include fires, toxic substances, explosions, release of flammable substances, corrosive substances and uncontrolled reactions (Nair, 2011). Common examples of hazards encountered during bioethanol production include high operation temperature and pressure, high storage pressure and temperature, overflow of tanks and reactors, improper selection of equipment and machinery and inadequate installation, inspection and maintenance (Nair, 2011).

In the bioethanol production process, accidents associated with operations include slips, trips, falls and major incidents like fires and explosions (Sinnott and Towler, 2020). Accidents can be caused by failure related to process equipment, machinery, control and instrumentation and operating parameters. The main safety concerns during large-

scale bioethanol production include corrosion of equipment due to the use of chemicals such as sulphuric acid, production of harmful byproducts and effluents especially during pretreatment, hydrolysis, fermentation and distillation (Humbird et al., 2011). Corrosion may lead to equipment failure which can cause injury to personnel working in the plant as well as loss of process materials and equipment. The use of corrosion resistant material of construction such as stainless steel, carbon steel and mild steel can help in mitigating the risk of equipment failure due to corrosion. The production and emission of harmful byproducts such as volatile organic carbons (VOCs) and effluents can be harmful to personnel working in the plant, nearby communities as well as the environment. Preventing and minimizing the formation of harmful byproducts and wastes through process optimization, proper equipment design and selection are some of the methods of addressing this concern (Sinnott and Towler, 2020). In addition, proper containment of process materials and wastes minimizes the possibility of release of these wastes to the environment. Flue gases from the combustor, consisting of CO_2, carbon monoxide (CO) and oxides of nitrogen (NOx) are also of concern. These gases can be managed through proper design of the combustion process and flue gas treatment. Wastewater generated during large-scale bioethanol production process can be managed through proper effluent treatment in anaerobic and aerobic digestion systems. The resultant methane -rich biogas from anaerobic digestion can be used to provide process heat (Humbird et al., 2011).

2.12 Process Modeling and Simulation

Evaluation of the techno-economic feasibility of large-scale production of 2GBE, requires assessment of the efficiencies of the pretreatment, hydrolysis, fermentation and the purification processes. If the efficiencies of these processes were to be assessed through experiments, the implications would be large in terms of resources (costs and

time) (Gebreyohannes, 2010). Therefore, an alternative way of evaluating the techno-economic performance of a large-scale process of producing 2GBE without performing experiments must be devised. Process modeling and simulation is a convenient technique of evaluating the techno-economic performance of large-scale bioethanol production processes without performing laboratory-based experiments (Gebreyohannes, 2010). Process models can be developed using theoretical and empirical model formulation approaches (Gebreyohannes, 2010). "Empirical models are based on experiments or experience without theoretical basis" (Gebreyohannes, 2010, p.22). They are used when it is complicated to develop a theoretical model. "Empirical models can be derived from experimental data using statistical regression techniques" (Gebreyohannes, 2010, p.22). On the other hand, "theoretical models are developed from theoretical considerations. They are used when the phenomena governing the process are well known" (Gebreyohannes, 2010, p.22). The first step in developing a process model entails preliminary process synthesis where different unit operations are selected in order to transform LGB to bioethanol. A base case design is then created by designing a process flow diagram (PFD). The PFD displays all the major processing units and provides stream information (Gebreyohannes, 2010). The simulation step is used to imitate an actual process using mathematical equations and to relate the parameters that describe the system (Gebreyohannes, 2010). Simulation of process models "requires large amount of data. These data include the physical and chemical properties of the various compounds involved in the process, thermodynamic models, reaction chemistry and process conditions" (Gebreyohannes, 2010, p.24). These data are feed into the simulator and upon simulation, the predicted "results are validated by comparing with experimental results" (Gebreyohannes, 2010, p.24). "If the model is in good agreement with the experimental results, it can be used for future

process analysis such as optimization, plant expansion, economic analysis etc" (Gebreyohannes, 2010, p.24). "However, if the model does not fit the experimental data, input parameters are changed until the model gives a reasonable fit" (Gebreyohannes, 2010, p.24).

2.12.1 Aspen Plus

Aspen Plus is used to model and simulate large-scale processes. It has built-in thermodynamic and equation of state (EOS) models, unit operation models that include reactors, distillation columns, separators, pressure changers, mixers etc (Schefflan, 2016; Aspen Plus, 2000). Using Aspen Plus, a PFD diagram can be developed easily by interconnecting different unit operation models. Unlike other simulators, Aspen Plus has a built-in thermodynamic model for solids (Schefflan, 2016; Aspen Plus, 2000). Additionally, Aspen Plus can be used to model and simulate the individual steps (unit operations) involved in the production of 2GBE (pretreatment, hydrolysis, fermentation, purification and dehydration), model and simulate the entire large-scale process of producing 2GBE, manipulate process flowsheet configurations, feed compositions and operating conditions in order to predict plant behavior and design better plants (Schefflan, 2016; Aspen Plus, 2000). Aspen Plus is also capable of performing sensitivity analysis. Sensitivity analysis is a tool for determining how a process reacts to varying key operating and design variables (Aspen Plus, 2000). Aspen Plus consist of a model library that contains a set of unit operation models that are used to construct the PFD (Schefflan, 2016; Aspen Plus, 2000). In addition, Aspen Plus has a data browser which is a sheet and form viewer with a hierarchical tree view of the available simulation input, results and objects that have been defined (Schefflan, 2016). The data browser is used to view and edit the forms and sheets that define the input and

display the results for the flowsheet simulation (Aspen Plus, 2000). According to Rao (2005), data from literature or operating plants is used during simulation studies.

2.12.2 Unit operation models

Unit operation models are used to represent actual pieces of equipment, such as distillation columns, separators or heat exchangers that are commonly found in processing plants (Aspen Plus, 2000). To run a flowsheet simulation, you must specify at least one-unit operation model. The unit operation model(s) are selected and placed on the main process flowsheet window in order to define the simulation flowsheet. Aspen Plus has a wide range of unit operation models to choose from. Unit operation models in Aspen Plus include mixers, separators, heat exchangers, columns, distillation columns and reactors (Aspen Plus, 2000). In this research study, the factors which were considered during selection of unit operation models included type of reaction, phases involved, availability of data and simplicity of the model.

2.12.3 Physical property methods

A property method is a collection of methods and models that Aspen Plus uses to compute thermodynamic and transport properties (Aspen Plus, 2000). Choosing the appropriate property method is often the key decision in determining the accuracy of your simulation results. The thermodynamic properties include fugacity coefficient (K-values), enthalpy, entropy, Gibbs free energy and volume (Schefflan, 2016). On the other hand, transport properties include viscosity, thermal conductivity, diffusion coefficient and surface tension (Aspen Plus, 2000). Aspen Plus includes a large number of built-in property methods that are sufficient for most applications. However, the user can create new property methods to suit his/her simulation needs. The user must select

one or more property methods to model the properties of specific systems in the flowsheet (Schefflan, 2016).

2.12.4 Chemical components

Aspen Plus has a large database of chemical compounds that are commonly used in the chemical industry (Aspen Plus, 2000). The built-in database has components covering organic, inorganic, aqueous and salt species. Also included in the data base are organic and inorganic electrolytic species (Schefflan, 2016).

2.12.5 Thermodynamic model selection

The physical and chemical behavior of a substance can be described by thermodynamic models. Aspen Plus has in –built thermodynamic property models which include the EOS models, activity coefficient models and special models. EOS models include the ideal gas law, Redlich-Kwong, Soave-Redlich-Kwong (SRK), Peng-Robinson, Lee-Kesler, Lee-Kesler-Plocker and Sanchez-Lacombe. Activity coefficient models include the Non-Random Two-Liquid (NRTL), Wilson, Van Laar and the Universal Quasi-Chemical while special models include the steam tables and Chao-Seader (Smith et al., 2021; Aspen Plus, 2000). The choice of property models used to predict the properties of the component determine the accuracy of the simulation, thus proper selection of thermodynamic models is necessary when using Aspen Plus simulation software. The choice of a thermodynamic model depends on the composition of the mixture (whether the mixture is polar or non-polar), operational pressure and temperature (Tosun, 2013). Properties that need to be calculated by Aspen Plus include enthalpy, entropy, density, vapor and liquid fractions, heat capacity and heat of formation. Distillation is a process in which the separation of components occurs from a liquid mixture with the help of condensation and boiling processes (Ray, 2023). A phase change is a physical process

where a substance changes state. The phase change that occurs during the process of distillation involves boiling followed by condensation. The liquid is converted into its vapour phase at its boiling point and the vapour is then condensed back to liquid on cooling (Ray, 2023). Distillation is based on multi-phase equilibrium. The tendency of a component or species in a mixture to leave or escape from its phase is measured by a parameter called fugacity (Smith et al., 2021). When the escaping tendency is the same for the two phases, they are in equilibrium with each other i.e., equilibrium is achieved when the fugacity of the component or species is equal in all phases involved. When the escaping tendency of a component or species is higher in one phase than another, that component or species will tend to transfer to the phase where its fugacity is lower (Smith et al., 2021). Therefore, phase equilibrium is calculated using fugacity. The ratio of the fugacity in solution to that of pure component is defined as the activity. The NRTL model is an activity coefficient model that correlates the activity coefficients of a compound with its mole fractions in the liquid phase concerned (Tosun, 2013). The model is used for non-ideal liquid solutions, such as the ethanol -water mixtures where the fugacity of the components in the solution deviates from that of the pure component (Tosun, 2013). Aspen Plus calculates chemical and vapor-liquid equilibria with activity coefficients calculated using the NRTL model. The NRTL, which includes the liquid activity coefficient model, Henry's law for the dissolved gases such as CO_2 and SRK EOS for the vapor phase was used to calculate properties for components in the liquid and vapor phases involved in large-scale 2GBE production process. The NRTL model was selected because during 2GBE production process, the pressure involved is below 10 bar and the system compounds are non-electrolyte polar substances (Humbird et al., 2011). This model takes into consideration the phase changes that occur during the entire 2GBE production process. Therefore, because of the need to distill bioethanol

and to handle dissolved gases, the NRTL thermodynamic property model was used in the current research study to calculate properties for components in the liquid and vapor phases.

2.13 Economics of the Bioethanol Production Process

The cost of pretreatment, hydrolysis, fermentation, product recovery, purification and dehydration are crucial to commercialization of the production of 2GBE. In order to compete in the market, the overall cost of producing 2GBE should be as low as possible. The main costs involved in the production of 2GBE include cost of LGB/substrate, pretreatment, hydrolysis, fermentation nutrients and microorganisms, sterilization of fermentation medium and equipments, bioethanol recovery and purification, research, waste management and human resource costs (Mustafa & Cahide, 2008).

2.13.1 Costing and Project Evaluation

Costing and project evaluation are an important activity during plant design. According to Sinnott and Towler (2020), cost estimates are used to decide between alternative designs during project evaluation. Chemical and process plants are designed, build and operated in order to make profits. In order to assess the profitability of a given or chosen plant design, an estimate of the investment and operation costs is required (Sinnott and Towler, 2020).

2.13.2 Economic analysis

Economic analysis is vital in evaluating the economic viability of a bioethanol production plant. In addition, this analysis helps to determine the profitability of the bioethanol production process. The output from this analysis can be used in decision making, i.e., whether or not to invest in such a process. The main factors affecting investment and production costs include cost of equipments, fluctuation in prices of

equipments, company policies, government policies, production rate and operating time (Sinnott and Towler, 2020).

2.13.2.1 Fixed capital investment

The total cost incurred in setting up the plant up to when it is ready for startup is called fixed capital investment (FCI) (Sinnott and Towler, 2020). This cost is incurred once and is only recovered at the end of the project life as the scrap or salvage value. This cost includes cost of purchase of equipment and their installation, design, engineering and construction supervision, piping, instrumentation and control systems, building and structures, utilities, land and civil engineering work (Sinnott and Towler, 2020)

2.13.2.2 Working capital investment

Working capital investment (WCI) refers to the investment needed to start up the plant operations and to support the operations until revenues are generated (Sinnott and Towler, 2020). This includes cost of startup, raw materials, catalysts and finished products inventories (Sinnott and Towler, 2020). Most of the WCI is recovered at the end of the plant life (Sinnott and Towler, 2020).

2.13.2.3 Direct costs

Direct costs cater for plant construction activities including erection of equipment, piping, insulation, painting, electrical, power and lighting, instrumentation, process buildings and structures, ancillary buildings (offices, laboratory buildings and workshops), raw materials and finished product storage, utilities (provision of plant for steam, water, air, firefighting services) and site preparation (Sinnott and Towler, 2020).

2.13.2.4 Indirect costs

Indirect cost includes design and engineering costs, contractor's fees and contingency allowance (Sinnott and Towler, 2020).

2.13.2.5 Operating cost

In order to produce a given product, the cost incurred is referred to as operating cost. It is used to judge the viability of a project and to make choices between possible alternative processing schemes (Sinnott and Towler, 2020). These costs can be estimated from the PFD, which gives the raw material and service requirements and the capital cost estimate. Operating costs are divided into fixed and variable operating costs (Sinnott and Towler, 2020).

2.13.2.5.1 Fixed operating costs

Costs that do not vary with the production rate are referred to as fixed operating costs (Sinnott and Towler, 2020). These costs have to be paid irrespective of the quantity of product produced. They include maintenance, operating labour, laboratory costs, supervision, plant overheads, capital charges, rates, insurance, license fees and royalty payments (Sinnott and Towler, 2020). For the operating labour, a labour burden is applied to the total salary costs to cater for items such as general engineering and plant maintenance, payroll overhead including fringe benefits, plant security, communication and lighting (Sinnott and Towler, 2020).

2.13.2.5.2 Variable operating costs

Variable operating costs depend on the amount of product produced. They include raw materials, miscellaneous operating materials, utilities, shipping and packaging (Sinnott and Towler, 2020).

2.13.3 Estimating capital costs

According to Humbird et al. (2011), the purchased cost for a given equipment reflects a baseline equipment size. As changes are made to the process, the equipment size required may be different than what was originally designed. Instead of re-costing in

detail, an exponential scaling expression can be applied (Humbird et al. 2011). Such scaled costs are easier to calculate and generally give nearly the same result as resizing the equipment for each scenario (Humbird et al. 2011).

2.13.4 Discounted cash-flow rate of return

The discounted cash-flow rate of return (DCFROR) is a measure of the maximum rate of interest that a project can pay and still break even by the end of the project life (Sinnott and Towler, 2020). The more profitable the project is, the higher the DCFROR that it can afford to pay (Sinnott and Towler, 2020). The TCI along with plant operating costs which are developed from mass balance flow rates from Aspen Plus are used to evaluate the DCFROR. This type of analysis is referred to as the techno-economic model. This model estimates the cost of bioethanol and the MBSP from a given production technology.

2.14 Reaction Kinetics

2.14.1 Chemical kinetics

Chemical kinetics deals with the experimental determination of reaction rates from which rate laws and rate constants are derived. Chemical reactions can either be homogeneous (one phase) or heterogeneous (multi-phase) (Fogler, 2016). On the other hand, reactions can be reversible or irreversible. A reversible reaction is one that proceeds in either direction, depending on the concentrations of reactants and products relative to the corresponding equilibrium concentrations (Fogler, 2016). An irreversible reaction is one that proceeds in only one direction and continues in that direction until one of the reactants is exhausted (Fogler, 2016).

2.14.2 Factors affecting reaction rate

The rate of a given reaction is affected by: nature of the reactants, physical state of the reactants, surface area of solid reactants, concentrations of the reactants, temperature at which the reaction occurs, pressure at which the reaction occurs and whether or not any catalysts are present in the reaction (Fogler, 2016).

2.14.3 Activation energy

The activation energy can be thought of as a barrier to energy transfer from kinetic energy to potential energy between reacting molecules that must be overcome (Fogler, 2016). Therefore, activation energy is the minimum increase in potential energy of the reactants that must be provided to transform the reactants into products. This increase can be provided by the kinetic energy of the colliding molecules (Fogler, 2016).

2.14.4 The Arrhenius equation

It was the great Nobel Prize–winning Swedish chemist Svante Arrhenius (1859–1927) who first suggested that the temperature dependence of the specific reaction rate, k_A, could be correlated by an equation of the type:

$$k_A(T) = A_o e^{-E_a/RT} \qquad 2.0$$

Where:

k_A = reaction rate constant

A_o = pre-exponential factor or frequency factor

E_a = activation energy, J/mol

R = universal gas constant = 8.314 J/mol*K

T = absolute temperature, K (Fogler, 2016).

The pre-exponential factor (A_o) relates to the frequency of collisions and the orientation of a favorable collision probability (Fogler, 2016). Both A_o and E_a are specific to a

particular reaction. Equation 2.0 is known as the Arrhenius equation (Fogler, 2016). The activation energy is determined experimentally by measuring the reaction rate at several different temperatures (Fogler, 2016). Taking the natural logarithm of Equation 2.0, we obtain:

$$\ln k_A = \ln A_o - \frac{E_a}{R}\left(\frac{1}{T}\right) \qquad 2.1$$

The activation energy can be found from a plot of ln k_A as a function of (1/T) (Fogler, 2016).

2.15 Kinetics of Glucose Production From LGB

According to Tizazu and Moholkar (2018), the chemical mechanism of acid hydrolysis of polysaccharides found in LGB is quite complex. This reaction system is heterogeneous because the LGB is in the solid phase while the catalyst (acid) is in the liquid phase (Tizazu & Moholkar, 2018). According to Kumar et al. (2015), the kinetics of acid hydrolysis of LGB is influenced by several factors that are related to the nature of the LGB and the reactions conditions. Some of the factors related to the nature of LGB include particle shape and size of LGB, porosity and surface area of LGB, crystallinity of the cellulosic fraction of LGB, the structure and composition of LGB and the chemical structure of the various compounds found in LGB (Kumar et al., 2015). Factors related to operating conditions include hydrolysis time and temperature, acid concentration, reaction pressure and intensity of mixing (Kumar et al., (2015). Acid hydrolysis of LGB can be carried out using dilute or concentrated acid (Alicia, 2013). Kinetics of dilute acid hydrolysis of LGB has been studied by several researchers, with few studies on kinetics of concentrated acid hydrolysis of LGB available.

2.15.1 Models used in kinetic studies during acid hydrolysis of LGB

Kinetic studies require the use of models. During hydrolysis of LGB, the widely used model is the one that was proposed by Saeman. The Saeman kinetic model was further refined into the biphasic or two fraction model (Tizazu and Moholkar, 2018).

2.15.1.1 The Saeman kinetic model

According to Yuan et al. (2021), Saeman studied kinetics of wood chips hydrolysis using H_2SO_4. Saeman reported that the reaction rate increased with an increase in reaction temperature and acid concentration (Yuan et al., 2021). According to Abril-González et al. (2023), simple kinetic models assume that hydrolysis proceeds directly from polysaccharides to monosaccharides without forming any intermediate products. Kinetics of cellulose hydrolysis using acids can be described by the Saeman model (Yuan et al., 2021). The model for cellulose hydrolysis proceeds as shown in Equation 2.2.

$$\text{Cellulose} \xrightarrow{1} \text{Glucose} \xrightarrow{2} \text{Degradation products} \qquad 2.2$$

According to Tizazu and Moholkar (2018), Equation 2.2 can be generalized for polysaccharides found in LGB as shown in Equation 2.3.

$$\underset{\text{(Cellulose/Hemicellulose)}}{\text{Polysaccharide}} \xrightarrow{1} \underset{\text{(Glucose/xylose)}}{\text{Sugar monomers}} \xrightarrow{2} \underset{\text{(HMF/furfural)}}{\text{Decomposition products}} \qquad 2.3$$
(Glucan/xylan)

Step 1 in Equation 2.3 represents hydrolysis of cellulose and hemicellulose to glucose and xylose respectively, while step 2 represents the degradation of glucose and xylose to HMF and furfural respectively. The Saeman model can be applied to study the kinetics of cellulose and hemicellulose hydrolysis (Yuan et al., 2021). Acid hydrolysis of cellulose present in LGB is a heterogeneous reaction (Kumar et al., 2015). However,

for modelling purposes the following assumptions are adopted during hydrolysis of cellulose:

1. The total cellulose/glucan content in the LGB comprises of the easy to hydrolyze and the hard to hydrolyze fractions (Kumar et al., 2015).
2. The main product from cellulose hydrolysis is glucose (Kumar et al., 2015).
3. The degradation product for glucose is HMF (Kumar et al., 2015).
4. The reaction of easy and hard to hydrolyze fractions follows homogeneous first order kinetic law.
5. The fast-reacting glucan reacts with a higher kinetic parameter while the slow reacting glucan reacts at a lower kinetic parameter (Tizazu & Moholkar, 2018).

The two steps in Equation 2.3 are considered to be pseudo homogenous first order reactions with Arrhenius type temperature dependence of reaction rate constants as shown by Equation 2.4. The pseudo homogeneous reactions occur near the glucan-water interface (Tizazu & Moholkar, 2018).

$$k_{1,2}(t) = (A_o)_{1,2}\exp\left(-\frac{E_{1,2}}{RT(t)}\right) \qquad 2.4$$

Where:

$E_{1,2}$ is the activation energy for reaction 1 and 2 respectively (Tizazu & Moholkar, 2018).

R = universal gas constant (Tizazu & Moholkar, 2018).

T (t) = temperature (K) at any time, t (Tizazu & Moholkar, 2018).

(A_o) 1,2 are the pre-exponential factor (Tizazu & Moholkar, 2018).

In order to calculate the kinetic parameters, $\ln(k)_{1,2}$ versus 1/T curves are plotted.

Using Equation 2.3, material balance for cellulose hydrolysis can be expressed as follows:

$$\frac{dC_A}{dt} = -k_1 C_A$$

$$\frac{dC_B}{dt} = -k_1 C_A - k_2 C_B \quad 2.5$$

$$\frac{dC_C}{dt} = k_2 C_B$$

Where:

C_A = concentration of cellulose/glucan

C_B = concentration of glucose

C_C = concentration of decomposition product

The proposed Saeman kinetic model is represented by Equation 2.6.

$$C_B(t) = \frac{k_1 C_{AO}}{(k_2 - k_1)} [\, e^{-k_1 t} - e^{-k_2 t}] \quad 2.6$$

Where:

C_B = instantaneous glucose concentration (g/L)

C_{AO} = initial cellulose/glucan concentration (g/L)

k_1 = kinetic constant for glucose formation (min^{-1})

k_2 = kinetic constant of glucose degradation (min^{-1})

t = time (minutes) (Mensah et al., 2020; Tizazu & Moholkar, 2018).

Using integration and Laplace transform, Equation 2.6 was obtained. The manner in which Equation 2.6 was arrived at is shown in Appendix D.

2.15.1.1 The biphasic kinetic model

The Saeman model is modified by introducing a parameter β so as to include the existence of two fractions i.e., the easy and hard to hydrolyze fractions of cellulose (Tizazu & Moholkar, 2018). The modified model is referred to as the biphasic or the two-fraction model. The parameter β represents the mass ratio of susceptible cellulose fraction to total cellulose in the raw LGB. Modification of Equation 2.6 leads to Equation 2.7.

$$C_B(t) = \frac{k_1 C_{Ao} \beta}{(k_2 - k_1)} [\, e^{-k_1 t} - e^{-k_2 t}] \qquad 2.7$$

The kinetic parameters are obtained after fitting the experimental data into Equation 2.7. Solver, Microsoft Excel software is used to calculate the rate constants by minimizing the sum of square deviations between experimental and calculated data (Kumar et al., 2015). If the value of k_1 in Equation 2.7 is greater than k_2, then it implies that the rate of glucose formation during hydrolysis of LGB is much faster than the rate of glucose degradation. In addition, lower values of k_2 are a consequence of higher activation energy of glucose degradation (Tizazu & Moholkar, 2018). The biphasic model is mostly applied during kinetic studies of LGB than the Saeman model because it fits the experimental data well (Yuan et al., 2021). In general, the rate constants and kinetic parameters obtained from acid hydrolysis of LGB depend on the type of LGB and the reaction conditions such as acid concentration, reaction temperature and reaction time. The LGB used in acid hydrolysis also differs in composition of cellulose, hemicellulose and lignin. In addition, the crystallinity of cellulose differs among the various types of LGB. This variation in composition and crystallinity leads to different values of kinetic parameters during hydrolysis of LGB (Kanchanalai et al., 2016). Therefore, all these factors need to be considered when modelling the kinetics of concentrated acid hydrolysis of LGB. Kinetic studies are aimed at establishing a suitable kinetic model that describe the hydrolysis of LGB. In addition, these studies aim at optimizing the hydrolysis reaction conditions, thus obtaining optimum conditions. In the hydrolysis of LGB, optimum conditions represent the ease with which the hydrolysis reaction proceeds. According to Kumar et al. (2015), the maximum concentration of glucose can be obtained from Equation 2.8

$$C_{Bmax} = C_{Ao} \left(\frac{k_1}{k_2}\right)^{\left(\frac{k_2}{k_2 - k_1}\right)} \qquad 2.8$$

Where:

C_{Bmax} - maximum concentration of glucose (g/L)

The hydrolysis time (t_{max}) at which maximum concentration of glucose occurs during kinetic studies is obtained from Equation 2.9 (Kumar et al., (2015).

$$t_{max} = \frac{\ln\left(k_2/k_1\right)}{(k_2 - k_1)} \qquad 2.9$$

In the current research study, the biphasic kinetic model was used to study the kinetics of SSS and maize cobs cellulose hydrolysis using concentrated H_2SO_4.

2.16 Optimization

Optimization studies entail exploring the process variables for maximum response. The experimental data obtained in any given research study is fitted into a suitable correlation and then plotted in surface and contour plots so as to depict optimal conditions. Response surface methodology (RSM) consists of statistical and mathematical techniques used to generate and analyze models with the sole aim of establishing optimum levels of factors that affect the response of interest (Montgomery, 2013).

2.16.1 Central Composite Design

Central Composite Design (CCD) is an established technique that is used in the optimization of experimental factors. In statistics, CCD is an experimental design, useful in RSM for generating second order quadratic polynomial for the response without the necessity of using a complete level factorial experiment (Montgomery, 2013). The Central Composite Rotatable Design (CCRD) was developed by Box and Hunter (Montgomery, 2013). The aim was to introduce rotatability in the CCD (Montgomery, 2013). CCRD consists of three sets of experimental runs which are:

i. A factorial design consisting of factors being studied. In this research there are three factors each with two levels.

ii. Center point experimental runs whose values of each factor are the medians of the values used in the factorial portion.

iii. A set of axial or star points experimental runs identical to the center points except for one factor which will take on the values below and above the median of the three factorial levels and typically outside their range (Montgomery, 2013).

The axial points are actually meant to ensure rotatability of the design. The distance of the axial points from the median is given by Equation 2.10.

$$\propto = (2^{k})^{1/4} \qquad 2.10$$

Where:

$\propto =$ Distance of axial points

k = Number of independent variables (Montgomery, 2013).

2.16.2 Full factorial design

In a full factorial experimental design, the total number of experimental combinations is given by Equation 2.11.

$$N = 2^{k} + 2k + n_o \qquad 2.11$$

Where:

N = Total number of experimental combinations

n_o = Central point experimental repetitions

The independent variables x_i are coded as shown in Equation 2.12.

$$x_i = \frac{X_i - \bar{x_i}}{\Delta x_j} \quad i = 1, 2, 3\ldots\ldots, k \qquad 2.12$$

Where:

x_i = Dimensionless values of the independent variables

X_i = Real value of the independent variable

$\bar{x_i} =$ Real value of the independent variable at the central point

$\Delta x_j =$ Step change (Montgomery, 2013).

The predicted response is given by the second order polynomial shown in Equation 2.13.

$$Y = \beta_o + \sum_{i=1}^{k} \beta_i x_i + \sum_{i=1}^{k} \beta_{ij} x_i^2 + \sum_{i_i<j}^{k} \sum_{j}^{k} \beta_{ij}\, x_i x_j + \varepsilon \qquad 2.13$$

Where:

Y = Predicted response

β = Regression coefficient

i, j = linear and quadratic coefficient respectively

ε = Random error (Montgomery, 2013).

2.16.3 The empirical model

In response surface designs, a complete description of the behaviour of the process may require a quadratic or cubic model (Montgomery, 2013). Equation 2.14 shows a model for three independent factors.

$$Y = \beta_o + \beta_1 X_1 + \beta_2 X_2 + \beta_3 X_3 + \beta_{11} X_1^2 + \beta_{12} X_1 X_2 + \beta_{13} X_1 X_3 + \beta_{23} X_2 X_3 + \beta_{22} X_2^2 + \beta_{33} X_3^2 \qquad 2.14$$

In Equation 2.14, Y is the dependent variable while X_1, X_2 and X_3 are the independent variables. The three terms in Equation 2.14 with single X are the main effects terms. Equation 2.14 depicts a full model with all possible terms. It is rare to have a model where all terms are required for a given application. If the researcher takes advantage of all tools available in multiple regression analysis as well as define factor limits appropriately, then it is quite unusual to find an industrial process that requires a third order model. This therefore implies that most response designs can be fitted by quadratic models (Montgomery, 2013).

2.16.4 Testing the significance of a regression

In order to determine the presence of a linear relation between a response y and a group of factors, the following hypothesis is employed.

$H_O: \beta_1 = \beta_2 = \cdots = \beta_{r+1} = 0$ 2.15

$H_1: \beta_{ij} \neq 0$ for at least one j 2.16

Where:

H_O = Null hypothesis

H_1 = Valid hypothesis

β_{ij} = Regression coefficient

The hypothesis H is only valid if at least one of the factors $x_1, x_2 \ldots \ldots \ldots, x_k$ contributes significantly to the regression model (Montgomery, 2013).

2.16.5 F- Test for regression model and lack of fit

F- test is used to test the significance of a model.

F statistics of $H_O: \beta_1 = \beta_2 = \cdots = \beta_{r+1} = 0$ is given by Equation 2.17.

$$F = \frac{SS_{R/r}}{SS_E/n-r-1} = \frac{MSS_R}{MSS_E} \quad 2.17$$

Where:

F = F- Value

MSS_E = Error Mean Sum of Squares

MSS_R = Regression Mean Sum of Squares

SS_E = Error Sum of Squares

SS_R = Regression Sum of Squares

r = Regression Degrees of Freedom

H_O is rejected if $F_O > F_{\alpha,r,n-r-1}$

Where:

H_O = Null hypothesis

F_O = Observed F- value

$F_{\alpha,r,n-r-1}$ = Critical F- value

2.16.6 Coefficient of determination

Coefficient of determination (R^2) is a measure of the variability of a response Y due to factors involved in the experiment. R^2 is given by Equation 2.18.

$$R^2 = \frac{SS_R}{SS_y} = 1 - \frac{SS_E}{SS_y} \quad 2.18$$

Where:

SS_y = Total Sum of Squares (Montgomery, 2013).

Addition of more variables affecting the response y will always increase the value of R^2 and never reduce it. The adjusted coefficient of determination R^2_{adj} is used to adjust for the number of X variables in the model. It alters R^2 by dividing each sum of squares by its associated degrees of freedom as shown by Equation 2.19 (Montgomery, 2013).

$$R^2_{adj} = 1 - \frac{SS_E/(N-r-1)}{SS_y/(N-1)} = 1 - \frac{(N-1)}{(N-r-1)}(1 - R^2) \quad 2.19$$

2.17 Software Application

In this research study, Aspen Plus software was used in modeling and simulation studies. Design-Expert 13 software was used in design of experiments, regression analyses, analysis of variance (ANOVA) and plotting of response surface and contour plots. Microsoft Excel software was used in kinetic studies.

2.18 Current Outlook for Large-Scale Bioethanol Production

In a review titled "Pretreatment methods for lignocellulosic biofuels production: current advances, challenges and future prospects", Cheah et al., (2020), concluded that "most

of the reports available in the literature were performed at lab scale and there is limited information on the real-world production cost arising from all the stages involved in biofuel production from lignocellulosic biomass, i.e., delignification, hydrolysis, and fermentation" (Cheah et al., 2020. p. 1124). "Therefore, future research works should be devoted to the optimization of operating parameters and assessment of total cost of biofuel production from lignocellulose biomass at large-scale by using different pretreatment methods" (Cheah et al., 2020. p. 1124). "Such information would pave the way for industrial scale lignocellulosic biofuels production" (Cheah et al., 2020. p. 1124).

According to da Silva et al. (2017), most studies involving the production of bioethanol report on experimental studies, with little concern given to large-scale 2GBE production processes. In addition, due to the presence of a variety of LGB and the existence of several pretreatment, hydrolysis and fermentation technologies, it is difficult to select the best 2GBE production technology (da Silva et al., 2018). Lack of sufficient techno-economic data on large-scale production of 2GBE impedes its commercialization. This is mainly due to scale-up problems caused by high costs involved as we move from the laboratory scale to pilot plant scale and eventually to large-scale (Beluhan et al., 2023; Gebreyohannes, 2010). Other issues that require consideration during commercialization of 2GBE, include the availability of the LGB and the chemical composition of the LGB. Variation in chemical composition of different LGB affects the yield of 2GBE, influences the choice of pretreatment and hydrolysis method to be used, the size of the equipment and the energy requirements for the entire process (Triana, 2016).

In conclusion, this study involved modeling and simulation of a large-scale process of producing bioethanol from SSS and maize cobs found in Kenya. The research study applied the concepts of process system engineering to develop and analyze feasible pathways to convert SSS and maize cobs into 2GBE. In addition, the study involved optimization and kinetics study of concentrated H_2SO_4 hydrolysis of SSS and maize cobs. The main concern was to address improvement of hydrolysis yield. The data obtained during kinetic studies was used to model and simulate a large-scale process of concentrated H_2SO_4 hydrolysis of SSS and maize cobs found in Kenya.

CHAPTER THREE: EXPERIMENTAL MATERIALS, EQUIPMENT AND PROCEDURE

3.1 Experimental Materials

3.1.1 Reagents and standards

The following reagents and standards were procured for use in the research: sodium hydroxide, H_2SO_4, calcium hydroxide, glucose standard, glucose HK reagent, ethanol standard and distilled water.

3.2 Experimental Equipment

Different types of equipment were used in this study for characterization, hydrolysis, kinetic studies, modeling and simulation. Detailed description of the equipments that were used in this research study are shown in Table 3.1.

3.3 Experimental Procedure

This research study was carried out through literature review, laboratory experimentation, modeling and simulation. CCRD was used to determine statistically the optimum combination of hydrolysis conditions (temperature, time and concentration of acid) under constrained particle size and SLR. Statistical software, Design-Expert 13 was used to generate the CCRD matrix, plotting of graphs and subsequent analysis of data. Three-dimensional Response Surface Plots (RSP) were generated using Design-Expert 13 in order to evaluate the effects of the variables on the response of interest. During kinetic studies, temperature and time were varied while the modified Saeman model was used to establish the rate constants. The kinetic parameters were established from the Arrhenius plot. Modeling and simulation software, Aspen Plus V8.4., (2013) was used in the study. The research study was done at Moi University, Kenya and Indian Institute of Technology Bombay, India.

Table 3. 1: Equipment used during the study

Equipment	Model	Purpose
Analytical balance	Mettler AE 160	Weighing chemicals and sample biomass
Oven	LabTech- LDO 150F	Drying of biomass
Furnace	CARBOLITE GERO-ELF 11/14B	Determination of ash content of biomass samples
Sieve and sieve shaker	Liya	Size classification
pH meter	Labtech Digital meter	Measuring pH during kinetic studies
Glass ware: Erlenmeyer flasks, volumetric flasks, test tubes, round bottom flasks, burettes, pipets, beakers, glass rods and droppers, boiling tubes, measuring cylinders and flasks, sample bottles/ tins for storing the samples, plastic bags	Assorted	Hydrolysis, kinetic studies and analysis of samples
UV-VIS-Spectrophotometer	SHIMADZU	Analysis of acid soluble lignin and glucose
Refrigerator /Freezer	LG	Storage of samples and reagents
Water bath	JOANLAB	Hydrolysis and kinetic studies
Vacuum filtration unit	ROCKER- Chemker 410	Filtration of hydrolysates during hydrolysis and kinetic studies
Desktop computer and Software (Aspen Plus V8.4)	LENOVO	Modeling and simulation
Laptop with Design-Expert 13 software	HP	Word processing, Excel, Microsoft Excel solver and Design and analysis of hydrolysis experiments, plotting of response surface & contour plots

3.3.1 Methodology

3.3.1.1 Collection of Samples

Sorghum stalks were obtained from a farm located in Bungoma County while maize cobs were obtained from a farm located in Nakuru County. Sorghum stalks were randomly picked from various sections within the farm after harvesting the sorghum grain. The stalks were packed in airtight plastic bags. Maize cobs were randomly picked from a pile after shelling was completed. The maize cobs samples were picked from the top, middle and bottom of the pile. The collected maize cobs were packed in airtight plastic bags. The biomass sampling technique used was based on a report by (Marinescu et al., 2015). The samples were then dispatched to the Chemical and Process Engineering laboratory within 24 hours after collection for further studies.

3.3.1.2 Drying and Milling of Substrate

SThe substrates (sorghum stalks and maize cobs) were cleaned using fresh water and dried under the sun for fourteen days. Further drying was done using a hot air oven set at 60°C for 24 hours. The substrates were then subjected to physical pretreatment through milling and thereafter sieved to pass 0.8 mm screen. The classified substrates were stored in sealed plastic containers. The chemical composition of substrates was analyzed in triplicate, using procedures described by National Renewable Energy Laboratory – Laboratory Analytical Procedures (NREL-LAP). The specific procedures which were used included: American Society for Testing and Materials (ASTM E 1757 – 01), NREL-LAP standard method No.001, **(**Tina, 1994), NREL-LAP standard method No. 002, (Ruiz, and Tina, 1996). NREL-LAP standard method No. 003, (David, and Tina, 1995), NREL-LAP standard method No. 004, (Tina, 1996), NREL- LAP standard method No.005, **(**Tina, 1994), NREL-LAP standard method No.008, **(**Hayward et al., 1995), NREL-LAP standard method No.010, **(**Tina, 1994) NREL-LAP standard

method No.011, **(**David, 1994) and NREL-LAP standard method No.012, **(**Tina, 1994). Plate 3.1 and Plate 3.2 shows samples used in the study.

Plate 3. 1: Sorghum stalks samples

Plate 3. 2: Maize cobs samples

3.3.2 Modeling and simulation

Process flow diagrams (PFDs) were modeled and simulated using Aspen Plus software (Aspen Plus V8.4, 2013). Capital and operating costs were estimated using data from literature. This information was used to calculate bioethanol production cost, IRR and

the MBSP. The average consumption of gasoline in Kenya was about 166 million liters per month between January-June 2019 (PIEA, 2019). Under the E10 policy (where 10% ethanol is blended with 90% gasoline), about 200 million liters of bioethanol will be required every year for blending with gasoline. It is on the basis of this requirements that this research study proposed a bioethanol production plant with a capacity to process 102,900 kg/h of LGB and an annual operation time of 7920 hours. This capacity and annual operation time was within the range reported for similar studies reported in literature (da Silva et al., 2019; da Silva et al., 2016; Humbird et al., 2011).

3.3.2.1 Chemical components

In developing the process model of producing 2GBE from sorghum stalks and maize cobs, all the chemical compounds that were involved in the process were selected from the built-in database found in Aspen Plus (Aspen Plus V8.4, 2013).

3.3.2.2 Thermodynamic model selection

Modeling and simulation of 2GBE production process from sorghum stalks and maize cobs was carried out by selecting proper thermodynamic models for each unit operation involved (Aspen Plus, 2000). In the pretreatment process, LGB (sorghum stalks and maize cobs) at ambient pressure and temperature were in solid phase. The activity coefficients for the water-ethanol mixture were calculated using the NRTL property model (Aspen Plus V8.4, 2013).

3.3.2.3 Reactor Models

Pretreatment, hydrolysis and fermentation process steps were modeled using the stoichiometric reactor model (Rstoic) (Aspen Plus V8.4, 2013). The Rstoic model was selected due to availability of reaction data for the above process steps. The Rstoic model in Aspen Plus performs mass and energy balances based on the reaction

stoichiometry and extent of conversion of the reactants during pretreatment, hydrolysis and fermentation (Aspen Plus V8.4, 2013).

3.3.2.3.1 Flush separation

Prior to conditioning of pretreated LGB, flushing was done. This was modeled using a flash separator in Aspen Plus (Aspen Plus V8.4, 2013). The SSCF process produces a product called beer, which mainly consists of ethanol, unreacted cellulose and hemicellulose, water, carbon dioxide and lignin. The beer stream from the SSCF process is sent to a flash separator in order to remove carbon dioxide followed by purification through distillation and molecular sieve dehydration in order to obtain ethanol which is the final product. The flash separator model was selected due to the phases involved.

3.3.2.3.2 Distillation models

Rigorous distillation model (RadFrac) was used to model the beer and the rectification column (Aspen Plus V8.4, 2013). The RadFrac model was selected due to the composition of the process stream involved and its simplicity. RadFrac model is most suitable for water -ethanol systems. In terms of simplicity, RadFrac model is suitable for process streams such as water-ethanol systems unlike PetroFrac model that is suitable for complex process streams such as those found in petroleum refining (Aspen, 2000).

3.3.2.3.3 Molecular sieves

Molecular sieve dehydration was modeled using a separation block (Aspen Plus V8.4, 2013).

3.3.2.3.4 Scrubbing

The scrubber was used to separate carbon dioxide and ethanol using water. The scrubber was modeled using an absorption tower found in RadFrac model (Aspen Plus V8.4, 2013).

3.3.2.4 Stream Input and equipment specification

The required input data was entered into the simulator. This was done for each unit operation. Temperature, feedstock flowrate, feedstock composition and pressure were specified in the input specification sheet for each stream. Using the specified input data, other parameters were calculated by the selected thermodynamic models (Aspen Plus V8.4, 2013).

3.3.2.5 Simulation output

After defining the input data for each unit operation, the simulator was run in order to performs mass and energy balance and the results were displayed in stream tables. The simulator gave the output temperature, pressure, heating and cooling demand for each unit operation.

3.3.2.6 Sensitivity analysis studies

Aspen Plus is equipped with model analysis tools. These tools include sensitivity analysis, optimization, constraint analysis and data fit (Aspen Plus V8.4, 2013). The sensitivity analysis tool was used to analyze and predict the behavior of the full process model to changes in key cost and process operating variables. The effect of changing cost and process parameters on bioethanol production cost and the MBSP was established by varying the LGB flowrate, conversion of cellulose to glucose in SSCF reactor, LGB and enzyme costs, FCI, plant life, discount rate and income tax rate. Results from the sensitivity analysis were used to indicate how the techno-economic

feasibility of the process behaved when carried out at different cost and operating conditions.

3.3.3 Summary of the process

Modeling and simulation of the pretreatment of sorghum stalks and maize cobs was performed using dilute H_2SO_4, steam explosion and sodium hydroxide pretreatment methods. This was followed by modeling and simulation of SHCF and SSCF process technologies using process streams from the three types of pretreatments mentioned above. Thereafter, the best pretreatment and hydrolysis method was selected based on ethanol production rate, energy demand and the energy intensity of the process. Using the models selected for pretreatment and hydrolysis, a full-scale process model that combined pretreatment, hydrolysis, fermentation, product recovery, purification and dehydration was modelled and simulated.

3.3.4 Pretreatment processes

The dilute H_2SO_4, steam explosion and alkaline pretreatment methods were modelled and simulated.

3.3.4.1 Dilute sulphuric acid pretreatment

The LGB (sorghum stalks and maize cobs) was delivered to the feed handling area from where it was conveyed to the pretreatment area using a screw conveyer (Humbird et al., (2011). In this process step, the LGB was treated with dilute sulphuric acid at a high temperature in order to liberate xylose from hemicellulose, decrystallize and depolymerize the cellulose fraction. Ammonia-water solution was then mixed with the whole pretreatment slurry in order to raise its pH from 1.0 to 5.0 for effective enzymatic hydrolysis (Humbird et al., 2011). The conditions used in this process are shown in Table 3.2.

Table 3. 2: Conditions for dilute sulphuric acid pretreatment (Humbird et al., 2011)

Parameter	Value	Units
Solid concentration	30	%, w/w
Acid concentration	22.1	mg/g dry biomass
Temperature	160	^{o}C
Pressure	6.0	atm
Ammonia	1.97	g/L of conditioned slurry

The main reactions that occur during dilute sulphuric acid pretreatment and ammonia conditioning of pretreated slurry are shown in Table 3.3 and Table 3.4. The percentage conversions and reaction conditions were selected based on literature (Humbird et al., 2011).

Table 3. 3: Main reactions that occur during dilute sulphuric acid pretreatment (Humbird et al., 2011)

Reaction	Product	Conversion (%)
$C_5H_8O_4 + H_2O \rightarrow C_5H_{10}O_5$	Xylose	90.0
$C_6H_{10}O_5 + H_2O \rightarrow C_6H_{12}O_6$	Glucose	9.9
$C_5H_8O_4 \rightarrow C_5H_4O_2 + 2H_2O$	Furfural	5.0

In the reactions shown in Table 3.3, 90% of the available hemicellulose was converted to xylose, 9.9% of the available cellulose was converted to glucose while 5% of the remaining hemicellulose was converted to furfural (Humbird et al., 2011).

Table 3. 4: Main reaction during ammonia conditioning (Humbird et al., 2011).

Reaction	Product	Conversion (%)
$2NH_3 + H_2SO_4 \rightarrow (NH_4)_2SO_4$	Ammonium sulphate	100.0

3.3.4.2 Steam explosion pretreatment

Steam explosion pretreatment of LGB was carried out under conditions shown in Table 3.5.

Table 3. 5: Conditions for steam explosion pretreatment (Ortiz & Oliveira, 2014)

Parameter	Value	Units
Solid concentration	30	%, w/w
Pressure	15.3	atm
Temperature	198	^{o}C
Steam	0.5	kg/kg biomass

The main reactions occurring during steam explosion pretreatment are shown in Table 3.6.

Table 3. 6: Reactions that occur during steam explosion pretreatment (Ortiz & Oliveira, 2014)

Reaction	Product	Conversion (%)
$C_5H_8O_4 + H_2O \rightarrow C_5H_{10}O_5$	Xylose	61.4
$C_6H_{10}O_5 + H_2O \rightarrow C_6H_{12}O_6$	Glucose	4.1
$C_5H_8O_4 + H_2O \rightarrow 2.5C_2H_4O_2$	Acetic acid	9.2
$C_5H_8O_4 \rightarrow C_5H_4O_2 + 2H_2O$	Furfural	5.1

In the reactions shown in Table 3.6, 61.4% of the available hemicellulose was converted to xylose, 4.1% of the available cellulose was converted to glucose while 9.2% and 5.1% of the remaining hemicellulose was converted to acetic acid and furfural respectively (Ortiz & Oliveira, 2014).

3.3.4.3 Alkaline pretreatment

Alkali pretreatment of LGB was carried out under conditions shown in Table 3.7.

Table 3. 7: Conditions for alkaline pretreatment (Davis et al., 2018)

Parameter	Value	Units
Solid concentration	30	%, w/w
Total NaOH loading	2	%, w/w
Temperature	87	^{o}C
Pressure	1	atm

During alkaline pretreatment, the substrates underwent a physical process (dissolution). The main constituents of the substrate were separated into liquid and solid streams as shown in Table 3.8. The solid stream was then taken to the SSCF reactor (Davis et al., 2018).

Table 3. 8: Output from separation unit during alkaline pretreatment

LGB fraction	Liquid stream (%, w/w)	Solid stream (%, w/w)
Cellulose	1	99
Hemicellulose	80	20
Lignin	80	20
Ash	100	-
Extractives	100	-
Water	90	10

3.3.5 Enzymatic hydrolysis

Enzyme cellulase was used to hydrolyze the pretreated LGB under conditions shown in Table 3.9. Enzymatic hydrolysis was selected because enzymes can be produced on-site from the LGB being processed (Humbird et al., 2011).

Table 3. 9: Conditions for separate hydrolysis (Humbird et al., 2011)

Parameter	Value	Units
Solid concentration	20	%, w/w
Temperature	50	^{o}C
Cellulase loading	20	mg protein/g cellulose

The main reactions occurring during separate hydrolysis are shown in Table 3.10.

Table 3. 10: Main reaction that occur during separate hydrolysis (Humbird et al., 2011)

Reaction	Product	Conversion (%)
$C_6H_{10}O_5 + H_2O \rightarrow C_6H_{12}O_6$	Glucose	90.0

During separate hydrolysis, 90% of the available cellulose was converted to glucose (Humbird et al., 2011).

3.3.5.1 Hydrolysis reactions

The hydrolysis reactions employ water to break the cellulose ($C_6H_{10}O_5$) and hemicellulose ($C_5H_8O_4$) carbohydrates into glucose ($C_6H_{12}O_6$) and xylose ($C_5H_{10}O_5$) respectively. The maximum amount of glucose and xylose that can be obtained from hydrolysis of cellulose and hemicellulose can be established using Equations 3.1 and 3.2 respectively (da Silva et al., 2018).

$$C_6H_{10}O_5 + H_2O \rightarrow C_6H_{12}O_6 \quad 3.1$$

One gram of cellulose (molecular weight = 1*162) produces 1.11 grams of glucose (molecular weight = 1*180)

$$C_5H_8O_4 + H_2O \rightarrow C_5H_{10}O_5 \quad 3.2$$

One gram of hemicellulose (molecular weight = 1*132) produces 1.136 grams of xylose (molecular weight = 1*150). Therefore, the maximum theoretical yield of glucose and xylose are 1.11 g/g and 1.136 g/g of cellulose and hemicellulose respectively (da Silva et al., 2018).

3.3.6 Fermentation

The co-fermentation reaction was done using *Zymomonas mobilis* (microorganism) under conditions shown in Table 3.11. The final product of fermentation (beer) was stored in the beer storage tank prior to product separation and purification (Humbird et al., 2011). In the case of SSCF, hydrolysis and fermentation were performed in one reactor (Humbird et al., 2011).

Table 3. 11: Conditions for co- fermentation (Humbird et al., 2011)

Parameter	Value	Units
Solid concentration	20	%, w/w
Temperature	35	^oC
Pressure	1.0	atm

The main reactions occurring during co-fermentation are shown in Table 3.12.

Table 3. 12: Main reactions that occur during co-fermentation (Humbird et al., 2011)

Reaction	Product	Conversion (%)
$C_6H_{12}O_6 \rightarrow 2C_2H_5OH + 2CO_2$	Ethanol	95.0
$3C_5H_{10}O_5 \rightarrow 5C_2H_5OH + 5CO_2$	Ethanol	85.0

During co-fermentation, 95% of the available glucose was converted to ethanol while 85% of the available xylose was converted to ethanol (Humbird et al., 2011).

The SSCF reaction was done under conditions shown in Table 3.13.

Table 3. 13: Conditions for SSCF (Humbird et al., 2011)

Parameter	Value	Units
Solid concentration	20	%, w/w
Temperature	32	^oC
Pressure	1.0	atm

The main reactions occurring during SSCF are shown in Table 3.14.

Table 3. 14: Main reactions that occur during SSCF (Humbird et al., 2011)

Reaction	Product	Conversion (%)
$C_6H_{10}O_5 + H_2O \rightarrow C_6H_{12}O_6$	Ethanol	85.5
$C_6H_{12}O_6 \rightarrow 2C_2H_5OH + 2CO_2$		
$3C_5H_{10}O_5 \rightarrow 5C_2H_5OH + 5CO_2$	Ethanol	85.0

During SSCF, 85.5% of the available cellulose and hemicellulose were converted to ethanol (Humbird et al., 2011).

3.3.6.1 Fermentation reactions

Microorganisms can degrade a variety of sugars such as glucose and xylose. The theoretical yield of bioethanol from these sugars can be calculated from the stoichiometric equations that describe the conversion of these sugars into bioethanol. Equation 3.3 and Equation 3.4 illustrate how maximum amount of ethanol (C_2H_5OH)

obtained during fermentation can be established for glucose and xylose respectively (da Silva et al., 2018).

$$C_6H_{12}0_6 \rightarrow 2C_2H_50H + 2CO_2 \quad 3.3$$

From Equation 3.3, one gram of glucose (molecular weight = 1*180) produces 0.511 grams of ethanol (molecular weight = 2*46) and 0.489 grams of carbon dioxide (molecular weight = 2*44). Similar equation can be written for xylose as shown in Equation 3.4, thus:

$$3C_5H_{10}0_5 \rightarrow 5C_2H_50H + 5CO_2 \quad 3.4$$

From Equation 3.4, one gram of xylose (molecular weight = 3*150) produces 0.511 grams of ethanol (molecular weight = 5*46) and 0.489 grams of carbon dioxide (molecular weight = 5*44).

Therefore, the maximum theoretical yield of ethanol from glucose and xylose is 0.511 g/g glucose or xylose (da Silva et al., 2018).

3.3.7 Product recovery and purification

Product recovery and purification involved distillation and dehydration. The fermentation broth was separated into ethanol, water and solids by distillation using the beer column and solid-liquid separation using a filter. Ethanol was then distilled to an azeotropic mixture in the rectification column. Solids (lignin, unreacted cellulose and hemicellulose) were recovered from the beer distillation column bottoms upon filtration, and were sent to the combustor while the liquid was sent to the wastewater treatment plant (Humbird et al., 2011).

3.3.8 Drying of ethanol

The product from the rectification column (ethanol vapor stream) was passed through a column packed with zeolite where water was removed from the stream. The final product was 99.85% (w/w) ethanol and was stored in the ethanol storage tanks.

3.3.9 Economic analysis

Table 3. 15: Parameters used in economic analysis

S/NO	Parameter	Formula/Source
1.	Total Product Cost (TPC)	Fixed Charges + Direct Production Cost
2.	Startup expense	5% of TCI (Sinnott and Towler, 2020)
3.	Total Product Cost (per liter)	Total product cost/Total annual production
4.	Direct Production Cost (per liter)	Direct production cost x cost of production (per liter) /Total annual sales
5.	Average annual depreciation	Total depreciation/Plant life in years
6.	TCI	FCI+WCI (Sinnott and Towler, 2020)
7.	Internal Rate of Return (IRR)	From Microsoft Excel
8.	Net Present Value (NPV)	From Microsoft Excel
9.	Return on Investment (ROR)	Annual profit/TCI (Sinnott and Towler, 2020)

Assumptions made in economic analysis:

i. The double declining method of depreciation was used. This method of depreciation was chosen since it results in larger depreciation expenses at the beginning of an asset life and smaller depreciation expenses later on (Sinnott and Towler, 2020; Humbird et al., 2011).

ii. The plant life was taken as 30 years. This was based on literature for plants of similar production capacity, technology and products (Sinnott and Towler, 2020; da Silva et al., 2016; Humbird et al., 2011).

The depreciation rate was found from the expression given by Equation 3.5.

$$\text{Depreciation}\,\frac{\text{rate}}{\text{factor}}\,(\text{f}) = \frac{100\%}{\text{n}} \times 2 = \frac{100}{30} \times 2 = 6.67\% = 0.067 \qquad 3.5$$

Where n is the plant life.

Let:

V = Initial value of assets

V_a = Value of assets in n years

V_s = Salvage value of assets

f = depreciation factor

Then:

$$V_a = V(1 - f)^n = V_s \quad 3.6$$

3.3.9.1 Purchased equipment costs

Capital cost estimates for the 2GBE production plant were based on an estimate of the purchase cost of the major equipments required for the process. According to Sinnott and Towler (2020), the capital cost of a proposed project can be estimated from the cost of existing projects that use similar manufacturing process. The capital cost of a project is related to capacity by Equation 3.7:

$$C_2 = C_1 \left(\frac{S_2}{S_1}\right)^n \quad 3.7$$

Where:

C_2 = Capital cost of project with capacity S_2 (New cost) (Sinnott and Towler, 2020; Humbird et al. 2011).

C_1 = Capital cost of project with capacity S_1 (Base cost) (Sinnott and Towler, 2020; Humbird et al. 2011).

n = Scaling exponent (typically in the range of 0.6 to 0.7) (Sinnott and Towler, 2020; Humbird et al. 2011).

The scaling exponent n in Equation 3.7 varies depending on the type of equipment. The basis for scaling is typically some characteristic of the equipment related to production capacity, such as flow or heat duty (Davis et al., 2018). In the current research study, n

was taken as 0.6 (Sinnott and Towler, 2020; Humbird et al. 2011). The estimated capital cost can be updated to the current year using cost index (chemical engineering plant cost index) from the base year in which the prices were quoted (Sinnott and Towler, 2020). From Equation 3.7, the current equipment cost can be estimated using Equation 3.8.

$$C_2 = C_1 \left(\frac{S_2}{S_1}\right)^n \frac{\text{Cost index B}}{\text{Cost index A}} \qquad 3.8$$

Where:

Cost index B: is the current year cost index (Sinnott and Towler, 2020; Humbird et al. 2011).

Cost index A: is the base year cost index (Sinnott and Towler, 2020; Humbird et al. 2011).

For the case where $S_1 = S_2$ in Equation 3.7, the cost of the current equipment is equal to the cost of the base equipment.

3.3.9.2 Raw material costs

The quantity of raw materials required to produce 2GBE were obtained from the PFDs and multiplied by the total operating hours per year in order to obtain the annual requirements (Sinnott and Towler, 2020; Humbird et al., 2011). The price of each raw material was obtained by getting quotations from suppliers and estimates from literature (Sinnott and Towler, 2020; Humbird et al., 2011).

3.3.9.3 Estimation of working capital investment, direct costs, indirect costs, service facilities and fixed charges

The WCI, direct costs, indirect costs, service facilities and fixed charges were established based on a percentage of FCI (Sinnott and Towler, 2020; da Silva et al.,

2016; Humbird et al., 2011). The various percentages used are shown in Table 3.16 to Table 3.20.

Table 3. 16: Working capital investment (Sinnott and Towler, 2020; da Silva et al., 2016; Humbird et al., 2011)

Component	% of FCI
WCI	5

Table 3. 17:Direct costs (Sinnott and Towler, 2020; Humbird et al., 2011)

Component	% of FCI
Purchased equipment	40
Purchase equipment installation	12
Instrumentation (installed)	2
Piping (installed)	4
Electrical (installed)	2
Buildings (including services)	4
Yard improvement	2
Service facilities (installed)	8
Land	1

Table 3. 18: Indirect costs (Sinnott and Towler, 2020; Humbird et al., 2011)

Component	% of FCI
Engineering and supervision	9
Construction expense	6
Contractor's fee	3
Legal expenses	2
Contingency	5

Table 3. 19: Service facilities (Sinnott and Towler, 2020; Humbird et al., 2011)

Component	% of FCI
Water supply	1.8
Water distribution	0.8
Electricity substation	1.3
Electricity distribution	1.0
Compressed air supply	1.0
Refrigeration	2.0
Fire protection system	0.5
Safety installation	0.4

Table 3. 20: Fixed charges (Sinnott and Towler, 2020; da Silva et al., 2016; Humbird et. al., 2011)

Component	% of FCI
Local taxes	0.7
Insurance	0.7

3.3.9.4 Estimation of labour costs

The number of employees required to work in the 2GBE production plant was based on similar plants (Sinnott and Towler, 2020; Humbird et al., 2011). According to the Kenya National Bureau of Statistics [KNBS] (2022), the results of economic survey which include the average wages and salaries are published each year. Labour costs were estimated based on existing average wages and salaries in Kenya. The average salaries and wages were obtained from (KNBS, 2022). A 90% labour burden was applied to the total salary requirements (Sinnott and Towler, 2020; da Silva et al., 2016; Humbird et al., 2011). The labour burden was added in order to cater for items such as safety, general engineering, general plant maintenance, payroll overhead (including benefits), plant security, janitorial and similar services, phone, light, heat, and plant communications (Sinnott and Towler, 2020; da Silva et al., 2016; Humbird et al., 2011).

3.3.9.5 Estimation of total capital investment

The total capital investment (TCI) required for a given project is given as the sum of FCI and WCI (Sinnott and Towler, 2020). Thus:

$$\mathrm{TCI} = \mathrm{FCI} + \mathrm{WCI} \quad (3.9)$$

$$\mathrm{WCI} = 0.05\ \mathrm{FCI} \quad (3.10)$$

$$\mathrm{TCI} = \mathrm{FCI} + 0.05\mathrm{FCI} \quad (3.11)$$

$$\mathrm{TCI} = 1.05\mathrm{FCI} \quad (3.12)$$

3.3.9.6 Discounted cash flow

According to Sinnott and Towler (2020), the net cash flow in each year of the project can be brought to its present worth at the start of the project by discounting it at some interest rate.

$$\text{Net present worth (NPW)} = \frac{\text{Estimated net cash flow in year n (NFW)}}{(1+r)^n} \quad 3.13$$

$$\text{Total NPW} = \sum_{n=1}^{n=t} \frac{\text{NFW}}{(1+r)^n} \quad 3.14$$

Where:

r = % discount rate (interest rate)

t = project life in years

NFW = Net Future Worth

The discount rate is chosen to reflect the earning power of money. It is considered equivalent to the current interest rate that the money could earn if invested.

3.3.10 Procedure for hydrolysis of substrate

15 grams of substrate was soaked in concentrated H_2SO_4 solution to form a SLR of 15.0% (w/v) in the hydrolysis reactor. The temperature, time and concentration of acid were determined from the experimental design matrix for each experimental run. The reactor was heated using a water bath to a temperature and for a period of time determined from the experimental design matrix. For each substrate, a total of 20 experimental runs were carried out based on the CCRD. At the end of each experimental run, the hydrolysate was separated from the spent solids through filtration. The spent solids were washed using distilled water in order to remove any adhering hydrolysate. The hydrolysate was then diluted using distilled water to form 1000 ml solution which was then treated with calcium hydroxide to a pH of 7.0 (Kanchanalai et al., 2016; Sarrouh et al., 2007). Table 3.21 and Table 3.22 shows the actual and coded levels of

hydrolysis factors that were investigated and the experimental design matrix respectively.

Table 3. 21: CCRD matrix for actual and coded level of hydrolysis factors

Independent variables	Symbol	Range and levels				
		Axial (- α)	Min (-1)	Center (0)	Max (+1)	Axial (+ α)
Temperature, (^oC)	X_1	26.4	40	60	80	93.6
Time (Min)	X_2	9.5	30	60	90	110.5
Acid Concentration (w/w, %)	X_3	16.36	30	50	70	83.64

3.3.11 Analysis of glucose: Summary

In this research study, the concentration of glucose released during hydrolysis of substrate was determined spectrophotometrically (Andrea, 2015; Bhattacharya et al., 2015). This procedure was based on Sigma glucose hexokinase (HK) assay kit (Andrea, 2015). The glucose assay method was based on a two-step enzymatic reaction, where glucose contained in the sample was first phosphorylated to glucose- 6-phosphate (G6P) by adenosine triphosphate (ATP) in the presence of HK. G6P was then reacted with nicotinamide-adenine dinucleotide phosphate (NADP+) in the presence of glucose-6-phosphate dehydrogenase (G6P-DH) to form gluconate-6-phosphate and reduced nicotinamide-adenine dinucleotide phosphate (NADPH). In order to estimate the concentration of glucose in the hydrolysis sample, the corresponding increase in NADPH was measured at 340 nm using a spectrophotometer. The resultant increase in absorbance due to the formation of NADH is directly proportional to the concentration of glucose in the sample being analyzed (Andrea, 2015; Gao et al., 2010; Zhao et al., 2010).

Table 3. 22: Experimental design matrix for the hydrolysis process: actual and coded levels of factors

STD	RUN	X1 (Temperature, ^oC)	X2 (Time, min)	X3 (Acid concentration, %, w/w)
8	1	26.4 (-1.682)	60 (0)	50 (0)
7	2	60 (0)	60 (0)	16..36 (-1.682)
20	3	80 (1)	30 (-1)	70 (1)
10	4	60 (0)	60 (0)	50 (0)
6	5	80 (1)	90 (1)	70 (1)
17	6	60 (0)	9.5 (-1.682)	50 (0)
11	7	80 (1)	30 (-1)	30 (-1)
2	8	40 (-1)	30 (-1)	30 (-1)
15	9	60 (0)	60 (0)	50 (0)
16	10	40 (-1)	90 (1)	30 (-1)
14	11	60 (0)	60 (0)	50 (0)
19	12	40 (-1)	30 (-1)	70 (1)
18	13	60 (0)	60 (0)	83.64 (1.682)
1	14	60 (0)	60 (0)	50 (0)
12	15	93.6 (1.682)	60 (0)	50 (0)
9	16	80 (1)	90 (1)	30 (-1)
4	17	60 (0)	60 (0)	50 (0)
3	18	60 (0)	110.5 (1.682)	50 (0)
13	19	40 (-1)	90 (1)	70 (1)
5	20	60 (0)	60 (0)	50 (0)

3.3.11.1 Procedure for analysis of glucose

HK assay reagent was reconstituted with 20 ml of deionised water and mixed several times by inversion. Standard glucose solution (1.0 mg/ml in 0.1% benzoic acid) was also prepared (Andrea, 2015). The samples to be analysed for glucose were then prepared for analysis by heating them to a temperature of 30^{o}C by immersing them into a water bath set 30^{o}C (Andrea, 2015 and Bhattacharya et al., 2015). The spectrophotometer was blanked using a cuvette containing deionised water. The absorbance of sample blank and reagent blank was also measured and recorded. 0.1 ml of sample was placed into a cuvette and 1.0 ml of reconstituted HK reagent added and the cuvette covered with a parafilm and the contents mixed by inversion and thereafter incubated at 30^{o}C for 15 minutes (Andrea, 2015 and Bhattacharya et al., 2015). After the reaction, the absorbance of the sample was measured at 340nm (Gao et al., 2010;

Zhao et al., 2010). The concentration of glucose in the sample was then calculated using Equation 3.15.

$$\text{Glucose concentration } \left(\frac{\text{g}}{\text{L}}\right) = \frac{(\Delta\text{A})(\text{TV})(\text{Glucose MW})}{(\varepsilon)(\text{d})(\text{SV})} \quad 3.15$$

Where:

$\Delta\text{A} = \text{A}_{\text{Test}} - \text{A}_{\text{Total Blank}}$

TV = total assay volume (mL) = 1.1 mL

SV = sample volume (mL) = 0.1 mL

MW = glucose molecular weight = 180.2 g/mole

ε = 6220 = Molar extinction coefficient for NADH at 340nm ($\text{L} \times \text{mol}^{-1}\text{cm}^{-1}$)

d = light path of the cuvette = 1cm

A_{Test} = absorbance of test sample at 340nm

$\text{A}_{\text{Total Blank}}$ = absorbance of sample blank + absorbance of reagent blank

Substituting the above values, Equation 3.15 reduces into:

$$\text{Glucose concentration}, \frac{\text{g}}{\text{L}} = 0.3187 \times \Delta\text{A} \quad 3.16$$

The yield of glucose for each experimental run was obtained using Equation 3.17.

$$\text{Glucose yield } (\%) = \frac{\left(\text{Glucose concentration}, \frac{\text{g}}{\text{L}}\right)(\text{HV})(\text{DF})(\text{AF})}{\text{Cellulose added during hydrolysis (grams)}} \times 100 \quad 3.17$$

Where:

$\text{Glucose concentration}, \frac{\text{g}}{\text{L}}$ = concentration of glucose obtained in Equation 3.16

HV = Volume of hydrolysate = 1 L

AF = 0.9 (anhydro factor that is used to correct for the water molecule added upon hydrolysis of the cellulose).

DF = dilution factor for sample preparation = 10.

3.3.12 Kinetic studies

Experiments on kinetic studies were conducted under varying temperature and treatment time. The SLR was kept constant at 1:15. At various time intervals between 0 and 60 minutes, a sample of hydrolysate was taken from the hydrolysis reactor and analysed for glucose concentration. The rate constants were established from the modified Saeman model (biphasic model) using Solver, Microsoft Excel. Using the Arrhenius equation, the rate constants were used to establish the kinetic parameters (activation energy and pre-exponential factor). Maximum glucose yield and time for maximum glucose yield were established using Equation 2.8 and Equation 2.9 respectively.

CHAPTER FOUR: EXPERIMENTAL RESULTS AND DISCUSSION

4.1 Introduction

This chapter presents results, analyses and discussions of various findings from the study.

4.2 Characterization of Substrates

The summary of the chemical composition of maize cobs and sorghum stalks is shown in Table 4.1.

Table 4. 1: Chemical composition of substrates

Composition (%, w/w)	Maize cobs	Sorghum stalks
Cellulose	28.97	27.49
Hemicellulose	43.79	23.51
Acid insoluble lignin	7.07	24.83
Acid soluble lignin	3.67	8.17
Ash	3.77	5.33
Moisture	8.67	9.98
Extractives	4.06	0.69

The cellulose content in maize cobs and sorghum stalks is 28.97% (w/w) and 27.49% (w/w) respectively while the hemicellulose content is 43.79% (w/w) and 23.51% (w/w) in maize cobs and sorghum stalks respectively. The presence of high cellulose and hemicellulose content in maize cobs (72.76%, w/w) and sorghum stalks (51%, w/w) is an indication of their potential for use as feedstock for the production of simple sugars (glucose and xylose) which can be fermented to bioethanol. The moisture content of 9.98% (w/w) and 8.67% (w/w) found in sorghum stalks and maize cobs respectively is below 10% (w/w). This is an indication that there was no effect of moisture content on the compositional analysis according to the standard method for determination of structural carbohydrates and lignin in biomass as the excess moisture is known to interfere with appropriate acid concentrations used in the compositional analysis (Ruiz & Tina, 1996). The composition of substrates used in the current study was compared with that of various LGB found in literature as shown in Table 4.2.

Table 4. 2: Comparison of substrate composition with literature data

Feedstock	Cellulose (%, w/w)	Hemicellulose (%, w/w)	Lignin (%, w/w)	Reference
Rice straw	41.00	21.50	19.60	da Silva et al. (2018)
Wheat straw	34.20	36.00	14.70	da Silva et al. (2018)
Newspaper	57.1	8.4	17.2	Jung et al. (2013)
Cocoa pod husk	23.04	38.08	18.19	Mensah et al. (2020)
Corn stover	37.60	25.70	15.50	da Silva et al. (2018)
Soybean straw	44.2	5.9	19.2	Kim et al. (2018)
Spruce	45.0	22.0	28.0	da Silva et al. (2017)
Switch grass	37.70	28.30	19.20	da Silva et al. (2018)
Corn cobs	41.0	22.6	14.1	Lukajtis et al. (2018)
Energetic willow	46.5	15.6	29.4	Lukajtis et al. (2018)
Beech	38.6	19.9	26.3	Lukajtis et al. (2018)
Sweet sorghum	32.65	20.80	27.87	Lopez-Sandin et al. (2022)
Sweet sorghum	35-50	20-30	15-25	Hu and Chen (2022)
Grasses	29-43	8.0-29	8.0-27	Cheah et al. (2020)
Wheat straw	33-40	20-25	15-20	Cheah et al. (2020)
Rice husk	42.49	19.34	15.05	Zhang et al. (2020)
Softwoods	-	-	25-35	Beluhan et al. (2023)
Grasses	-	-	10-30	Beluhan et al. (2023)
Sorghum bagasse	39.07	34.57	13.29	Liu et al. (2012)
Nut shells	25-30	25-30	30-40	Muktham et al. (2016)
Sorghum bagasse	21-49	14-33	17-30	Roziafanto et al. (2023)
Sorghum stalks	34.87	30.95	24.9	Roziafanto et al. (2023)
Banana pseudostem	24.27	22.56	14.14	Legodi et al. (2021)
Coconut husk	29.58	27.77	31.04	Telleria et al. (2018)
Elephant grass	29.9	20.2	21.1	Kolo et al. (2020)
Maize cobs	41.27	46	7.4	Boonyisa et al. (2012)
Maize cobs	38.8	44.4	11.9	Pointner et al. (2014)

The composition of sorghum stalks and maize cobs is within the range reported in literature for other substrates.

4.3 Process Modeling and Simulation: Sorghum Stalks and Maize Cobs

This section presents the various PFDs that were modeled and simulated in order to achieve the first specific objective of this research study for sorghum stalks and maize cobs.

4.3.1 Modeling and simulation of dilute sulphuric acid pretreatment and SSCF process

The model for dilute sulphuric acid pretreatment and SSCF process is shown in Figure 4.1.

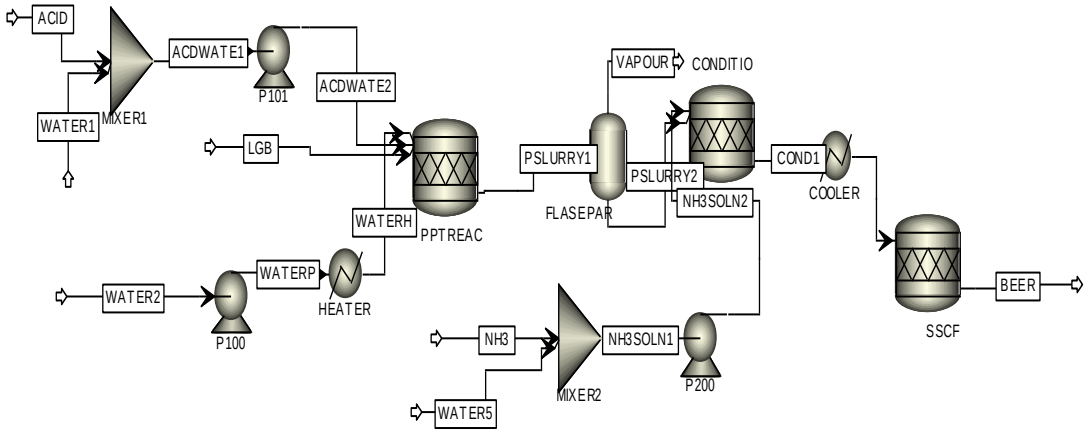

Figure 4. 1: PFD for dilute sulphuric acid pretreatment and SSCF process

4.3.2 Modeling and simulation of dilute sulphuric acid pretreatment and SHCF process

The model for dilute sulphuric acid pretreatment and SHCF process is shown in Figure 4.2.

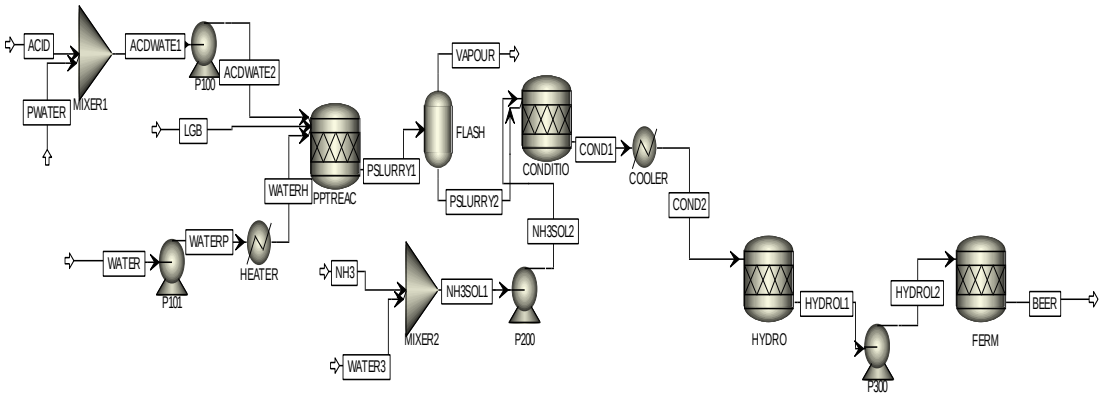

Figure 4. 2: PFD for dilute sulphuric acid pretreatment and SHCF process

4.3.3 Modeling and simulation of steam explosion pretreatment and SSCF process

The model for steam explosion pretreatment and SSCF process is shown in Figure 4.3.

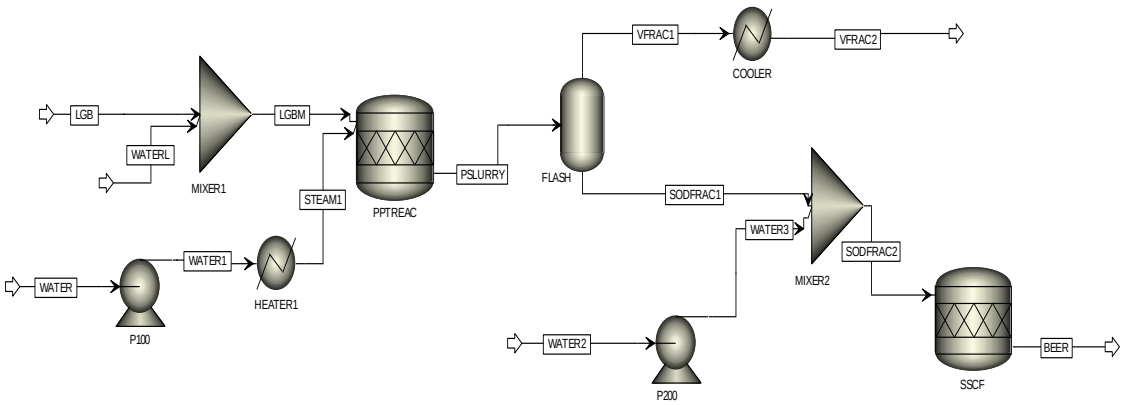

Figure 4. 3: PFD for steam explosion pretreatment and SSCF process

4.3.4 Modeling and simulation of the steam explosion pretreatment and SHCF process

The model for steam explosion pretreatment and SHCF process is shown in Figure 4.4.

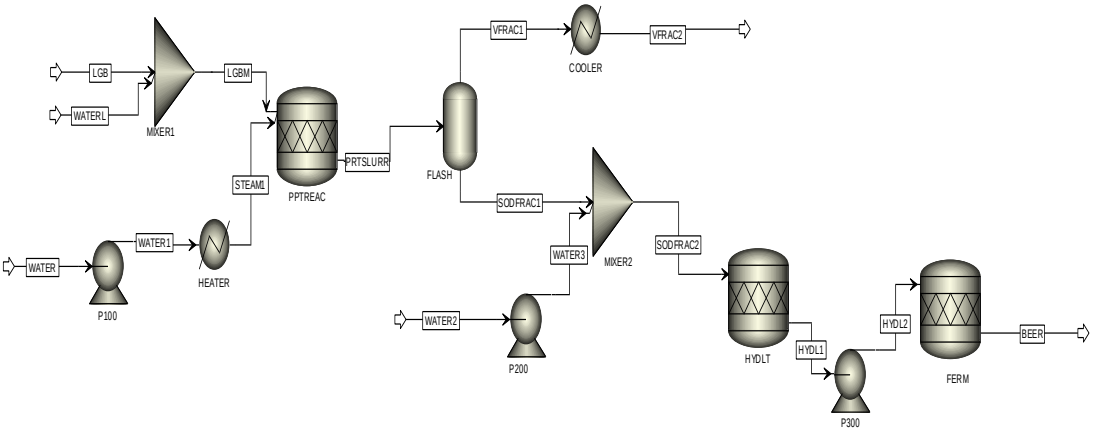

Figure 4. 4: PFD for steam explosion pretreatment and SHCF process

4.3.5 Modeling and simulation of the alkaline pretreatment and SSCF process

The model for alkaline pretreatment and SSCF process is shown in Figure 4.5.

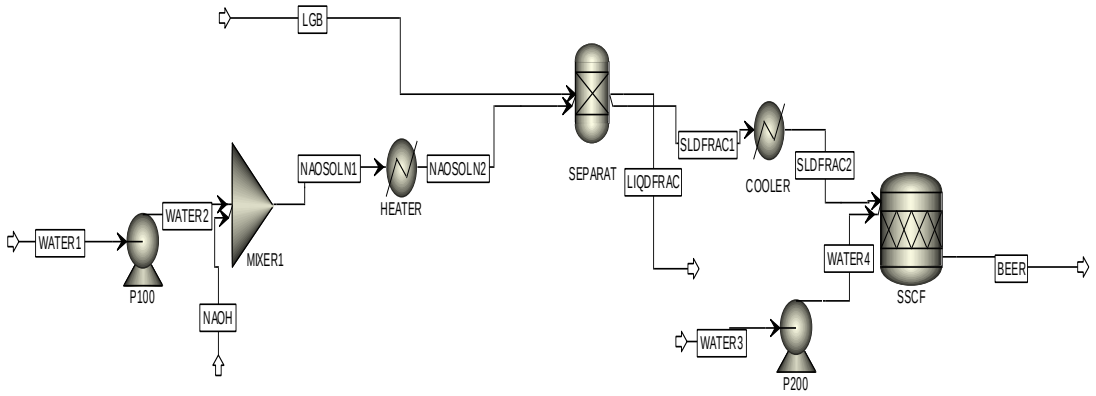

Figure 4. 5: PFD for alkaline pretreatment and SSCF process

4.3.6 Modeling and simulation of the alkaline pretreatment and SHCF process

The model for alkaline pretreatment and SHCF process is shown in Figure 4.6.

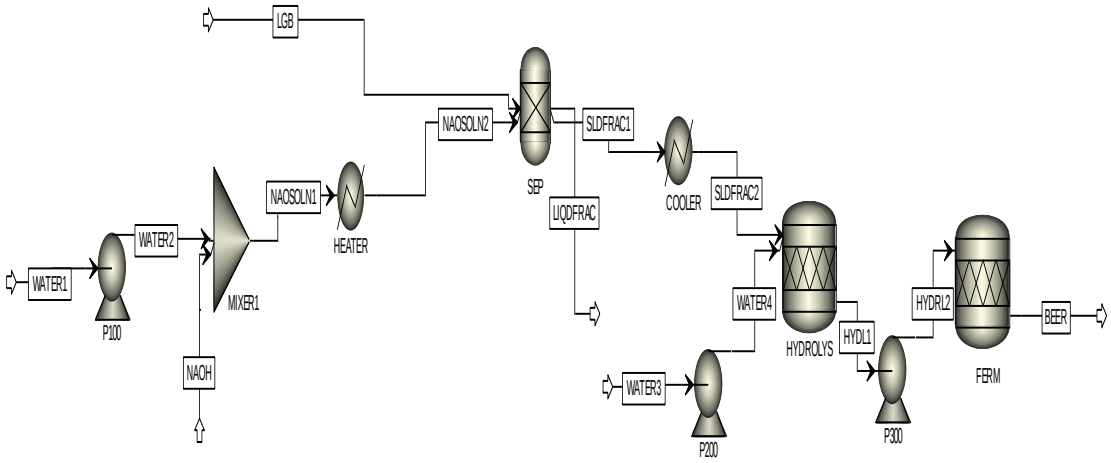

Figure 4. 6: PFD for alkaline pretreatment and SHCF process

4.3.7 Modeling and simulation of the beer column, rectification column, molecular sieve dehydration and energy recovery process

The model for beer purification, molecular sieve dehydration and energy recovery process is shown in Figure 4.7.

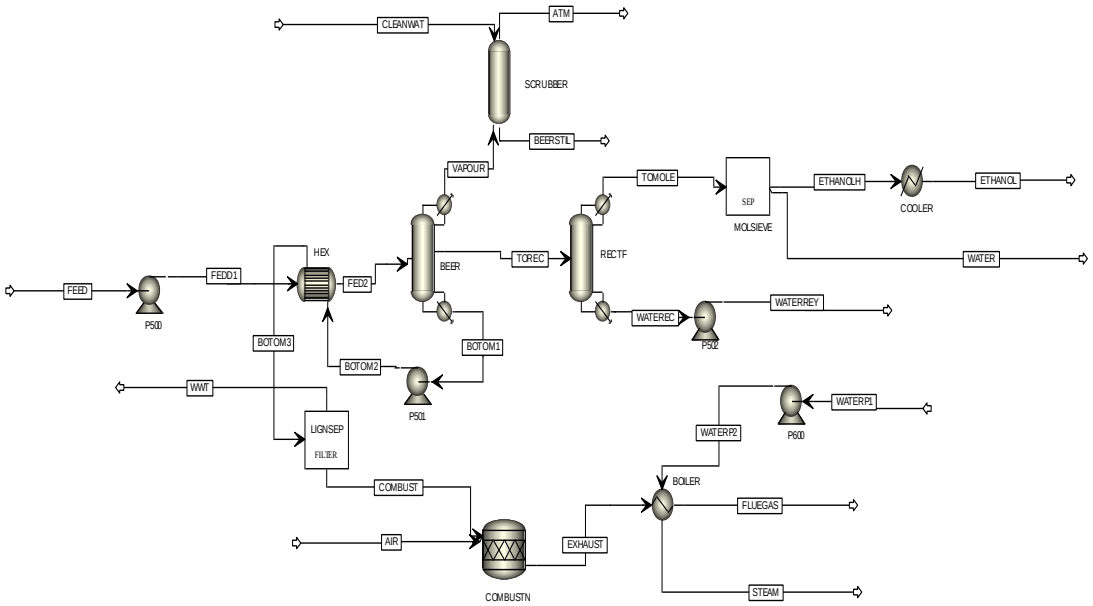

Figure 4. 7: PFD for ethanol purification, dehydration and energy recovery

4.4 Sorghum Stalks: Simulation Results Obtained From Various Models

The results of simulation for the various models representing the different pretreatment, SHCF and SSCF bioethanol production technologies are presented in this section for sorghum stalks. All the results were obtained from Aspen Plus simulation software.

4.4.1 Simulation results for dilute sulphuric acid pretreatment and SSCF process for sorghum stalks

The model for dilute sulphuric acid pretreatment and SSCF process is shown in Figure 4.1. The results obtained after simulating the model are shown in Table 4.3. The flow rate of each stream component is given in kilomole per hour (kmol/h) while the total flow rate is given in kilogram per hour (kg/h).

Table 4. 3: Results of dilute sulphuric acid pretreatment and SSCF process for sorghum stalks

Stream/component	COND2 (kmol/h)	BEER1 (kmol/h)
Water	18935.99	18815.84
Hemicellulose	8.14	8.14
Ethanol	0.00	476.96
Glucose	15.35	0.77
Xylose	146.47	21.97
Sulphuric acid	0.13	0.13
Extractives	20.84	20.84
Furfural	3.99	3.99
Ammonium sulphate	23.06	23.06
Lignin	198.35	198.35
Carbon dioxide	0.00	476.96
Ash	86.90	86.90
Cellulose	139.70	19.56
Total Flow (kmol/h)	19578.92	20153.46
Total Flow (kg/h)	428740	428740

4.4.2 Simulation results for dilute sulphuric acid pretreatment and SHCF process for sorghum stalks

The model for dilute sulphuric acid pretreatment and SHCF process is shown in Figure 4.2. The results obtained after simulating the model are shown in Table 4.4.

Table 4. 4: Results of dilute sulphuric acid pretreatment and SHCF process for sorghum stalks

Stream/component	HYDROL2 (kmol/h)	BEER (kmol/h)
Water	18810.26	18810.26
Hemicellulose	8.14	8.14
Ethanol	0.00	475.56
Glucose	141.08	7.05
Xylose	146.47	21.97
Sulphuric acid	0.13	0.13
Extractives	20.84	20.84
Furfural	3.99	3.99
Ammonium sulphate	23.06	23.06
Lignin	198.35	198.35
Carbon dioxide	0.00	475.56
Ash	86.90	86.90
Cellulose	13.97	13.97
Total Flow (kmol/h)	19453.19	20145.78
Total Flow (kg/h)	428740	428740
Temperature (^{O}C)	50	35

4.4.3 Simulation results for steam explosion pretreatment and SSCF process for sorghum stalks

The results obtained after simulating the model for steam explosion pretreatment and SSCF process (Figure 4.3) are shown in Table 4.5.

Table 4. 5: Results of steam explosion pretreatment and SSCF process for sorghum stalks

Stream/component	SODFRAC2 (kmol/h)	BEER (kmol/h)
Water	18385.85	18257.97
Hemicellulose	39.55	39.55
Ethanol	0.00	409.40
Glucose	6.36	0.32
Xylose	99.93	14.99
Furfural	2.70	2.70
Lignin	198.35	198.35
Carbon dioxide	0.00	409.40
Ash	86.90	86.90
Acetic acid	31.66	31.66
Extractives	20.84	20.84
Cellulose	148.69	20.82
Total Flow (kmol/h)	19020.83	19492.89

4.4.4 Simulation results for steam explosion pretreatment and SHCF process for sorghum stalks

The results obtained after simulating the model for steam explosion pretreatment and SHCF process (Figure 4.4) are shown in Table 4.6.

Table 4. 6: Results of steam explosion pretreatment and SHCF process for sorghum stalks

Stream/component	HYDL2 (kmol/h)	BEER (kmol/h)
Water	18252.03	18252.03
Hemicellulose	39.55	39.55
Ethanol	0.00	407.91
Glucose	140.18	7.01
Xylose	99.93	14.99
Furfural	2.70	2.70
Lignin	198.35	198.35
Carbon dioxide	0.00	407.91
Ash	86.90	86.90
Acetic acid	31.66	31.66
Extractives	20.84	20.84
Cellulose	14.87	14.87
Total Flow (kmol/h)	18887.01	19484.71

4.4.5 Simulation results for alkaline pretreatment and SSCF process for sorghum stalks

The model for alkaline pretreatment and SSCF process is shown in Figure 4.5. The results obtained after simulating the model are shown in Table 4.7.

Table 4. 7: Results of alkaline pretreatment and SSCF process for sorghum stalks

Stream/component	WATER4 (kmol/h)	SLDFRAC2 (kmol/h)	BEER (kmol/h)
Water	6105.93	1879.41	7853.26
Hemicellulose	0.00	32.71	32.71
Ethanol	0.00	0.00	264.16
Lignin	0.00	45.02	45.02
Carbon dioxide	0.00	0.00	264.16
Cellulose	0.00	153.58	21.50
Total Flow (kmol/h)	6105.93	2110.72	8480.81
Total Flow (kg/h)	110000	69932	179932
Temperature (ºC)	27	32	32

4.4.6 Simulation results for alkaline pretreatment and SHCF process for sorghum stalks

The model for alkaline pretreatment and SHCF process is shown in Figure 4.6. The results obtained after simulating the model are shown in Table 4.8.

Table 4. 8: Results of sodium hydroxide pretreatment and SHCF process for sorghum stalks

Stream/component	HYDRL2 (kmol/h)	BEER (kmol/h)
Water	7847.11	7847.11
Hemicellulose	32.71	32.71
Ethanol	0.00	262.62
Glucose	138.22	6.91
Lignin	45.02	45.02
Carbon dioxide	0.00	262.62
Cellulose	15.36	15.36
Total Flow (kmol/h)	8078.43	8472.36
Total Flow (kg/h)	179932	179932
Temperature (ºC)	50	35

The overall mass balance for dilute acid, steam explosion and alkaline pretreatment methods for SSS is shown in appendix A.

4.5 Sorghum Stalks: Energy Analysis and Ethanol Production Rate for Pretreatment, Hydrolysis and Fermentation Processes

In order to compare and select the most suitable pretreatment, hydrolysis and fermentation technology in terms of ethanol production rate, energy demand and energy intensity, analysis of these parameters was done as shown in this section. All the results were obtained from Aspen Plus simulation software. The units for heating and cooling demand are megajoules per hour (MJ/h).

4.5.1 Energy analysis for dilute sulphuric acid, steam explosion, alkaline pretreatment and SHCF process

The heating and cooling demand for dilute sulphuric acid, steam explosion and alkaline pretreatment methods and SHCF process for sorghum stalks is shown in Table 4.9.

Table 4. 9: Heating and cooling demand for dilute sulphuric acid, steam explosion and alkaline pretreatment methods and SHCF process for sorghum stalks

Equipment/ process unit	Pretreatment method combined with SHCF					
	Dilute sulphuric acid		Steam Explosion		Alkaline	
	Heating demand (MJ/h)	Cooling demand (MJ/h)	Heating demand (MJ/h)	Cooling demand (MJ/h)	Heating demand (MJ/h)	Cooling demand (MJ/h)
Heater	13449.31	-	41830.92		93411	-
Pretreatment reactor	149414.76	-	158222.16	-	-	-
Conditioning	6923.16	-	-		-	-
Cooler	-	39537.72	-	121308.84	-	6356.79
Hydrolysis reactor	-	123306.48	-	150058.44	-	125025.9
Fermentation reactor	-	54021.24	-	46792.8	-	19263.31
Total	**169787.23**	**216865.44**	**200053.08**	**318160.08**	**93411**	**150646**

4.5.2 Energy analysis for dilute sulphuric acid, steam explosion, alkaline pretreatment and SSCF process

The heating and cooling demand for dilute sulphuric acid, steam explosion and alkaline pretreatment methods and SSCF process for sorghum stalks is shown in Table 4.10.

Table 4. 10: Heating and cooling demand for dilute sulphuric acid, steam explosion and alkaline pretreatment methods and SSCF process for sorghum stalks

Equipment/ process unit	Pretreatment method combined with SSCF					
	Dilute sulphuric acid		Steam Explosion		Alkaline	
	Heating demand (MJ/h)	Cooling demand (MJ/h)	Heating demand (MJ/h)	Cooling demand (MJ/h)	Heating demand (MJ/h)	Cooling demand (MJ/h)
Heater	13449.31		41830.92		93411	
Pretreatment reactor	149414.76		158222.16			
Conditioning reactor	6923.16					
Cooler		67261.68		121308.84		9293.65
SSCF reactor		148887.72		195441.84		137299.32
Total	**169787.23**	**216149.40**	**200053.08**	**316750.68**	**93411**	**146592.97**

4.6 Sorghum Stalks: Summary of Energy Analysis and Ethanol Production Rate for Pretreatment, Hydrolysis and Fermentation Processes

A summary of heating demand, cooling demand, ethanol production rate and ethanol yield for dilute sulphuric acid, steam explosion and alkaline pretreatment methods combined with SHCF and SSCF processes for sorghum stalks is presented in this section.

4.6.2 Summary of heating, cooling demand and ethanol production rate for SHCF process for sorghum stalks

A summary of heating demand, cooling demand, ethanol production rate and ethanol yield for dilute sulphuric acid, steam explosion and alkaline pretreatment methods and SHCF process for sorghum stalks is shown in Table 4.11.

Table 4. 11: Summary of heating, cooling demand and ethanol production rate for SHCF processes for sorghum stalks

Energy requirements	Unit	Pretreatment method combined with SHCF		
		Acid	Steam Explosion	Alkaline
Heating demand	MJ/h	169787.23	200053.08	93411
Cooling demand	MJ/h	216865.44	318160.08	150646
Electricity (Pumps)	kWh	57.42	106.25	68.68
Ethanol production rate	kg/h	21899.5	18784.2	12093.7
Ethanol in beer stream	%, w/w	5.11	4.53	6.72
Ethanol yield	L/Tonne dry LGB	336.75	288.84	185.96

4.6.3 Summary of heating, cooling demand and ethanol production rate for SSCF processes for sorghum stalks

A summary of heating demand, cooling demand, ethanol production rate and ethanol yield for dilute sulphuric acid, steam explosion and alkaline pretreatment methods and SSCF process for sorghum stalks is shown in Table 4.12.

Table 4. 12: Summary of heating, cooling demand and ethanol production rate for SSCF processes for sorghum stalks

Parameter	Unit	Pretreatment method combined with SSCF		
		Acid	Steam Explosion	Alkaline
Heating demand	MJ/h	169787.23	200053.08	93411
Cooling demand	MJ/h	216149.40	316750.68	146592.97
Electricity (Pumps)	kWh	42.88	68.50	42.84
Ethanol production rate	kg/h	21963.80	18852.70	12164.40
Ethanol in beer stream	%, w/w	5.12	4.55	6.76
Ethanol yield	L/Tonne dry LGB	337.73	289.89	187.05

The results shown in Table 4.11 and Table 4.12 indicate that the SSCF bioethanol production technology has a higher ethanol production rate and higher ethanol yield per tonne of dry LGB than the SHCF bioethanol production technology for all the three types of pretreatment methods. In addition, the concentration of bioethanol in the fermentation broth is higher in SSCF than in SHCF. A closer look at the PFDs for both technologies (Figure 4.1 and Figure 4.2) indicate that SSCF has fewer process units than SHCF. Therefore, SHCF bioethanol production technology has higher capital costs compared to SSCF technology because the process requires separate hydrolysis and fermentation reactors (Beluhan et al., 2023). In addition, the pumping requirement for SHCF is higher than that in SSCF. This leads to higher operation costs (in terms of kWh of electricity) in SHCF than in SSCF. Jarunglumlert and Prommuak (2021) reported that SSCF require less energy to run the hydrolysis and fermentation process in a single

reactor. This results in lower capital and operational costs (Jarunglumlert and Prommuak, 2021). From the foregoing, the SSCF bioethanol production technology is more suitable than SHCF. It was therefore chosen as the best technology based on these findings.

4.7 Sorghum Stalks: Energy Analysis and Ethanol Production Rate for Pretreatment, Hydrolysis, Fermentation, Beer Purification and Energy Recovery Process

In order to compare and select the most suitable pretreatment, hydrolysis, fermentation, beer purification and energy recovery process in terms of ethanol production rate, energy demand, energy intensity and energy recovery, analysis of these parameters was done and presented in this section. The feed to the beer purification section consisted of the output stream (beer) from each model representing dilute sulphuric acid pretreatment and SSCF, steam explosion pretreatment and SSCF and alkaline pretreatment and SSCF processes. All the results were obtained from Aspen Plus simulation software.

4.7.1 Heating and cooling demand for purification of beer from dilute sulphuric acid, steam explosion, alkaline pretreatment methods and SSCF process

The heating and cooling demand for purification of beer from dilute sulphuric acid, steam explosion, alkaline pretreatment methods and SSCF process is shown in Table 4.13.

Table 4. 13: Heating and cooling demand for purification of beer from dilute sulphuric acid, steam explosion, alkaline pretreatment methods and SSCF process

Equipment/process unit	Pretreatment method combined with SSCF					
	Dilute sulphuric acid		Steam Explosion		Alkaline	
	Heating demand (MJ/h)	Cooling demand (MJ/h)	Heating demand (MJ/h)	Cooling demand (MJ/h)	Heating demand (MJ/h)	Cooling demand (MJ/h)
Beer column reboiler	127173.96	-	130557.24	-	124211.88	-
Beer column condenser	-	25361.32	-	24657.34	-	10788.59
Rectification reboiler	37414.08	-	53717.40	-	81287.28	-
Rectification condenser	-	88394.04	-	104451.84	-	131994.72
Cooler		21835.91	-	19027.04	-	12507.26
Total	**164588.04**	**135591.27**	**184274.64**	**148136.22**	**205499.16**	**155290.57**

4.8 Sorghum Stalks: Summary of Energy Analysis and Ethanol Production Rate for Pretreatment, SSCF and Beer Purification Processes

A summary of heating demand, cooling demand, ethanol production rate, ethanol yield, energy intensity and recovered energy for dilute sulphuric acid, steam explosion and alkaline pretreatment methods, SSCF and purification processes for sorghum stalks is shown in Table 4.14.

Table 4. 14: Combined summary of results for dilute sulphuric acid, steam explosion, alkali pretreatment, SSCF and purification process for sorghum stalks

Parameter	Unit	Pretreatment method with purification		
		Acid	Steam Explosion	Alkaline
Heating demand	MJ/h	334375.27	384327.72	298910.16
Cooling demand	MJ/h	351740.67	464886.90	301883.54
Electricity (Pumps)	kWh	1529.23	1720.13	705.3
Ethanol production rate	kg/h	21664.5	18698.6	12032.7
Ethanol production rate	L/h	27423.42	23669.11	15231.27
Ethanol yield	L/Tonne dry LGB	333.13	287.53	185.03
Energy intensity	MJ/L	12.39	16.50	19.79
Energy recovered	MJ/h	725870.16	784293.84	241460.28

The bioethanol production rate and bioethanol yield are higher for dilute sulphuric acid pretreatment, SSCF and purification technology than for steam explosion and alkaline pretreatment, SSCF and purification technologies. In addition, the energy intensity for dilute sulphuric acid pretreatment is lower than for steam explosion and alkaline

pretreatment methods. From the results shown in Table 4.14, dilute sulphuric acid pretreatment with SSCF was selected as the most suitable bioethanol production technology from sorghum stalks. The results shown in Table 4.10 indicate that the energy requirement for the pretreatment reactor is 88% of the total energy demand for dilute sulphuric acid pretreatment and SSCF 2GBE production technology. In addition, the cooling demand for SSCF reactor is 69% of the total cooling demand for dilute sulphuric acid pretreatment and SSCF technology. From the results shown in Table 4.12, Table 4.13 and Table 4.14, the energy demand for the pretreatment process is 50.78% while the energy demand for the distillation process is 49.22% of the total energy demand for pretreatment, SSCF and beer purification. This indicates that the pretreatment process consumes most of the energy during the production of bioethanol from sorghum stalks through dilute sulphuric acid pretreatment, SSCF and purification. According to da Silva et al. (2018), AFEX pretreatment consumed 72% and 73.9% of the total heating and cooling demand respectively. Porzio et al. (2012) reported that the pretreatment process consumes 72.33% of the total process energy requirements. Similar observations were made by Shukla et al. (2023); Beluhan et al. (2023); da Silva et al., 2016 and Humbird et al. (2011). Jarunglumlert and Prommuak (2021) reported that pretreatment and product purification are the most energy consuming processes during production of 2GBE. The recovered energy is able to cater for the energy demand required in dilute sulphuric acid pretreatment, SSCF and purification and steam explosion pretreatment, SSCF and purification processes. However, additional external source of energy is required to meet the energy demand in alkaline pretreatment, SSCF and purification process.

4.9 Sila Sorghum Stalks: Development and Simulation of Full-Scale Model for 2GBE Production

This section presents the various results obtained in order to achieve the second specific objective of this research study. The dilute sulphuric acid pretreatment and SSCF process was selected as the most promising technology in terms of energy intensity and ethanol production rate. This technology was used to develop and simulate a full-scale model for producing 2GBE. The process model is a shown in Figure 4.8.

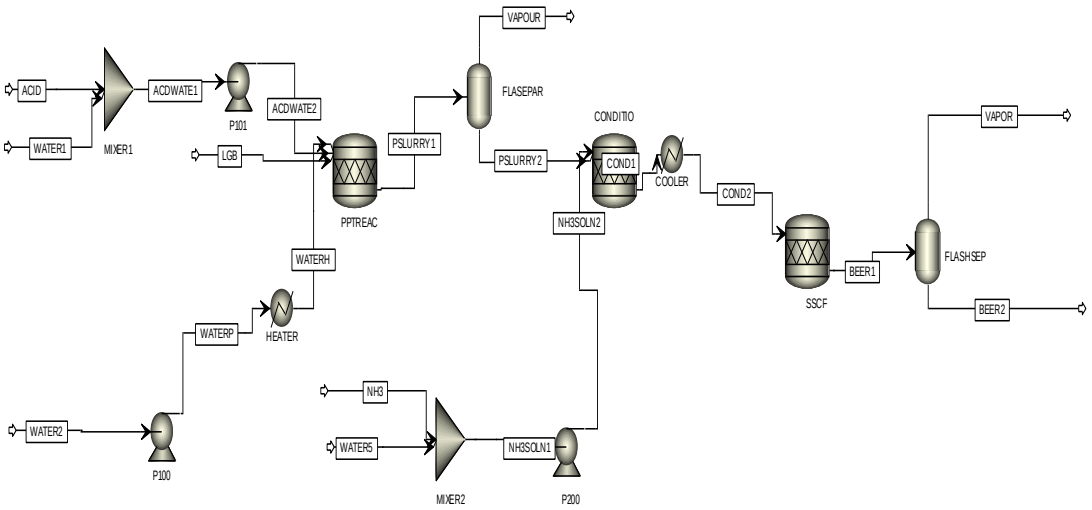

Figure 4. 8: PFD of dilute acid pretreatment and SSCF process for sorghum stalks

The results obtained after simulating the model are shown in Table 4.15.

Table 4. 15: Results of dilute sulphuric acid pretreatment and SSCF process with flash separator for sorghum stalks (Source: Aspen Plus simulator)

Stream/component	BEER (kmol/h)
Water	18805.54
Hemicellulose	8.14
Ethanol	474.37
Glucose	0.77
Xylose	21.97
Sulphuric acid	0.13
Extractives	20.84
Furfural	3.99
Ammonium sulphate	23.06
Lignin	198.35
Carbon dioxide	262.18
Ash	86.90
Cellulose	19.56
Total Flow (kmol/h)	19925.79
Total Flow (kg/h)	418983
Temperature (°C)	32

The beer stream indicated in Table 4.15 was fed into the ethanol purification, dehydration and energy recovery model shown in Figure 4.7. The results obtained after simulating this model are shown in Table 4.16.

Table 4. 16: Composition of product stream from the purification and dehydration section (Source: Aspen Plus simulator)

Stream/component	Ethanol
Ethanol (kmol/h)	469.73
Water (kmol/h)	1.358
Total Flow (kmol/h)	471.09
Total Flow (kg/h)	21664.61

4.10 Economic Analysis: Production of Bioethanol from Sorghum Stalks

During economic analysis, the assumptions stated in Table 4.17 were used.

Table 4. 17: Assumptions for techno-economic analysis

Parameter	Value
Plant life	30 years
Currency	USA dollars ($)
Discount rate	10%
Daily plant operation time	24 hours
Number of shifts	3 shifts
Number of operation days per year	330 days
Plant depreciation	Double declining method
Tax rate	30% (Republic of Kenya [ROK], 2021)
Construction period	3 years
First 12 months expenditure	8% (Davis et al., 2018; Humbird et al., 2011)
Next 12 months expenditure	60% (Davis et al., 2018; Humbird et al., 2011)
Last 12 months expenditure	32% (Davis et al., 2018; Humbird et al., 2011)
Working capital	5% of FCI

The construction period is important to the cash flow analysis because no income is earned during construction, but large sums of money are being expended (Davis et al. 2018). According to Davis et al. (2018), small projects (ussually less than $10 million investment) can be constructed in less than 18 months while larger projects can take up to 42 months. In the current study, a construction period of 36 months was used and the capital expenditure was spread out during the construction period as shown in Table

4.17. The construction period was inclusive of twelve months required before the start of actual construction for planning and engineering purposes.

4.10.1 Purchased equipment costs

The estimated purchased equipment costs are shown in Table 4.18.

Table 4. 18: Purchased equipment costs (Sinnott and Towler, 2020; Humbird et al., 2011)

Purchased equipment	Cost ($)
Handling and storage of substrate	15,697,389
Pretreatment	21,998,453.6
Conditioning	1,658,174.88
SSCF	20,450,823.7
Distillation and solid recovery	12,270,494.22
Waste water treatment	54,498,681.53
Boiler combustion	40,348,922.43
Utilities	4,421,799.72
Product storage	3,095,259.80
Total cost	**174,439,998.88**

4.10.2 Direct costs, indirect costs, TCI, fixed charges and service facilities

The direct costs, indirect costs, TCI, fixed charges and service facilities were estimated based on a percentage of FCI (Sinnott and Towler, 2020; Humbird et al., 2011). The results are shown in Table 4.19 to Table 4.23.

Table 4. 19: Direct costs (Sinnott and Towler, 2020; Humbird et al., 2011)

Component	% of FCI	Cost ($)
Purchased equipment	40	174,439,998.88
Purchase equipment installation	12	52,331,999.67
Instrumentation (installed)	2	8,721,999.94
Piping (installed)	4	17,443,999.89
Electrical (installed)	2	8,721,999.94
Buildings (including services)	4	17,443,999.89
Yard improvement	2	8,721,999.94
Service facilities (installed)	8	34,887,999.78
Land	1	4,360,999.97
Total direct costs		**327,074,997.90**

Table 4. 20: Indirect costs (Sinnott and Towler, 2020; Humbird et al., 2011)

Component	% of FCI	Cost ($)
Engineering and supervision	9	39,248,999.75
Construction expense	6	26,165,999.83
Contractor's fee	3	13,082,999.92
Legal expenses	2	8,721,999.94
Contingency	5	21,804,999.86
Total indirect costs		**109,024,999.30**

Table 4. 21: Total capital investment (Sinnott and Towler, 2020; Humbird et al., 2011)

Component	Cost ($)
FCI = Direct Cost + Indirect Cost	436,099,997.20
WCI = 5% FCI	21,804,999.86
Total Capital Investment (TCI)	**457,904,997.06**

Table 4. 22: Fixed charges (Sinnott and Towler, 2020; Humbird et al., 2011)

Component	Rate/% of FCI	Cost ($)
Depreciation (Rate: 0.067)	0.067	12,721,509.8
Local taxes	0.7	3,052,699.98
Insurance	0.7	3,052,699.98
Total fixed charges		**18,826,909.76**

Table 4. 23: Service facilities (Sinnott and Towler, 2020; Humbird et al., 2011)

Component	% of FCI	Cost ($)
Water supply	1.8	7,849,799.95
Water distribution	0.8	3,488,799.98
Electricity substation	1.3	5,669,299.96
Electricity distribution	1.0	4,360,999.97
Compressed air supply	1.0	4,360,999.97
Refrigeration	2.0	8,721,999.94
Fire protection system	0.5	2,180,499.99
Safety installation	0.4	1,744,399.99
Total service facilities		**38,376,799.75**

4.10.3 Total labour costs

The total labour costs were estimated based on the description in section 3.3.9.4. The distribution of labour requirements is shown in Appendix B, Table B.1. A summary of total labour costs is shown in Table 4.24.

Table 4. 24: Total labour costs (KNBS, 2022; Sinnott and Towler, 2020; Humbird et al., 2011)

Position	Number of personnel	Average monthly salary ($)	Annual salary ($)
Administration	12	1314	189,216
Finance	3	1578	56,808
Technical	11	1120	147,840
Manufacturing	79	432	409,536
Total salaries			**803,400**
Labour burden (90%)			**723,060**
Total labour costs			**1,526,460**

A summary of direct production costs is shown in Table 4.25.

Table 4. 25: Summary of direct production costs (Sinnott and Towler, 2020; Humbird et al., 2011)

Component	Cost ($)
Raw material costs	78,358,062.31
Total service facilities	38,376,799.76
Total labour costs	1,526,460
Total Direct Production Cost	**118,261,322.07**

A summary of total product costs is shown in Table 4.26.

Table 4. 26: Total product costs (Sinnott and Towler, 2020; Humbird et al., 2011)

Component	Cost ($)
Fixed charges	18,826,909.76
Direct production cost	118,261,322.07
Total Product Cost (TPC)	**137,088,231.83**

4.10.4 Analysis of cash flow

Cash flow was analyzed using parameters shown in Table 4.27.

Table 4. 27: Analysis of cash flow (Sinnott and Towler, 2020; Humbird et al., 2011)

Selling price of Ethanol	$ 1.0 per liter (for iteration purpose)
TCI	FCI+WCI
Start –up expense	5% of TCI
Gross profit for the first year	Total sales –TPC –Start –up cost – Depreciation
Gross profit after the first year	Total Sales –TPC- Depreciation
Net profit	Gross profit (1- income tax rate)
Annual Operating Cash Flow	Net profit +Depreciation –TCI
Cumulative Cash Flow	Net profit + Depreciation

The results of the cash flow analysis are shown in Table 4.28. All prices are in United States of America (USA) dollar ($).

Table 4. 28: Summary of cash flow analysis

Total Product Cost (TPC)	$137,088,231.83
Startup expense	$22,895,249.85
Total Product Cost per liter	$0.63/L
Direct production cost per liter	$0.34/L
Total Capital Investment (TCI)	$457,904,997.06
Internal Rate of Return (IRR)	11.47%

The results obtained during economic analysis were used to study the effect of varying cost and process parameters on the MBSP and the cost of producing bioethanol as presented in section 4.18.

4.11 Maize Cobs: Simulation Results Obtained From Various Models

The results of simulation for the various models representing the different pretreatment and SSCF bioethanol production technologies from maize cobs are presented in this section. All the results were obtained from Aspen Plus simulation software.

4.11.1 Simulation results for dilute sulphuric acid pretreatment and SSCF process for maize cobs

The model for dilute sulphuric acid pretreatment and SSCF process is shown in Figure 4.1. The results obtained after simulating the model are shown in Table 4.29.

Table 4. 29: Results of dilute sulphuric acid pretreatment and SSCF process for maize cobs

Stream/component	COND2 (kmol/h)	BEER1 (kmol/h)
Water	20988.00	20855.47
Hemicellulose	15.83	15.83
Ethanol	0.00	700.99
Glucose	16.93	0.85
Xylose	285.01	42.75
Sulphuric acid	0.13	0.13
Extractives	130.57	130.57
Furfural	8.25	8.25
Ammonium sulphate	23.06	23.06
Lignin	68.10	68.10
Carbon dioxide	0.00	700.99
Ash	64.41	64.41
Cellulose	154.10	21.57
Total Flow (kmol/h)	21754.39	22632.97
Total Flow (kg/h)	472769	472769

4.11.2 Simulation results for steam explosion pretreatment and SSCF process for maize cobs

The model for steam explosion pretreatment and SSCF process is shown in Figure 4.3.

The results obtained after simulating the model are shown in Table 4.30.

Table 4. 30: Results of steam explosion pretreatment and SSCF process for maize cobs

Stream/component	SODFRAC2 (kmol/h)	BEER (kmol/h)
Water	19714.51	19573.45
Hemicellulose	76.95	76.95
Ethanol	0.00	570.89
Glucose	7.01	0.35
Xylose	194.44	29.17
Furfural	5.74	5.74
Lignin	68.10	68.10
Carbon dioxide	0.00	570.89
Ash	64.41	64.41
Acetic acid	61.46	61.46
Extractives	130.57	130.57
Cellulose	164.02	22.96
Total Flow (kmol/h)	20487.21	21174.95
Total Flow (kg/h)	444515	444515

4.11.3 Simulation results for alkaline pretreatment and SSCF process for maize cobs

The model for alkaline pretreatment and SSCF process is shown in Figure 4.5. The results obtained after simulating the model are shown in Table 4.31.

Table 4. 31: Results of alkaline pretreatment and SSCF process for maize cobs

Stream/component	WATER4 (kmol/h)	SOLFRA2 (kmol/h)	BEER (kmol/h)
Water	6550	2056.23	8460.53
Hemicellulose	0.00	63.65	63.65
Ethanol	0.00	0.00	291.38
Lignin	0.00	15.46	15.46
Carbon dioxide	0.00	0.00	291.38
Cellulose	0.00	169.41	23.72
Total Flow (kmol/h)	6550	2304.75	9146.12
Total Flow (kg/h)	118000	75273	193273

The overall mass balance for dilute sulphuric acid, steam explosion and alkaline pretreatment methods for maize cobs is shown in appendix A.

4.12 Maize Cobs: Energy Analysis and Ethanol Production Rate for Pretreatment, Hydrolysis and Fermentation Processes

In order to compare and select the most suitable pretreatment, hydrolysis and fermentation technology in terms of ethanol production rate, energy demand and energy intensity, analysis of these parameters was done and presented in this section. All the results were obtained from Aspen Plus simulation software.

4.12.1 Energy analysis for dilute sulphuric acid, steam explosion, alkaline pretreatment and SSCF process

The heating and cooling demand for dilute sulphuric acid, steam explosion and alkaline pretreatment methods and SSCF process for maize cobs is shown in Table 4.32.

Table 4. 32: Heating and cooling demand for dilute sulphuric acid, steam explosion, alkaline pretreatment methods and SSCF process

Equipment/ process unit	Pretreatment method combined with SSCF					
	Dilute sulphuric acid		Steam Explosion		Alkaline	
	Heating demand (MJ/h)	Cooling demand (MJ/h)	Heating demand (MJ/h)	Cooling demand (MJ/h)	Heating demand (MJ/h)	Cooling demand (MJ/h)
Heater	18312.7	-	41909.76	-	104211	-
Pretreatment reactor	197828.64	-	200942.28	-	-	-
Conditioning reactor	9566.17	-	-	-	-	-
Cooler	-	75355.92	-	130121.64	-	10267.24
SSCF reactor	-	181440	-	226206.72	-	151522.92
Total	**225707.51**	**256795.92**	**242852.04**	**356328.36**	**104211**	**161790.16**

4.13 Maize Cobs: Summary of Energy Analysis and Ethanol Production Rate for Pretreatment, Hydrolysis and Fermentation Processes

A summary of heating demand, cooling demand, ethanol production rate and ethanol yield for dilute sulphuric acid, steam explosion and alkaline pretreatment methods and SSCF processes for maize cobs is shown in Table 4.33.

Table 4. 33: Summary of heating demand, cooling demand and ethanol production rate for SSCF processes for maize cobs

Parameter	Unit	Pretreatment method		
		Acid	Steam Explosion	Alkaline
Heating demand	MJ/h	225707.51	242852.04	104211
Cooling demand	MJ/h	256795.92	356328.36	161790.16
Ethanol production rate	kg/h	32280.60	26289.60	13418.1
Ethanol in beer stream	%, w/w	6.83	5.91	6.94
Ethanol yield	L/Tonne dry LGB	467.18	380.47	194.19

The results shown in Table 4.33 indicate that dilute sulphuric acid pretreatment and SSCF technology has a higher bioethanol production rate and yield per tonne of dry LGB than steam explosion and alkaline pretreatment methods. Similar observations were made for sorghum stalks.

4.14 Maize Cobs: Energy Analysis and Ethanol Production Rate for Pretreatment, Hydrolysis, Fermentation, Beer Purification and Energy Recovery Process

In order to compare and select the most suitable pretreatment, hydrolysis, fermentation, beer purification and energy recovery process in terms of ethanol production rate, energy demand, energy intensity and energy recovery, analysis of these parameters was done and presented in this section. The feed to the beer purification section consisted of the output stream (beer) from each model representing dilute sulphuric acid pretreatment and SSCF, steam explosion pretreatment and SSCF and alkaline pretreatment and SSCF processes. All the results were obtained from Aspen Plus simulation software.

4.14.1 Energy analysis and ethanol production rate for dilute sulphuric acid pretreatment, SSCF and beer purification process

The heating and cooling demand for purification of beer from dilute sulphuric acid, steam explosion, alkaline pretreatment methods and SSCF process is shown in Table 4.34.

Table 4. 34: Heating and cooling demand for purification of beer from dilute sulphuric acid, steam explosion, alkaline pretreatment methods and SSCF process

Equipment/ process unit	Pretreatment method combined with SSCF					
	Dilute sulphuric acid		Steam Explosion		Alkaline	
	Heating demand (MJ/h)	Cooling demand (MJ/h)	Heating demand (MJ/h)	Cooling demand (MJ/h)	Heating demand (MJ/h)	Cooling demand (MJ/h)
Beer column reboiler	194935.32	-	125829.72	-	123317.64	-
Beer column condenser	-	28932.7	-	27070.42	-	11753.86
Rectification reboiler	46117.08	-	51778.08		27902.66	-
Rectification condenser	-	134578.8	-	95928.84	-	90811.08
Cooler	-	31368.71	-	24913.33	-	13601.3
Total	**241052.4**	**194880.21**	**177607.8**	**147912.59**	**151220.3**	**116166.24**

4.15 Maize Cobs: Summary of Energy Analysis and Ethanol Production Rate for Pretreatment, SSCF and Beer Purification Processes

A summary of heating demand, cooling demand, ethanol production rate, ethanol yield, energy intensity and recovered energy for dilute sulphuric acid, steam explosion and alkaline pretreatment methods, SSCF and purification processes for maize cobs is shown in Table 4.35.

Table 4. 35: Combined summary of results for dilute sulphuric acid, steam explosion, alkali pretreatment, SSCF and purification processes for maize cobs

Parameter	Unit	Pretreatment, SSCF and Purification		
		Acid	Steam Explosion	Alkaline
Heating demand	MJ/h	466759.91	420459.84	255431.30
Cooling demand	MJ/h	451676.13	504240.95	277956.40
Electricity (Pumps)	kWh	1049.37	945.23	591.53
Ethanol production rate	kg/h	31074.40	24749.40	13266.60
Ethanol production rate	L/h	39334.68	31328.35	16793.16
Ethanol yield	L/Tonne dry LGB	449.72	358.18	192.00
Energy intensity	MJ/L	11.96	13.53	15.34
Energy recovered	MJ/h	297728.78	386603.28	194622.91

The results shown in Table 4.35 indicate that the bioethanol production rate and yield are higher for dilute sulphuric acid pretreatment than for steam explosion pretreatment and alkaline pretreatment. In addition, the energy intensity for dilute sulphuric acid pretreatment is lower than for steam explosion pretreatment and alkaline pretreatment. Therefore, dilute sulphuric acid pretreatment of maize cobs with SSCF was selected as the most suitable bioethanol production technology. The results shown in Table 4.32 indicate that the energy requirement for the pretreatment reactor is 87.65% of the total energy demand for dilute sulphuric acid pretreatment and SSCF. In addition, the cooling demand for SSCF reactor is 70.66% of the total cooling demand for dilute sulphuric acid pretreatment and SSCF. From the results shown in Table 4.32, Table

4.34 and Table 4.35, the energy demand for the pretreatment process is 48.36% while the energy demand for the distillation process is 51.64% of the total energy demand for pretreatment, SSCF and beer purification. This indicates that purification and dehydration processes consume most of the energy during the production of bioethanol from maize cobs through dilute sulphuric acid pretreatment, SSCF, recovery, purification and dehydration. According to Tgarguifa et al. (2018), purification and dehydration of bioethanol from the fermentation broth is one of the most energy demanding process steps in the production of 2GBE. The recovered energy is not able to cater for the energy demand required for bioethanol production using dilute sulphuric acid, steam explosion and alkaline pretreatment processes and additional external source of energy is required to meet the energy demand.

4.16 Economic Analysis: Production of Ethanol from Maize Cobs

During economic analysis, the assumptions stated in Table 4.17 were used. For maize cobs, the purchased equipment costs, direct costs, indirect costs, TCI, service facilities, fixed charges and raw material costs were estimated using the method applied for sorghum stalks. The results are as shown in Table 4.36 to Table 4.43.

Table 4. 36: Purchased equipment costs (Sinnott and Towler, 2020; Humbird et al., 2011)

Purchased equipment	**Cost ($)**
Handling and storage of substrate	19,508,466.95
Pretreatment	27,339,330.44
Conditioning	2,060,753.55
SSCF	25,415,960.46
Distillation and solid recovery	15,249,576.28
Waste water treatment	67,730,100.03
Boiler combustion	50,145,003.07
Utilities	5,495,342.80
Product storage	3,846,739.96
Total cost	**216,791,273.54**

Table 4. 37: Direct costs (Sinnott and Towler, 2020; Humbird et al., 2011)

Component	% of FCI	Cost ($)
Purchased equipment	40	216,791,273.54
Purchase equipment installation	12	65,037,382.06
Instrumentation (installed)	2	10,839,563.68
Piping (installed)	4	21,679,127.35
Electrical (installed)	2	10,839,563.68
Buildings (including services)	4	21,679,127.35
Yard improvement	2	10,839,563.68
Service facilities (installed)	8	43,358,254.71
Land	1	5,419,781.84
Total direct costs		**406,483,637.89**

Table 4. 38: Indirect costs (Sinnott and Towler, 2020; Humbird et al., 2011)

Component	% of FCI	Cost ($)
Engineering and supervision	9	48,778,036.55
Construction expense	6	32,518,691.03
Contractor's fee	3	16,259,345.52
Legal expenses	2	10,839,563.68
Contingency	5	27,098,909.19
Total indirect costs		**135,494,545.97**

Table 4. 39: Total capital investment (Sinnott and Towler, 2020; Humbird et al., 2011)

FCI = Direct Cost + Indirect Cost **($)**	541,978,183.86
WCI = 5% FCI **($)**	27,098,909.19
Total Capital Investment (TCI) **($)**	**569,077,093.05**

Table 4. 40: Service facilities (Sinnott and Towler, 2020; Humbird et al., 2011)

Component	% of FCI	Cost ($)
Water supply	1.8	9,755,607.31
Water distribution	0.8	4,335,825.47
Electricity substation	1.3	7,045,716.39
Electricity distribution	1.0	5,419,781.84
Compressed air supply	1.0	5,419,781.84
Refrigeration	2.0	10,839,563.68
Fire protection system	0.5	2,709,890.92
Safety installation	0.4	2,167,912.74
Total service facilities		**47,694,080.19**

Table 4. 41: Fixed charges (Sinnott and Towler, 2020; Humbird et al., 2011)

Component	Rate/% of FCI	Cost ($)
Depreciation ($) (Rate: 0.067)	0.067	15,810,091.31
Local taxes	0.7	3,793,847.29
Insurance	0.7	3,793,847.29
Total fixed charges ($)		**23,397,785.89**

A summary of direct production costs is shown in Table 4.42.

Table 4. 42: Direct production costs (Sinnott and Towler, 2020; Humbird et al., 2011)

Component	Cost ($)
Raw material costs	85,625,222.60
Total service facilities	47,694,080.19
Total labour costs	1,526,460
Total Direct Production Cost	**134,845,762.79**

A summary of total product costs is shown in Table 4.43.

Table 4. 43: Total product cost (Sinnott and Towler, 2020; Humbird et al., 2011)

Component	Cost ($)
Fixed charges	23,397,785.89
Direct production cost	134,845,762.79
Total Product Cost (TPC)	**158,243,548.68**

4.16.1 Analysis of cash flow

A summary of cash flow analysis is shown in Table 4.44.

Table 4. 44: Summary of cash flow analysis

Total Product Cost (TPC)	$158,243,548.68
Startup expense	$28453854.65
Total product cost per liter	$0.51/L
Direct production cost per liter	$0.22/L
Total Capital Investment (TCI)	$569,077,093.05
Internal Rate of Return (IRR)	17.10%

The results obtained during economic analysis were used to study the effect of varying cost and process parameters on the MBSP and the cost of producing bioethanol as presented in section 4.18.

4.17 Production of Bioethanol from Sorghum Stalks and Maize Cobs: Overall Results and Discussion

Table 4. 45: Combined summary of heating, cooling demand and ethanol production rate for acid pretreatment, SSCF and purification process for sorghum stalks and maize cobs

Parameter	Unit	Acid Pretreatment, SSCF with purification	
		Sorghum stalks	Maize cobs
Heating demand	MJ/h	334375.27	466759.91
Cooling demand	MJ/h	351740.67	451676.13
Electricity (Pumps)	kWh	1529.23	1049.37
Ethanol production	kg/h	21664.50	31074.40
Ethanol production	L/h	27423.42	39334.68
Ethanol yield	L/Tonne dry LGB	333.13	449.72
Energy intensity	MJ/L	12.39	11.96
Energy recovered	MJ/h	725870.16	297728.78

The results shown in Table 4.45 indicate that the energy recovered from the bioethanol production process involving sorghum stalks is sufficient to cater for the energy demand for the entire process. However, in the process involving maize cobs, additional energy is required to meet the energy demand for the process. The cooling demand for the process involving maize cobs is higher than that involving sorghum stalks. The process involving maize cobs has lower energy intensity than the process involving sorghum stalks. The results from the current research study indicate that bioethanol yield from sorghum stalks and maize cobs is 333.13 and 449.72 liters per tonne of dry LGB respectively. This shows that maize cobs have higher 2GBE yield than sorghum stalks. This can be attributed to the presence of high carbohydrate content (cellulose and hemicellulose) in maize cobs than in sorghum stalks. The energy intensity (process energy requirements per liter of bioethanol produced) is 12.39 MJ/L and 11.96 MJ/L for sorghum stalks and maize cobs respectively. Porzio et al. (2012) reported that the total process energy requirement was 18.32 MJ/L of ethanol. According to Jarunglumlert and Prommuak (2021), the energy required for the production of 2GBE

from rice straw and sugarcane was about 29–30 MJ/L. This was higher than that required for wheat straw (12–15 MJ/L) and potatoes (17.7 MJ/L). da Silva et al. (2016) reported that the process energy required was 11.88 MJ/L, 31.0 MJ/L and 24.54 MJ/L of ethanol for dilute acid, LHW and AFEX pretreatment technologies respectively. The values of energy intensity obtained from the current study are lower than those reported in literature. The differences can be attributed to the type of biomass, production technology and process conditions considered in the study. The 2GBE production rate from this study was compared with results found in literature for other substrates and production technologies as shown in Table 4.46.

Table 4. 46: Ethanol production rate: comparison between results from the current study with results from literature

Pretreatment method	Liters/tonne dry biomass	Literature
Steam explosion (General)	229.75	Conde-Mejíaa et al. (2012)
Steam explosion (Sorghum stalks)	287.53	This study
Steam explosion (maize cobs)	358.18	This study
Liquid hot water (General)	357.47	Conde-Mejíaa et al. (2012)
Dilute sulphuric acid (General)	366.33	Conde-Mejíaa et al. (2012)
Dilute sulphuric acid (Sorghum stalks)	333.13	This study
Dilute sulphuric acid (maize cobs)	449.72	This study
Ammonia fiber explosion (General)	372.53	Conde-Mejíaa et al. (2012)
Alkaline with Lime (General)	265.32	Conde-Mejíaa et al. (2012)
Sodium hydroxide (Sorghum stalks)	185.03	This study
Sodium hydroxide (maize cobs)	192.0	This study
Organosolvent (General)	233.05	Conde-Mejíaa et al. (2012)
Ozonolysis (blue agave bagasse)	431.38	Barreraa et al. (2016)
Ozonolysis (sugarcane bagasse)	389.08	Barreraa et al. (2016)
Steam catalyzed by SO_2 Pulp wood	310.0	Frankó et al. (2016)
Steam catalyzed by SO_2 (Early thinning	330.0	Frankó et al. (2016)
Steam catalyzed by SO_2 (Tops and branches	310.0	Frankó et al. (2016)
Steam catalyzed by SO_2 (Hog fuel)	240.0	Frankó et al. (2016)
Steam catalyzed by SO_2 (Fuel logs)	340.0	Frankó et al. (2016)
Steam catalyzed by SO_2 (Sawdust)	350.0	Frankó et al. (2016)
Modified AFEX (corn stover)	342.65	da Silva et al. (2018)
Sulphuric acid catalyzed ethanol organo-solvent (spruce biomass)	344.2	da Silva et al. (2017)
Dilute sulphuric acid (corn stover)	356.3	da Silva et al. (2016)
LHW (corn stover)	235.3	da Silva et al. (2016)
AFEX (corn stover)	239.9	da Silva et al. (2016)
Steam catalyzed by H_2SO_4 (Poplar)	316.0	Porzio et al. (2012)

The results of ethanol production rate, concentration of ethanol in the fermentation broth, heating demand and cooling demand obtained in the current study were compared with the results reported in literature as shown in Table 4.47.

Table 4. 47: Ethanol production rate, concentration of ethanol in the fermentation broth, heating demand and cooling demand: comparison between results from the current study with results from literature

Type of pretreatment	LGB	Ethanol production rate (kg/h)	Ethanol in broth (%, w/w)	Heating demand (MJ/h)	Cooling demand (MJ/h)	Reference
Dilute sulphuric acid	Sorghum stalks	21664.5	5.12	334375.27	351740.67	This study
Steam explosion	Sorghum stalks	18698.6	4.55	384327.72	464886.90	This study
Sodium hydroxide	Sorghum stalks	12032.7	6.76	298910.16	301883.54	This study
Dilute sulphuric acid	Maize cobs	31074.4	6.83	466759.91	451676.13	This study
Steam explosion	Maize cobs	24749.4	5.91	420459.84	504240.95	This study
Sodium hydroxide	Maize cobs	13266.6	6.94	255431.30	277956.40	This study
Modified AFEX	Corn stover	26284	6.67	623016	569808	da Silva et al. (2018)
Organo-solvent	Spruce biomass	24063	11.25	1271880	1408680	da Silva et al. (2017)
Dilute sulphuric acid	Corn stover	24922	5.85	374295.60	543344.40	da Silva et al. (2016)
LHW	Corn stover	16460	5.20	645706.8	193658.4	da Silva et al. (2016)
AFEX	Corn stover	16781	5.40	361026	722167.20	da Silva et al. (2016)

Frankó, et al. (2016) reported that the concentration of bioethanol in the fermentation broth ranged from 2.1%, w/w to 5.3 %, w/w from fuel logs, sawdust and shavings, hog fuel, pulpwood, tops and branches and early thinning forest residues. According to da Silva et al. (2016), the concentration of ethanol in the fermentation broth (beer) was 5.85% (w/w), 5.20% (w/w) and 5.40% (w/w) for dilute acid, LHW and AFEX pretreatment methods respectively. In the current study, the concentration of bioethanol

in the fermentation broth was 5.12% (w/w) and 6.83% (w/w) for the process involving dilute sulphuric acid pretreatment and SSCF of sorghum stalks and maize cobs respectively. The maximum possible concentration of bioethanol in the fermentation broth is 6.24% (w/w) and 8.49% (w/w) for the process involving dilute sulphuric acid pretreatment and SSCF of sorghum stalks and maize cobs respectively. According to da Silva et al. (2019), a higher ethanol concentration in the fermentation broth contributes to energy savings during distillation and dehydration processes. A comparison between pretreatment energy consumption results obtained in the current study with those found in literature is shown in Table 4.48.

Table 4. 48: Pretreatment energy consumption: comparison between results from the current study with results from literature

Pretreatment method	LGB	Pretreatment Energy Consumption	Reference
LHW	Palm oil residue	2.90 –16.52 MJ/kg dry LGB	Cheah et al., (2020)
Microwave-assisted organo-solvent	Mixed saw mill	12.5 –19.0 MJ/kg dry LGB	Cheah et al., (2020)
Hydrothermal liquefaction	Eucalyptus	26 MJ/kg of dry LGB	Cheah et al., (2020)
Dilute acid	SSS	2.06 MJ/kg dry LGB	This study
Steam explosion	SSS	2.43 MJ/kg dry LGB	This study
Alkaline	SSS	1.13 MJ/kg dry LGB	This study
Dilute acid	Maize cobs	2.58 MJ/kg dry LGB	This study
Steam explosion	Maize cobs	2.78 MJ/kg dry LGB	This study
Alkaline	Maize cobs	1.19 MJ/kg dry LGB	This study
Organosolvent	LGB	11.6 MJ/kg dry LGB	Conde-Mejíaa et al. (2012)
Dilute acid	Rice straw	1.23 MJ/kg dry LGB	Bakari et al. (2010)
Milling	LGB	4.0 –12.5 MJ/kg dry LGB	Shukla et al., (2023)
Steam explosion	LGB	0.2 –0.6 MJ/kg dry LGB	Shukla et al., (2023)
Organosolvent	Corn stover	15.07 MJ/kg dry LGB	da Silva et al., (2019)
Steam explosion	Corn stover	4.84 MJ/kg dry LGB	da Silva et al., (2019)
LHW	Corn stover	5.62 MJ/kg dry LGB	da Silva et al., (2019)
Steam	Poplar	13.25 MJ/L of ethanol	Porzio et al. (2012)
AFEX	Corn stover	8.34 MJ/kg dry LGB	da Silva et al., (2019)
Hydrothermal	Sugarcane bagasse	1.65-1.72 MJ/kg dry LGB	Jarunglumlert and Prommuak (2021)

A comparison between energy intensity results obtained in the current study with those found in literature is shown in Table 4.49.

Table 4. 49: Energy intensity: comparison between results from the current study with results from literature

Pretreatment method	LGB	Energy intensity (MJ/L of Ethanol)	Reference
Dilute acid	SSS	12.39	This study
Dilute acid	Maize cobs	11.96	This study
Modified AFEX	Corn stover	18.75	da Silva et al., (2018)
Organosolvent	Spruce (softwood tree)	41.82	da Silva et al., (2017)
Dilute acid	Corn stover	11.88	da Silva et al., (2016)
LHW	Corn stover	31.00	da Silva et al., (2016)
AFEX	Corn stover	24.54	da Silva et al., (2016)
Dilute acid	Wheat straw	12-15	Jarunglumlert and Prommuak (2021)
Dilute acid	Rice straw & SCB	29-30	Jarunglumlert and Prommuak (2021)
Dilute acid	Rice straw	10.16	Bakari et al. (2010)
Steam	Poplar	18.32	Porzio et al. (2012)

A comparison between bioethanol production cost from sorghum stalks and maize cobs is shown in Table 4.50.

Table 4. 50: Comparison of bioethanol production cost from sorghum stalks and maize cobs

LGB	Sorghum stalks		Maize cobs	
Component	$/L	Share of total cost (%)	$/L	Share of total cost (%)
Raw material	0.36	57.14	0.27	52.94
Total labour costs	0.01	1.59	0.01	1.96
Total service facilities	0.17	26.98	0.15	29.41
Total fixed charges	0.09	14.29	0.08	15.69
Total	**0.63**	**100**	**0.51**	**100.00**

The results shown in Table 4.50 indicate that the cost of raw materials is the main cost contributor in the production of bioethanol from sorghum stalks and maize cobs. From a study by Quintero et al. (2013) the yield of ethanol from empty fruit branches, coffee cut stems, sugarcane bagasse and rice husks were 313.83, 305.11, 298.21 and 250.56

liters per tonne of LGB respectively. The authors reported that the cost of producing ethanol was $0.5779/L, $0.6393/L, $0.6807/L and $0.7662/L from empty fruit branches, rice husks, coffee cut stems and sugar cane bagasse respectively. According to Quintero et al. (2013), ethanol derived from empty fruit bunches had the lowest cost of production because the cost of empty fruit bunches was the lowest compared to the other substrates. Barreraa et al. (2016) reported that the cost of producing bioethanol from sugarcane bagasse and blue agave bagasse pretreated by ozonolysis followed by SHCF was $0.384/L and $0.352/L respectively. Overall cost of raw materials was 35% of the total production cost (Barreraa et al., 2016). Frankó, et al. (2016) reported that MBSP from forest residues (fuel logs, sawdust and shavings, hog fuel, pulpwood, tops and branches and early thinning) ranged from $0.77/L to $1.52/L. Boakye-Boaten et al. (2017) reported that the cost of producing bioethanol from *Miscanthus x giganteus* pretreated by dilute sulphuric acid followed by SHCF varied between $0.65/L and $0.714/L upon varying the cost of feedstock at between $0.08/kg to $0.10/kg. According to da Silva et al. (2019), the pretreatment process contributes about one-third of the total production cost in 2GBE production process. The cost of producing bioethanol from maize cobs is lower than that reported by Quintero et al. (2013) because the yield of bioethanol obtained from maize cobs is higher than that produced from empty fruit branches, coffee cut stems, sugar cane bagasse and rice husks. However, the cost of producing bioethanol from sorghum stalks is higher than that of producing bioethanol from empty fruit branches and lower than that of producing bioethanol from rice husks, coffee cut stems and sugar cane bagasse as reported by Quintero et al. (2013). MBSP for sorghum stalks and maize cobs in the current study is $0.95/L and $0.79/L respectively at 10% discount rate. Jarunglumlert and Prommuak, (2021) reported that MBSP was $0.34/L and $0.63/L from sweet sorghum bagasse and

sugarcane bagasse respectively. According to Jarunglumlert and Prommuak (2021), the cost of raw materials and the pretreatment method used were the keys factors that had an impact on MBSP. From the above discussion, the range of 2GBE yield, MBSP and production cost of 2GBE from sorghum stalks and maize cobs is consistent with that of 2GBE from other substrates reported in literature. The differences in 2GBE production cost and the MBSP can be attributed to differences in composition of LGB, cost of raw materials and the type of technology used in the production of bioethanol (Jarunglumlert and Prommuak, 2021).

4.18 Effect of Varying Cost and Process Parameters on Bioethanol Production Rate, Bioethanol Production Cost and MBSP

This section presents the various results obtained in order to achieve the third specific objective of this research study. The effect of varying LGB flow rate, cost of LGB and enzymes, conversion of cellulose to glucose in the SSCF reactor, FCI, discount rate, income tax rate and plant life on bioethanol production rate, bioethanol production cost and the MBSP is presented in this section. MBSP was calculated from the DCFROR model. MBSP is the selling price of 2GBE that makes the NPV of the 2GBE production process equal to zero at a given discount rate and income tax rate within the entire plant life. MBSP does not include any taxes, levies or government subsidies. MBSP was compared with the landed cost of gasoline in Kenya. According to the Energy and Petroleum Regulatory Authority [EPRA, 2023], the landed cost of gasoline in Kenya was $0.70/L in the month of November 2023.

4.18.1 Effect of varying LGB flow rate on bioethanol production rate

The flow rate of LGB was varied between 10000 kg/h and 300000 kg/h and the impact of this variation on bioethanol production rate was established as shown in Figure 4.9

and Figure 4.10 for SSS and maize cobs respectively. During variation in LGB flow rate, the study assumed that the supply of LGB was guaranteed throughout the year, the same number of employees was able to handle the increased capacity and the quality of ethanol produced was not affected by the increase in capacity.

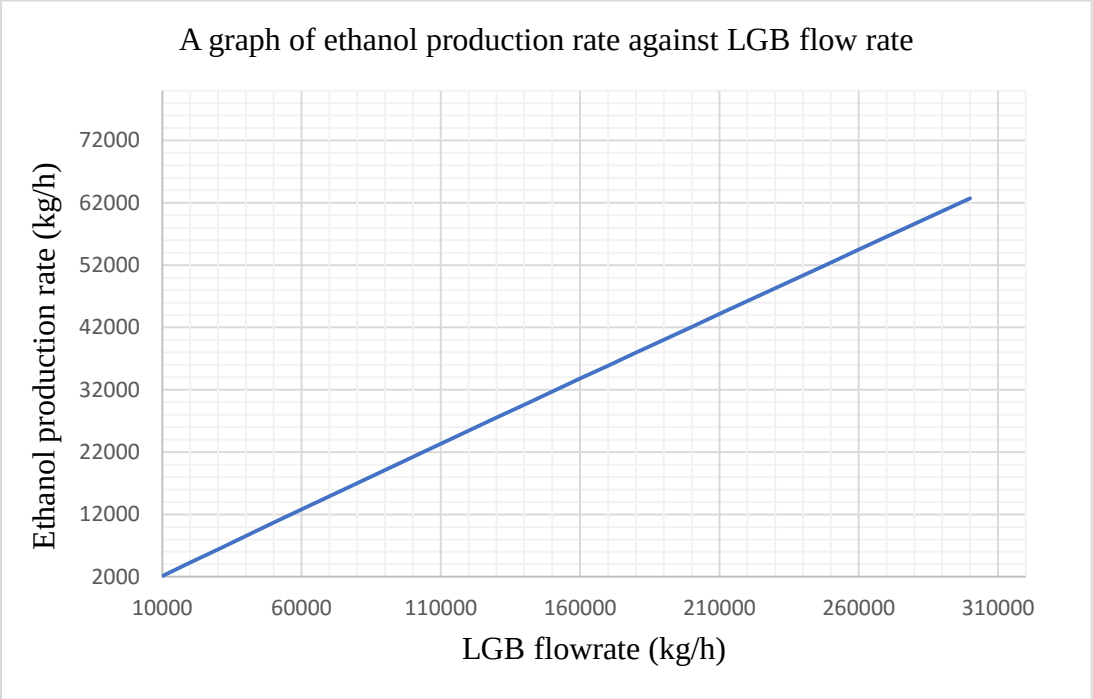

Figure 4. 9: Effect of varying LGB flow rate on ethanol production rate for sorghum stalks

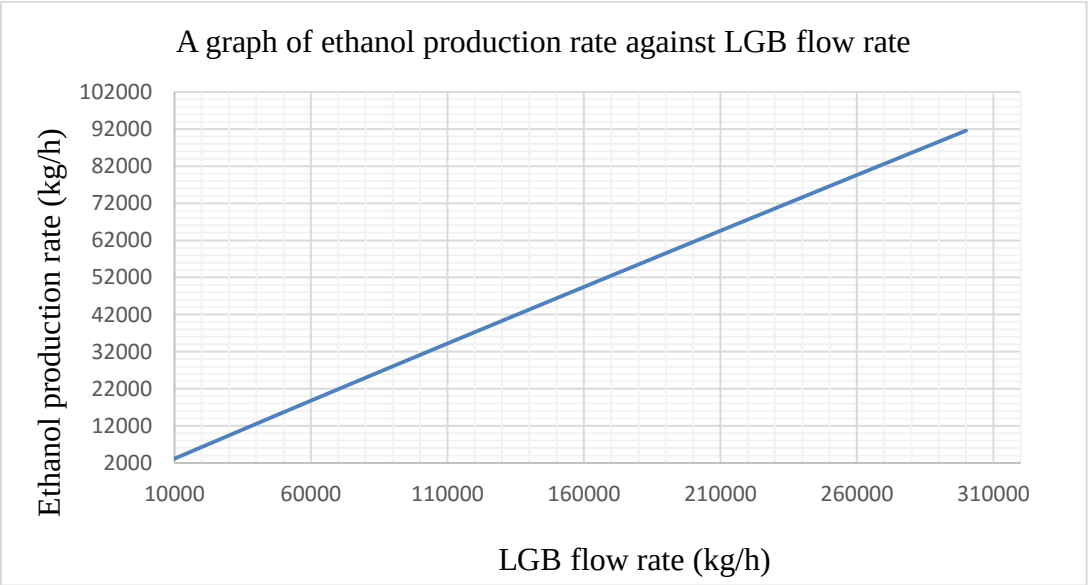

Figure 4. 10: Effect of varying LGB flow rate on ethanol production rate for maize cobs

Figure 4.9 and Figure 4.10 indicate that as the flow rate of LGB increases, the production rate of bioethanol increases. This is because of an increase in the quantity of cellulose and hemicellulose which are the main sources of glucose and xylose that are fermented to bioethanol. In addition, when the LGB flow rate was set at 80,000 kg/h, the product cost was $0.7/L and $0.56/L while the IRR was 6.96% and 12.67% for sorghum stalks and maize cobs respectively. On the other hand, at a feed rate of 130,000 kg/h, the product cost was $0.57/L and $0.45/L while the IRR was 16.77% and 23.80% for sorghum stalks and maize cobs respectively. The design feed rate was 102,900 kg/h with a product cost of $0.63/L and $0.51/L while IRR was 11.47% and 17.10% for sorghum stalks and maize cobs respectively. From the above comparison, increasing the flow rate of LGB results into a reduction in the product cost of about 9.52% and 11.76% for sorghum stalks and maize cobs respectively. Barreraa et al. (2016) reported that the cost of producing bioethanol from sugarcane bagasse and blue agave bagasse pretreated by ozonolysis followed by SHCF was $0.384/L and $0.352/L respectively. Quintero et al. (2013) reported that the cost of producing bioethanol was $0.5779/L, $0.6393/L, $0.6807/L and $0.7662/L from empty fruit branches, rice husks, coffee cut stems and sugar cane bagasse respectively. The cost of bioethanol obtained from the current study is higher than that reported by Barreraa et al. (2016). However, it is within the same range as reported by Quintero et al. (2013). Therefore, the flow rate of LGB has a significant impact on bioethanol production rate and production cost.

4.18.2 Effect of varying the conversion of cellulose to glucose in the SSCF reactor on ethanol production rate

The conversion of cellulose to glucose in the SSCF reactor was varied from 0.1 to 1.0 and the impact of this variation on ethanol production rate was established as shown in Figure 4.11 and Figure 4.12 for sorghum stalks and maize cobs respectively.

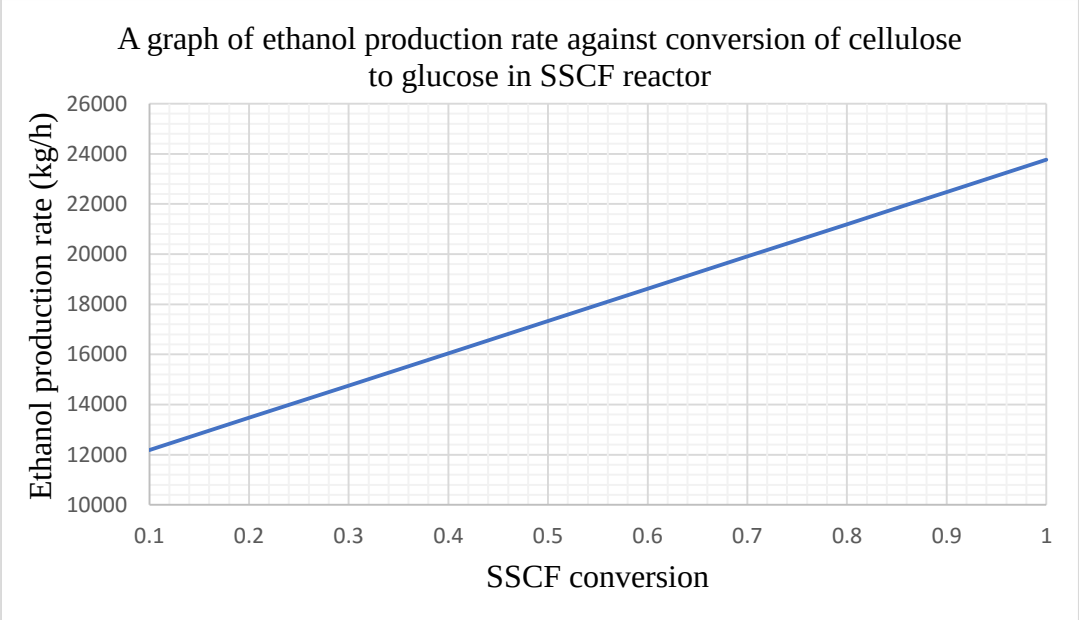

Figure 4. 11: Effect of varying SSCF conversion on ethanol production rate for sorghum stalks

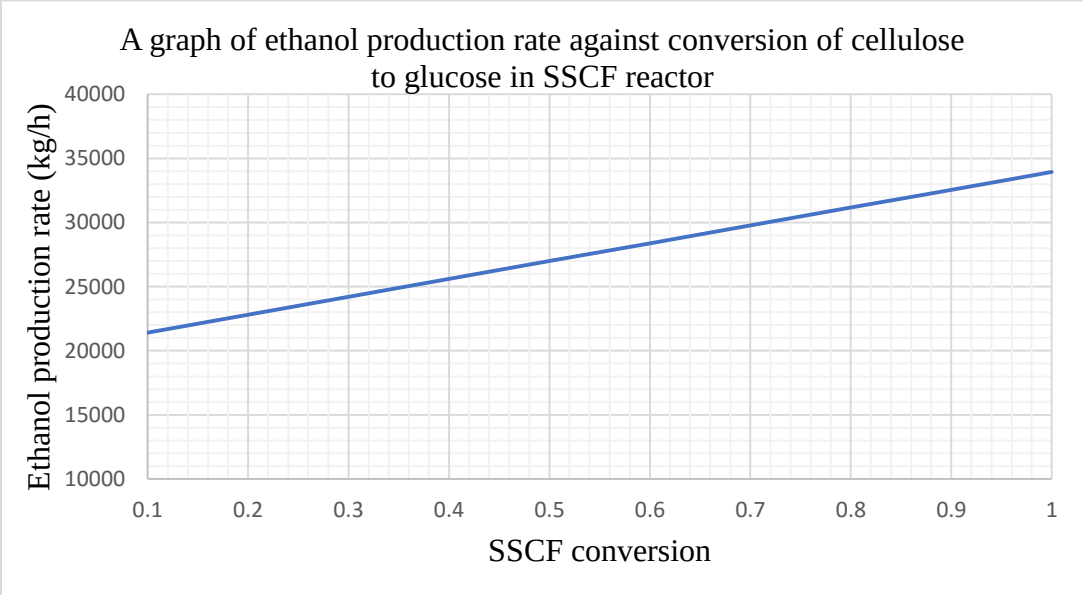

Figure 4. 12: Effect of varying SSCF conversion on ethanol production rate for maize cobs

Figure 4.11 and Figure 4.12 indicate that as the conversion of cellulose to glucose in the SSCF reactor increases, the production rate of bioethanol increases. This is because of an increase in the quantity of glucose produced from the conversion of cellulose which in turn is fermented to bioethanol. According to da Silva et al. (2019), high conversion of substrate to fermentable sugars increases the overall productivity of a

large-scale 2GBE production process. High conversion can be achieved by optimizing the pretreatment and hydrolysis processes through better equipment design and laboratory studies (da Silva et al., 2019). From an economic analysis point of view, at a conversion rate of 0.8, 0.9 and 1.0, the product cost was $0.64/L, $0.61/L, $0.57/L and $0.51/L, $0.48/L, $0.46/L for sorghum stalks and maize cobs respectively. On the other hand, at a conversion rate of 0.8, 0.9 and 1.0, the IRR was 10.94%, 12.58%, 14.60% and 17.17%, 18.81%, 20.17% for sorghum stalks and maize cobs respectively. In the current study, the base case conversion of cellulose to glucose in the SSCF reactor was 0.855 (Humbird et al., 2011). This resulted in a product cost of $0.63/L and $0.51/L and IRR of 11.47% and 17.10% for sorghum stalks and maize cobs respectively. From the above analysis, an increase in conversion from 0.8 to 1.0 resulted into a 10.94% and 9.80% reduction in product cost for sorghum stalks and maize cobs respectively. These results are within the range reported by Quintero et al. (2013) but higher than those reported by Barreraa et al. (2016). On the other hand, the impact of varying the conversion of cellulose to glucose in the SSCF reactor on the MBSP indicated that at a conversion rate of 0.8, 0.9 and 1.0, MBSP was $0.97/L, $0.92/L, $0.86/L and $0.79/L, $0.75/L, $0.71/L for sorghum stalks and maize cobs respectively.

Based on the above results, the MBSP would not compete with landed gasoline in the Kenyan market, where the landed cost of gasoline was approximately $0.70/L in the month of November 2023 (EPRA, 2023). However, upon adding distribution and storage costs, margins, levies and taxes to the landed cost of gasoline, the retail price of gasoline in Kenya was $1.35/L in the month of November 2023 (EPRA, 2023). Therefore, 2GBE is able to compete with gasoline in Kenya under the current conditions when no taxes and levies are imposed on the MBSP. These results further

indicate that a conversion of 0.7 and above is able to meet the E-10 bioethanol policy requirement in Kenya for both substrates.

4.18.3 Effect of varying LGB cost on bioethanol production cost and MBSP

The cost of LGB was varied between $20/tonne to $100/tonne and the impact of this variation on bioethanol production cost and the MBSP was established as shown in Figure 4.13 and Figure 4.14 respectively.

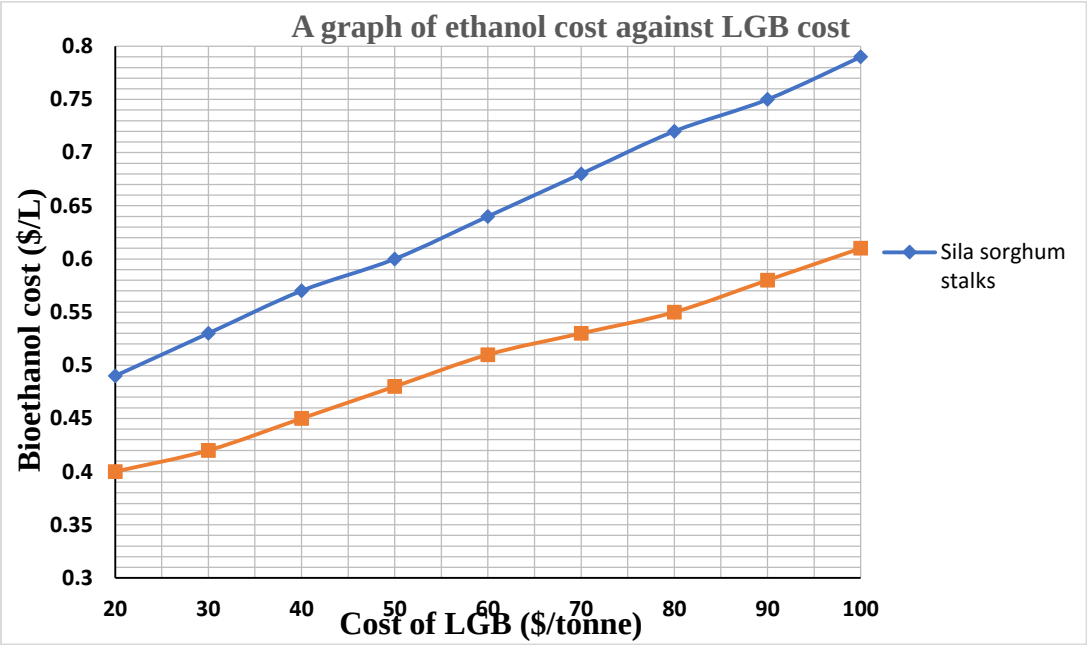

Figure 4. 13: Effect of varying LGB cost on bioethanol cost

Figure 4.13 indicate that changing the cost of LGB from $20/tonne to $100/tonne increases the production cost of bioethanol from $0.49/L and $0.40/L to $0.79/L and $0.61/L for sorghum stalks and maize cobs respectively. On the other hand, changing the cost of LGB from $20/tonne to $100/tonne increases the MBSP from $0.81/L and $0.68/L to $1.11/L and $0.89/L for sorghum stalks and maize cobs respectively. This is shown in Figure 4.14. Boakye-Boaten et al. (2017) reported that varying the cost of LGB from $0.08/kg to $0.10/kg increased the MBSP from $0.65/L to $0.71/L. Kazi et al. (2010) reported that the cost of producing bioethanol increased by 11% when the

cost of LGB was changed from $83/Mg to $110/Mg. Zhao et al. (2015) reported that the plant gate price of bioethanol ranged between $4.68–$6.05/gal.

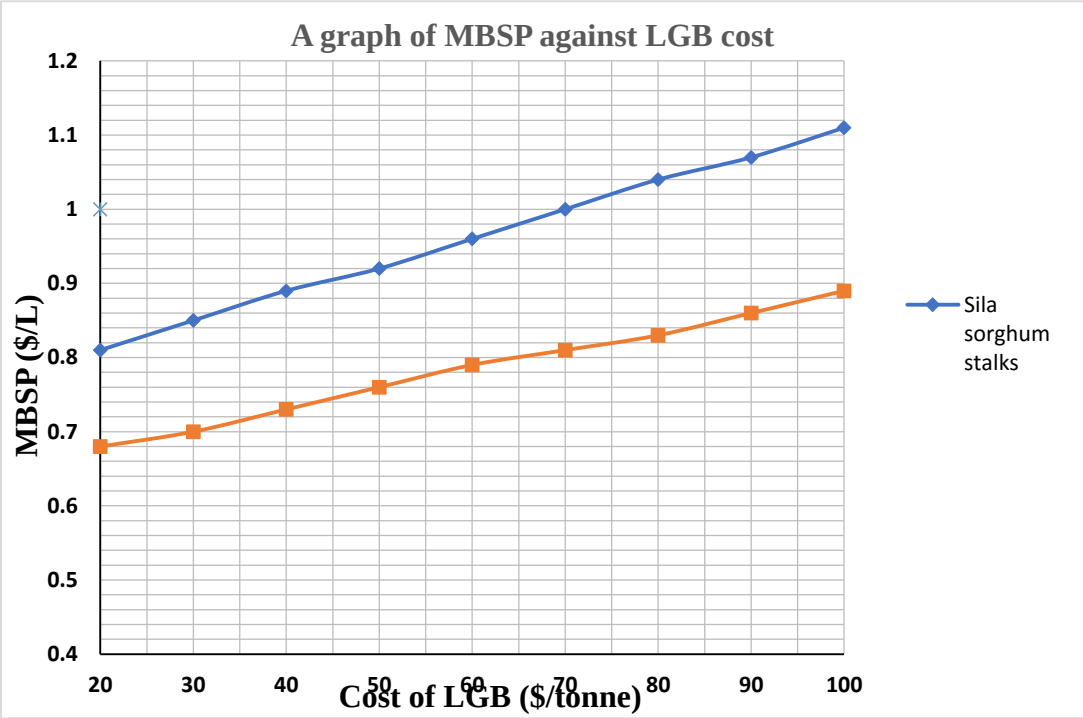

Figure 4. 14: Effect of varying cost of LGB on MBSP

Quintero et al. (2013) reported that the cost of producing bioethanol was $0.5779/L, $0.6393/L, $0.6807/L and $0.7662/L from empty fruit branches, rice husks, coffee cut stems and sugar cane bagasse respectively. Barreraa et al. (2016) reported that the cost of producing bioethanol from sugarcane bagasse and blue agave bagasse pretreated by ozonolysis followed by SHCF was $0.384/L and $0.352/L respectively. Frankó et al. (2016) reported that the MBSP from forest residues (fuel logs, sawdust and shavings, hog fuel, pulpwood, tops and branches and early thinning) ranged from $0.77/L to $1.52/L. From the above comparison, the range of the MBSP and bioethanol production cost from maize cobs and SSS is similar to that reported for other substrates and process technologies. From the foregoing, the cost of LGB has a significant impact on the cost of producing bioethanol and the MBSP. The differences in cost of producing bioethanol

and the MBSP are attributed to the type of LGB under consideration, country where the plant is located and the type of technology used in the production of bioethanol. The cost of LGB includes the amount that is paid to the farmer, transportation cost to the proposed plant site and size reduction of the LGB. One way of reducing the cost of LGB is by locating the plant near the source of substrate.

4.18.4 Effect of varying cost of enzyme on MBSP

Table 4. 51: Effect of varying enzyme cost on MBSP

Variation in enzyme cost	MBSP ($/L)	
	Sorghum stalks	Maize cobs
-50%	0.9	0.75
0	0.95	0.78
50%	1.0	0.82

The cost of enzymes was varied by $\pm$ 50% and the impact of this variation on the MBSP was established as shown in Table 4.51. Reducing the cost of enzyme by 50% resulted in a 5.3% and 3.8% reduction in the MBSP for sorghum stalks and maize cobs respectively. Kazi et al. (2010) reported that reducing the cost of enzyme within the same range resulted in a 10% reduction in bioethanol production cost.

Table 4. 52: Cost contribution for sorghum stalks and maize cobs

Parameter	Sorghum stalks		Maize cobs	
	Cost ($/L)	% Contribution	Cost ($/L)	% Contribution
LGB	0.22	61.11	0.16	59.26
Enzymes	0.09	25.0	0.07	25.93

The main cost contributors during the production of bioethanol in the current research study are shown in Table 4.52. In the raw material category, the cost of LGB is the largest cost contributor at 61.11% and 59.26% followed by the cost of enzymes at 25.0% and 25.93% for sorghum stalks and maize cobs respectively. These results are consistent with those reported in literature (Kazi et al., 2010; Humbird et al., 2011). Boakye-Boaten et al. (2017) reported that the cost of feedstock and enzymes contributes

39% and 15.7% of the total cost of producing bioethanol respectively. Telleria et al. (2018) reported that the cost of feedstock contributes between 30-40% of the overall cost while enzymes contribute 13%. Therefore, the cost of enzymes has a significant contribution to the overall cost of producing bioethanol and the MBSP (Humbird et al., 2011).

4.18.5 Effect of varying discount rate on MBSP

The discount rate was varied between 5% and 30% and the impact of this variation on the MBSP was established as shown in Figure 4.15.

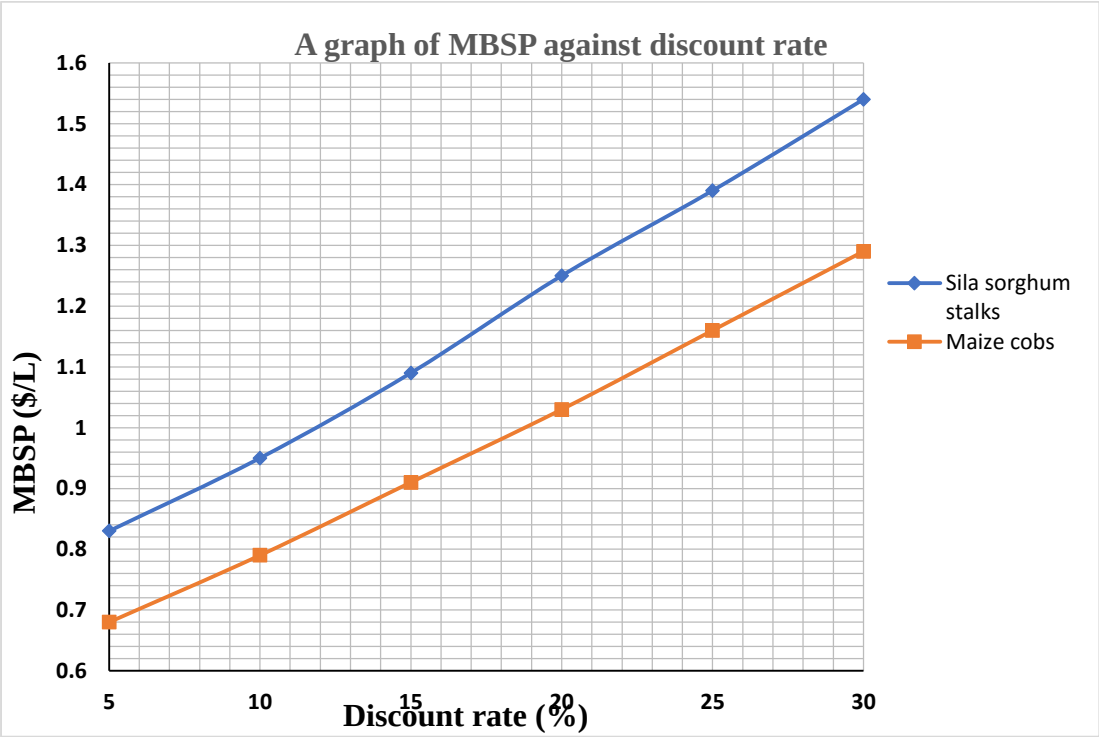

Figure 4. 15: Effect of varying discount rate on MBSP

The MBSP increased from $0.83/L and $0.68/L to $1.54/L and $1.29/L for sorghum stalks and maize cobs respectively when the discount rate was varied from 5% to 30%. Boakye-Boaten et al. (2017) reported similar results. The percentage change in the MBSP when the discount rate is varied between 10% and 20% is quite minimal for both substrates. These results indicate that the impact of discount rate on the MBSP is

insignificant. According to EPRA (2023), the landed cost of gasoline for the month of November, 2023 was $0.70/L. Comparing the cost of gasoline with the MBSP in Figure 4.15, the MBSP is beyond the present market value of landed gasoline in the Kenyan market, hence 2GBE produced from Sila sorghum stalks and maize cobs under the current techno-economic conditions cannot compete with gasoline in Kenya unless favourable policy interventions are enacted. In order to compete with fossil fuels, subsidies are currently used to support the production of biofuels (Beluhan et al., 2023).

4.18.6 Effect of varying FCI on MBSP

FCI was varied by $\pm$ 35% and the impact of this variation on the MBSP was established as shown in Table 4.53 for sorghum stalks and maize cobs respectively.

Table 4. 53: Effect of varying FCI on MBSP

Parameter	**Sorghum stalks**			**Maize cobs**		
Variation of FCI	**-35%**	**0**	**35%**	**-35%**	**0**	**35%**
MBSP ($/L)	0.85	0.95	1.06	0.69	0.79	0.88
% Change in MBSP	-10.53%	0	+11.59%	-11.54%	0	+12.82%

FCI affects the MBSP because changing the FCI by 35% increased the MBSP by 11.59% and 12.82% for sorghum stalks and maize cobs respectively, while a reduction in FCI by 35%, decreased the MBSP by 10.53% and 11.54% for sorghum stalks and maize cobs respectively. Similar observation was reported by Kazi et al. (2010). Therefore, FCI has a significant impact on the MBSP and a reduction in FCI would contribute to the techno-economic viability of large-scale bioethanol production from maize cobs and sorghum stalks found in Kenya.

4.18.7 Effect of varying plant life on MBSP

The effect of varying plant life on the MBSP was explored by varying the plant life from 10 to 30 years as shown on Figure 4.16.

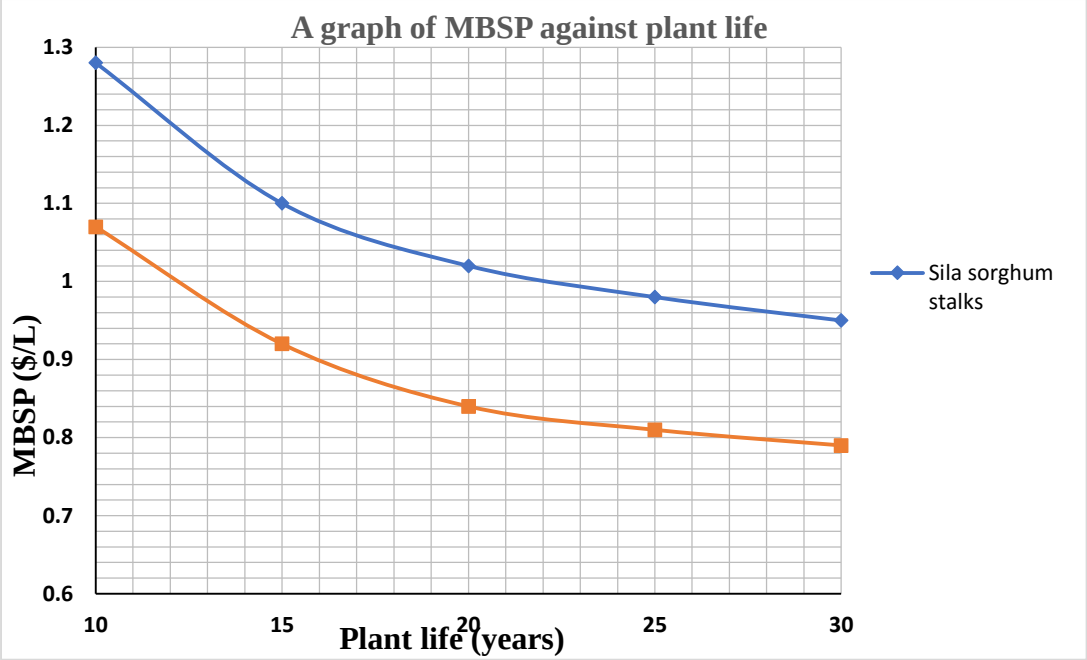

Figure 4. 16: Effect of varying plant life on MBSP

Figure 4.16 shows the impact of varying plant life on the MBSP, where by the MBSP decreases as plant life increases. Similar results were reported by Piccolo and Benzzo (2009). For both substrates, the most significant change in the MBSP was realized when the plant life increased from 10 to 15 years. However, there was insignificant change in the MBSP when plant life increased from 25 to 30 years. Therefore, plant life had insignificant impact on the MBSP especially when the 2GBE production plant was to operate beyond 25 years.

4.18.8 Effect of varying income tax rate on MBSP

The impact of varying income tax rate on the MBSP was explored by varying the applicable income tax rate from 0% to 40% as shown in Figure 4.17.

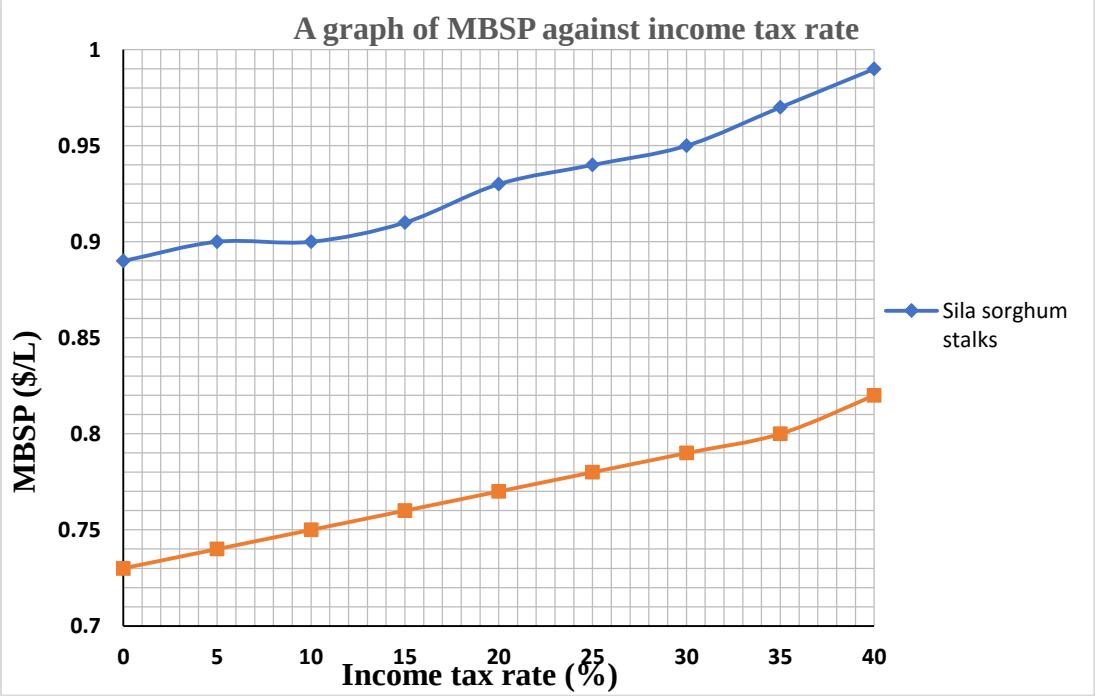

Figure 4. 17: Effect of varying income tax rate on MBSP

Figure 4.17 shows that changing the income tax rate from 0% to 40% increased the MBSP from $0.89/L and $0.73/L to $0.99/L and $0.82/L for sorghum stalks and maize cobs respectively. The percentage change in the MBSP was small (less than 2.5%), thus the impact of income tax rate on the MBSP was insignificant. Similar observation was reported by Boakye-Boaten et al. (2017). The current income tax rate in Kenya is 30% (ROK, 2021). This rate has no impact on the MBSP if a large-scale 2GBE production plant were to be built in Kenya.

4.19 Optimal Hydrolysis Conditions

This section presents the various results obtained in order to achieve the fourth specific objective of this research study.

4.19.1 Glucose yield from sorghum stalks

The actual and predicted yield of glucose from sorghum stalks under various experimental conditions is shown in Table 4.54. The manner in which the yield of glucose was obtained is shown in Appendix C.

Table 4. 54: Glucose yield from sorghum stalks

STD	RUN	X_1	X_2	X_3	Glucose Actual (g/L)	Glucose Yield (%, w/w) Actual)	Predicted
8	1	-1.682	0	0	2.91	70.55	72.65
7	2	0	0	-1.682	1.88	45.59	47.59
20	3	1	-1	1	2.75	66.68	67.25
10	4	0	0	0	3.48	84.38	86.22
6	5	1	1	1	3.36	81.47	80.77
17	6	0	-1.682	0	2.28	55.29	57.45
11	7	1	-1	-1	2.45	59.41	57.15
2	8	-1	-1	-1	2.15	52.13	51.21
15	9	0	0	0	3.59	87.05	86.22
16	10	-1	1	-1	2.26	54.8	52.6
14	11	0	0	0	3.48	84.38	86.22
19	12	-1	-1	1	3.19	77.35	75.02
18	13	0	0	1.682	3.29	79.78	80.08
1	14	0	0	0	3.61	87.54	86.22
12	15	1.682	0	0	3.18	77.11	77.33
9	16	1	1	-1	2.69	65.23	65.93
4	17	0	0	0	3.61	87.54	86.22
3	18	0	1.682	0	2.88	69.84	69.98
13	19	-1	1	1	3.32	80.5	81.14
5	20	0	0	0	3.58	86.81	86.22

By applying multiple regression analysis on the experimental data, a second-degree polynomial was found to represent the relationship between glucose yield (response) and the independent variables (hydrolysis temperature, hydrolysis time and acid concentration) adequately. The quadratic model (Equation 4.1) was selected as suggested by Design-Expert 13 software. Prediction of glucose yield from concentrated acid hydrolysis of sorghum stalks was done using Equation 4.1.

$$Y_{GSS} = 86.22 + 1.39X_1 + 3.73X_2 + 9.66X_3 + 1.85X_1X_2 - 3.43X_1X_3 + 1.18X_2X_3 - 3.97X_1^2 - 7.95X_2^2 - 7.91X_3^2 \quad 4.1$$

Where:

Y_{GSS} = Predicted yield of glucose from sorghum stalks (%)

In order to test the significance of the model depicting the yield of glucose from sorghum stalks, Design-Expert 13 was used to perform ANOVA. The results are shown in Table 4.55.

Table 4. 55: ANOVA for testing significance of the model equation

Source	Sum of squares	df	Mean square	F-value	p-value	
Model	3368.12	9	374.24	88.25	< 0.0001	significant
X_1	26.47	1	26.47	6.24	0.0315	
X_2	189.7	1	189.7	44.73	< 0.0001	
X_3	1274.75	1	1274.75	300.6	< 0.0001	
X_1X_2	27.35	1	27.35	6.45	0.0294	
X_1X_3	93.85	1	93.85	22.13	0.0008	
X_2X_3	11.18	1	11.18	2.64	0.1355	not significant
X_1^2	227.11	1	227.11	53.55	< 0.0001	
X_2^2	912.2	1	912.2	215.11	< 0.0001	
X_3^2	902.4	1	902.4	212.79	< 0.0001	
Residual	42.41	10	4.24			
Lack of Fit	31.19	5	6.24	2.78	0.1431	not significant
Pure Error	11.22	5	2.24			
Total	3410.53	19				
R^2	0.9876					
Adjusted R^2	0.9764					
Predicted R^2	0.9218					

The results of ANOVA for testing the significance of Equation 4.1 are shown in Table 4.55. From Table 4.55, the model representing the yield of glucose has an F- value of 88.25. This indicates that the experimental data involving the yield of glucose from sorghum stalks is well evaluated by Equation 4.1. The model F – value (88.25) implied that the model was significant and there was negligible chance (0.01%) that an F- value this large can occur because of noise. The implication of a higher F – value is that there is a high likelihood that the results did not happen by chance. The lack of fit F-value of 2.78 implies that the lack of fit is not significant relative to pure error. In addition, from Table 4.55, the coefficient of determination (R^2) for the model was 0.9876 with an adjusted R^2 of 0.9764 and predicted R^2 of 0.9218 for the yield of glucose from sorghum stalks, which indicated that Equation 4.1 adequately represented the relationship between hydrolysis time, hydrolysis temperature and concentration of sulphuric acid. R^2 value of 0.9876 means that 98.76% of the variability was explained by the model

and only 1.24% was as a result of chance. The validity of the model is supported by high R^2. This suggests that the model obtained can be used for prediction and simulation of the dependency of the yield of glucose on hydrolysis time, hydrolysis temperature and concentration of sulphuric acid within the range of investigation. The ANOVA results shown in Table 4.55 also indicate that acid concentration showed significant influence on glucose yield, followed by reaction time, while reaction temperature showed less significance on glucose yield. In addition, the interaction between acid concentration and reaction temperature showed significant influence on glucose yield followed by the interaction between reaction temperature and reaction time, while the interaction between reaction time and acid concentration showed less significance on glucose yield.

4.19.2 Optimization of concentrated acid hydrolysis of sorghum stalks

In order to optimize the variables that influence concentrated acid hydrolysis of sorghum stalks, response surface and contour plots (RSM plots) were generated using Design-Expert 13. These plots were generated by keeping one variable constant at the centre point (0) and varying the other two variables within the experimental range. The RSM plots were generated in terms of coded factors as shown in Table 3.21. The resulting plots depicted the effect of hydrolysis temperature (X1), time (X2) and acid concentration (X3) on the yield of glucose from sorghum stalks.

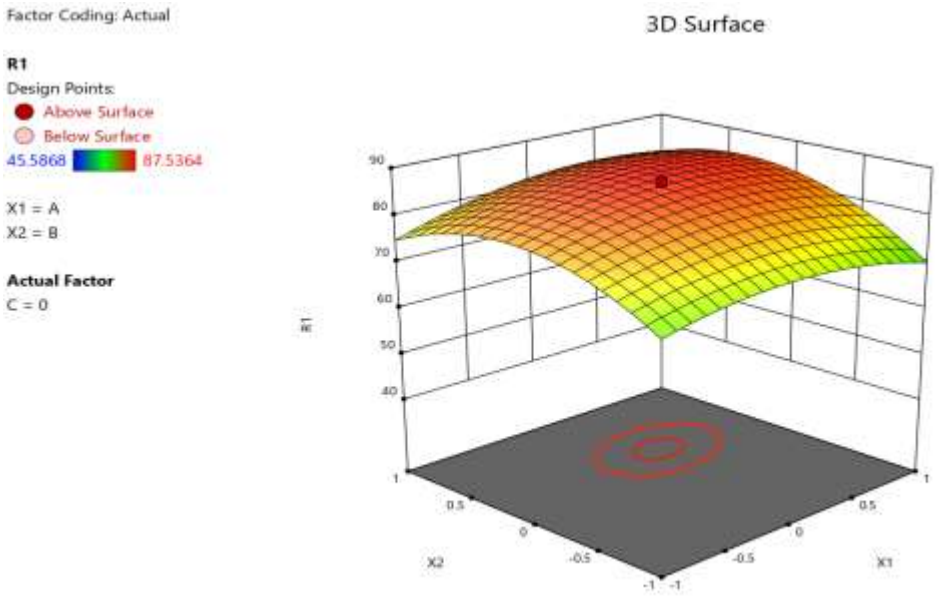

Figure 4. 18: RSM plot: effect of temperature (X1) and time (X2) on glucose yield (R1)

Figure 4.18 shows the effect of hydrolysis temperature (X1) and hydrolysis time (X2) on the yield of glucose (R1). This plot depicts how the yield of glucose from sorghum stalks varied with hydrolysis temperature and hydrolysis time. From the plot, maximum glucose yield was 87.54%, w/w which was realized when hydrolysis temperature and hydrolysis time were 60^{o}C and 60 minutes respectively. From Table 3.21, the level of these factors (temperature and time) was at the central setting and corresponded to the smallest eclipse as illustrated by the contour plot. The experimental observations were compared with the results depicted by the RSM plot. There was good agreement between experimental and predicted results which showed that optimum yield of glucose from sorghum stalks (87.54%, w/w) was realized at 60^{o}C (temperature) and 60 minutes (hydrolysis time). An increase in hydrolysis temperature and time resulted in an increase in glucose yield until the optimum value (87.54%, w/w). Any further increase in hydrolysis temperature and time was found to be unfavourable for the yield of glucose as explained by the decreasing trend observed. This could be attributed to the degradation of glucose due to increased hydrolysis temperature and time. Swiatek

et al. (2020) reported that increasing the hydrolysis temperature led to a decrease in glucose concentration. Similar observations were reported by Kanchanalai et al. (2016) and Wijaya et al. (2014).

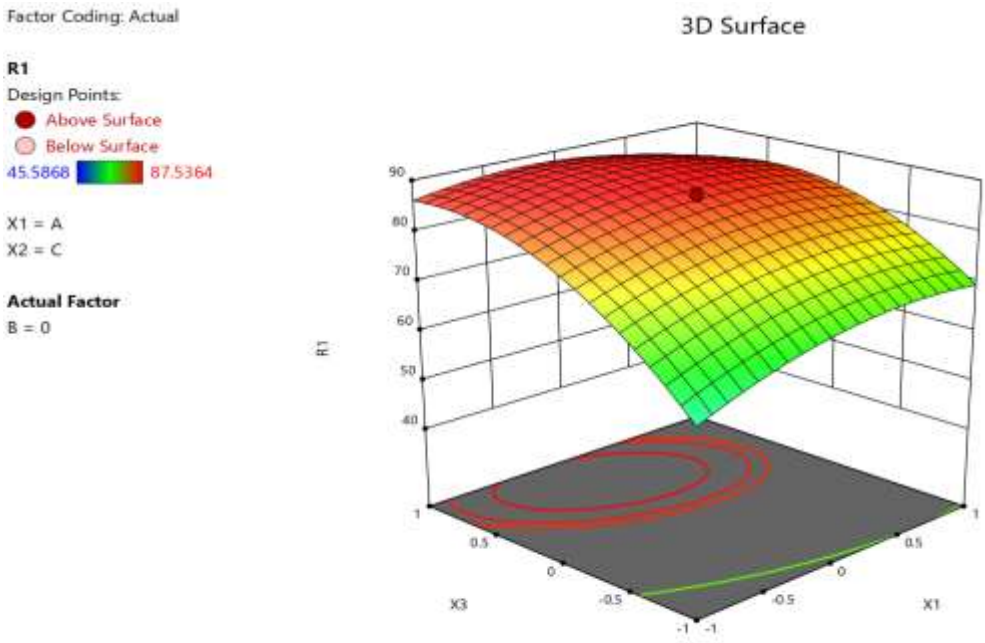

Figure 4. 19: RSM plot: effect of temperature (X1) and acid concentration (X3) on glucose yield (R1)

The effect of hydrolysis temperature (X1) and acid concentration (X3) on the yield of glucose (R1) is shown in Figure 4.19. An increase in hydrolysis temperature along with a steady increase in acid concentration resulted in an increase in glucose yield until the optimum value (87.54%, w/w). This was realized at 60^{o}C (temperature) and 50.0%, w/w (acid concentration). Under conditions of high acid concentration, the crystalline fraction of cellulose found in LGB is disintegrated and more glucose is produced. Since the acid acts as a catalyst, high concentration of acid increases the rate of the hydrolysis reaction, consequently increasing the yield of glucose. Further increase in hydrolysis temperature and acid concentration beyond the optimum level led to a decrease in glucose yield. According to Tizazu and Moholkar (2018), glucose mainly forms from amorphous fraction of cellulose during hydrolysis of LGB at low acid concentration.

However, at relatively higher acid concentration, the crystalline fraction of cellulose also undergoes hydrolysis, thus resulting into higher glucose yields (Tizazu & Moholkar, 2018). Similar observations were reported by (Kolo et al., 2020; Swiatek et al.,2020; Wijaya et al., 2014; Ioelovich, 2012; Janga et al., 2012; Chandel et al., 2012).

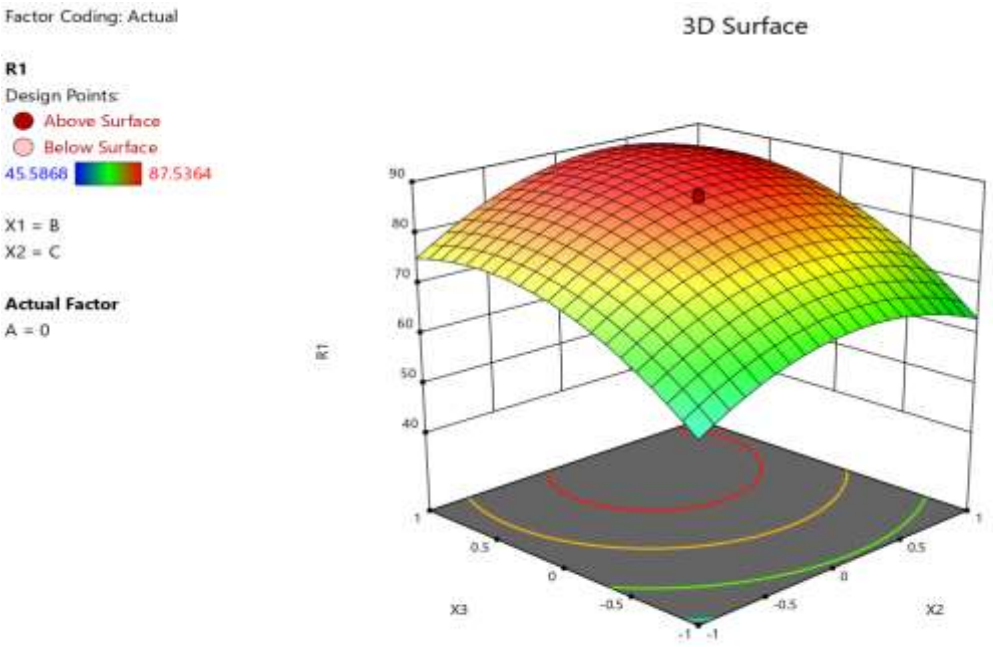

Figure 4. 20: RSM plot: effect of time and acid concentration on glucose yield

Figure 4.20 shows the effect of hydrolysis time (X2) and acid concentration (X3) on the yield of glucose (R1). The centre point of Figure 4.20 reveals the optimal values of hydrolysis time and acid concentration that may be combined to obtain optimal yield of glucose from sorghum stalks (87.54%, w/w). This was revealed to be 60 minutes hydrolysis time and 50.0% (w/w) acid concentration. At time levels higher than 60 minutes (central setting), the yield of glucose started to decrease slightly. This could be attributed to the degradation of glucose due to prolonged hydrolysis period. Swiatek et al. (2020) reported that prolonged hydrolysis period led to a decrease in the concentration of glucose due to inhibitor formation. Wijaya et al. (2014) reported that

the hydrolysis reaction time affected the concentration of sugar at higher temperature (100^{o}C) because extending the hydrolysis reaction time decreased the overall sugar yield at this temperature. Similar observations were made by Sarrouh et al. (2007) and Kanchanalai et al. (2016). In order to select the optimum conditions and their respective levels, the model was analysed. The maximum response (glucose yield) predicted from the model was 86.22 % (w/w). There was no significant difference between experimental (87.54%, w/w) and predicted (86.22%, w/w) values of glucose yield. The final optimized hydrolysis conditions obtained using RSM were 60^{o}C (temperature), 60 minutes (hydrolysis time) and 50.0% (w/w) (acid concentration).

4.19.3 Glucose yield from maize cobs

The actual and predicted yield of glucose from maize cobs under various experimental conditions is shown in Table 4.56. The manner in which the yield of glucose was obtained is shown in Appendix C. By applying multiple regression analysis on the experimental data, a second-degree polynomial was found to represent the relationship between glucose yield (response) and the independent variables (hydrolysis temperature, hydrolysis time and acid concentration) adequately.

Table 4. 56: Glucose yield from maize cobs

STD	RUN	X_1	X_2	X_3	Glucose		Glucose Yield (%, w/w)	
					Actual (g/L)	Predicted (g/L)	Actual	Predicted
9	1	-1.682	0	0	3.19	3.26	72.34	73.97
13	2	0	0	-1.682	2.29	2.38	51.93	53.89
6	3	1	-1	1	3.14	3.16	71.2	71.74
20	4	0	0	0	3.83	3.92	86.85	88.96
2	5	1	1	1	3.76	3.76	85.26	85.25
4	6	0	-1.682	0	2.67	2.76	60.54	62.52
12	7	1	-1	-1	2.82	2.73	63.95	61.98
7	8	-1	-1	-1	2.53	2.48	57.37	56.24
8	9	0	0	0	3.89	3.92	88.21	88.96
5	10	-1	1	-1	2.62	2.55	59.41	57.73
18	11	0	0	0	3.96	3.92	89.8	88.96
16	12	-1	-1	1	3.48	3.41	78.91	77.22
11	13	0	0	1.682	3.67	3.65	83.22	82.88
1	14	0	0	0	3.97	3.92	90.02	88.96
15	15	1.682	0	0	3.58	3.58	81.18	81.16
17	16	1	1	-1	3.14	3.16	71.2	71.75
14	17	0	0	0	3.95	3.92	89.57	88.96
3	18	0	1.682	0	3.33	3.31	75.51	75.15
19	19	-1	1	1	3.6	3.64	81.63	82.45
10	20	0	0	0	3.95	3.92	89.57	88.96

The quadratic model (Equation 4.2) was selected as suggested by Design-Expert 13. Prediction of glucose yield from concentrated sulphuric acid hydrolysis of maize cobs was done using Equation 4.2.

$$Y_{GMC} = 88.96 + 2.14X_1 + 3.75X_2 + 8.62X_3 + 2.07X_1X_2 - 2.81X_1X_3 + 0.9354X_2X_3 - 4.03X_1^2 - 7.11X_2^2 - 7.27X_3^2 \quad 4.2$$

Where:

Y_{GMC} = Predicted yield of glucose from maize cobs (%)

In order to test the significance of the model depicting the yield of glucose from maize cobs, Design-Expert 13 was used to perform ANOVA. The results are shown in Table 4.57.

Table 4. 57: ANOVA for testing significance of the model equation

Source	Sum of squares	df	Mean square	F-value	p-value	
Model	2839.24	9	315.47	103.88	< 0.0001	Significant
X_1	62.26	1	62.26	20.5	0.0011	
X_2	192.31	1	192.31	63.32	< 0.0001	
X_3	1014.51	1	1014.51	334.05	< 0.0001	
X_1X_2	34.25	1	34.25	11.28	0.0073	
X_1X_3	62.99	1	62.99	20.74	0.0011	
X_2X_3	7	1	7	2.3	0.1599	not significant
X_1^2	233.71	1	233.71	76.95	< 0.0001	
X_2^2	729.23	1	729.23	240.11	< 0.0001	
X_3^2	762.47	1	762.47	251.06	< 0.0001	
Residual	30.37	10	3.04			
Lack of Fit	22.79	5	4.56	3.0	0.1263	not significant
Pure Error	7.58	5	1.52			
Total	2869.61	19				
R^2	0.9894					
Adjusted R^2	0.9799					
Predicted R^2	0.9334					

The results of ANOVA for testing the significance of Equation 4.2 are shown in Table 4.57. From Table 4.57, the model representing the yield of glucose has an F- value of 103.88. This indicates that the experimental data involving the yield of glucose from maize cobs is well evaluated by Equation 4.2. The model F – value (103.88) implied that the model was significant and there was negligible chance (0.01%) that an F- value this large can occur because of noise. The implication of a higher F – value is that there is a high likelihood that the results did not happen by chance. The lack of fit F-value of 3.0 implies that the lack of fit is not significant relative to pure error. There is a 12.63 % chance that a lack of fit F-value this large could occur due to noise. In addition, from Table 4.57, R^2 for the model was 0.9894 with an adjusted R^2 of 0.9799 and predicted R^2 of 0.9334 for the yield of glucose from maize cobs, which indicated that Equation 4.2 adequately represented the relationship between hydrolysis time, hydrolysis temperature and concentration of sulphuric acid. R^2 value of 0.9894 means that 98.94% of the variability was explained by the model and only 1.06% was as a result of chance. The validity of the model is supported by high R^2. This suggests that the model obtained

can be used for prediction and simulation of the dependency of the yield of glucose on hydrolysis time, hydrolysis temperature and concentration of sulphuric acid within the range of investigation. The ANOVA results shown in Table 4.57 also indicate that acid concentration showed significant influence on glucose yield, followed by reaction time, while reaction temperature showed less significance on glucose yield. In addition, the interaction between acid concentration and reaction temperature showed significant influence on glucose yield followed by the interaction between reaction temperature and reaction time, while the interaction between reaction time and acid concentration showed less significance on glucose yield.

Model reduction

In order to test the significance of the various regression coefficients that describe the yield of glucose from maize cobs in Equation 4.2, Design-Expert 13 was used during the analysis. From Table 4.57, P-values lower than 0.05 indicate that the model terms are significant. In the present study, X_1, X_2, X_3, X_1X_2, X_1X_3, X_1^2, X_2^2 and X_3^2 are significant model terms. However, P-values greater than 0.05 indicate that the model terms are not significant. If there are many insignificant model terms (not including those required to support model hierarchy), model reduction may improve the model. From ANOVA (Table 4.57), the interaction term X_2X_3 is not significant (P-value is 0.1599). This term was removed and the reduced model is shown as Equation 4.3.

$$Y_{GMCR} = 88.96 + 2.14X_1 + 3.75X_2 + 8.62X_3 + 2.07X_1X_2 - 2.81X_1X_3 - 4.03X_1^2 - 7.11X_2^2 - 7.27X_3^2 \quad 4.3$$

Where:

Y_{GMCR} = Predicted glucose yield from maize cobs (%)

Table 4. 58: ANOVA for testing significance of the reduced model

Source	Sum of squares	df	Mean square	F-value	p-value	
Model	2832.25	8	354.03	104.21	< 0.0001	significant
X_1	62.26	1	62.26	18.33	0.0013	
X_2	192.31	1	192.31	56.61	< 0.0001	
X_3	1014.51	1	1014.51	298.63	< 0.0001	
X_1X_2	34.25	1	34.25	10.08	0.0088	
X_1X_3	62.99	1	62.99	18.54	0.0012	
X_1^2	233.71	1	233.71	68.79	< 0.0001	
X_2^2	729.23	1	729.23	214.65	< 0.0001	
X_3^2	762.47	1	762.47	224.44	< 0.0001	
Residual	37.37	11	3.4			
Lack of Fit	29.79	6	4.96	3.27	0.1071	not significant
Pure Error	7.58	5	1.52			
Total	2869.61	19				
R^2	0.9870					
Adjusted R^2	0.9775					
Predicted R^2	0.9399					

The results of ANOVA for testing the significance of the reduced model equation representing the hydrolysis of maize cobs are shown in Table 4.58. From Table 4.58, the reduced model representing the yield of glucose from maize cobs has an F- value of 104.21. This indicates that the experimental data involving the yield of glucose from maize cobs is well evaluated by Equation 4.3. The model F – value (104.21) implied that the reduced model was significant and there was negligible chance (0.01%) that an F- value this large can occur because of noise. The implication of a higher F – value is that there is a high likelihood that the results did not happen by chance. The lack of fit F-value of 3.27 implies that the lack of fit is not significant relative to pure error. There is a 10.71% chance that a lack of fit F-value this large could occur due to noise. In addition, from Table 4.58, R^2 for the reduced model was 0.9870 with an adjusted R^2 of 0.9775 and predicted R^2 of 0.9399 for the yield of glucose from maize cobs which indicated that the reduced model adequately represented the real relationship between hydrolysis time, hydrolysis temperature and concentration of sulphuric acid.

4.19.4 Optimization of concentrated acid hydrolysis of maize cobs

In order to optimize the variables that influence concentrated sulphuric acid hydrolysis of maize cobs, response surface and contour plots were generated using Design-Expert 13. The RSM plots depicted the effect of hydrolysis temperature (X1), time (X2) and acid concentration (X3) on the yield of glucose from maize cobs.

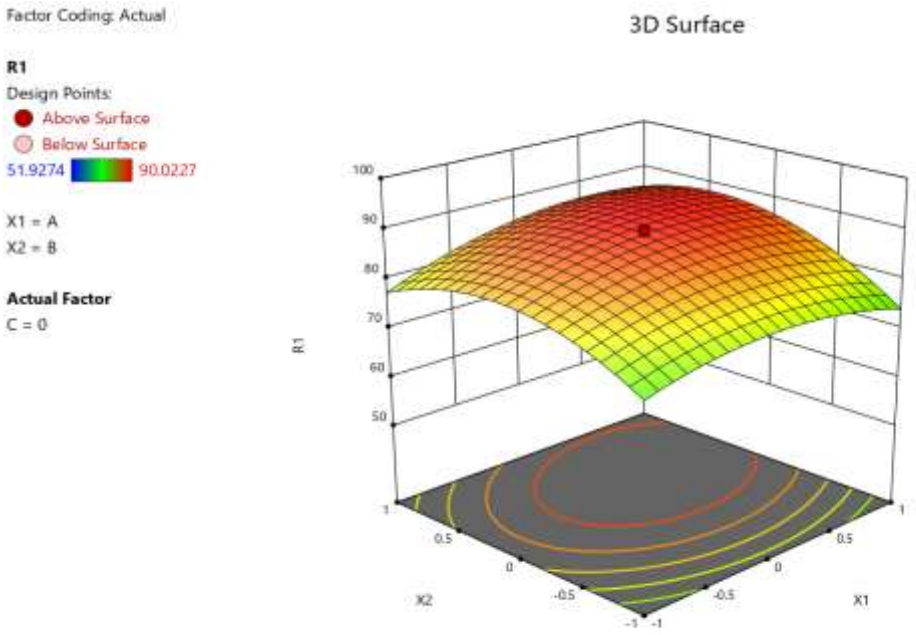

Figure 4. 21: RSM plot: effect of temperature (X1) and time (X2) on glucose yield (R1)

Figure 4.21 shows the RSM plot for the yield of glucose as a function of hydrolysis temperature (X1) and hydrolysis time (X2). This plot depicts how the yield of glucose from maize cobs varied with hydrolysis temperature and hydrolysis time. From the plot, maximum glucose yield was 90.02% (w/w) which was realized when hydrolysis temperature and hydrolysis time were 60^{o}C and 60 minutes respectively. From Table 3.21, the level of these factors (temperature and time) was at the central setting and corresponded to the smallest eclipse as illustrated by the contour plot. The experimental observations were compared with the results depicted by the RSM plot. There was good agreement between experimental and predicted results which showed that optimum

yield of glucose from maize cobs (90.02%, w/w) was realized at 60^{o}C (temperature) and 60 minutes (hydrolysis time). An increase in hydrolysis temperature and time resulted in an increase in glucose yield until the optimum value (90.02%, w/w). Any further increase in hydrolysis temperature and time was found to be unfavourable for the yield of glucose as explained by the decreasing trend observed. This could be attributed to the degradation of glucose due to increased hydrolysis temperature and time. Similar observations were reported by Swiatek et al. (2020), Kanchanalai et al. (2016) and Wijaya et al. (2014).

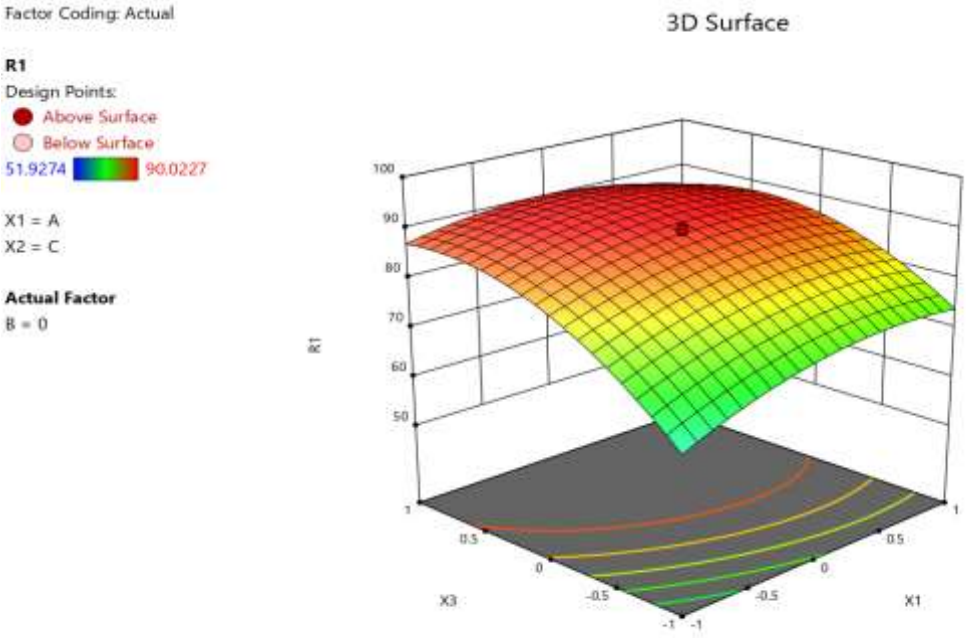

Figure 4. 22: RSM plot: effect of temperature (X1) and acid concentration (X3) on glucose yield (R1)

Figure 4.22 shows how hydrolysis temperature (X1) and acid concentration (X3) affected the yield of glucose from maize cobs. An increase in temperature along with a steady increase in acid concentration resulted in an increase in glucose yield until the optimum value (90.02%, w/w). This was realized at 60^{o}C (temperature) and 50.0%, w/w (acid concentration). Further increase in hydrolysis temperature and acid concentration beyond the optimum level resulted in a decrease in the yield of glucose.

Similar observations were reported by Kolo et al. (2020), Swiatek et al. (2020) and Wijaya et al. (2014).

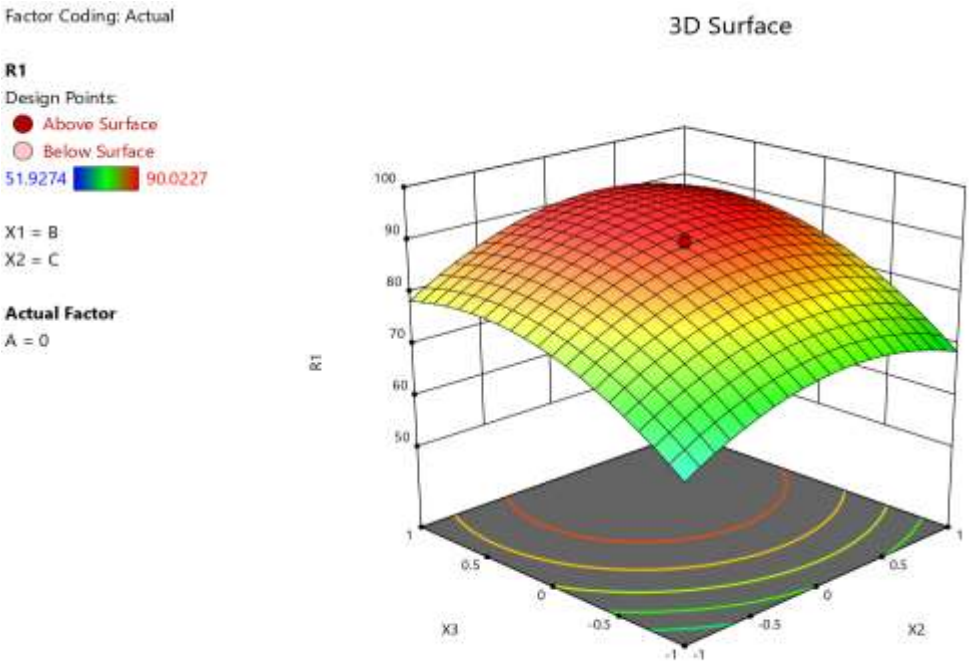

Figure 4. 23: RSM plot: effect of time (X2) and acid concentration (X3) on glucose yield (R1)

Figure 4.23 shows the effect of the interaction between hydrolysis time and acid concentration on the yield of glucose. The centre point of Figure 4.23 reveals the optimal values of hydrolysis time (X2) and acid concentration (X3) that may be combined to obtain optimal yield of glucose from maize cobs (90.02%, w/w). This was revealed to be 60 minutes hydrolysis time and 50.0% (w/w) acid concentration. There was no appreciable increase in the yield of glucose when the hydrolysis time and acid concentration were both increased after the optimum levels. At time levels higher than 60 minutes (central setting), the yield of glucose started to decrease slightly. This could be attributed to the degradation of glucose due to prolonged hydrolysis period. Swiatek et al. (2020) reported that prolonged hydrolysis period led to a decrease in the concentration of glucose due to inhibitor formation. Wijaya et al. (2014) reported that

the hydrolysis reaction time affected the concentration of sugar at higher temperature (100^{o}C) because extending the hydrolysis reaction time decreased the overall sugar yield at this temperature (Wijaya et al., 2014). Similar observations were made by Sarrouh et al. (2007) and Kanchanalai et al. (2016). In order to select the optimum conditions and their respective levels, the model was analysed. The maximum response predicted from the model was 88.96 % (w/w) glucose yield. There was no significant difference between experimental (90.02%, w/w) and predicted (88.96%, w/w) values of glucose yield. The final optimized hydrolysis conditions obtained using RSM were 60^{o}C (temperature), 60 minutes (hydrolysis time) and 50.0% (w/w) (acid concentration).

4.20 Model Validation

In order to validate the models obtained in the current study, the levels of factors that were found to be the optimum values (60^{o}C, 60 minutes and 50.0% (w/w) (acid concentration)) were used in carrying out separate experiments using sorghum stalks and maize cobs as substrates. The results of these experiments gave rise to a maximum glucose yield of 86.84% (w/w) and 89.43% (w/w) for sorghum stalks and maize cobs respectively. These results were similar to those obtained in the model prediction shown in Table 4.54 and Table 4.56 for sorghum stalks and maize cobs respectively. The generated models were thus considered to be accurate and reliable for predicting the yield of glucose from sorghum stalks and maize cobs.

4.21 Glucose Yield from Sorghum Stalks and Maize Cobs: Literature Based Comparison

The results of hydrolysis yield from sorghum stalks and maize cobs using concentrated sulphuric acid are displayed in Table 4.54 and Table 4.56 respectively. The optimum

yield of glucose is 87.54% (w/w) and 90.02% (w/w) from sorghum stalks and maize cobs respectively. This was obtained at 60°C hydrolysis temperature, 60 minutes hydrolysis period and 50 % (w/w) concentration of sulphuric acid from sorghum stalks and maize cobs respectively. Similarly, the lowest yield of glucose obtained was 45.59% (w/w) and 51.93% (w/w) from sorghum stalks and maize cobs respectively. This was obtained at 60°C hydrolysis temperature, 60 minutes hydrolysis period and 16.36 % (w/w) sulphuric acid concentration. The manner in which the yield of glucose was obtained is shown in Appendix C. The results obtained in the current study for glucose yield from sorghum stalks and maize cobs are within the range reported in literature. The difference between the results from the current study and those in literature can be attributed to different type of LGB under consideration, differences in structure and composition of LGB and the use of different hydrolysis reaction conditions. A summary of comparison of hydrolysis yield between the results obtained from the current study with results found in literature is shown in Table 4.59.

Table 4. 59: Comparison of hydrolysis yield results from this study with results from literature

Substrate	Optimum hydrolysis conditions	Response (%, w/w)	Reference
Cotton	78.22%. w/w formic acid, 65^{o}C, 5 h	32.0% (reducing sugars)	Chu et al. (2011)
Cotton	55%, w/w H_2SO_4, 40^{o}C, 90 min	73.9% (reducing sugars)	Chu et al. (2011)
Elephant grass	2%, w/w H_2SO_4, 95^{o}C, 30 min	66.57% hydrolysis efficiency	Kolo et al. (2020)
SCB	7%, w/w H_2SO_4, 125^{o}C, 120 min	29.0% (reducing sugars)	Chu et al. (2011)
SCB	4%, w/w H_2SO_4, 122^{o}C, 300 min	23.2% (reducing sugars)	Chu et al. (2011)
Newspaper	70.8%, w/w H_2SO_4, 30^{o}C, 3.6h	92.1% glucose conversion	Jung et al. (2013)
SSS	50%, w/w H_2SO_4, 50^{o}C, 60 min	87.54% (glucose)	This study
Maize cobs	50%, w/w H_2SO_4, 50^{o}C, 60 min	90.02% (glucose)	This study
Aspen wood	70%, w/w H_2SO_4, 38^{o}C, 60 min	74 % (total sugar)	Janga et al. (2012)
Pine wood	66.4%, w/w H_2SO_4, 39.6^{o}C, 60 min	91% (total sugar)	Janga et al. (2012)
Cocoa pod husk	4%, w/w H_2SO_4, 121^{o}C, 60 min	43.49% (glucose yield)	Mensah et al. (2020)
Energetic willow	Viscozyme & glucosidase enzymes, 42^{o}C, 24h	79.7% (glucose efficiency)	Lukajtis et al. (2018)
SCB	70%, w/w H_2SO_4, 50^{o}C, 60 min	87.6% (sugar)	Sarrouh et al. (2007)
Oakwood	75%, w/w H_2SO_4, 80^{o}C, 30 min	34.53% (glucose)	Wijaya et al. (2014)
Pine wood	80%, w/w H_2SO_4, 80^{o}C, 30 min	29.94% (glucose)	Wijaya et al. (2014)
Mature coconut husk	CTec2 and HTec2 enzymes, 30^{o}C, 48h	90.72% (enzymatic conversion)	Telleria et al. (2018)
BPS	29.2 mg/g dry substrate enzyme, 50^{o}C, 76 h	86.7% (hydrolysis efficiency)	Legodi et al. (2021)
Soybean straw	CTec2 cellulase, 42^{o}C, 48h	90.9% (glucose yield efficiency)	Kim et al. (2018)
Empty fruit bunch	80%, w/w H_2SO_4, 80^{o}C, 30 min	31.68% (glucose)	Wijaya et al. (2014)

4.22 Kinetics Studies

This section presents the various results obtained in order to achieve the fifth specific objective of this research study. The results of the rate constants are shown in Table 4.60 and Table 4.61 for sorghum stalks and maize cobs respectively.

Table 4. 60: Rate constants for glucose formation and degradation during kinetic studies of sorghum stalks

Temperature		k_1	k_2	k_1/k_2	t_{max}	1/T	Ln	Ln
°C	K	(min^{-1})	(min^{-1})		(min)		k1	k2
30	303	0.0573	0.00009	636.67	112.85	0.0033	-2.86	-9.32
40	313	0.0718	0.00034	211.18	74.90	0.0032	-2.63	-7.99
50	323	0.0944	0.00087	108.51	50.11	0.0031	-2.36	-7.05
60	333	0.1177	0.00099	118.89	40.94	0.0030	-2.14	-6.92
70	343	0.1823	0.00358	50.92	21.99	0.0029	-1.70	-5.63
80	353	0.2336	0.00822	28.42	14.85	0.00283	-1.45	-4.80

Table 4. 61: Rate constants for glucose formation and degradation during kinetic studies of maize cobs

Temperature		k_1	k_2	k_1/k_2	t_{max}	1/T	Ln k1	Ln k2
°C	K	(min^{-1})	(min^{-1})		(min)			
30	303	0.0656	0.0005	131.20	74.91	0.0033	-2.72	-7.60
40	313	0.0856	0.0011	77.82	51.53	0.0032	-2.46	-6.81
50	323	0.1244	0.002	62.20	33.74	0.0031	-2.08	-6.21
60	333	0.1558	0.00245	63.59	27.08	0.0030	-1.86	-6.01
70	343	0.2205	0.00616	35.80	16.69	0.0029	-1.51	-5.09
80	353	0.2756	0.01017	27.10	12.43	0.0028	-1.29	-4.59

The results shown in Table 4.60 and Table 4.61 indicate that the values of k_2 are small compared to k_1. In addition, the results indicate that, in the temperature range of 30°C – 80°C, the hydrolysis of cellulose to glucose is faster than the degradation of glucose. This scenario depicts a situation where glucose formation from cellulose during concentrated H_2SO_4 hydrolysis of sorghum stalks and maize cobs occurs at a faster rate than decomposition of glucose into HMF. The low values of k_2 are attributed to higher activation energy of glucose degradation and lower activation energy for cellulose hydrolysis to glucose as shown by the results of this study. High activation energy is an indication of how difficult it is to degrade glucose into HMF. Similar results were reported by Tizazu and Moholkar (2018). Comparing the values of rate constants, in

the case of $^{k_1}/_{k_2} > 1.0$, the rate of glucose formation from cellulose is faster than the rate of glucose degradation with a corresponding lower activation energy, while values of $^{k_1}/_{k_2} < 1.0$ implies that the rate of glucose degradation is faster than the rate of glucose formation which has a corresponding higher activation energy (Tizazu & Moholkar, 2018). In the reaction where temperature is varied from 30^{o}C to 80^{o}C, the quantity of glucose increases as temperature increases from 30^{o}C to 80^{o}C. This can be attributed to faster hydrolysis reaction as temperature increases (Mensah et al., 2020). In addition, lower temperature (30^{o}C) requires longer hydrolysis period while higher temperature (80^{o}C) requires shorter hydrolysis period. On the other hand, the rate of degradation of glucose increases as the hydrolysis temperature increases. This is supported by the results in Table 4.60 and Table 4.61, where the values of rate constants for glucose degradation are lower at low hydrolysis temperature and higher at high hydrolysis temperature. Similar observations were reported by Liu, et al. (2012). High temperature and prolonged hydrolysis period favour the degradation of glucose which in turn lead to substrate loss. The loss of substrate during hydrolysis impacts negatively on the fermentation yield due to low yield of fermentable sugars and high content of fermentation inhibitors (Liu, et al., 2012). The rate constants shown in Table 4.60 and Table 4.61 were used to establish the activation energy and pre-exponential factor (kinetic parameters) shown in Table 4.62 for sorghum stalks and maize cobs. The kinetic parameters were obtained from Arrhenius plots of $\ln k_{1,2}$ against 1/T for glucose production and degradation from sorghum stalks and maize cobs respectively (Figure 4.24 to Figure 4.27).

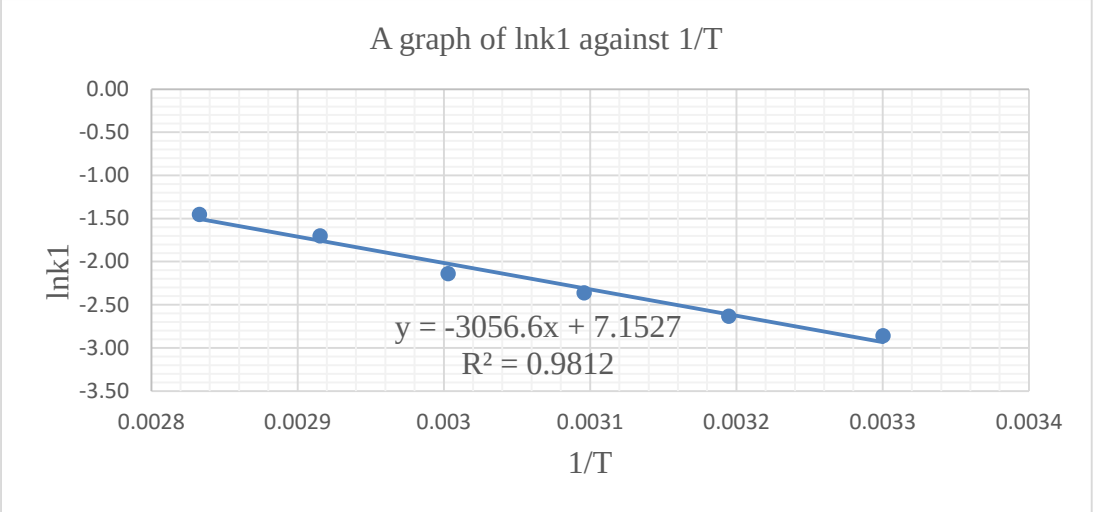

Figure 4. 24: Arrhenius plot of lnk1 against 1/T for sorghum stalks (Source: Table 4.60)

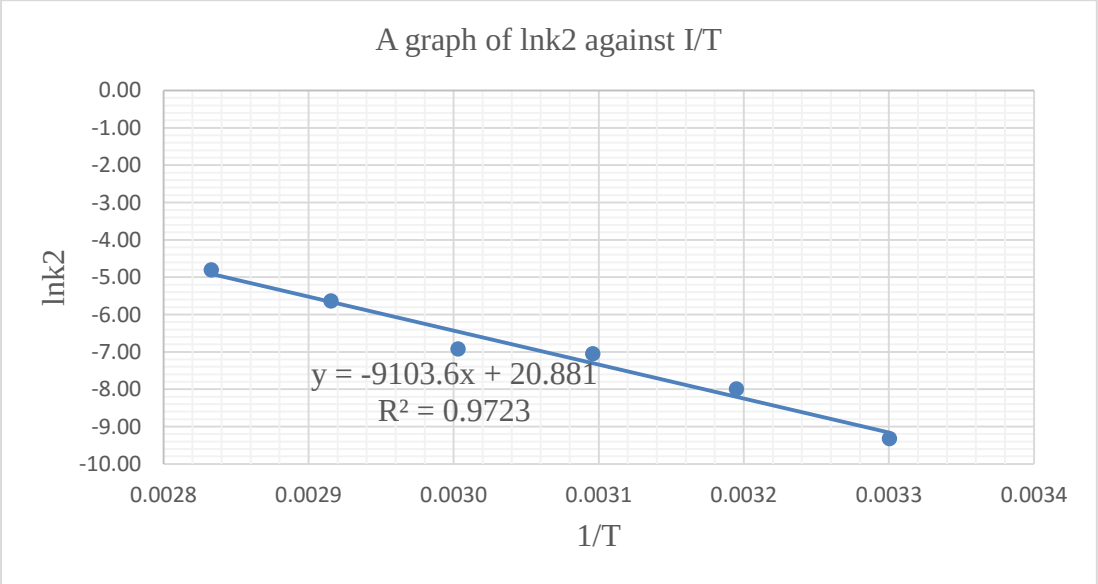

Figure 4. 25: Arrhenius plot of lnk2 against 1/T for sorghum stalks (Source: Table 4.60)

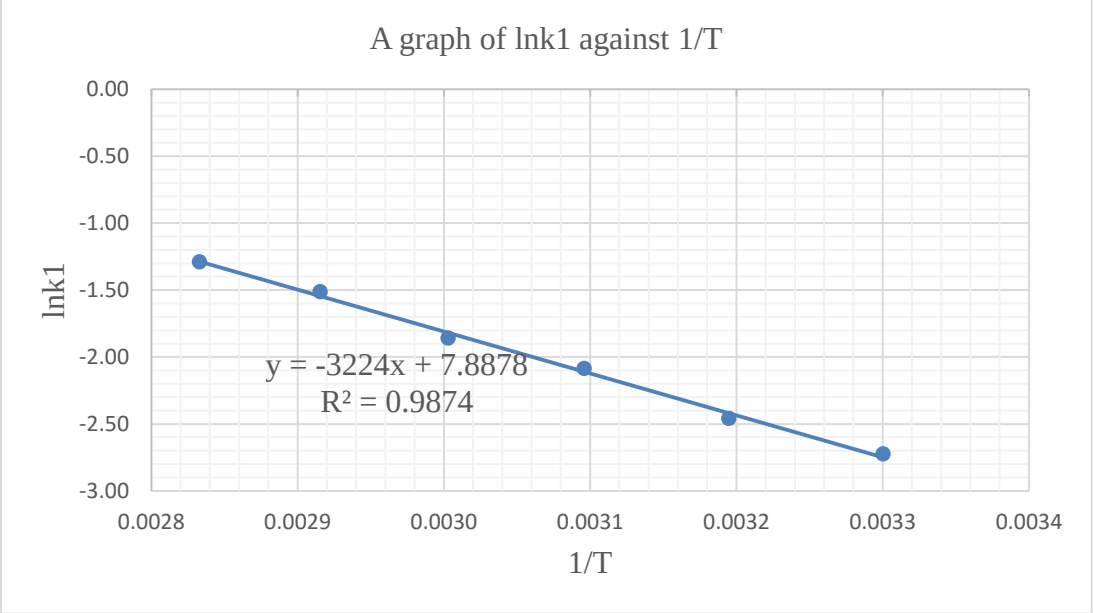

Figure 4. 26: Arrhenius plot of lnk1 against 1/T for maize cobs (Source: Table 4.61)

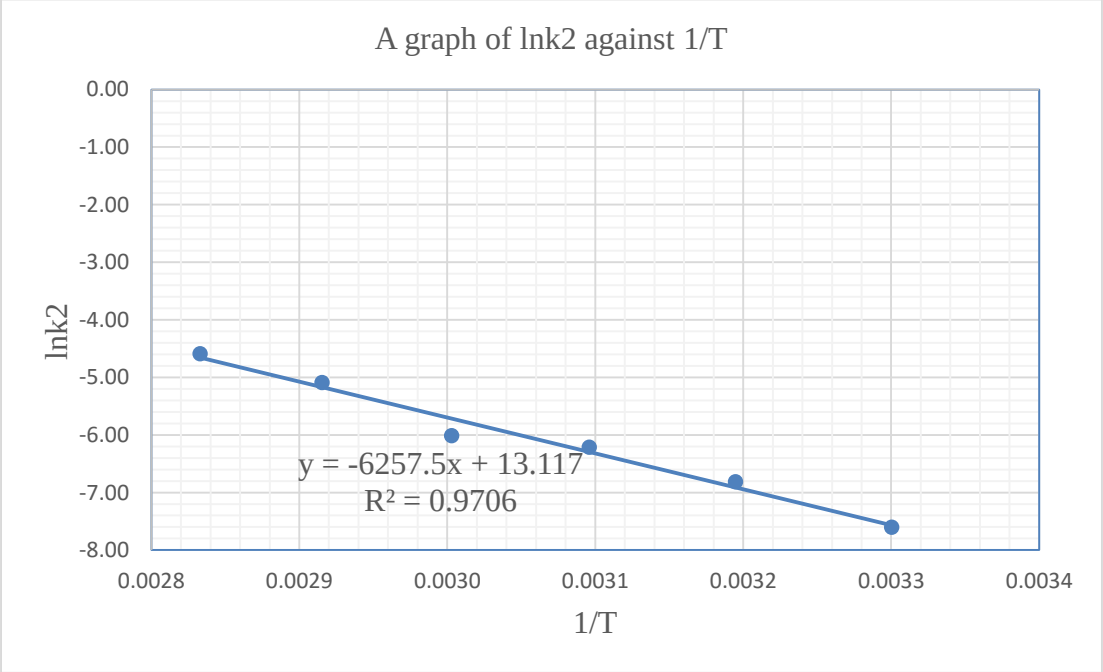

Figure 4. 27: Arrhenius plot of lnk2 against 1/T for maize cobs (Source: Table 4.61)

Table 4. 62: Kinetic parameters for glucose formation and degradation during hydrolysis of sorghum stalks and maize cobs

Substrate	Reaction	Activation energy (E, kJ/mol)	Pre-exponential factor (A, min^{-1})	R^2
Sorghum stalks	Glucose production (k_1)	25.41	$1.28x10^3$	0.9812
	Glucose degradation (k_2)	75.69	$1.17x10^9$	0.9723
Maize cobs	Glucose production (k_1)	26.80	$2.66x10^3$	0.9874
	Glucose degradation (k_2)	52.02	$4.97x10^5$	0.9706

The activation energy for glucose degradation during hydrolysis of sorghum stalks is higher than that in maize cobs. This is an indication of how difficult it is to degrade glucose during hydrolysis of sorghum stalks. This is advantageous since it results in high glucose yield during hydrolysis of sorghum stalks compared to hydrolysis of maize cobs. Esther et al. (2012) reported that the rate of degradation of glucose to HMF was negligible due to high activation energy. The authors noted that the decomposition of glucose to HMF can occur during the hydrolysis of LGB, but at a very low rate such that the resulting HMF is too minimal to be detected through analysis (Esther et al., 2012). In sorghum stalks and maize cobs, the activation energy for glucose formation was lower than the activation energy for glucose degradation. The slow rate of glucose degradation results in high yield of glucose, which in turn increases the concentration of ethanol during the fermentation process. During hydrolysis of LGB, glucose is mainly obtained from amorphous and crystalline fractions of cellulose (Tizazu & Moholkar, 2018). At low acid concentration, the amorphous fraction of cellulose is easily hydrolyzed to glucose while the crystalline fraction resists hydrolysis at low acid concentration (Tizazu & Moholkar, 2018). However, as the concentration of acid increases, the crystalline fraction of cellulose begins to degrade/decrystalize into glucose thus contributing to the increase in glucose yield (Tizazu & Moholkar, 2018). Similarly, at low hydrolysis temperature, the amorphous fraction of cellulose is easily hydrolysed to glucose while the crystalline fraction resists hydrolysis. However, at

relatively higher temperature, the crystalline fraction of cellulose may also undergo hydrolysis, thus resulting in higher glucose yields (Tizazu & Moholkar, 2018). Similar observations were made by Kumar et al. (2015) and Kanchanalai et al. (2016).

4.22.1 Optimization of glucose production during kinetics studies

The main aim of kinetic studies during hydrolysis of LGB is to develop kinetic models that describe the hydrolysis reaction. In addition, kinetic studies aim at optimizing the reaction conditions for glucose production from LGB. The maximum concentration of glucose (C_{BMax}) and the optimum time (t_{max}) for maximum amount of glucose were calculated from first order rate constants using Equation 2.8 and Equation 2.9 respectively (Kumar et al., 2015). The results of G_{MMax} and t_{max} are shown in Table 4.63 for sorghum stalks and maize cobs.

Table 4. 63: Hydrolysis of sorghum stalks and maize cobs: Results of optimization

Temperature (K)	Sorghum stalks			Maize cobs		
	t_{max} (min)	Glucose yield (%, w/w)		t_{max} (min)	Glucose yield (%, w/w)	
		Experimental results	Model results		Experimental results	Model results
303	112.85	80.02	89.1	74.91	77.11	86.7
313	74.9	82.44	87.75	51.53	81.64	85.05
323	50.11	89.72	86.17	33.74	86.18	84.13
333	40.94	94.57	86.43	27.08	92.98	84.23
343	21.99	89.72	83.19	16.69	88.44	81.21
353	14.85	92.14	79.67	12.43	88.44	79.32

The calculated values of t_{max} were found to decrease with an increase in hydrolysis temperature. This further confirms that hydrolysis of LGB occurs at a faster rate with increase in temperature (Mensah et al., 2020). The results shown in Table 4.63 indicate that the ideal conditions for the hydrolysis of sorghum stalks and maize cobs are 60^{o}C for a period of 41 minutes and 60^{o}C for a period of 27 minutes respectively. Under these conditions, the yield of glucose reached was 94.57% and 92.98% by weight of initial glucan content in sorghum stalks and maize cobs respectively.

4.23 Modeling and Simulation of Concentrated Sulphuric Acid Hydrolysis of Sorghum Stalks and Maize Cobs

The results shown in Table 4.60 to Table 4.62 were used to model and simulate a process to hydrolyze sorghum stalks and maize cobs using concentrated H_2SO_4. The process model is shown in Figure 4.28. The results obtained after simulating the model are shown in Table 4.64 and Table 4.65 for sorghum stalks and maize cobs respectively.

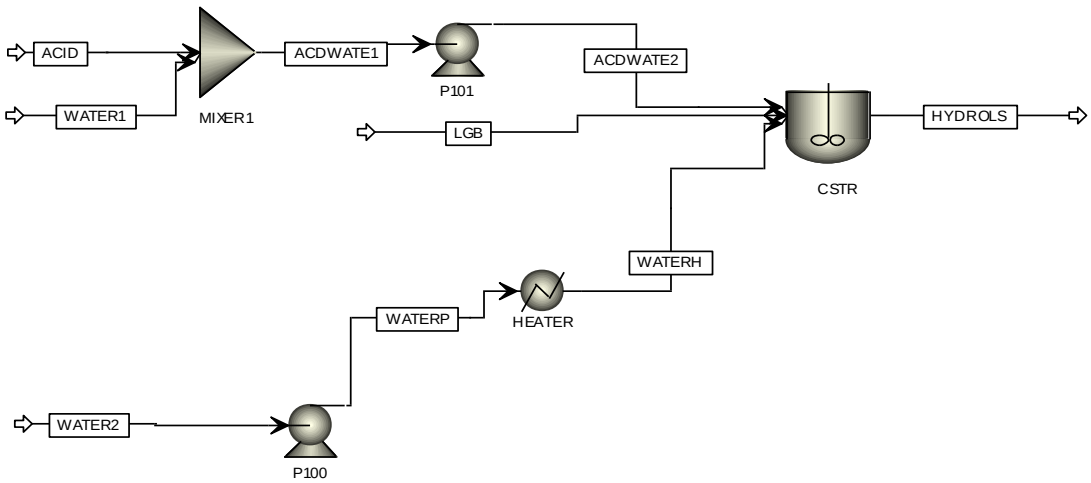

Figure 4. 28: PFD for concentrated acid hydrolysis of sorghum stalks and maize cobs

Table 4. 64: Results of modeling and simulation of concentrated acid hydrolysis of sorghum stalks

Stream/Component	ACDWATE2 (kmol/h)	LGB (kmol/h)	WATERH (kmol/h)	HYDROLS (kmol/h)
Water	7225.59	1142.36	2559.55	10787.41
Cellulose	0.00	155.05	0.00	14.96
Hemicellulose	0.00	162.75	0.00	162.75
Glucose	0.00	0.00	0.00	140.09
Sulphuric acid	23.19	0.00	0.00	23.19
Extractives	0.00	20.84	0.00	20.84
Lignin	0.00	198.35	0.00	198.35
Ash	0.00	86.90	0.00	86.90
Total Flow (kmol/h)	7248.77	1766.25	2559.55	11434.49
Total Flow (kg/h)	132445	102900	46111	281456

Table 4. 65: Results of modeling and simulation of concentrated acid hydrolysis of maize cobs

Stream/Component	ACDWATE2 (kmol/h)	LGB (kmol/h)	WATERH (kmol/h)	HYDROLS (kmol/h)
Water	7225.59	856.77	3774.57	11699.84
Cellulose	0	171.03	0	13.94
Hemicellulose	0	316.68	0	316.68
Glucose	0	0	0	157.09
Sulphuric acid	23.19	0	0	23.19
Extractives	0	130.57	0	130.57
Lignin	0	68.10	0	68.10
Ash	0	64.41	0	64.41
HMF	0	0	0	0
Total Flow (kmol/h)	7248.77	1607.57	3774.57	12473.82
Total Flow (kg/h)	132445	102900.00	68000	303345

From the simulation results, glucose yield was 90.42% (w/w) and 91.85% (w/w) of theoretical yield for sorghum stalks and maize cobs respectively. In addition, a comparison was made between the yield of glucose for experimental, model and simulation results. The results of this comparison are as shown in Table 4.66 for sorghum stalks and maize cobs.

Table 4. 66: Comparison of glucose yield for experimental, model and simulation results at 60oC for sorghum stalks and maize cobs

Substrate	Glucose yield (%, w/w)		
	Experimental results	Model results	Simulation results
Sorghum stalks	94.57	86.43	90.42
Maize cobs	92.98	84.23	91.85

From the results shown in Table 4.66, the kinetic model gave lower values of glucose yield compared to experimental results. There was 8.6% and 9.4% difference between the experimental and model glucose yield for sorghum stalks and maize cobs respectively. The difference could be attributed to the assumptions made during kinetic modeling of LGB hydrolysis. Due to the complex nature of LGB hydrolysis, kinetic models are simplified by:

1. Hydrolysis of cellulose to glucose and degradation of glucose to HMF are assumed to be first order reactions (Tizazu & Moholkar, 2018; Kumar et al.,2015).
2. Even though mass and heat transfer effects are involved in the reaction, they are neglected during kinetic studies of LGB (Tizazu & Moholkar, 2018; Kumar et al.,2015).
3. The reaction is heterogeneous since the LGB is in the solid phase while the acid (catalyst) is in the liquid phase, but we assume it is pseudo-homogeneous reaction. (Tizazu & Moholkar, 2018; Kumar et al., 2015).

Kumar et al. (2015) made similar observations on the main cause of variance between experimental and model results of glucose yield. The results of modeling and simulation of concentrated H_2SO_4 hydrolysis of sorghum stalks and maize cobs were compared with the results of modeling and simulation of dilute H_2SO_4 pretreatment and enzymatic hydrolysis of sorghum stalks and maize cobs shown in Table 4.67.

Table 4. 67: Heating demand, glucose production rate and glucose yield: Comparison between concentrated acid hydrolysis and dilute acid pretreatment and enzymatic hydrolysis of sorghum stalks and maize cobs

Parameters	Unit	Hydrolysis method (Sorghum stalks)		Hydrolysis method (maize cobs)	
		Concentrated acid	Dilute acid & enzymatic	Concentrated acid	Dilute acid & enzymatic
Heating demand	MJ/h	46945.73	169787.23	51572.34	225707.51
Glucose production rate	Kg/h	25,233.30	25,411.65	28295.36	28030.65
Glucose yield	%, w/w	90.42	91.06	91.85	90.72

The results shown in Table 4.67 indicate that concentrated H_2SO_4 hydrolysis has a slightly lower glucose production rate than dilute H_2SO_4 pretreatment and enzymatic hydrolysis process for the case of sorghum stalks. However, the energy demand for concentrated H_2SO_4 hydrolysis is lower than for dilute H_2SO_4 pretreatment and

enzymatic hydrolysis. In addition, the results shown in Table 4.67, indicate that concentrated H_2SO_4 hydrolysis has a slightly higher glucose production rate than dilute H_2SO_4 pretreatment and enzymatic hydrolysis process for the case of maize cobs. In addition, the energy demand for concentrated H_2SO_4 hydrolysis is lower than for dilute H_2SO_4 pretreatment and enzymatic hydrolysis of maize cobs.

4.23.1 Comparison of kinetic parameters for glucose formation and degradation

A comparison of kinetic parameters obtained from the current study with kinetic parameters for other substrates found in literature is shown in Table 4.68.

Table 4. 68: Comparison of kinetic parameters in this study with those from literature for acid catalysed hydrolysis of cellulose

LGB	Reaction conditions (T(°C) & Acid concentration (%, w/w)	Activation energy: Glucose formation (kJ/mol)	Activation energy: Glucose degradation (kJ/mol)	Reference
Cellulose	200°C, 20% formic acid	201	153	Kupiainen et al. (2014)
Wheat straw	140°C,3.0% H_2SO_4	60.7	14.5	Liu et al. (2012)
SCB	120°C, 2.0% H_2SO_4	60.33	83.4	Tizazu & Moholkar (2018)
SCB	121°C,1.8% H_2SO_4	86.7	82.9	Kumar at al. (2015)
SCB	80°C, 18.0% H_2SO_4	84.7	56.5	(Kumar et al., 2015)
Douglas fir	170-190°C, 0.4-1.0% H_2SO_4	179.5	137.5	Girisuta et al., (2007)
Kraft paper slurries	180-240°C, 0.2-1.0% H_2SO_4	188.7	137.2	Girisuta et al., (2007)
Filter paper	200-240°C, 0.4-1.5% H_2SO_4	178.9	137.2	Girisuta et al., (2007)
Cotton cellulose	40°C, 55% H_2SO_4	98.98	-	Chu et al., (2011)
MSW	200-240°C, 1.3-4.4% H_2SO_4	171.7	142.4	Girisuta et al., (2007)
SSS	60°C, 50.0% H_2SO_4	25.41	75.69	This study
Maize cobs	60°C, 50.0% H_2SO_4	26.8	50.02	This study

The activation energies for glucose formation from sorghum stalks and maize cobs are lower than those reported for other substrates in literature. This suggests that sorghum stalks and maize cobs are easily hydrolyzed to glucose using concentrated acid. The

kinetic parameters show significant differences due to the fact that the substrates differ in structure, chemical composition and the hydrolysis conditions are different. In summary, sample preparation, analytical procedures, hydrolysis and kinetic experiments, modeling and simulation using Aspen Plus, design and analysis of hydrolysis experiments using Design-Expert 13 were successful.

CHAPTER FIVE: CONCLUSIONS AND RECOMMENDATIONS

5.1 Conclusions

This research study was aimed at modeling and simulation of bioethanol production from sorghum stalks and maize cobs found in Kenya. Techno-economic analysis of large-scale 2GBE production process was conducted using literature-based experimental data. Three pretreatment methods (dilute H_2SO_4, steam explosion and alkaline) and two hydrolysis and co-fermentation technologies (SSCF and SHCF) were compared in terms of bioethanol production rate, bioethanol yield and energy intensity. Economic analysis was performed on a large-scale process of producing bioethanol that involved dilute H_2SO_4 pretreatment, SSCF, recovery, purification and dehydration. The research study also investigated the impact of varying process and economic parameters on bioethanol production rate, bioethanol production cost and the MBSP. The parameters that were varied included the flowrate of LGB, conversion of cellulose to glucose in the SSCF reactor, cost of LGB and enzymes, plant life, FCI, discount rate and income tax rate. Optimization of hydrolysis conditions and kinetic study of concentrated H_2SO_4 hydrolysis of sorghum stalks and maize cobs was also done. Kinetic data obtained during kinetic study was used to model and simulate a large-scale process involving concentrated H_2SO_4 hydrolysis of sorghum stalks and maize cobs. A summary of the findings from this study are:

a. Sorghum stalks and maize cobs were found to have high carbohydrate content of 51.0% (w/w) and 72.76% (w/w) respectively. This is an indication that these agri-wastes are essential raw materials for the production of fermentable sugars.
b. The bioethanol production rate from dilute H_2SO_4, steam explosion, alkaline pretreatment and SSCF technologies was 21664.5, 18698.6, 12032.7 and 31074.4, 24749.4 and 13266.6 kg/h from sorghum stalks and maize cobs respectively.

c. The energy demand for pretreatment and SSCF was 169787.23, 200053.08 and 93411 MJ/h for sorghum stalks and 225707.51, 242852.04 and 104211 MJ/h for maize cobs when using dilute H_2SO_4, steam explosion and alkaline pretreatment respectively.

d. The energy intensity was 12.39 MJ/L, 16.50 MJ/L and 19.79 MJ/L of ethanol for sorghum stalks and 11.96 MJ/L, 13.53 MJ/L and 15.34 MJ/L for maize cobs respectively from dilute H_2SO_4 pretreatment, SSCF and purification process, steam explosion pretreatment, SSCF and purification process and alkaline pretreatment, SSCF and purification process respectively.

e. In terms of bioethanol production rate, energy demand and energy intensity, the dilute H_2SO_4 pretreatment and SSCF technology was selected as the most suitable technology for the production of bioethanol from sorghum stalks and maize cobs.

f. For a large-scale 2GBE production plant, the total product cost and IRR were \$0.63/L, 11.47% and \$0.51/L, 17.10% for a plant processing Sila sorghum stalks and maize cobs respectively. The TCI was \$ 458 million and \$ 569 million for a plant processing Sila sorghum stalks and maize cobs respectively.

g. The MBSP increased from \$0.81/L and \$0.68 /L to \$1.11/L and \$0.89/L using sorghum stalks and maize cobs respectively when the cost of substrate increased from \$20/ton to \$100/ton. MBSP increased from \$0.9/L and \$0.75/L to \$1.0/L and \$0.82/L using sorghum stalks and maize cobs respectively when the cost of enzymes was varied by − 50% and + 50%. MBSP increased from \$0.83/L and \$0.68/L to \$1.54/L and \$1.29/L using sorghum stalks and maize cobs respectively when discount rate varied by 5% and 30%. MBSP increased from \$0.85/L and \$0.69/L to \$1.06/L and \$0.88/L using sorghum stalks and maize cobs respectively when fixed capital investment was varied by -35% and + 35%. MBSP reduced

from \$1.28/L and \$1.07/L to \$0.95/L and \$0.79/L using sorghum stalks and maize cobs respectively when plant life varied from 10 to 30 years. MBSP increased from \$0.89/L and \$0.73/L to \$0.99/Land \$0.82/L using sorghum stalks and maize cobs respectively when income tax rate varied from 0 to 40%.

h. This study verifies that the main factors that impact the bioethanol production rate, bioethanol production cost and the MBSP are cost of LGB and enzymes, conversion of cellulose to glucose in the SSCF reactor, FCI and the flow rate of LGB. On the other hand, plant life, income tax rate and discount rate have insignificant impact on the MBSP.

i. Optimum glucose yield of 87.54% (w/w) and 90.02% (w/w) from sorghum stalks and maize cobs respectively were obtained at 60^{o}C hydrolysis temperature, 50.0% (w/w) concentration of H_2SO_4 and 60 minutes hydrolysis time. Lowest glucose yield of 45.59% (w/w) and 51.93% (w/w) from sorghum stalks and maize cobs respectively were obtained at 60^{o}C hydrolysis temperature, 60 minutes hydrolysis time and 16.36% (w/w) concentration of H_2SO_4.

j. During kinetic studies, the hydrolysis time at which maximum concentration of glucose occurs decreases with increase in hydrolysis temperature. The ideal conditions for the hydrolysis of sorghum stalks and maize cobs are 60^{o}C for a period of 41 minutes and 60^{o}C for a period of 27 minutes respectively. Under these conditions, the yield of glucose reached was 94.57% and 92.98% by weight of initial glucan content in sorghum stalks and maize cobs respectively.

k. Studying of large-scale processes of producing bioethanol from lignocellulosic biomass using modeling and simulation saves time and money since modeling and simulation studies are fast and less expensive. It is possible to explore many

scenarios within a short time by varying different techno-economic parameters when using modeling and simulation software.

l. In the current research study, the main limitation was the assumptions made on costs and process parameters and the absence of kinetic data for use in modeling of pretreatment, hydrolysis and fermentation reactors.

m. 2GBE produced from sorghum stalks and maize cobs under the current techno-economic conditions and assumptions cannot compete with gasoline in Kenya unless favourable policy interventions are enacted in order to support large-scale 2GBE production.

n. The study has come up with data on the impact of varying process and economic factors on the techno-economic viability of large-scale 2GBE production process involving Sila sorghum stalks and maize cobs. This data can be used in decision making as to whether or not investment in large-scale 2GBE should be done. Optimum hydrolysis conditions involving sorghum stalks and maize cobs have been obtained in a single stage LGB hydrolysis process. In addition, data on kinetic study of concentrated H_2SO_4 hydrolysis of sorghum stalks and maize cobs was obtained. This data was applied in modeling and simulation of a large-scale LGB hydrolysis process. The study has shown that solid wastes generated during 2GBE production can be used as source of energy to meet process heat requirements.

o. Implementing the findings of the current study in terms of setting up a large-scale 2GBE production plant in Kenya will have the following implications to the community and society as a whole:

    i. Suppliers of biomass will earn income which will go a long way in improving their living standards.

ii. Creating of employment opportunities to the local community.

iii. Improving the economic status of rural Kenya.

iv. Environmental protection in terms of avoiding disposal and burning of biomass during land preparation.

5.2 Recommendations

The current research study addresses issues regarding the use of sorghum stalks and maize cobs as substrates for large-scale production of 2GBE. However, numerous challenges remain that need to be addressed in order to fully commercialize the use of these substrates for the production of 2GBE. The following recommendations describe approaches that can build on the current research so as to support large-scale production of 2GBE from sorghum stalks and maize cobs.

a. For optimal operation, 2GBE plants require constant supply of quality LGB and at a reasonable cost. Therefore, large-scale 2GBE production from sorghum stalks and maize cobs can be supported by locating the plant within the vicinity of low cost and sustainable LGB supplies. Further research should be done in order to identify other substrates that can be used to produce fermentable sugars in Kenya. In addition, the government should provide tax rebates to bioethanol producers that source raw materials directly from local farmers.

b. For 2GBE to be able to compete with gasoline in Kenya, the government should not impose taxes and levies on the MBSP. This will make 2GBE competitive in the Kenyan market. In addition, the existing petroleum distribution and marketing infrastructure in Kenya can be used to distribute and market bioethanol produced in Kenya.

c. The government of Kenya should support the E-10 policy through mandatory use of 2GBE - gasoline blended energy source in the transport sector. In addition, the

government can support increased usage of bioethanol in households by removing import duty, excise duty and value added tax levied on bioethanol cook stoves and other equipment and machinery that use bioethanol.

d. Future work on kinetic studies of fermentation of glucose and xylose should be performed in order to come up with kinetic data on fermentation of these sugars. The data obtained can be used in modeling and simulation of a large-scale fermentation process.

e. In order to develop a single model that can handle alternative substrates, further research is recommended to update the models used in this study so as to handle other types of substrates. In addition, further research is recommended to update the economic model used in the current study in order to take into consideration current technological improvements and changes in economic factors such as cost of equipment and raw materials. There is need to revise and update operating conditions and conversions based on future improvements in 2GBE production. This will ensure that the models are consistent with the present techno-economic conditions.

f. Performing process heat integration of the entire 2GBE production plant in order to identify areas for energy demand reduction, optimizing energy supply methods, heat recovery systems and process operating conditions.

g. Further research involving the biorefinery concept is recommended. In the biorefinery concept, 2GBE, biogas and other by-products such as xylitol and fertilizer are produced in the same plant. The biogas can be produced from the fermentation residues and organic waste found in the wastewater streams from the plant. The liquid fraction obtained after distillation can also be sold as fertilizer. Alternatively, the solid residues can be used to produce electricity for use in the

plant and any excess electricity be sold to the national grid. Performing a techno-economic analysis on the biorefinery will establish the impact of these by-products on the MBSP since they will act as sources of additional revenue.

h. In order to address the limitations identified in this study, further research is recommended on techno-economic analysis of a large-scale 2GBE production process using current economic data. Actual cost of equipment, raw materials, utilities etc should be used in the analysis. In addition, all reactors involved in the process should be modeled and simulated using respective kinetic data and a sensitivity analysis should be done on each reactor by varying parameters such as temperature and pressure.

i. The current research study did not consider the environmental impact of large-scale 2GBE production. In order to evaluate the environmental performance of a large-scale 2GBE production process from sorghum stalks and maize cobs, a life cycle analysis of the entire process that will take into account the flow of material, energy and pollution is recommended.

REFERENCES

Abril-González, M., Vele-Salto, A., & Pinos-Vélez, V. (2023). Kinetic Study of Acid Hydrolysis of the Glucose obtained from Banana Plant. *Chemical engineering*, 7, 39.

Agfax On-line. (2011). Super Sorghum: High yielding and drought tolerant. Retrieved March 20, 2019, from http://www.agfax.net.

Akpinar, O., Erdogan, K., & Bostanci, S. (2009). Production of xylooligosaccharides by controlled acid hydrolysis of lignocellulosic materials. *Carbohydydrates Resources*, 344, 660–666.

Ali, Z., Hussain, M., & Arshad, M. (2014). Saccharification of corn cobs an agro-industrial waste by sulphuric acid for the production of monomeric sugars. *International Journal of Biosciences*, *5*(3), 204-213.

Alicia, M. (2013). Sodium hydroxide pretreatment of corn stover and subsequent enzymatic hydrolysis: An investigation of yields, kinetic modeling and glucose recovery, PhD thesis, University of Kentucky, USA.

Anderson, J.L., Berthod, A., Estevez, V.P., & Stalcup, A, M. (Eds.). (2015). Analytical Separation Science, (1st edn.). Wiley-VCH Verlag GmbH & Co. KGaA.

Andrea, F. (2015). Enzymatic assay kits for nutrients. Retrieved April 15, 2019, from http://www.sigmaaldrich.com/technicaldocuments.

Aspen Plus V8.4. (2013). AspenTech Inc., Burlington, MA, USA.

Aspen Plus. (2000). *Aspen Plus User Guide, version 10.2,* Aspen Technology, Inc. Ten Canal Park, Cambridge, MA 02141-2201 USA.

ASTM E. (2003). Standard practice for preparation of biomass for compositional analysis 1757 – 01. Annual book of ASTM Standards, *11*(5).

Australian Government. (2008). The Biology of *Zea mays L. ssp mays* (maize or corn), Australia, Department of Health and Ageing. Office of the Gene Technology Regulator.

Bakari, M., Ngadi, M., & Bergthorson, T. (2010). Energy Analysis of Biochemical Conversion Processes of Biomass to Bioethanol. XVIIth World Congress of the International Commission of Agricultural and Biosystems Engineering (CIGR),13-17 June, 2010. Quebec City, Canada.

Barreraa, I., Amezcua-Allieri, M.A, Estupinan, L., Martínez, T., & Aburtob, J. (2016). Technical and economical evaluation of bioethanol production from lignocellulosic residues in Mexico: Case of sugarcane and blue agave bagasses. *Chemical Engineering Research and Design*, 107, 91–101.

Beckendorff, A., Lamp, A., & Kaltschmitt, M. (2021). Optimization of hydrolysis conditions for xylans and straw hydrolysates by HPLC analysis. *Biomass Conversion and Biorefinery*, 9, 1-14.

Beluhan, S., Mihajlovski, K., Santek, B., & Santek, M.I. (2023). The Production of Bioethanol from Lignocellulosic Biomass: Pretreatment Methods, Fermentation, and Downstream Processing. *Energies*, 16, 7003.

Bhattacharya, A., & Pletschke, B.I. (2015). Strategic optimization of xylanase–mannanase combi-CLEAs for synergistic and efficient hydrolysis of complex lignocellulosic substrates. *Journal of Molecular Catalysis B: Enzymatic*, 115, 140–150.

Boakye-Boaten, N.A., Kurkalova, L., Xiu, S., & Shahbazi, A. (2017). Techno-economic analysis for the biochemical conversion of *Miscanthus x giganteus* into bioethanol. *Biomass and Bioenergy*, 98, 85-94.

Boonyisa, W., Apanee, L., & Sujitra, W. (2012). Characterization of Corn Cobs from Microwave and Potassium Hydroxide Pretreatment. *International Journal of Chemical and Biological Engineering*, 6.

Camacho, F., Tello, P.G., Jurado, E., & Robles, A. (1996). Microcrystalline-Cellulose Hydrolysis with Concentrated Sulphuric Acid. *Chemical Technology & Biotechnology*, 67, 350-356.

Chandel, A.K., Antunes, F.A.F, Arruda, P.V., Milessi, T.S.S, da Silva, S.S., & Felipe, M.G.A. (2012). Dilute Acid Hydrolysis of Agro-Residues for the Depolymerization of Hemicellulose: State-of-the-Art. Springer-Verlag Berlin Heidelberg.

Chandel, A.K., Chan, E.S., Rudravaram, R., Narasu, M.L., Rao, V., & Ravindra, P. (2007). Economics and environmental impact of bioethanol production technologies: an appraisal. *Biotechnology and Molecular Biology*, *2*(1), 014-032.

Chang, J.K.W., Duret, X., Berberi, V., Niaki, H.Z., & Lavoie, J.M. (2018). Two-Step Thermochemical Cellulose Hydrolysis with Partial Neutralization for Glucose Production. *Frontiers in Chemistry*, 6: 117.

Cheah, W.Y., Sankaran, R., Show, P.L., Ibrahim, T.N.B., Chew, K.W., Culaba, A., & Chang, J.S. (2020). Pretreatment methods for lignocellulosic biofuels production: current advances, challenges and future prospects. *Biofuel Research Journal*, 25, 1115-1127.

Chu, C.Y., Wub, S.Y., Tsai, C.Y., & Lin, C.Y. (2011). Kinetics of cotton cellulose hydrolysis using concentrated acid and fermentative hydrogen production from hydrolysate. *International Journal of Hydrogen Energy*, 36, 8743-8750.

Conde-Mejíaa, C., Jiménez-Gutiérreza, A., & *El*-Halwagi, M. (2012). A comparison of pretreatment methods for bioethanol production from lignocellulosic materials. *Process Safety and Environmental Protection*, 90, 189–202.

da Silva, A.R.G., Errico, M., & Rong, B.G. (2017). Evaluation of organosolv pretreatment for bioethanol production from lignocellulosic biomass: solvent recycle and process integration. *Biomass conversion and biorefinery*, 1-15.

da Silva, A.R.G., Errico, M., & Rong, B.G. (2018). Systematic procedure and framework for synthesis and evaluation of bioethanol production processes from lignocellulosic biomass. *Bioresource Technology Reports*, 4, 29-39.

da Silva, A.R.G., Giuliano, A., Errico, M., & Rong, B.G. and Barletta, D. (2019). Economic value and environmental impact analysis of lignocellulosic ethanol production: assessment of different pretreatment processes. *Clean Technologies and Environmental Policy*, 21, 637-654.

da Silva, A.R.G., Ortega, C.E.T., & Rong, B.G. (2016). Techno-economic analysis of different pretreatment processes for lignocellulosic-based bioethanol production. *Bioresource Technology*, 218, 561–570.

David, T. W. (1994). Determination of Ethanol Concentration in Biomass to Ethanol Fermentation Supernatants by Gas Chromatography, NREL Ethanol Project, LAP 011, ISSUE DATE: 05/05/1994.

David, T., & Tina, E. (1995). Standard Method for the Determination of Acid – Insoluble Lignin in Biomass, in NREL Ethanol Project, LAP 003, ISSUE DATE: 01/30/1995.

Davis, R. E., Grundl, N. J., Tao, L., Biddy, M. J., Tan, E. C., Beckham, G. T., Humbird, D., Thompson, D. N., & Roni, M. S. (2018). Process Design and Economics for the Conversion of Lignocellulosic Biomass to Hydrocarbon Fuels and Coproducts: 2018 Biochemical Design Case Update; Biochemical Deconstruction and Conversion of Biomass to Fuels and Products via Integrated Biorefinery Pathways. United States. https://doi.org/10.2172/1483234.

Dias, M.O.S., Cunha, M.P., Jesus, C.D.F., Rocha, G.J.M., Pradella, J.G.C., Rossell, C.E.V., & Bonomi, A. (2011). Second generation ethanol in Brazil: Compete with electricity production. *Bioresource Technology*, 102, 8964–8971.

East African Breweries Limited (EABL). (2014). Increasing Climate Resilience through the Promotion of Sorghum-based Beer, Climate Change and Your Business Briefing Note Series.

El Bari, H., Lahboubi, N., Habchi, S., Rachidi, S., Bayssi, O., Nabil, N., Mortezaei, Y., & Villa, R. (2022). Biohydrogen production from fermentation of organic waste, storage and applications. *Cleaner Waste Systems*, 3, 100043.

Energy and Petroleum Regulatory Authority. (2023). Maximum Retail Petroleum Prices in Kenya for the period 15th December 2023 to 14th January 2024, Press release, Nairobi.

Energy Institute. (2023). Statistical Review of World Energy, (72nd edn.), Energy Institute. Retrieved December 02, 2023, from https://www.energyinst.org/statistical-review.

Esther, G.R., Oscar, M. P., Lorenzo, J.E., Jose, A. R., & Manuel, V. (2012). Acid hydrolysis of wheat straw: A kinetic study. *Biomass and bioenergy*, 36, 3 4 6-355.

Fogler, S.H. (2016). *Elements of Chemical Reaction Engineering*, (5th edn.), USA: Prentice Hall.

Frankó, B., Galbe, M., & Wallberg, O. (2016). Bioethanol production from forestry residues: A comparative techno-economic analysis. *Applied Energy*, 184, 727–736.

Fukaya, Y., Hayashi, K., Wada, M., & Ohno, H. (2008). Cellulose dissolution with polar ionic liquids under mild conditions: Required factors for anions. *Green Chemistry*, 10, 44-46.

Galbe, M., & Wallberg, O. (2019). Pretreatment for biorefineries: a review of common methods for efficient utilization of lignocellulosic materials. *Biotechnology for Biofuels*, 12, 294.

Gao, D., Chundawat, S.P.S., Krishnan, C., Balan, V., & Dale, B.E. (2010). Mixture optimization of six core glycosyl hydrolases for maximizing saccharification of ammonia fiber expansion (AFEX) pretreated corn stover. *Bioresource Technology*, 101, 2770–2781.

Gebreyohannes, S. (2010). Process design and economic evaluation of an ethanol production process by biomass gasification. MSc Thesis. Oklahoma State University, USA.

Girisuta, B., Janssen, L. P. B. M., & Heeres, H.J. (2007). Kinetic Study on the Acid-Catalyzed Hydrolysis of Cellulose to Levulinic Acid. *Industrial & Engineering Chemistry Research*, 46, 1696-1708.

Habibi, Y., Lucia, L. A., & Rojas, O. J. (2010). Cellulose nano crystals: chemistry, self-assembly and applications. *Chemistry Reviews, 110*(6), 3479-3500.

Hayward, K. T., Combs, S.N., Schmidt, S.L., & Philippidis, G.P. (1995). Lignocellulosic Biomass Hydrolysis and Fermentation, in NREL Ethanol Project, LAP 008, ISSUE DATE: 05/31/1995.

Hector, H., Hughes, S., & Liang-Li, X. (2008). Developing yeast strains for biomass to ethanol production. *Ethanol Producer Magazine*, June 2008 Issue.

Hu, G., Heitmann, J., & Roja, O. (2008). Feedstock pretreatment strategies for producing ethanol from wood, bark, and forest residues. *BioResources, 3*(1), 270-294.

Hu, W., Zhou, L., & Chen, J. (2022). Conversion sweet sorghum biomass to produce value-added products. *Biotechnology for Biofuels and Bioproducts*, 15, 72.

Humbird, D., Davis, R., Tao, L., Kinchin, C., Hsu, D., & Aden, A. (2011). Process Design and Economics for Biochemical Conversion of Lignocellulosic Biomass to Ethanol. Dilute-Acid Pretreatment and Enzymatic Hydrolysis of Corn Stover, National Renewable Energy Laboratory Golden, Colorado.

Ibrahim, A.E., Elhenawee, M., Saleh, H., & Sebaiy, M.M. (2021). Overview on liquid chromatography and its greener chemistry application. *Annals of Advances in Chemistry*, 5, 004-012.

International Energy Agency (2023). World Energy Outlook 2023. Retrieved December 02, 2023, from https://www.iea.org/reports/world-energy-outlook-2023/executive-summary.

Ioelovich, M. (2012). Study of Cellulose Interaction with Concentrated Solutions of Sulphuric Acid. *ISRN Chemical Engineering*. Article ID: 428974.

Ioelovich, M. (2015). Recent findings and the Energetic Potential of Plant Biomass as a Renewable Source of Biofuels – A Review. Biofuels Energy Potential. *BioResources, 10*(1), 1-10.

Janga, K.K., Hägg, M.B., & Moe, S.T. (2012). Concentrated acid hydrolysis of wood. *BioResources*, *7*(1), 391-411.

Jarunglumlert, T., & Prommuak, C. (2021). Net Energy Analysis and Techno-Economic Assessment of Co-Production of Bioethanol and Biogas from Cellulosic Biomass. *Fermentation*, 7, 229.

Jeevan, P., R. Nelson, R., & Rena, A.E. (2011). Optimization studies on acid hydrolysis of Corn cob hemicellulosic hydrolysate for Microbial production of xylitol. *Journal of Microbiology & Biotechnology Research*, *1*(4), 114-123.

Joshi, B., Bhatt, M.R., Sharma, D., Joshi, J., Malla, R., & Sreerama, L. (2011). Lignocellulosic ethanol production: Current practices and recent developments: Review. *Biotechnology and Molecular Biology*, *6*(8), 172-182.

Joy, S.P., Kumar, A.A., Gorthy, S., Jaganathan, J., Kunappareddy, A., Gaddameedi, A ., & Krishnan, C. (2021). Variations in structure and saccharification efficiency of biomass of different sorghum varieties subjected to aqueous ammonia and glycerol pretreatments. *Industrial Crops & Products*, 159, 113072.

Jung, J.Y., Choi, M.S., & Yang, J.K. (2013). Optimization of Concentrated Acid Hydrolysis of Waste Paper Using Response Surface Methodology. *Journal of Korean Wood Science and Technology*, *41*(2), 87-99.

Kanchanalai, P., Temani, G., Kawajiri, Y., & Realff, M. (2016). Reaction Kinetics of Concentrated Acid Hydrolysis for Cellulose and Hemicellulose and Effects of Crystallinity. *BioResources, 11*(1), 1672-1689.

Kazi, F.K., Fortman, J.A., Anex, R.P., Hsu, D.D., Aden, A., Dutta, A., & Kothandaraman, G. (2010). Techno-economic comparison of process technologies for biochemical ethanol production from corn stover. *Fuel*, 89, S20–S28.

Kenya National Bureau of Statistics. (2022). Economic Survey 2022, Nairobi, Kenya National Bureau of Statistics.

Khandelwal, A., Chhabra, M., & Lens P.N.L. (2023). Integration of third generation biofuels with bio-electrochemical systems: Current status and future perspective. *Frontiers in Plant Science*, 14:1081108.

Kim, S. (2018). Evaluation of alkali-pretreated soybean straw for lignocellulosic bioethanol production. *International Journal of Polymer Science*, vol. 2018,1–7.

Kolo, S.M.D., Wahyuningrum, D., & Hertadi, R. (2020). The Effects of Microwave-Assisted Pretreatment and Cofermentation on Bioethanol Production from Elephant Grass. *International Journal of Microbiology*, vol. 2020, 1-11.

Kumar R., Tabatabaei M., Karimi K., & Sárvári Horváth I. (2016). Recent updates on lignocellulosic biomass derived ethanol - A review. *Biofuel Research Journal*, 9, 347-356.

Kumar, P., Barrett, D.M., Delwiche, M.J., & Stroeve, P. (2009). Methods for pretreatment of lignocellulosic biomass for efficient hydrolysis and biofuel production. *Industrial and engineering chemistry research*, *48*(8), 3713-3729.

Kumar, S., Dheeran, P., Singh, S.P., Mishra, I.M., & Adhikari, D.K. (2015). Kinetic studies of two-stage sulphuric acid hydrolysis of sugarcane bagasse. *Renewable Energy*, 83, 850-858.

Kupiainen, L., Ahola, J., & Tanskanen J. (2014). Kinetics of Formic Acid Catalyzed Cellulose Hydrolysis. *BioResources*, *9*(2), 2645-2658.

Legodi, L.M., LaGrange, D.C., van Rensburg, E.L.J., & Ncube, I. (2021). Enzymatic Hydrolysis and Fermentation of Banana Pseudostem Hydrolysate to Produce Bioethanol. *International Journal of Microbiology*, vol. 2021, 1-14.

Lenihan, P., Orozco, A., O'Neil, E., Ahmad, M., N., M., Rooney, D., W., & Walker G. M. (2010). Dilute acid hydrolysis of lignocellulosic biomass. *Chemical Engineering Journal*, *156*(2), 395-403.

Liu, X., Lu, M., Ai, N., Yu, F., & Ji, J. (2012). Kinetic model analysis of dilute sulfuric acid- catalyzed hemicellulose hydrolysis in sweet sorghum bagasse for xylose production. *Industrial Crops and Products*, 38, 81– 86.

Lopes, T.F., Cabanas, C., Silva, A., Fonseca, D., Santos, E., Guerra, L.T., Sheahan, C., Reisa, A., & Girioa, F. (2019). Process simulation and techno-economic assessment for direct production of advanced bioethanol using a genetically modified *Synechocystis* sp. *Bioresource Technology Reports*, 6, 113–122.

Lopez-Sandin, I., Rodríguez-Jasso, R.M., Gutiérrez-Soto, G., Rosero-Chasoy, G., S., González-Gloria, K.D., & Ruiz, H.A. (2022). Energy Assessment of Second Generation (2G) Bioethanol Production from Sweet Sorghum (Sorghum bicolor (L.) Moench) Bagasse. *Agronomy*, 12, 3106.

Lu, Y., He, Q., Fan, G., Cheng, Q., & Song, G. (2021). Extraction and modification of hemicellulose from lignocellulosic biomass: A review. *Green Processing and Synthesis*, 10, 779–804.

Lugani, Y., Rai, R., Prabhu, A.A., Maan, P., Hans, M., Kumar, V., Kumar, S., Chandel, A.K., & Sengar, R.S. (2020). Recent advances in bioethanol production from lignocelluloses: a comprehensive review with a focus on enzyme engineering and designer biocatalysts. *Biofuel Research Journal*, 28, 1267-1295.

Lukajtis, R., Rybarczyk, P., Kucharska, K., Łyskawa, D.K., Słupek, E., Wychodnik, K., & Kaminski, M. (2018). Optimization of Saccharification Conditions of Lignocellulosic Biomass under Alkaline Pre-Treatment and Enzymatic Hydrolysis. *Energies*, 11, 886, 1-27.

Mailu S.K., & Mulinge, W. (2016). Excise tax changes and their impact on Gadam sorghum demand in Kenya, 5th international conference of AAAE, 23-26th September, 2016, United Nations Conference Centre, Addis Ababa- Ethiopia.

Marinescu, M., Volpe, S., Desrochers, L., & Roser, D. (2015). Basic procedures for sampling and analyzing woody biomass. Advantage Report Vol. 13, No. 10. FPInnovations, Vancouver, British Columbia. Retrieved August 22, 2018 from https://library.fpinnovations.ca/media/FOP/ADV15N5.PDF.

McKinsey & Company. (2022). Global Energy Perspective 2022. Retrieved December 02, 2023, from https://www.mckinsey.com/industries/oil-and-gas/our-insights/global-energy-perspective-2022.

Mensah, M., Asiedu, N.Y., Neba, F.A., Amaniampong, P.N., Boakye, P., & Addo, A. (2020). Modeling, optimization and kinetic analysis of the hydrolysis process of waste cocoa pod husk to reducing sugars. *SN Applied Sciences*, 2:1160.

Mezule, L., Dalecka, B., & Juhna, T. (2015). Fermentable sugar production from lignocellulosic waste. *Chemical Engineering Transactions*, 43, 619-624.

Ming C. Liming. X., & Peijian, X. (2007). Enzymatic hydrolysis of corncob and ethanol production from cellulosic hydrolysate. *International Biodeterioration & Biodegradation*, 59, 85–89.

Ministry of Energy. (2018). National Energy Policy, Nairobi, Government of Kenya.

Miya, S.P. (2015). Maize (*Zea mays* L.) Seed Quality in Response to Simulated Hail Damage, Msc Thesis. Pietermaritzburg. University of KwaZulu-Natal, South Africa.

Moe, S.T., Janga, K.K., Hertzberg, T., Hagg, M.B., Oyaas, K., & Dyrset, N. (2012). Saccharification of Lignocellulosic Biomass for Biofuel and Biorefinery Applications – A Renaissance for the Concentrated Acid Hydrolysis. *Energy Procedia*, 20, 50-58.

Monir, M.U., Aziz, A.A., Yousuf, A., & Alam, M.Z. (2020). Hydrogen-rich syngas fermentation for bioethanol production using *Saccharomyces cerevisiae*. *International Journal of Hydrogen Energy*, *45*(36), 18241-18249.

Montgomery, D.C. (2013). Design and Analysis of Experiments, (8th edn.), Arizona State University. John Wiley & Sons, Inc.

Muktham, R., Bhargava, S.K., Bankupalli, S., & Ball, A.S. (2016). A Review on 1st and 2nd Generation Bioethanol Production – Recent Progress. *Journal of Sustainable Bioenergy Systems*, 6, 72-92.

Mustafa, B., Havva, B., & Cahide, O. (2008). Progress in Bioethanol Processing. *Progress in energy and combustion science*, 34, 551-573.

Nair, S. (2011). Identifying and Managing Process Risks Related to Biofuel Projects and Plants. Symposium Series No. 156, Hazards XXII, IChemE.

Nasohaa, Z., Luthfia, A.A., Hariza, H.B., Roslana, F., Bukhari, N.A., & Manaf, S.F. (2023). Xylose Recovery from Pineapple Peel Biomass by Mild Acid Hydrolysis. *Chemical Engineering Transactions*, 106, 1087-1092.

New Agriculturist On-line. (2011). New sorghum variety gives hopes to farmers. Retrieved March 20, 2019, from http://www.new ag.info/en/news.

Njagi, T., Onyango, K., Kirimi, L., & Makau, J. (2019). Sorghum Production in Kenya: Farm-level Characteristics, Constraints and Opportunities, Technical Report, Tegemeo Institute of Agricultural Policy and Development, Egerton University, pp. 1-43.

Obieogu K.N., Chiemenem L.I., & Adekunle, K.F. (2016). Utilization of Agricultural Waste for Bioethanol Production- A Review. *International Journal of Current Research, 8*(19), 1-5.

Ortiz, P.S., & Oliveira, S. (2014). Exergy analysis of pretreatment processes of bioethanol production based on sugarcane bagasse. *Energy*, 76, 130-138.

Parameswaran, B., Janu, K.U., Raveendran, S., & Ashok P. (2011). Hydrolysis of lignocellulosic biomass for bioethanol production. Centre for biofuels, biotechnology division. *National Institute for Interdisciplinary Science and Technology*, 229-250.

Phyllis, B., & Kathryn, D. (1997). *Handbook of Instrumental techniques for analytical chemistry*. pp. 147-164. Editor: High Performance Liquid Chromatography, Settle: Prentice Hall.

Piccolo, C., & Bezzo, F. (2009). A techno-economic comparison between two technologies for bioethanol production from lignocellulose. *Biomass and bioenergy*, 33, 478-491.

PIEA. (2019). Petroleum Institute of East Africa: quarterly industry report on petroleum sale in Kenya, Nairobi, PIEA.

Pointner, M., Kuttner, P., Obrlik, T., Jager, A., & Kahr, H. (2014). Composition of corncobs as a substrate for fermentation of biofuels. *Agronomy Research*, *12*(2), 391–396.

Porzio, G.F., Prussi, M., Chiaramonti, D., & Pari, L. (2012). Modeling lignocellulosic bioethanol from poplar: estimation of the level of process integration, yield and potential for co-products. *Journal of Cleaner Production*, 34, 66-75.

Puttaswamy, C.T., Sagar, B.R., Simha, U., Manjappa, S., & Kumar, V.C.S. (2016). Production of Bioethanol from Lignocellulosic Biomass. *Indian Journal of Advances in Chemical Science*, 239-244.

Quintero, J.A., Moncada, J., & Cardona, C.A. (2013). Techno-economic analysis of bioethanol production from Lignocellulosic residues in Colombia: A process simulation approach. *Bioresource Technology,* 139, 300–307.

Rahman, S.H.A., Choudhury, J.P., & Ahmad, A.L. (2006). Production of xylose from oil palm empty fruit bunch fiber using sulfuric acid. *Biochemical Engineering*, 30, 97–103.

Rao., S.R. (2005). Biomass to Ethanol: Process Simulation, Validation and Sensitivity Analysis of a Gasifier and a Bioreactor. MSc Thesis. Karnataka. National Institute of Technology, India.

Rasmey, A.M., Hassan, H.H, Akram, A., Aboseidah, A.A., & Abdul- Wahid, OA. (2017). Chemical pretreatment and saccharification of sugarcane bagasse for bioethanol fermentation by *Saccharomyces cerevisiae* Y17 -KP096551. *Basic Research Journal of Microbiology*, *4*(1), 01-11.

Ray, K.A. (Ed.). (2023). Coulson and Richardson's Chemical Engineering: Volume 2B: Separation Processes, (6th edn.), Elsevier Science

Republic of Kenya. (2021). The Income Tax Act (CAP 470). Kenya Government Press, Nairobi.

Roberto, I.C., Mussatto, S.I., & Rodrigues, R.C.L.B. (2003). Dilute-acid hydrolysis for optimization of xylose recovery from rice straw in a semi-pilot reactor. *Industrial Crops Production,* 17, 171–176.

Rodrigues, R.C.L.B., Rocha, G.J.M., Rodrigues. J. D., Filho, H.J.I., Felipe, M.G.A., & Pessoa, J.A. (2010). Scale up of diluted sulfuric acid hydrolysis for producing sugarcane bagasse hemicellulosic hydrolysate (SBHH). *Bioresource Technology*, 101, 1247-1253.

Roziafanto, A.N., Lazuardi, R.L., Ghozali, M., Sofyan, N., & Chalid, M. (2023). Hydrothermal treatment of sorghum (Sorghum bicolor (L.) Moench) stalks for enhanced microfibrillated cellulose production. *Material Research Express*, 10, 095303.

Ruiz, R., & Tina, E. (1996). Determination of Carbohydrates in Biomass by High Performance Liquid Chromatography, in NREL Ethanol Project, LAP 002, ISSUE DATE: 08/12/1996.

Rusanen, A., Lappalainen, K., Kärkkäinen, J., Tuuttila, T., Mikola, M., & Lassi, U. (2019). Selective hemicellulose hydrolysis of Scots pine sawdust. *Biomass Conversion and Biorefinery*, 9, 283–291.

Salimi, M.N., Lim, S.E., Yusoff, A.H., & Jamlos, M.F. (2017). Conversion of rice husk into fermentable sugar by two stage hydrolysis. *Journal of Physics*, 908: 012056.

Sanchez, G., Pilcher, L., Roslander, C., Modig, T., Galbe, M., & Liden, G. (2004). Dilute- acid hydrolysis for fermentation of the Bolivian straw material *Paja brava*. *Bioresource Technology,* 93, 249–256.

Sarrouh, B.F., Silva, S.S., Santos, D.T., & Converti, A. (2007). Technical/Economical Evaluation of Sugarcane Bagasse Hydrolysis for Bioethanol Production. *Chemical Engineering Technology, 30*(2), 270-275.

Schefflan, R. (2016). Teach Yourself the Basics of Aspen Plus, (2nd edn.), John Wiley & Sons.

Shawn, D.M., John, N., & Saddler, J.N. (2003). Application of enzyme to lignocellulosics. *American chemical society,* 885, 230-243.

Shukla, A., Kumar, D., Girdhar, M., Kumar, A., Goya, A., Malik, T., & Mohan, A. (2023). Strategies of pretreatment of feedstocks for optimized bioethanol production: distinct and integrated approaches. *Biotechnology for Biofuels and Bioproducts*, 16:44.

Sinnott, R. K., & Towler, G. P. (2020). Chemical engineering design, (6th edn.). Oxford: Butterworth-Heinemann Linacre House.

Sjulander N., & Kikas, T. (2020). Origin, Impact and Control of Lignocellulosic Inhibitors in Bioethanol Production—A Review. *Energies*, 13, 4751.

Skoog, H., & Nieman, S. (1998). Principles of Instrumental Analysis. (5th edn.). NY: College Publishing.

Smith, J.M., Van Ness H.C., Abbott, M.M., & Swihart, M. (2021). Introduction to Chemical Engineering Thermodynamics. (9th edn.). New York: Mc Graw Hill.

Standard Newspaper On-line. (2014). Sorghum farmers to earn Kshs 200m in EABL deal. Retrieved April 15, 2019, from http://www.standardgroup.co.ke.

Stroud, K.A. (2001). Engineering mathematics, (5th edn.). New York, Industrial Press, Inc.

Suryadi, H., Yanuar, A., Harmita, R., & Rachmadani, P.W. (2020). Response Surface Methodology Applied to Oxalic Acid Hydrolysis of Oil Palm Empty Fruit Bunch Biomass for D-Xylose Production. *International Journal of Applied Pharmaceutics*, *12*(1), 1-5.

Svetlana, N., Jelena, P., & Ljiljana, M. (2016). Challenges in Bioethanol Production: Utilization of Cotton Fabrics as a Feedstock. *Chemical Engineering*, *22* (4), 375−390.

Swiatek, K., Gaag, S., Klier, A., Kruse, A., Sauer, J., & Steinbach, D. (2020). Acid Hydrolysis of Lignocellulosic Biomass: Sugars and Furfurals Formation. *Catalysts*, 10, 437.

Taherzadeh, M. J., & Karimi, K. (2007). Acid based Hydrolysis processes for Ethanol from Lignocellulosic Materials: A review. *BioResources, 2*(3), 472-499.

Taherzadeh, M.J., & Karimi, K. (2008). Pretreatment of Lignocellulosic Wastes to Improve Ethanol and Biogas Production: A Review. *International Journal of Molecular Science,* 9, 1621-1651.

Tandzi, L.N., & Mutengwa, C.S. (2019). Estimation of Maize (Zea mays L.) Yield Per Harvest Area: Appropriate Methods. *Agronomy, 10*(29), 1-18.

Tarus, C.B.K. (2019). Maize Crisis: A Position Paper on Strategies for Addressing Challenges Facing Maize Farming in Kenya. *East African Scholars Journal of Education, Humanities and Literature, 2*(3), 149-158.

Telleria, B. M., Turbay, C., Favarato, L., Carneiro, T., de Biasi, R.S., Fernandes, A.R., Santos, A.M.C., & Fernandes, P.M.B. (2018). Second-Generation Bioethanol from Coconut Husk. *BioMed Research International*, Volume 2018, ,1- 20.

Tgarguifa, A., Abderafi, S., & Bounahmidi, T. (2017). Modeling and optimization of distillation to produce bioethanol. *Energy Procedia*, 139, 43-48.

Tgarguifa, A., Abderafi, S., & Bounahmidi, T. (2018). Energy efficiency improvement of a bioethanol distillery, by replacing a rectifying column with a pervaporation unit. *Renewable Energy*, 122, 239-250.

Tina, E. (1994). Standard method for ash in biomass, in NREL Ethanol Project, LAP 005, ISSUE DATE: 04/28/1994.

Tina, E. (1994). Standard method for determination of total solids in biomass, in NREL Ethanol Project, LAP 001, ISSUE DATE: 11/01/1994.

Tina, E. (1994). Standard Method for the Determination of Extractives in Biomass, in NREL Ethanol Project, LAP 010, ISSUE DATE: 04/22/1994.

Tina, E. (1994). Standard Test Method for Moisture, Total Solids and Total Dissolved Solids in Biomass Slurry and Liquid Process Samples, in NREL Ethanol Project, LAP 012, ISSUE DATE: 07/05/1994.

Tina, E. (1996). Determination of Acid – Soluble Lignin in biomass, in NREL Ethanol Project, LAP 004, ISSUE DATE: 09/25/1996.

Tizazu, B.Z., & Moholkar, V.S. (2018). Kinetic and thermodynamic analysis of dilute acid hydrolysis of sugarcane bagasse. *Bioresource Technology*, 250, 197–203.

Tosun, I. (2013). The Thermodynamics of Phase and Reaction Equilibria, (1st edn.), Elsevier B.V.

Triana, F.C. (2016). Towards Improved Ethanol Production from Lignocellulosic Biomass. PhD thesis. London. University College London.

UNEP. (2013). Technologies for Converting Waste Agricultural Biomass to Energy. United Nations Environmental Programme Division of Technology, Industry and Economics International Environmental Technology Centre, Osaka.

Wijaya, Y.P., Putra, R.D.D., Widyaya, V.T., Ha, J., Suh, D.J., & Kim, C.S. (2014). Comparative study on two-step concentrated acid hydrolysis for the extraction of sugars from lignocellulosic biomass. *Bioresource Technology*, 164, 221-231.

Wyman, C. E. (1994): Ethanol from Lignocellulosic Biomass: Technology, Economics and Opportunities. *Bioresource Technology*, 50, 3-16.

Xiao, M.Z., Sun, Q., Hong, S., Chen, W.J., Pang, B., Du, Z.Y., Yang, W.B., Sun, Z., & Yuan, T.Q. (2021). Sweet sorghum for phytoremediation and bioethanol production. *Journal of Leather Science and Engineering*, 3,32.

Yolcan, O.O. (2023). World energy outlook and state of renewable energy: 10-Year Evaluation. *Innovation and Green Development*, 2, 100070.

Yuan, Q., Liu, S., Ma, M.G., Ji, X.X., Choi, S.E., & Si. C. (2021). The Kinetics Studies on Hydrolysis of Hemicellulose. *Frontiers in Chemistry*, 9:781291.

Zhang, M., Wang, Y., Hui, K.S., Liu, L., & Zhang, C. (2020). Microwave-assisted Acid-catalyzed Hydrolysis of Hemicelluloses in Rice Husk into Xylose. *Earth and Environmental Science*, 513, 012016.

Zhao, H., Baker, G.A., & Cowins, J.V. (2010). Fast Enzymatic Saccharification of Switchgrass After Pretreatment with Ionic Liquids. *Biotechnology Progress*, *26*(1), 127-133.

Zhao, L., Zhang, X., Xu, J., Ou, X., Chang, S., & Wu, M. (2015). Techno-Economic Analysis of Bioethanol Production from Lignocellulosic Biomass in China: Dilute-Acid Pretreatment and Enzymatic Hydrolysis of Corn Stover. *Energies*, 8, 4096-4117.

Zhu, T., Li, P., Wang, X., Yang, W., Chang, H., & Ma, S. (2014). Optimization of formic acid hydrolysis of corn cob in xylose production. *Korean Journal of Chemical Eng*ineering, *31*(9), 1624-1631.

APPENDIXES

Appendix A: Modeling and Simulation results

Table A. 1: Overall mass balance around the dilute sulphuric acid pretreatment reactor for SSS

Stream/Component	LGB (kg/h) (IN)	WATERH (kg/h) (IN)	ACDWATE 2 (kg/h) (IN)	PSLURRY1 (kg/h) (OUT)
Water	20580	46111	130171	194386
Hemicellulose	21502	0	0	1055
Glucose	0	0	0	2700
Xylose	0	0	0	21901.5
Sulphuric acid	0	0	2274	2274
Extractives	625.66	0	0	625.66
Furfural	0	0	0	768
Lignin	30178.5	0	0	30178.5
Ash	4873.34	0	0	4873.34
Cellulose	25140.5	0	0	22694
Total Flow (kg/h)	**102900**	**46111**	**132445**	**281456**

Table A. 2: Overall mass balance around the dilute sulphuric acid pretreatment reactor for maize cobs

Stream/Component	LGB (kg/h) (IN)	WATERH (kg/h) (IN)	ACDWATE 2 (kg/h) (IN)	PSLURRY1 (kg/h) (OUT)
Water	15435	68000	130171	208782.25
Hemicellulose	41839.10	0	0	2090.28
Glucose	0	0	0	3047.96
Xylose	0	0	0	42755.27
Sulphuric acid	0	0	2274	2274
Extractives	3920.49	0	0	3920.49
Furfural	0	0	0	1521.35
Lignin	10362	0	0	10362
Ash	3611.81	0	0	3611.81
Cellulose	27731.60	0	0	24979.59
Total Flow (kg/h)	102900	68000	132445	303345

Table A. 3: Overall mass balance around the steam explosion pretreatment reactor for SSS

Stream/Component	LGBM (kg/h) (IN)	STEAM1 (kg/h) (IN)	WATERL (kg/h) (IN)	PRTSLURR (kg/h) (OUT)
Water	20580	51450	120000	190168.26
Hemicellulose	21502			5220.79
Glucose	0			1144.35
Xylose	0			14990.34
Furfural	0			797.49
Lignin	30178.50			30178.50
Ash	4873.34			4873.34
Acetic acid	0			2247.83
Extractives	625.66			625.66
Cellulose	25140.50			24103.44
Total Flow (kg/h)	**102900**	**51450**	**120000**	**274350**

Table A. 4: Overall mass balance around the steam explosion pretreatment reactor for maize cobs

Stream/Component	LGBM (kg/h) (IN)	STEAM1 (kg/h) (IN)	WATERL (kg/h) (IN)	PRTSLURR (kg/h) (OUT)
Water	15435	51450	137000	200352.81
Hemicellulose	41839.10	0		10158.75
Glucose	0	0		1262.29
Xylose	0	0		29168.59
Furfural	0	0		1551.78
Lignin	10362	0		10362
Ash	3611.81	0		3611.81
Acetic acid	0	0		4373.89
Extractives	3920.49	0		3920.49
Cellulose	27731.60	0		26587.59
Total Flow (kg/h)	**102900**	**51450**	**137000**	**291350**

Table A. 5: Overall mass balance around the alkaline pretreatment reactor for SSS

Stream/Component	NAOSOLN2 (kg/h) (IN)	LGB (kg/h) (IN)	LIQDFRAC (kg/h) (OUT)	SLDFRAC1 (kg/h) (OUT)
Water	318000	20580	304819	33761
Hemicellulose	0	21502	17146	4356
Lignin	0	30178.50	23326.50	6852
Ash	0	4873.34	4873.34	0
Cellulose	0	25140.50	177.50	24963
Sodium Hydroxide	5762	0	5762	0
Extractives	0	625.66	625.66	0
Total Flow (kg/h)	**323762**	**102900**	**356730**	**69932**

Table A. 6: Overall mass balance around the alkaline pretreatment reactor for maize cobs

Stream/Component	NAOSOLN 2 (kg/h) (IN)	LGB (kg/h) (IN)	LIQDFRAC (kg/h) (OUT)	SLDFRAC1 (kg/h) (OUT)
Water	355000	15435	333391.49	37043.51
Hemicellulose	0	41839.10	33436.19	8402.91
Lignin	0	10362	8007.88	2354.12
Ash	0	3611.81	3611.81	0
Cellulose	0	27731.60	270.69	27460.91
Sodium Hydroxide	5762	0	5762	0
Extractives	0	3920.49	3920.49	0
Total Flow (kg/h)	360762	102900	388400.55	75261.45

Appendix B: Economic analysis and variation of techno-economic parameters

Table B. 1: Distribution of labour requirements (Sinnott and Towler, 2020; Humbird et al., 2011)

Position	Number of personnel	Broad category	Total number of personnel
General manager	1	Administration	**12**
Human resource manager	1		
Procurement manager	1		
Marketing manager	1		
Sales manager	1		
Plant manager	1		
Lab manager	1		
Secretaries	4		
Sales representative	1		
Finance manager	1	Finance	**3**
Accountant	2		
Plant engineer	2	Technical	**11**
Maintenance supervisor	4		
Shift supervisor	4		
Quality control Officer	1		
Maintenance technician	12	Manufacturing	**79**
Lab technician	3		
Shift operators	27		
Support staff	15		
Yard employees	12		
Clerks	10		

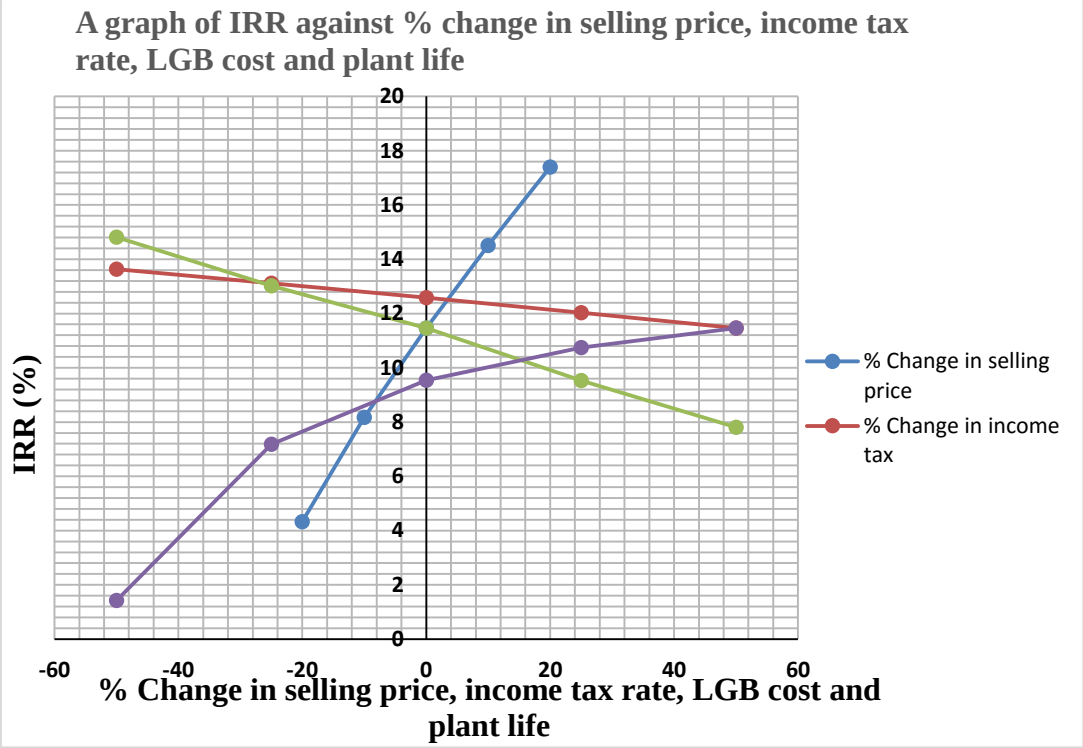

Figure B. 1: IRR against % change in selling price, income tax rate, LGB cost and plant Life for SSS

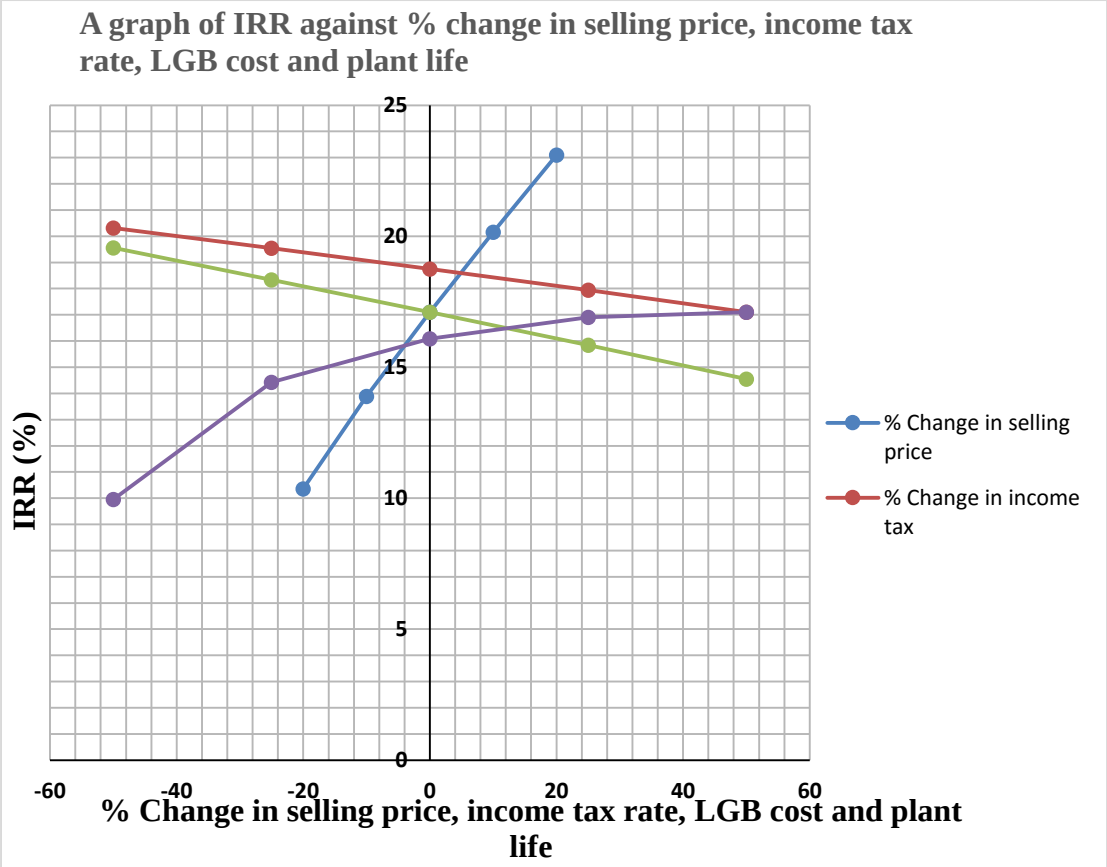

Figure B. 2: IRR against % change in selling price, income tax rate, LGB cost and plant Life for maize cobs

Appendix C: Calculations involving glucose yield

Appendix C. 1: Determination of glucose yield

For SSS, the cellulose content is 27.49% (w/w) **(Table 4.1)**

For every experiment, 15 grams of substrate was used.

15 grams of sample contains $15\text{g} \times 0.2749 = 4.1235$ grams of cellulose

The SSS sample contains 9.98% (w/w) moisture content **(Table 4.1)**

On a dry weight basis, cellulose content in sample = $4.1235 \times (1 - 0.0998) = 3.7119747$ grams of cellulose

Therefore, in every experiment, 3.712 grams of cellulose was subjected to hydrolysis. Assuming that this was the only source of glucose, the percentage yield is expressed in terms of this amount of cellulose. During hydrolysis of SSS, the data on the amount of glucose obtained is shown in Table 4.54.

Using data for experiment on row one in Table 4.54, 2.91 grams of glucose was obtained.

This amount of glucose is corrected for hydration by multiplying the glucose reading by 0.9 to correct for the water molecule added upon hydrolysis of cellulose (da Silva et al., 2018).

Therefore, actual glucose obtained = $2.91 \times 0.9 = 2.619$ grams

$$\text{Percentage Yield} = \frac{\text{Actual glucose obtained}}{\text{Initial cellulose present}} \times 100$$

Therefore, yield is given by:

$$\text{Percentage Yield} = \frac{2.619 \text{ grams}}{3.712 \text{ grams}} \times 100 = 70.55\ \%, \text{(w/w)}$$

Similar approach was done for all the other experimental runs and the results are as shown in Table 4.54 for SSS. The same analysis was done for maize cobs and the results are shown in Table 4.56.

Appendix C. 2: Maximum/theoretical yield of glucose

The composition of cellulose in SSS and maize cobs is 27.49% (w/w) and 28.97% (w/w) respectively. During hydrolysis, 15 grams of substrate was used.

For SSS:

15 grams of sample contains $15\text{g} \times 0.2749 = 4.1235$ grams of cellulose

SSS sample contains 9.98% (w/w) moisture content **(Table 4.1)**

On a dry weight basis, cellulose content in sample = $4.1235 \times (1 - 0.0998) = 3.712$ grams of cellulose

The maximum/theoretical amount of glucose that can be obtained from SSS is given by Equation C.1.

$$C_6H_{10}O_5 + H_2O \rightarrow C_6H_{12}O_6 \qquad \text{C.1}$$

From Equation C.1:

162 grams of cellulose + 18 grams of water gives 180 grams of glucose. Therefore, 3.712 grams of cellulose gives:

$\frac{3.712\text{g} \times 180}{162} = 4.124$ grams of Glucose

This is the maximum amount of glucose that can be obtained from SSS sample

The same calculation is done for maize cobs, thus

15 grams of maize cobs sample contains $15\text{g} \times 0.2897 = 4.3455$ grams of cellulose

Maize cobs sample contains 8.67% (w/w) moisture content **(Table 4.1)**

On a dry weight basis, cellulose content in sample = $4.3455 \times (1 - 0.0867) = 3.969$ grams of cellulose. Using Equation C.1:

$\frac{3.969g \times 180}{162} = 4.41$ grams of Glucose

This is the maximum amount of glucose that can be obtained from maize cobs sample.

Appendix D: Saeman and biphasic model

Appendix D. 1: Integration of the proposed Saeman model

According to Tizazu and Moholkar (2018)

$$\underset{\text{(Cellulose/Hemicellulose)}}{\text{Polysaccharide}} \xrightarrow{K_1} \underset{\text{(Glucose/xylose)}}{\text{Sugar monomers}} \xrightarrow{K_2} \underset{\text{(HMF/furfural)}}{\text{Decomposition products}} \quad \textbf{2.3}$$

Using Equation 2.3, material balance is performed to obtain a system of ordinary differential equations that describe the hydrolysis process for cellulose.

The material balance for cellulose hydrolysis is given by:

$$r_A = \frac{dC_A}{dt} = -k_1 C_A \quad \text{D.1}$$

$$r_B = \frac{dC_B}{dt} = -k_1 C_A - k_2 C_B \quad \text{D.2}$$

$$r_C = \frac{dC_C}{dt} = k_2 C_B \quad \text{D.3}$$

Where:

C_A = polymer concentration

C_B = monomer concentration

C_C = concentration of decomposition product

From Equation D.1

$$\frac{dC_A}{dt} = -k_1 C_A$$

$$\int_{C_{AO}}^{C_A} \frac{dC_A}{C_A} = -k_1 \int_0^t dt$$

$$\ln \frac{C_A}{C_{AO}} = -k_1 t$$

$$C_A = C_{AO} e^{-k_1 t} \quad \text{D.4}$$

Where:

C_{AO} = initial polymer concentration

t = hydrolysis reaction time

Substituting Equation D.4 into Equation D.2

$$\frac{dC_B}{dt} = k_1 C_{AO} e^{-k_1 t} - k_2 C_B$$

$$\frac{dC_B}{dt} + k_2 C_B = k_1 C_{AO} e^{-k_1 t} \quad \text{D.5}$$

Applying Laplace transform to Equation D.5 (Stroud, 2001)

$$L\left[\frac{dC_B}{dt}\right] + k_2 L[C_B] = k_1 C_{AO} L\left[e^{-k_1 t}\right]$$

$$L\left[\frac{dC_B}{dt}\right] = -k_2 L[C_B] + k_1 C_{AO} L\left[e^{-k_1 t}\right]$$

$$sC_B(s) - C_B(0) = -k_2 C_B(s) + \frac{k_1 C_{AO}}{S+k_1}$$

$C_B(0) = 0$, because there is no monomer at time = 0

$$sC_B(s) = -k_2 C_B(s) + \frac{k_1 C_{AO}}{S+k_1}$$

$$sC_B(s) + k_2 C_B(s) = \frac{k_1 C_{AO}}{S+k_1}$$

$$C_B(s)[s + k_2] = \frac{k_1 C_{AO}}{S+k_1}$$

$$C_B(s) = \frac{k_1 C_{AO}}{(S+k_1)(S+k_2)} \quad \text{D.6}$$

Resolving Equation D.6 into partial fraction (Stroud, 2001)

$$\frac{k_1 C_{AO}}{(S+k_1)(S+k_2)} = \frac{A}{(S+k_1)} + \frac{B}{(S+k_2)}$$

$$k_1 C_{AO} = A(s + k_2) + B(s + k_1)$$

Let:

$$s = -k_1$$

$$k_1 C_{AO} = A(k_2 - k_1)$$

$$A = \frac{k_1 C_{AO}}{(k_2 - k_1)} \quad \text{D.7}$$

Let:

$s = -k_2$

$k_1 C_{AO} = A(-k_2 + k_1) + B(k_1 - k_2)$

$$B = \frac{k_1 C_{AO}}{(k_1 - k_2)} \quad \text{D.8}$$

$$C_B(s) = \frac{k_1 C_{AO}}{(s+k_1)(s+k_2)} = \frac{k_1 C_{AO}}{(k_2 - k_1)(s+k_1)} + \frac{k_1 C_{AO}}{(k_1 - k_2)(s+k_2)}$$

$$C_B(s) = \frac{k_1 C_{AO}}{(k_2 - k_1)(s+k_1)} - \frac{k_1 C_{AO}}{(k_2 - k_1)(s+k_2)} \quad \text{D.9}$$

$$C_B(s) = \frac{k_1 C_{AO}}{(k_2 - k_1)} \left[\frac{1}{(s+k_1)} - \frac{1}{(s+k_2)}\right] \quad \text{D.10}$$

Find the Laplace inverse of Equation D.10 (Stroud, 2001)

$$C_B(t) = \frac{k_1 C_{AO}}{(k_2 - k_1)} [\, e^{-k_1 t} - e^{-k_2 t}] \quad \text{D.11}$$

Equation D.11 is similar to Equation 2.6.

Appendix E: Scientific Output

Publications

1. Ngigi, W., Siagi, Z., Kumar, A. and Arowo, M., Predicting the techno-economic performance of a large-scale second-generation bioethanol production plant: a case study for Kenya. *Int. J. Energy Environ Eng.* (2022). https://doi.org/10.1007/s40095-022-00517-1

2. Wiseman Ngigi, Zachary Siagi, Anil Kumar, Moses Arowo, "Optimization of Concentrated Sulphuric Acid Hydrolysis of Gadam Sorghum Stalks Found in Kenya for Fermentable Sugar Production", *Journal of Energy*, vol. 2022, Article ID 2064600, 13 pages, 2022. https://doi.org/10.1155/2022/2064600

Exchange programme report

1. World Bank-India Government PhD Funded Exchange Program: https://excellencecenter.mu.ac.ke/wp-content/uploads/2020/09/WISEMAN-EXCHANGE-PROGRAM-AT-IITB.pdf

Appendix F: Plagiarism Awareness Certificate

SR177

THESIS WRITING COURSE

PLAGIARISM AWARENESS CERTIFICATE

This certificate is awarded to

WISEMAN TUMBO NGIGI

ENG/DPHIL/MP/01/18

In recognition for passing the University's plagiarism
Awareness test with a similarity index of 17% and
Striving to maintain academic integrity.

Awarded by:

Prof. Anne Syomwene Kisilu , CERM-ESA Project Leader

19th /05/2023